

# Fundamentals of OPEN CHANNEL FLOW



# Fundamentals of OPEN CHANNEL FLOW

Glenn E. Moglen

*Occoquan Laboratory, Virginia Tech*



CRC Press

Taylor & Francis Group

Boca Raton London New York

---

CRC Press is an imprint of the

Taylor & Francis Group, an **Informa** business

A SPOON PRESS BOOK

CRC Press  
Taylor & Francis Group  
6000 Broken Sound Parkway NW, Suite 300  
Boca Raton, FL 33487-2742

© 2015 by Taylor & Francis Group, LLC  
CRC Press is an imprint of Taylor & Francis Group, an Informa business

No claim to original U.S. Government works

Printed on acid-free paper  
Version Date: 20150303

International Standard Book Number-13: 978-1-4665-8006-0 (Paperback)

This book contains information obtained from authentic and highly regarded sources. Reasonable efforts have been made to publish reliable data and information, but the author and publisher cannot assume responsibility for the validity of all materials or the consequences of their use. The authors and publishers have attempted to trace the copyright holders of all material reproduced in this publication and apologize to copyright holders if permission to publish in this form has not been obtained. If any copyright material has not been acknowledged please write and let us know so we may rectify in any future reprint.

Except as permitted under U.S. Copyright Law, no part of this book may be reprinted, reproduced, transmitted, or utilized in any form by any electronic, mechanical, or other means, now known or hereafter invented, including photocopying, microfilming, and recording, or in any information storage or retrieval system, without written permission from the publishers.

For permission to photocopy or use material electronically from this work, please access [www.copyright.com](http://www.copyright.com) (<http://www.copyright.com/>) or contact the Copyright Clearance Center, Inc. (CCC), 222 Rosewood Drive, Danvers, MA 01923, 978-750-8400. CCC is a not-for-profit organization that provides licenses and registration for a variety of users. For organizations that have been granted a photocopy license by the CCC, a separate system of payment has been arranged.

**Trademark Notice:** Product or corporate names may be trademarks or registered trademarks, and are used only for identification and explanation without intent to infringe.

Visit the Taylor & Francis Web site at  
<http://www.taylorandfrancis.com>

and the CRC Press Web site at  
<http://www.crcpress.com>

*To my wife,  
Jenny, and to my children,  
Rachel and Richard*



# Contents

<i>Preface</i>	<i>xi</i>
<b>1 Introductory Material</b>	<b>1</b>
1.1 Introduction: What Is Open Channel Flow?	1
1.2 Quantification of Open Channel Flow	2
1.3 Foundational Equations	4
1.4 Classes of Problems	7
1.5 The Need for Critical Thinking	8
Reference	10
Problems	10
<b>2 Energy</b>	<b>13</b>
2.1 Specific Energy	13
2.2 The $E-y$ Diagram	16
2.3 Critical Flow	18
2.4 The Froude Number	21
2.5 Alternate Depths	24
2.6 Energy Considerations on Upward and Downward Steps	26
2.7 Energy Considerations in Constrictions and Expansions	35
2.8 Chokes, Flow Accessibility, Critical Flow, and Transients	39

2.9	Longitudinal Changes in Flow Conditions and the Froude Number	46
2.10	Energy in Non-Rectangular Channels	49
2.10.1	Alternate Depths in Non-Rectangular Channels	51
2.10.2	Critical Depth and Energy in Non-Rectangular Channels	55
2.11	Summary	63
	Reference	65
	Problems	65
<b>3</b>	<b>Momentum</b>	<b>69</b>
3.1	Introductory Comments	69
3.2	The Momentum Function	71
3.3	Hydraulic Jump	74
3.4	Energy and Momentum Losses	78
3.5	Dimensionless Energy and Momentum	83
3.6	Momentum in Non-Rectangular Channels	86
3.7	Summary	97
	References	99
	Problems	99
<b>4</b>	<b>Friction and Uniform Flow</b>	<b>103</b>
4.1	Introductory Comments	103
4.2	Uniform Flow	104
4.3	Shear Stress in Open Channel Flow	106
4.4	Chézy and Manning's Equations	108
4.5	Uniform Flow and Normal Depth	112
4.6	Reach Classification	114
4.7	Summary	121
	References	122
	Problems	123
<b>5</b>	<b>Qualitative Gradually Varied Flow</b>	<b>125</b>
5.1	Introductory Comments	125
5.2	Non-Uniform Flow	126
5.2.1	Scenario 1	127
5.2.2	Scenario 2	127
5.3	Profile Taxonomy	129
5.4	In-Stream Obstructions	132
5.5	Composite Profiles	140

5.6	Drowned Hydraulic Jump	151
5.7	Generalized Boundary Conditions	153
5.7.1	Downstream Boundary Conditions	153
5.7.2	Upstream Boundary Conditions	155
5.7.2.1	Case 1: Incoming Supercritical Flow	155
5.7.2.2	Case 2: Incoming Subcritical Flow	156
5.8	Conjugate Curve Concept	159
5.9	Summary	161
	Problems	162
<b>6</b>	<b>Quantitative Gradually Varied Flow</b>	<b>167</b>
6.1	Introductory Comments	167
6.2	Governing Equation	168
6.3	Standard Step Method	170
6.4	Variations of and Alternatives to the Standard Step Method	176
6.5	Conjugate Curve: Quantitative Application	185
6.6	HEC-RAS: an Industry Standard Software Package for Surface Water Profiles	194
6.7	Summary	205
	References	205
	Problems	205
<b>7</b>	<b>Fundamentals of Sediment Transport</b>	<b>209</b>
7.1	Introductory Comments	209
7.2	Characterization of Water and Sediment	210
7.2.1	Manning's $n$ as a Function of Channel and Sediment Characteristics	214
7.3	Sediment Motion	215
7.3.1	Particle Fall Velocity: Stokes' Law	215
7.3.2	Incipient Motion and Shields' Diagram	221
7.4	Sediment Transport	227
7.4.1	Bed Load Transport Rate	228
7.4.2	Suspended Load Transport Rate	232
7.4.3	Sediment Load Estimation	235
7.5	Estimation of Sediment Transport: Accuracy and Precision	240
	References	242
	Problems	243
<i>Appendix</i>		245
<i>Index</i>		251



# Preface

As with many students of open channel flow from my generation, I first was exposed to this topic as an undergraduate senior using the excellent and wonderful book authored by Henderson (1966). With a further nod toward Henderson, the alert reader will notice that the sequence of material presentation in this text is the same as in the early chapters of his book. So a fair question is, “What do I feel I have to offer to this topic that Henderson did not already address?” My answer is twofold.

First, Henderson’s book was broader than this one, presenting the fundamentals of open channel flow along with more advanced topics. This book, by contrast, is intended for exclusive use in a first course on this topic, as it appears in the curriculum of most undergraduate civil engineering programs. Advanced courses will necessarily draw on other material beyond this text. I have written this text with the intention of making up for limited scope with what I hope is a thorough and clear examination of the nuances of the most fundamental concepts.

Second, I have endeavored to bring this topic into the twenty-first century by emphasizing tools and programs that did not exist in Henderson’s time. Tools such as the “Goal Seek” function in Excel, computer animations of basic open channel phenomena, and an exploration of surface water profiles as modeled using both spreadsheet applications and the US Army Corps of Engineers Hydrologic Engineering Center River Analysis System (HEC-RAS) program should serve the current reader well. These items reduce mindless repetition, tap into the reader’s innate ability to understand complex concepts visually, and expose the reader to the industry-standard tools of the day.

This book offers a few other new contributions. At this writing, I am unaware of any text that presents an analytical solution relating one alternate depth to the other in a rectangular channel. While the analog of this equation relating conjugate depths has existed since before Henderson's time, the rather simple equation for alternate depths has remained elusive. Ironically, I developed this relationship directly from the mathematics offered by Henderson. In his book, he not only presented the equation relating one conjugate depth to the other, but he showed the surprising duality that exists between  $y'$  and  $1/y'$  in dimensionless forms of the energy and momentum equations. I reasoned that if these two equations could be made equivalent in a dimensionless presentation, then the conjugate depth relationship must likewise have an alternate depth counterpart. That derivation appears in this text.

Another theme I have emphasized in this book is graphical interpretation of the  $E\text{-}y$  and  $M\text{-}y$  relationships. I have had the benefit of presenting this material to students over many years. While many students capably manipulate the relevant equations when solving open channel flow problems, a fair number of others struggle. I have found that by focusing the problem interpretation into a shift along either or both of the  $E\text{-}y$  and  $M\text{-}y$  curves, students are able to gain the insights necessary to solve the problem at hand. Those insights then guide the mathematics. Many of the examples and animations provided here reinforce the correspondence between these graphical and mathematical realms.

\*\*\*

As I write this, I feel strongly aware of my place in the teaching and learning continuum of those who have studied open channel flow. I have learned immensely from three people who merit special recognition. First, I owe a debt of gratitude to my original teacher of this subject, Dr. Yaron Sternberg at the University of Maryland. Ron's classroom was a joy to enter because he so skillfully encouraged quiet contemplation as the source of true understanding. I remember his classroom as being an almost magical sanctuary, where deep and careful thought could prevail over any problem. Second, I owe the trajectory of my life in academia to Dr. Richard McCuen, also at the University of Maryland. It was Rick who so impressed me as an undergraduate as to what was possible in my life's work. It was Rick who planted the seed and helped me believe my future was in academics. And it is Rick who has steadfastly supported my efforts to complete this book. Third, I would like to recognize Dr. Michael Casey for his unique role in my life. Unlike Ron and Rick, Mike was once my student, never formally my teacher. But he has taught me so much more than I ever taught him. Mike was my student when I was a struggling assistant professor. Intellectually, he taught me GIS, how to be a clever programmer, and how to integrate apparently disparate tools into a unique

whole. And he was the person who actually suggested I write this book. Mike has been a remarkable friend to me. He is the younger brother I never had.

There is no better way to learn a subject than to teach it. In keeping with my earlier statement of the continuum, this work has benefitted enormously from the hundreds of students whom I've had the good fortune to lead through this material, both at the University of Maryland and now at Virginia Tech. These students have patiently sat through numerous iterations of past material that now appears in this book. They have asked insightful questions and pointed out errors in algebra, in computation, and in logic. They have forced me to hone presentations, to pare down needless and confusing examples, and to demonstrate what might have been obvious to me but not to them. This book exists because of these students.

Finally, I would like to thank my family and friends for their support. My wife and children have seen me labor on this book at all hours and in all places. There have been occasions when they have sacrificed my time with them so that I could pursue the completion of this work. They have never complained and have remained supportive and encouraging to the end.

## Reference

Henderson, F.M. (1966). *Open Channel Flow*, Macmillan, New York.

**Glenn Moglen**  
September 2014  
Manassas, Virginia



# Introductory Material

## CHAPTER OBJECTIVES

1. Define open channel flow.
2. Define basic quantities relevant to open channel flow.
3. Present and discuss fundamental governing equations.
4. Identify different classes of open channel flow problems.
5. Emphasize the value and importance of critical thinking.

### 1.1 INTRODUCTION: WHAT IS OPEN CHANNEL FLOW?

As used in this text, the term *open channel flow* covers the range of natural and artificial conveyances of water in settings that are open to atmospheric pressure. Some examples of open channels include water flowing in creeks and rivers, through irrigation canals, within open air conveyances in wastewater treatment plants, and along the curb and gutter at the edges of streets and parking lots. The channel, therefore, varies from a natural surface lined with naturally occurring sediment to a man-made surface made of concrete, metal, or graded soil and sediment.

To properly study open channel flow, we first need to define the basic quantities that are at the heart of the physical system, to enumerate the most fundamental governing equations, and to develop a classification system for different kinds of problems that will be addressed. These items are discussed in this chapter. The chapter concludes with a brief discussion on the value

of critical thinking. This last item is a nod toward the author's experience teaching this subject for many years.

## 1.2 QUANTIFICATION OF OPEN CHANNEL FLOW

Figure 1.1 presents a longitudinal view of flow in an open channel. The figure shows many of the basic quantities that govern solutions to open channel flow problems.

The flow depth,  $y$ , is arguably the most important quantity when approaching problems in open channel flow. Depth is measured in the vertical plane, from channel bottom to the water surface. The reader may be concerned that depth is apparently not measured perpendicular to the channel bottom. While this is true, the channel slope,  $S_0$ , is generally very small (see Problem 1.1) so that the difference between measuring the channel depth perpendicular to channel bottom and measuring the depth in the vertical plane is minuscule. By basic geometry Figure 1.1 also shows that  $\theta = \tan^{-1}(S_0)$ . The quantity,  $z$ , is generally used to represent any topography presented by the channel bottom itself, relative to the horizontal datum.

The flow velocity,  $v$ , is also of primary importance to solving open channel flow problems. In reality, velocity varies in the vertical from essentially zero at the channel bottom to generally a maximum value at or near the water surface. Velocity also varies across the width of the channel in potentially very complex ways depending upon the channel shape. In this text, however, we rarely consider this variation. Instead we work with a single, aggregate value of velocity that represents a mean value across both the depth and width of the channel cross-section.

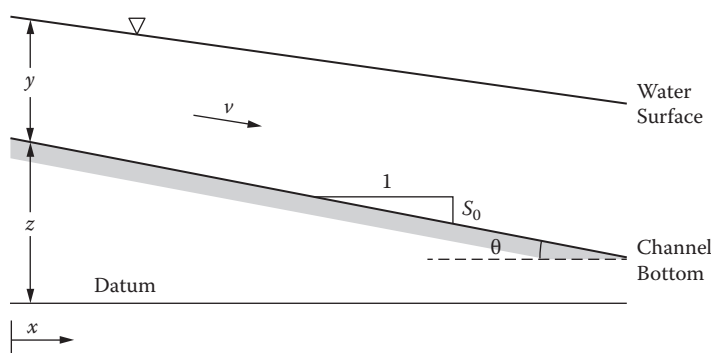


**FIGURE 1.1** Profile view of basic open channel flow quantities.

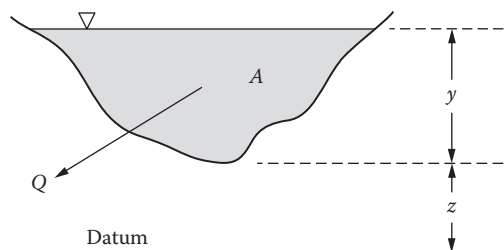


**FIGURE 1.2** Cross-sectional view of basic open channel flow quantities.

Figure 1.2 presents a cross-sectional view of flow in an open channel. Like velocity, the channel cross-section is potentially quite complex in shape. It should be apparent to the reader that the cross-sectional area of the channel,  $A$ , is dependent on the flow depth,  $y$ . More than anything else, this observation is what distinguishes channel flow from flow in a closed conduit. In a closed conduit such as a pipe, assumed to be flowing full, the cross-sectional area is fixed and constant. Thus, the physics of the flow are constrained largely to understanding the flow velocity, issues of friction, and of total energy possessed by the flow. In open channel flow, the depth plays a dual role: (1) it controls the energy possessed by the flow, and (2) it determines the cross-sectional area of the flowing volume. This is the challenge of solving open channel flow problems. It is also the beauty of solving such problems. Although it should be understood by the reader that the natural world offers an endless range of possible channel shapes, this text focuses almost exclusively on regular channel shapes: rectangular, trapezoidal, and circular. An emphasis is placed on rectangular channels, not because they are widely used, but because the mathematics of flow in a rectangular channel are as simple as possible and allow the reader to focus attention on other more pressing open channel flow phenomena.

Discharge,  $Q$ , is the last of the basic open channel flow quantities the reader must consider. Dimensionally,  $Q$  has units of  $L^3T^{-1}$  such as cubic meters per second or cubic feet per second. Like velocity,  $Q$  also varies continuously in both the vertical and horizontal planes. But like velocity,  $Q$  is generally treated in this text as an aggregate average over the cross-sectional area of the flow.

Not shown in either Figure 1.1 or Figure 1.2 but still relevant in some open channel problems are several properties of water. One fundamental property of water is density,  $\rho$  (in  $ML^{-3}$ ). The density of water is roughly  $1000 \text{ kg/m}^3$ . Closely related is the unit weight of water,  $\gamma$  (in  $FL^{-3}$ ), which is simply the product of density and gravitational acceleration:

$$\gamma = \rho \cdot g \quad (1.1)$$

A typical value of  $\gamma$  is about 9810 N/m<sup>3</sup> in metric units or 62.4 lb/ft<sup>3</sup>. Density and unit weight vary slightly with temperature.

Another fundamental quality of water is its viscosity, which is reported in two different ways. The kinematic viscosity of water,  $\nu$  (in L<sup>2</sup>T<sup>-1</sup>) is roughly  $1.8 \times 10^{-6}$  m<sup>2</sup>/s at 0°C, but diminishes considerably (by more than a factor of two) as it warms to say, 30°C. The other way viscosity is measured and reported is as dynamic viscosity,  $\mu$  (in FTL<sup>-2</sup>). Dynamic and kinematic viscosity are related according to the following equation:

$$\mu = \rho \cdot \nu \quad (1.2)$$

The dynamic viscosity of water is approximately  $1.8 \times 10^{-3}$  N-s/m<sup>2</sup> at 0°C, and also diminishes by a factor of two as it warms to 30°C. Chapter 7 deals most closely with issues of water density, unit weight, and viscosity. Table 7.1 (Chapter 7) shows the variation of these quantities with temperature.

### 1.3 FOUNDATIONAL EQUATIONS

This text is premised on essentially four foundational equations that quantify the concepts of continuity, energy, momentum, and friction. Energy and momentum are the immediate focus of Chapters 2 and 3, respectively. Chapter 4 first introduces friction, but it requires that chapter, along with Chapters 5 and 6, to more fully examine both qualitatively and quantitatively the nuances of friction. Of course, these concepts do not exist separate from one another, so the full development of friction concepts in Chapters 4 through 6 draws heavily on continuity, energy, and momentum. All must be understood in order to adequately address most problems relating to open channel flow.

We defer the proper discussion of energy, momentum, and friction to subsequent chapters. For now, we assume the reader is already familiar with continuity and Bernoulli's energy equations and use these to motivate the central concept of the Froude number by deriving the speed of shallow wave propagation in an open channel.

Inspired by Henderson (1966), Figure 1.3 provides a definition sketch of a shallow wave moving at velocity,  $c$ , that is set in motion by a wall pushing a flow of water at velocity  $\Delta v$ . At location 1, to the left of the shallow wave front, the velocity of the flow is  $\Delta v$ . At location 2, to the right of the wave front, the water is stationary (i.e.,  $v = 0$ ). The depth is slightly greater at location 1,  $y + \Delta y$ , than at location 2 where the depth is simply,  $y$ . We now make use of continuity and Bernoulli's equation to determine the velocity at which the shallow wave is propagating. Taking the perspective of an observer on the banks of the

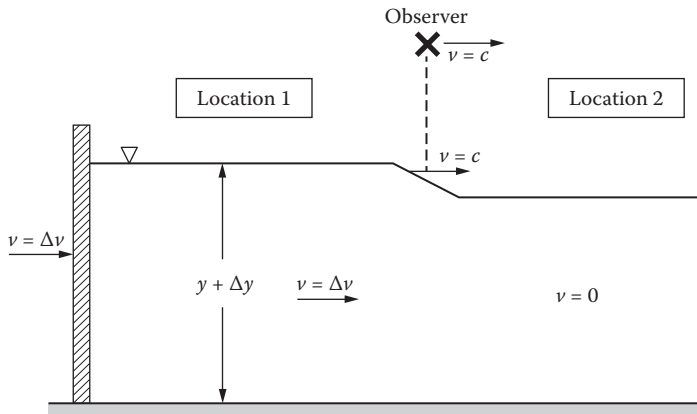


**FIGURE 1.3** A shallow wave moving at velocity,  $c$ , is set up by a wall traveling at velocity,  $\Delta v$ , to the right.

stream, the observer moves in synchronization with the shallow wave so that from the observer's perspective the wave is stationary. Because the observer is moving at velocity  $c$  to the right, the apparent velocity (velocity taken as positive moving from left to right in Figure 1.3) of the flow at location 1 is  $v_1 = c - \Delta v$ . Similarly, at location 2, the apparent velocity of the flow is  $v_2 = c$ .

Applying continuity and assuming a rectangular channel with width,  $w$ , we have

$$Q_1 = Q_2 \quad (1.3)$$

$$v_1 \cdot y_1 \cdot w = v_2 \cdot y_2 \cdot w \quad (1.4)$$

Dividing through by  $w$  and substituting for  $y_1$  and  $y_2$ , we get

$$(c - \Delta v) \cdot (y + \Delta y) = c \cdot y \quad (1.5)$$

$$c \cdot y + c \cdot \Delta y - \Delta v \cdot y - \Delta v \cdot \Delta y = c \cdot y \quad (1.6)$$

By definition,  $\Delta v$  is much smaller than  $c$ , and  $\Delta y$  is small relative to  $y$ . Thus the product,  $\Delta v \cdot \Delta y$ , is very small and can be neglected. Equation 1.6 can be simplified and rearranged to

$$\frac{c}{y} = \frac{\Delta v}{\Delta y} \quad (1.7)$$

The wave height,  $\Delta y$ , is small, so the energy dissipated by the wave is treated as negligible. Using Bernoulli's equation between locations 1 and 2 and noting that the pressure term (i.e.,  $p_1 = p_2$ ) is unchanged between these locations,

$$y + \Delta y + \frac{(c - \Delta v)^2}{2g} = y + \frac{c^2}{2g} \quad (1.8)$$

$$y + \Delta y + \frac{c^2 - 2c \cdot \Delta v + \Delta v^2}{2g} = y + \frac{c^2}{2g} \quad (1.9)$$

As we previously neglected  $\Delta v \cdot \Delta y$  as small in equation 1.6, we similarly neglect  $\Delta v^2$  as small. Canceling common terms on both sides of equation 1.9 and dismissing  $\Delta v^2$  as small, we get

$$\Delta y - \frac{c \cdot \Delta v}{g} = 0 \quad (1.10)$$

Equation 1.10 can be rearranged to

$$\frac{g}{c} = \frac{\Delta v}{\Delta y} \quad (1.11)$$

The right-hand sides of both equations 1.7 and 1.11 are identical, so we equate the left-hand sides of these two equations which yields

$$\frac{c}{y} = \frac{g}{c} \quad (1.12)$$

Finally, solving for  $c$  in equation 1.12 gives

$$c = \sqrt{gy} \quad (1.13)$$

Thus, the velocity at which a shallow wave propagates in a rectangular channel is given by equation 1.13. The ratio of the bulk velocity of the water,  $v$ , to this wave velocity is known as the Froude number,  $F_r$

$$F_r = \frac{v}{\sqrt{gy}} \quad (1.14)$$

The magnitude of the Froude number relative to unity has deep implications for open channel flow as is discussed thoroughly in the coming chapters of this text.

## 1.4 CLASSES OF PROBLEMS

Flow in open channels can vary or remain constant in both space and time. Examination of flow from this perspective provides a natural classification scheme for differentiating between the kinds of problems that can be considered.

A problem in which the flow is not changing as a function of time is said to be *steady state*. The overwhelming majority of problems considered in this book fall into this class. When flow is changing as a function of time we might refer to it as *unsteady* or *transient*. Transient conditions are considered occasionally throughout this book—especially in Chapter 2, primarily in the context of chokes where energy conditions do not support the discharge as it originally encounters an obstacle in the channel.

*Uniform* flow refers to the condition of flow not changing as a function of space or position along the channel. Uniform flow will be the dominant condition considered in the early chapters of this text through the presentation of the concept of normal depth in Chapter 4. However, the early part of this text repeatedly turns to a fixed set of channel obstacles (e.g., gates, steps, and constrictions) that represent discrete elements that tend to disrupt uniform flow conditions. Hydraulic jumps, first introduced in Chapter 3, serve as an additional example of non-uniform flow. Non-uniform flow becomes the primary focus of discussion in Chapters 5 and 6 as we examine gradually varied flow both qualitatively and quantitatively, respectively.

A special note on the myriad animations presented in the text and provided as electronic material to accompany this text is merited. The provided animations illustrate “movement,” but this movement does not generally correspond to a transient behavior. Instead, most of these animations show the continuum of steady-state solutions to a set of similar problems in which one input is allowed to vary. This varying input is generally not something that varies with time such as channel roughness, channel slope, or the size of a sluice gate opening. Thus, a transient behavior is not being illustrated. Rather, what is being illustrated is how the behavior of the overall channel system varies along a continuum as a function of that varying input.

## 1.5 THE NEED FOR CRITICAL THINKING

Calculators, computers, software, and the ever-increasing speed and availability of tools to perform engineering analyses can create the illusion of accuracy and rigor when quite the opposite is true. These tools have enormous value, but the greatest asset an engineer brings to bear on a problem is critical thought. Critical thought requires the engineer to be perpetually asking such questions as:

- Roughly what magnitude answer do I expect to this problem?
- Can I think of limiting cases or extremes of this problem whose outcomes are known to me?
- Are the underlying assumptions to this problem consistent with the solution approach? Are the underlying assumptions consistent with one another?
- What is the sensitivity of my answer to the specific inputs I have used?
- Does my final answer convey uncertainty appropriately given the uncertainty in the inputs that have supported the solution?

The engineer who faithfully asks these questions during and after an analysis will find such questions serve as an internal compass, pointing toward the correct solution and raising warning flags when a flawed solution is at hand.

We expand on the items enumerated above as a series of critical thinking “Rules”:

- *Rule 1: Have an expectation of the answer:* I am too young to have used a slide rule. Calculators were commonplace long before I began my university studies. A senior colleague of mine is fond of saying that one of the greatest values of using a slide rule was that it forced one to estimate the order of magnitude of the answer. If the expectation is that the answer should be, for instance, on the order of 1 meter, arriving at a final answer of 1 centimeter (or 1 kilometer) would be troubling and suggest that an error may have been made somewhere along the way. With a calculator, an answer of 1 or 0.01 or 1000 may be unconsciously accepted a bit more readily because of the speed of the device and the lack of going through the exercise of anticipating the answer. With a computer the impression of authority of the device might further limit the engineer’s tendency to question the result. Critical thought prompts the engineer to question the result, perhaps returning to some intermediate calculations that might have been faulty.

- *Rule 2: Does the answer “smell” right?* The phrasing of this rule is obviously a bit tongue-in-cheek. An answer “smells” wrong if some element of it is clearly inconsistent with the information provided in posing the problem. For instance, consider a problem that is seeking a discharge as part of the solution. The provided information might include several velocities and a stream cross-section. Assuming reasonable depths, a cross-sectional area can be determined which can be multiplied by the velocities to determine one or more “back-of-the-envelope” discharges. If the solution obtained is suggestive of a discharge that corresponds to a slight fraction of, or an overwhelming multiplier of, the back-of-the-envelope discharges, this could suggest trouble. The reader has to assess the quantitative meaning of “slight fraction” or “overwhelming multiplier” as used here, but these terms are suggestive of orders of magnitude. Thus, Rule 2 follows as a corollary of Rule 1.
- *Rule 3: Explore the sensitivity of the answer to inputs:* The majority of the provided examples and problems posed in this text force the calculation of the state of a system under specific, well-defined conditions. The clichéd expression “textbook example” generally refers to a classic, straightforward problem with an equally straightforward solution. Real life is often not so straightforward. Quantities such as the slope of the channel or the size of a cross-section may not be known precisely but rather they may vary over some range. When quantities are known, there is nonetheless uncertainty in their measurement. The sum of all this is that the textbook example may have value in being studied, but it does not begin to address natural variability or uncertainty. Sensitivity analysis is a valuable tool because it allows the reader/engineer to consider the real-world fuzziness of inputs and to explore the possible range of influence of this fuzziness on the solution. Sensitivity analysis may show that the solution undergoes no appreciable change over a reasonable range of, say, Input 1, but that a small change in Input 2 produces profound changes in the solution. Of particular note is the potential presence of threshold behavior. This behavior is perhaps the most dramatic example of a profound sensitivity. Sensitivity analysis ultimately provides the reader a level of confidence in the solution. Where strong sensitivity is identified, the reader/engineer will naturally place enhanced effort at understanding and measuring the relevant inputs so as to maximize both the accuracy and precision of the outputs to a solution.

- **Rule 4: Be vigilant in the use of significant figures:** On the topic of precision, significant figures demand a special form of critical thinking to be called upon when presenting final answers to an analysis. I have found that students can be deeply invested in reporting an answer to three, four, and five or more significant figures. That one of the givens in their analysis was only known to one or two significant figures is easily overlooked, especially when the calculator gives an answer with seven or eight digits of precision. Critical thought allows the engineer to use significant figures to accurately convey the answer and also indicate, through degree of precision used, the degree of belief or uncertainty in that answer. This text will endeavor to obey such rules as well, straying slightly for purposes of clarity of calculation when necessary. The reader is strongly encouraged to obey the rules germane to significant figures when solving problems posed by this text and elsewhere.

## Reference

Henderson, F.M. (1966). *Open Channel Flow*, Macmillan, New York, NY.

## Problems

- 1.1. What slope would lead to a 1% difference between depth in the vertical plane rather than depth measured perpendicular to the channel bottom? Compare this slope to the observation that a channel slope of  $S_0 = 0.01 \text{ m/m}$  is generally considered quite steep for open channel flow.
- 1.2. Using Bernoulli's equation, write the energy balance in general terms for flow in an open channel from location 1 to 2 where  $h_L$  is the head loss between these two locations. Simplify the equation by taking the perspective of a point on the water surface at both locations. Note: your solution should show that the pressure term from Bernoulli's equation is not relevant for open channel flow.
- 1.3. Parts (a), (b), and (c) require simple multiplication/division and/or addition/subtraction to solve. The reader is cautioned to pay special attention to significant digits when reporting the final answer.
  - a. If the density of water is  $1000 \text{ kg/m}^3$  and gravitational acceleration is  $9.81 \text{ m/s}^2$ , what is the unit weight of water?

- b. If the density of water is  $1.0 \times 10^3 \text{ kg/m}^3$  and gravitational acceleration is  $9.81 \text{ m/s}^2$ , what is the unit weight of water?
- c. The cross-sectional area of a channel is broken into three separate subareas with the following sizes:  $1.3 \text{ m}^2$ ,  $0.92 \text{ m}^2$ , and  $15 \text{ m}^2$ . What is the total cross-sectional area of the channel?
- 1.4. The mean or bulk velocity of flow in a stream is observed to be  $1.1 \text{ m/s}$ . A rock tossed into this same flow sets up ripples that radiate outward in all directions. It is noted that the ripples propagating directly upstream travel at a velocity of  $0.67 \text{ m/s}$  in the opposite direction to the direction of the flowing stream.
- What is the Froude number for this flow?
  - Estimate the depth of flow in this stream.
- 1.5. In the final chapter of this book we study sediment transport. In a particular stream, it is found that the sediment transport rate can be approximated as:

$$Q_s = c(\tau_0 - \tau^*)^p$$

where  $c$ ,  $p$ , and  $\tau^*$  are positive constants.

- Write an analytical expression for the sensitivity,  $dQ_s/d\tau_0$ .
- Let  $c = 1$ ,  $p = 2.2$ , and  $\tau^*$  be 1.4.
  - Plot  $dQ_s/d\tau_0$  for  $\tau_0 \geq 1.4$ .
  - Determine the value of the sensitivity at  $\tau_0 = 1.5$  and  $\tau_0 = 1.7$ .
- Briefly discuss how “Rule 3” as presented in Section 1.5 relates to your findings in Part (b) of this problem.



## Chapter 2

# Energy

## CHAPTER OBJECTIVES

1. Define specific energy and understand how it varies as a function of depth, velocity, and discharge.
2. Introduce concept of alternate depth.
3. Define the Froude number and derive conditions of critical flow.
4. Introduce classic flow problems: the gate, the step, and the constriction.
5. Introduce concepts of flow accessibility, chokes, and flow transients.
6. Identify conditions along the direction of channel flow that may cause critical flow conditions.
7. Examine specific energy in non-rectangular channels.
  - a. Quantify alternate depths in non-rectangular channels.
  - b. Quantify critical depth and energy in non-rectangular channels.

## 2.1 SPECIFIC ENERGY

As learned in fluid mechanics, the energy possessed by a flow of water is quantified by Bernoulli's equation:

$$H = \frac{p}{\gamma} + \frac{v^2}{2g} + z \quad (2.1)$$

where  $H$  is total head (in L),  $p$  is pressure (in  $\text{FL}^{-2}$ ),  $v$  is velocity (in  $\text{LT}^{-1}$ ),  $z$  is the elevation of the flow above some datum (in L),  $\gamma$  is the unit weight

of water (in  $\text{FL}^{-3}$ ), and  $g$  is gravitational acceleration (in  $\text{LT}^{-2}$ ). The utility of Bernoulli's equation is that it can be applied at two locations in a system and used to quantify the head difference between those points.

Bernoulli's equation is applied to open channel flow at two locations, and gives:

$$\frac{p_1}{\gamma} + \frac{v_1^2}{2g} + z_1 = \frac{p_2}{\gamma} + \frac{v_2^2}{2g} + z_2 + h_L \quad (2.2)$$

where the subscripts 1 and 2 indicate locations 1 and 2, and  $h_L$  is the head loss between the two locations (in L). As the term suggests, in open channel flow, the system is open to the surroundings, usually atmospheric pressure, which is assumed to be constant over the length scales typically considered in open channel flow problems. Thus,  $p_1 = p_2$  and the pressure term from Bernoulli's equation can be dropped. It should be emphasized that the pressure term is being dropped because it does not vary across the system, not because it is equal to zero. We thus define a new term, *specific energy*, which is simply the sum of the velocity head and elevation terms of Bernoulli's equation:

$$E = \frac{v^2}{2g} + z \quad (2.3)$$

where  $E$  is specific energy (in L).

Specific energy is perhaps the most important concept in open channel flow. Nevertheless, students often fail to recognize that they have seen this equation before when doing mechanics in physics. In physics we learn about the motion of a frictionless pendulum. We learn that the total energy possessed by the pendulum is constant and that as the pendulum swings, it is simply storing that energy in varying proportions between kinetic and potential energy. Kinetic energy ( $KE$ ) is

$$KE = \frac{mv^2}{2} \quad (2.4)$$

where  $m$  is the mass of the pendulum, and  $v$  is the velocity of the pendulum. Recall that kinetic energy of a pendulum is greatest when the pendulum is at the bottom of its swing and moving at its greatest speed. Potential energy ( $PE$ ) is

$$PE = mgh \quad (2.5)$$

where  $h$  is the height of the pendulum mass above some datum. Recall that the potential energy of a pendulum is greatest when the pendulum is at the top of its swing and has an instantaneous velocity of zero. The total energy ( $TE$ ) held by the pendulum is simply the sum of equations 2.4 and 2.5:

$$TE = \frac{mv^2}{2} + mgh = c \quad (2.6)$$

where  $c$  is a constant (assuming no friction), so the moving pendulum simply swings back and forth, forever trading  $KE$  for  $PE$  and vice versa such that the gains in energy in one form come at an equal loss of energy in the other form.

If we divide equation 2.6 by  $mg$ , we get:

$$\frac{TE}{mg} = \frac{v^2}{2g} + h \quad (2.7)$$

If we replace  $h$  in equation 2.7 with  $z$  (both are in units of length), we find that the right-hand side of equation 2.7 is the same as our definition of specific energy. This derivation is provided in an effort to help the student draw a quick understanding and level of comfort with the concept of specific energy.

We have defined specific energy in equation 2.3, but we have been silent on two questions: (1) Where is the datum of the system? And, (2) What about energy loss? With regard to the first question, the channel (for now) is horizontal and its bottom thus becomes convenient to use as the datum of our system as shown in Figure 2.1. The term  $z$  in the specific energy equation can thus be more clearly written as the depth of flow,  $y$ . Equation 2.3 (Bakhmeteff 1932) becomes:

$$E = \frac{v^2}{2g} + y \quad (2.8)$$

Concerning energy loss, it is a thermodynamic imperative, as suggested by the  $h_L$  term in equation 2.2, that energy be lost as water flows from location 1 to location 2. For now, however, we ask the reader to suspend disbelief and accept that energy is conserved in our idealized system. We will relax this idealization in the coming chapters.

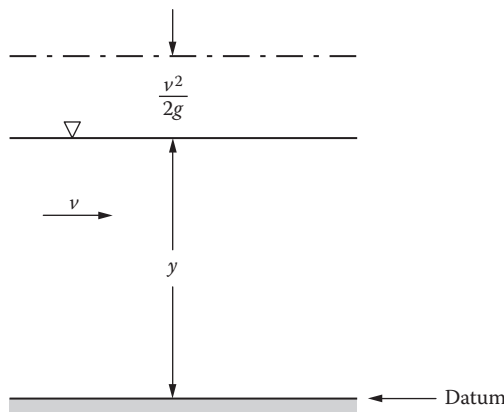


**FIGURE 2.1** A typical open channel flowing at depth,  $y$ , with velocity,  $v$ . The channel bottom shows the datum of the system.

## 2.2 THE E-y DIAGRAM

Let us first introduce a new quantity,  $q$  (in  $L^2/T$ ), called the unit discharge or specific discharge. The unit discharge is defined by

$$q = \frac{Q}{w} \quad (2.9)$$

where  $w$  is the width of the rectangular channel which is carrying the discharge,  $Q$ . The reader should be sure to note that  $q$  can only be determined under conditions where the channel shape is rectangular. If the channel is non-rectangular,  $q$  cannot be determined. This book will frequently use examples with rectangular channels because of the analytical simplifications this channel shape often provides. The reader, however, is cautioned to remain mindful to discriminate between equations that apply to rectangular channels only and equations that are broadly applicable to all channel shapes.

In fluid mechanics, before we learned Bernoulli's equation we likely learned the continuity equation:

$$Q = A \cdot v \quad (2.10)$$

where  $Q$  is the discharge (in  $L^3T^{-1}$ ),  $A$  is cross-sectional area (in  $L^2$ ), and  $v$  is velocity. In a rectangular channel we can focus on unit discharge with the continuity equation becoming

$$q = y \cdot v \quad (2.11)$$

Note that for a channel carrying a fixed unit discharge,  $q$ , this discharge can be reached through an infinite number of pairings of  $y$  and  $v$ . The pairing may be small  $y$  and large  $v$  or large  $y$  and small  $v$ —either pairing can produce the same unit discharge. But does specific energy vary across these pairings? And, if so, what does this variation look like?

Consider a rectangular channel carrying unit discharge,  $q$ . From equation 2.11 we observe that  $q/y = v$  and thus the specific energy equation can be rewritten as:

$$E = \frac{q^2}{2gy^2} + y \quad (2.12)$$

This formulation of the specific energy equation is handy because it expresses  $E$  solely as a function of depth,  $y$ . All other terms are constants. The relationship between  $E$  and  $y$  can now be easily explored by choosing a value for the unit discharge, say  $q = 3 \text{ m}^2/\text{s}$ , and simply varying  $y$  from a small depth to a large depth. The result is the  $E$ - $y$  diagram shown in Figure 2.2. There are several things to note in this diagram:

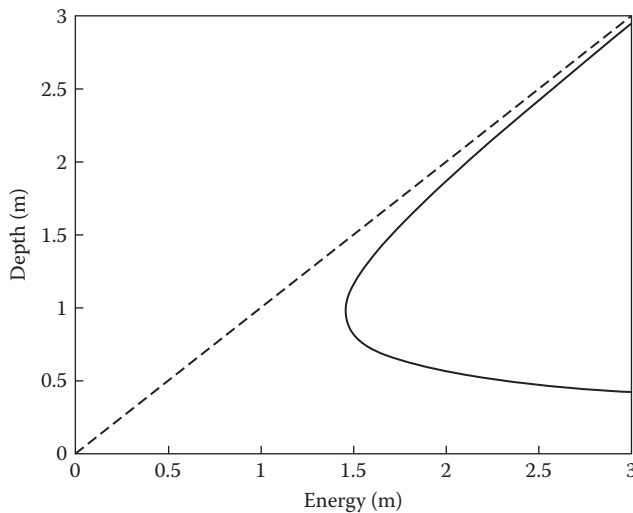


**FIGURE 2.2**  $E$ - $y$  diagram for  $q = 3 \text{ m}^2/\text{s}$ . The dashed line shows the  $E = y$  asymptote.

**Observation 1.** The traditional convention of plotting the independent variable on the horizontal axis and the dependent variable on the vertical axis is flipped around. This is because the depth of flow,  $y$ , is inherently a vertical quantity, and so it is naturally visualized on the vertical axis presented here. This convention will be followed throughout this book.

**Observation 2.** It should be clear to the reader from examination of Figure 2.2 and/or equation 2.8, that for very large  $y$ , velocity becomes negligible and  $E \approx y$ . The asymptote  $E = y$  in Figure 2.2 is drawn to reinforce this observation.

**Observation 3.** Finally, the shape of the  $E$ - $y$  relationship is striking in that there is clearly a minimum value of  $E$  indicated by the figure. The figure shows us that for the unit discharge illustrated, no value of  $E$  less than this minimum value (approximately 1.5 meters) can be observed, regardless of the depth of flow. Additionally, for any  $E$  value greater than this minimum, there are actually two depths that produce the same energy,  $E$ .

We explore the minimum energy value in Section 2.3, and the two depths with the same energy in Section 2.5, but let us briefly examine how the  $E$ - $y$  relationship varies as  $q$  varies. Focusing on equation 2.12, we see that if depth,  $y$ , is kept constant,  $E$  will increase as  $q$  increases. In other words, we expect the  $E$ - $y$  curve in Figure 2.2 to shift to the right, to higher energy levels, as  $q$  increases. Figure 2.3 confirms this, showing a family of  $E$ - $y$  curves that shift to the right as  $q$  increases from 2 to 5  $\text{m}^2/\text{s}$ . A few observations can be drawn from Figure 2.3:

**Observation 4.** The  $E = y$  asymptote applies to any value of  $q$  we choose.

**Observation 5.** The dashed line drawn through the minimum energy location of each  $q$  curve has an apparent slope of  $y = 2/3E$ . We will return to this observation in the next section.

## 2.3 CRITICAL FLOW

Let us analytically determine the value of the minimum energy and the depth corresponding to this minimum energy. This is accomplished by taking the derivative of the specific energy equation with respect to depth,  $y$ , and setting the derivative to zero:

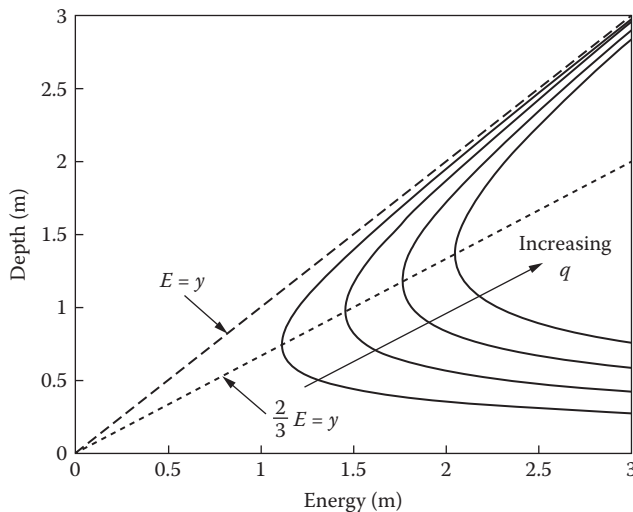


**FIGURE 2.3** A family of  $E$ - $y$  curves for  $q = \{2, 3, 4, 5\} \text{ m}^2/\text{s}$ . Note that the dashed line for  $\frac{2}{3}E = y$  crosses each curve at its minimum energy value.

$$0 = \frac{dE}{dy} = \frac{d}{dy} \left( \frac{q^2}{2gy_c^2} + y_c \right)$$

$$0 = -2 \cdot \left( \frac{q^2}{2gy_c^3} \right) + 1$$

$$\frac{q^2}{gy_c^3} = 1$$

$$\therefore y_c = \left( \frac{q^2}{g} \right)^{1/3} \quad (2.13)$$

where we use the term *critical depth*,  $y_c$ , to indicate the depth at which energy is minimized for a given unit discharge. The critical energy associated with critical depth is readily calculated by substituting the result from equation 2.13 above into equation 2.12:

$$E_c = \frac{q^2}{2gy_c^2} + y_c = \left( \frac{1}{2y_c^2} \right) \cdot \left( \frac{q^2}{g} \right) + y_c = \left( \frac{1}{2y_c^2} \right) \cdot y_c^3 + y_c = \frac{y_c}{2} + y_c = \frac{3}{2}y_c \quad (2.14)$$

Notice that equation 2.14 can be rearranged to get:

$$y_c = \frac{2}{3} E_c \quad (2.15)$$

This result shows why the dashed line in Figure 2.3 passes through the minima of each of the curves corresponding to a different specific discharge. Whether we focus on equation 2.14 or 2.15, the physical interpretation is the same:

**Observation 6.** At critical conditions in a rectangular channel for a given specific discharge, the energy is at a minimum value and is equal to 1.5 times the critical depth.

Another way to examine critical conditions is to hold energy at a fixed value,  $E^*$ , and examine how specific discharge varies with depth of flow. Analytically,

$$E^* = \frac{q^2}{2gy^2} + y \quad (2.16)$$

For a given value of  $E^*$ , we can vary  $y$  from just greater than zero to a maximum of  $E^*$  and solve for  $q$  (see Problem 2.2). Logically the specific discharge,  $q$ , reaches some maximum value at a depth somewhere between 0 and  $E^*$ . This relationship is shown in Figure 2.4.

The precise location of the maximum can be calculated by rearranging equation 2.16, and differentiating with respect to depth we get

$$\frac{d}{dy} [(2gy^2)(E^* - y)] = \frac{d}{dy}(q^2)$$

$$\frac{d}{dy} [(2gy^2E^* - 2gy^3)] = \frac{d}{dy}(q^2)$$

$$4gyE^* - 6gy^2 = 2q \cdot \frac{dq}{dy}$$

At the maximum discharge we know that  $dq/dy = 0$ ; thus,

$$4gyE^* = 6gy^2$$

which simplifies to

$$E^* = \frac{3}{2}y \quad (2.17)$$

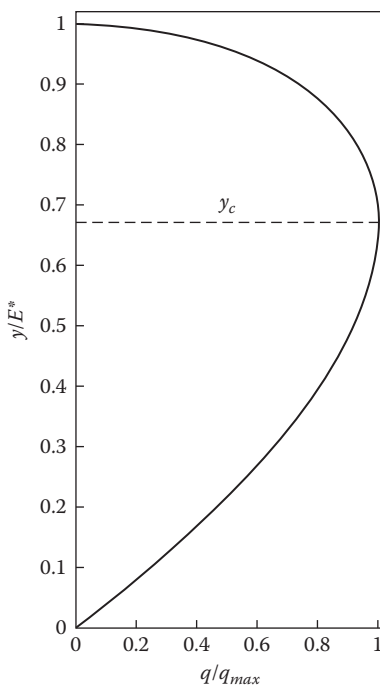


**FIGURE 2.4** Specific discharge ( $q$ ) normalized by the maximum specific discharge ( $q_{max}$ ) as it varies with depth ( $y$ ) normalized by a fixed specific energy,  $E^*$ .

This is the same relationship we arrived at for critical conditions in equation 2.14. To interpret, this means that:

**Observation 7.** For a fixed specific energy, specific discharge is maximized at critical conditions.

We will make great use of Observations 6 and 7 in problems that we consider later in this chapter.

## 2.4 THE FROUDE NUMBER

Returning to equation 2.12 and differentiating with respect to  $y$ , we get:

$$\frac{d}{dy}(E) = \frac{d}{dy} \left( y + \frac{q^2}{2gy^2} \right)$$

So,

$$\frac{dE}{dy} = 1 - \frac{q^2}{gy^3}$$

Substituting  $q^2 = v^2y^2$  and then simplifying,

$$\frac{dE}{dy} = 1 - \frac{v^2}{gy} \quad (2.18)$$

As derived and defined earlier in Chapter 1, we note that the Froude number,  $F_r$ , in a rectangular channel is:

$$F_r = \frac{v}{\sqrt{gy}} \quad (2.19)$$

Thus, equation 2.18 can be rewritten as:

$$\frac{dE}{dy} = 1 - F_r^2 \quad (2.20)$$

As we learned earlier, at critical conditions  $dE/dy = 0$  when  $y = y_c$ , so it follows from equation 2.20 that the Froude number equals 1 at critical flow conditions. Returning to Figures 2.2 or 2.3, it should be clear to the reader that for depths less than  $y_c$ ,  $v > \sqrt{gy}$ , and thus, from equation 2.19, the Froude number,  $F_r > 1$ . When the Froude number is greater than 1, the flow that results is referred to as *supercritical flow*. (By analogy, we trust that the reader has heard of supersonic flow which occurs when the Mach number is greater than 1.) Finally, when the flow depth is greater than  $y_c$ , we find that  $v < \sqrt{gy}$ , and the  $F_r < 1$ . This is referred to as *subcritical flow*. This is summarized in Table 2.1.

In addition to the discussion above, the Froude number has a very useful physical interpretation. In Chapter 1, we derived that the velocity at which a shallow wave propagates in a rectangular channel is  $\sqrt{gy}$ . The magnitude of the Froude number relative to 1 is thus of crucial importance with regard to the ability of the presence of downstream disturbances to propagate upstream.

What does this mean? Imagine an observer on the bank of a river with a rectangular cross-section and channel depth,  $y$ . The river can potentially flow at three different velocities  $v_1 < v_2 = v_c < v_3$ . The observer tosses a rock into the center of the river and observes the ripples that propagate outward from

**TABLE 2.1** Flow Conditions as Characterized by the Froude Number

Flow Type	Depth Relative to $y_c$	Froude Number	Qualitative Flow Description
Supercritical flow	$y < y_c$	$F_r > 1$	Fast and shallow
Critical flow	$y = y_c$	$F_r = 1$	Intermediate
Subcritical flow	$y > y_c$	$F_r < 1$	Slow and deep

the point of impact. The ripples will propagate outward from the point of impact at velocity  $\sqrt{gy}$ , so in a time  $t = t^*$ , they will have propagated outward a distance,  $d = \sqrt{gy} \cdot t^*$ . Meanwhile, the center of the ripple will have propagated downstream a distance  $v_x t^*$  where  $x$  is any of the three different velocities being considered. An illustration of this system is shown in Figure 2.5. For the system with the river flowing at  $v_1$  the ripples propagating directly upstream are able to travel faster than the center of the ripple is able to travel downstream. The net result is the stationary observer sees ripples propagating upstream from the location where the rock was originally thrown. In contrast, for the system with the river flowing at  $v_3$ , the ripples propagating directly upstream cannot travel as quickly as the center of the ripple is able to travel downstream. The net result is the observer sees all ripples propagating downstream, even those that are attempting to propagate upstream. For the system with the river flowing at  $v_2 = v_c$ , the distance covered by the ripples propagating

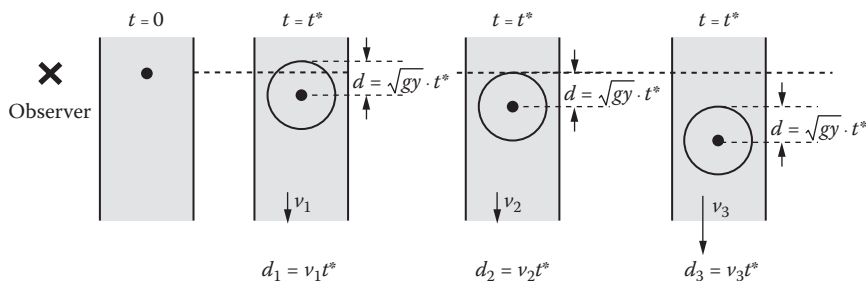


**FIGURE 2.5** Propagation of shallow waves (ripples) from an object thrown into subcritical, critical, and supercritical flows. At  $v_1$  (subcritical), some ripples propagate upstream. At  $v_2 = v_c$  (critical) the upstream edge of the ripple forms a standing wave at the location of observer. At  $v_3$  (supercritical) all ripples are washed downstream.

upstream is the same as the distance covered by the center of the ripple in the downstream direction. The observer sees a standing wave that corresponds to the edge of the ripple that is attempting to propagate directly upstream. Thus, for a system flowing subcritically (e.g.,  $v_1 < v_c$ ,  $F_r < 1$ ), "information" about downstream disturbances can travel upstream. Likewise, for a system flowing supercritically (e.g.,  $v_3 > v_c$ ,  $F_r > 1$ ), "information" about downstream disturbances cannot travel upstream.

## 2.5 ALTERNATE DEPTHS

A sluice gate is an obstruction that can be introduced into a flow that, under appropriate conditions, imposes subcritical flow upstream and supercritical flow downstream. The left side of Figure 2.6 shows a sluice gate introduced into a rectangular channel with depth  $y_1$  upstream and depth  $y_2$  downstream. We assume that the gate in Figure 2.6 has been in place long enough for the system to reach steady state. In this case, the continuity equation applies with:

$$q = y_1 \cdot v_1 = y_2 \cdot v_2 \quad (2.21)$$

In this book, unless otherwise indicated, all sluice gates we analyze will be handled as idealized devices that conserve energy. Thus, in Figure 2.6, the energy at location 1 is the same as the energy at location 2. Applying equation 2.12 to locations 1 and 2 we get

$$\frac{q^2}{2gy_1^2} + y_1 = \frac{q^2}{2gy_2^2} + y_2 \quad (2.22)$$

The right side of Figure 2.6 shows the  $E$ - $y$  relationship for the channel/sludge gate system depicted on the left. In Observation 3, it was stated for any energy greater than  $E_c$ , there are two depths that correspond to the same energy. Depths  $y_1$  and  $y_2$  are such a pair. Any pair of depths that correspond to the same specific energy for a given discharge are referred to as *alternate depths*. In this case,  $y_1$  corresponds to the subcritical alternate and  $y_2$  corresponds to the supercritical alternate.

In a rectangular channel with specific discharge,  $q$ , if one depth ( $y_1$ ) is known the other can be calculated with the following equation:

$$y_2 = \frac{2y_1}{-1 + \sqrt{1 + \frac{8gy_1^3}{q^2}}} = \frac{2y_1}{-1 + \sqrt{1 + \frac{8}{F_{r,1}^2}}} \quad (2.23)$$

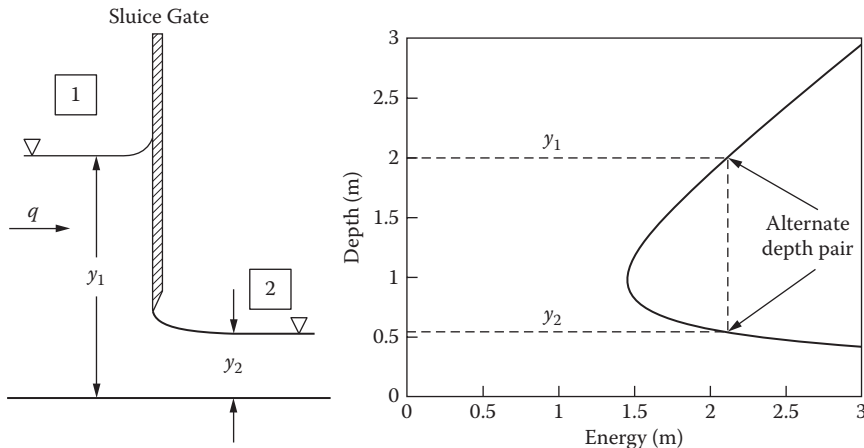


**FIGURE 2.6** A sluice gate introduced to a flow imposes subcritical flow upstream of the gate and supercritical flow downstream of the gate. Depths  $y_1$  and  $y_2$  make up an alternate depth pair.

The derivation of equation 2.23 is presented in Chapter 3.

### Example 2.1

The system shown in Figure 2.6 has a specific discharge of  $3 \text{ m}^2/\text{s}$ . The depth,  $y_1$ , upstream of the sluice gate is 2 meters. Determine:

- The upstream Froude number,  $F_{r,1}$ .
- The specific energy upstream of the sluice gate,  $E_1$ .
- The downstream depth,  $y_2$ .
- The downstream specific energy,  $E_2$ .
- The downstream Froude number,  $F_{r,2}$ .

#### Solution:

- Noting that  $q = v \cdot y_1$ , the upstream Froude number is:

$$F_{r,1} = \frac{v}{\sqrt{gy_1}} = \frac{q}{\sqrt{gy_1^3}} = \frac{3.0}{\sqrt{(9.81)(2.0)^3}} = 0.34$$

Notice that  $F_{r,1} < 1$ , so this confirms our expectation that the Froude number upstream of the gate is subcritical.

- b. Specific energy upstream of the sluice gate is:

$$E_1 = \frac{q^2}{2gy_1^2} + y_1 = \frac{(3.0)^2}{2(9.81)(2.0)^2} + 2.0 = 2.11 \text{ m}$$

Notice that this result is visually consistent with the right side of Figure 2.6, which indicates an energy slightly greater than 2 m.

- c. The downstream depth is (using equation 2.22 and the result from Example 2.1a):

$$y_2 = \frac{2(2.0)}{-1 + \sqrt{1 + \frac{8}{(0.34)^2}}} = 0.54 \text{ m}$$

Again, this is visually consistent with the right side of Figure 2.6.

- d. The downstream specific energy is:

$$E_2 = \frac{q^2}{2gy_2^2} + y_2 = \frac{(3.0)^2}{2(9.81)(0.54)^2} + 0.54 = 2.11 \text{ m}$$

Notice the  $E_1 = E_2$  as we would expect since  $y_1$  and  $y_2$  are alternate depths.

- e. The downstream Froude number is:

$$F_{r,2} = \frac{q}{\sqrt{gy_2^3}} = \frac{3.0}{\sqrt{(9.81)(0.54)^3}} = 2.41$$

$F_{r,2} > 1$ , confirming our expectation that the Froude number downstream of the gate is supercritical.

## 2.6 ENERGY CONSIDERATIONS ON UPWARD AND DOWNWARD STEPS

Another obstruction that a flow can encounter is a smooth, energy-conserving upward or downward step. Figure 2.7 shows a flow entering from the left and encountering an upward step of height  $\Delta z$ . For purposes of calculating specific energy, we have been using as our datum the horizontal bottom of the channel. With the addition of a vertical step we have set up essentially two datums

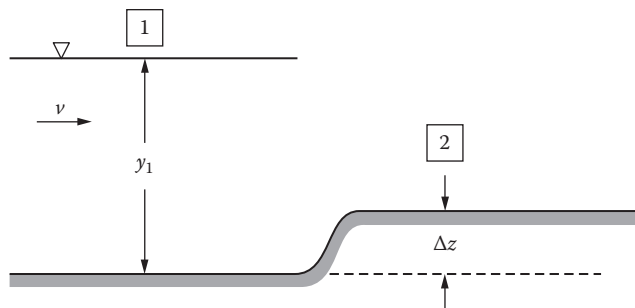


**FIGURE 2.7** Definition sketch for flow encountering an upward step of height,  $\Delta z$ .

that differ by height  $\Delta z$ . The important observation to make is that the relationship between specific energy with regard to these two datums is:

$$E_1 = E_2 + \Delta z \quad (2.24)$$

and thus,

$$\frac{q^2}{2gy_1^2} + y_1 = \frac{q^2}{2gy_2^2} + y_2 + \Delta z \quad (2.25)$$

We now investigate the implications of equations 2.24 and 2.25 through an example.

### Example 2.2

The system shown in Figure 2.7 has a specific discharge of  $3 \text{ m}^2/\text{s}$ . The depth,  $y_1$ , upstream of the step is 2 meters. The upward step height is 0.2 meters.

- Determine the downstream specific energy,  $E_2$ .
- Determine the downstream depth,  $y_2$ .
- Determine the absolute change in the water surface from location 1 to location 2.
- Determine the downstream Froude number,  $F_{r,2}$ .
- Interpret the results in the context of an  $E-y$  diagram.

**Solution:**

- a. The flow conditions upstream of the step are the same as in Example 2.1, where it was previously determined that  $E_1 = 2.11$  meters. Therefore,

$$E_2 = E_1 - \Delta z = 2.11 - 0.2 = 1.91 \text{ m}$$

Thus, a flow encountering an upward step can be thought of as paying an “energy tax” equal to the step height in order to continue flowing downstream.

- b. The downstream depth,  $y_2$ , is determined by trial and error using the specific energy equation:

$$E_2 = \frac{q^2}{2gy_2^2} + y_2 = \frac{(3.0)^2}{2(9.81)y_2^2} + y_2 = 1.91 \text{ m}$$

There are two positive solutions for  $y_2$ : 0.59 m and 1.76 m. These two depths are an alternate depth pair that both produce a specific energy of 1.91 m. As the conditions upstream of the step are subcritical, the solution will proceed with the subcritical value for  $y_2 = 1.76$  m, but there will be a need for further discussion of the rationale for this choice outside of this example problem.

- c. The absolute change in water depth,  $\Delta w_s$ , between locations 1 and 2 is determined from a quick examination of the solved system:

$$\Delta w_s = y_2 + \Delta z - y_1 = 1.76 + 0.2 - 2.0 = -0.04 \text{ m}$$

Thus, the additional presence of the step serves to actually *lower* the water surface slightly, by 0.04 m.

- d. The downstream Froude number,  $F_{r,2}$  is:

$$F_{r,2} = \frac{q}{\sqrt{gy_2^3}} = \frac{3.0}{\sqrt{(9.81)(1.76)^3}} = 0.41$$

Comparing the upstream (calculated in Example 2.1 as 0.34) and downstream Froude numbers shows that the Froude number remains subcritical but increases in the downstream direction. This indicates that the effect of the upward step is to drive the flow closer to critical conditions.

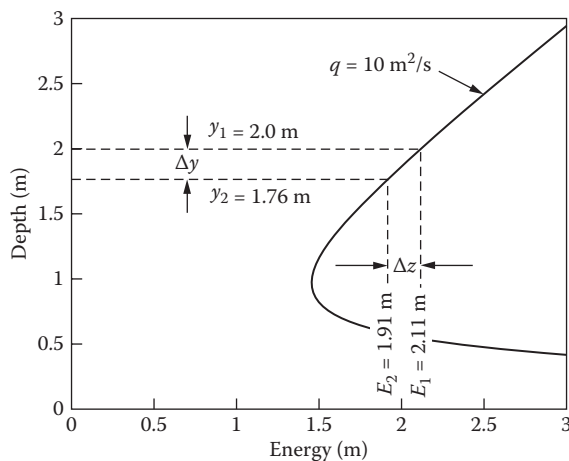


**FIGURE 2.8** *E-y* diagram showing solutions to Example 2.2.

- e. Figure 2.8 shows the *E-y* diagram that corresponds to Example 2.2. The “energy tax” alluded to in Example 2.2a corresponds physically to a horizontal shift from  $E_1$  to  $E_2$  equal to the height of the step.

Figure 2.9 shows a flow entering from the left and encountering a downward step of height  $\Delta z$ . A downward step has the effect of increasing the energy at the downstream location and can be thought of as an “energy gift” rather than the “energy tax” that an upward step represents. This will be illustrated in Example 2.3.

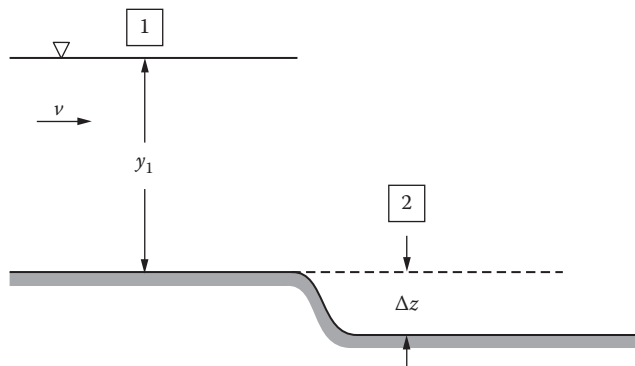


**FIGURE 2.9** Definition sketch for flow encountering a downward step of height,  $\Delta z$ .

***Example 2.3***

Consider a system with a specific discharge of  $3 \text{ m}^2/\text{s}$ . The depth,  $y_1$ , upstream of the step is 2 meters. The downward step height is 0.2 meters.

- Determine the downstream specific energy,  $E_2$ .
- Determine the downstream depth,  $y_2$ .
- Determine the absolute change in the water surface from location 1 to location 2.
- Determine the downstream Froude number,  $F_{r,2}$ .
- Contrast the results of this example with the results from Example 2.2.

***Solution:***

- The flow conditions upstream of the step are the same as in Example 2.1, where it was previously determined that  $E_1 = 2.11$  meters. Therefore,

$$E_2 = E_1 + \Delta z = 2.11 + 0.2 = 2.31 \text{ m}$$

- Thus, a flow encountering a downward step can be thought of as receiving an “energy gift” equal to the step height.
- The downstream depth,  $y_2$ , is determined by trial and error using the specific energy equation:

$$E_2 = \frac{q^2}{2gy_2^2} + y_2 = \frac{(3.0)^2}{2(9.81)y_2^2} + y_2 = 2.31 \text{ m}$$

There are two positive solutions for  $y_2$ : 0.50 m and 2.22 m. These two depths are an alternate depth pair that both produce a specific energy of 2.31 m. As in Example 2.2, the solution will proceed with the subcritical value for  $y_2 = 2.22$  m.

- The absolute change in water depth,  $\Delta w_s$ , between locations 1 and 2 is:

$$\Delta w_s = y_2 - \Delta z - y_1 = 2.22 - 0.2 - 2.0 = 0.02 \text{ m}$$

**TABLE 2.2** Summary and Contrast in Findings from Examples 2.2 and 2.3

Quantity	Example 2.2	Example 2.3
Step height, $\Delta z$	+0.2 m	-0.2 m
$E_1 - E_2$	+0.2 m	-0.2 m
$y_1$ relative to $y_2$	$y_1 > y_2$	$y_1 < y_2$
$\Delta w_s$	-0.04 m	+0.02 m
$F_{r,1}$ relative to $F_{r,2}$	$F_{r,1} < F_{r,2}$	$F_{r,1} > F_{r,2}$

Thus, the downward step results in a *higher* water surface by 0.02 m.

d. The downstream Froude number,  $F_{r,2}$  is:

$$F_{r,2} = \frac{q}{\sqrt{gy_2^3}} = \frac{3.0}{\sqrt{(9.81)(2.22)^3}} = 0.29$$

Comparing the upstream (calculated in Example 2.1 as 0.34) and downstream Froude numbers shows that the Froude number becomes more subcritical. That is, the downward step serves to drive the flow away from critical conditions.

e. Contrasting Example 2.3 with Example 2.2 shows, not surprisingly, that the effect of a subcritical flow encountering a downward step is generally opposite to that of the same flow encountering an upward step. Results are summarized in Table 2.2.

---

This section concludes with one more example. This case considers a supercritical upstream flow encountering an upward step.

### Example 2.4

Consider a system with a specific discharge of  $3 \text{ m}^2/\text{s}$ . The depth,  $y_1$ , upstream of the step is 0.54 meters. The upward step height is 0.2 meters.

- a. Determine the upstream Froude number,  $F_{r,1}$ .
- b. Determine the downstream specific energy,  $E_2$ .

- c. Determine the downstream depth,  $y_2$ .
- d. Determine the absolute change in the water surface from location 1 to location 2.
- e. Determine the downstream Froude number,  $F_{r,2}$ .
- f. Using an  $E$ - $y$  diagram, illustrate schematically the shift in flow conditions associated with Examples 2.2, 2.3, and 2.4.

**Solution:**

- a. The upstream Froude number was calculated in Example 2.1(e) as 2.41.
- b. The reader should recognize that the flow depth upstream of the step is the supercritical alternate to the upstream flow depth from Examples 2.1, 2.2, and 2.3. We therefore have the same upstream specific energy,  $E_1 = 2.11$  meters. As in Example 2.2,

$$E_2 = E_1 - \Delta z = 2.11 - 0.2 = 1.91 \text{ m}$$

- c. The downstream depth,  $y_2$ , is determined by trial and error using the specific energy equation:

$$E_2 = \frac{q^2}{2gy_2^2} + y_2 = \frac{(3.0)^2}{2(9.81)y_2^2} + y_2 = 1.91 \text{ m}$$

In Example 2.2, we determined two positive solutions for  $y_2$ : 0.59 m and 1.76 m. These two depths are an alternate depth pair that both produce a specific energy of 1.91 m. Now, because the conditions upstream of the step are supercritical, the solution will proceed with the supercritical value for  $y_2 = 0.59$  m.

- d. The absolute change in water depth,  $\Delta w_s$ , between locations 1 and 2 is:

$$\Delta y_2 + \Delta z - y_1 = 0.59 + 0.2 - 0.54 = 0.25 \text{ m}$$

Thus, the flow depth has increased and added to the step height, the downstream water surface is actually 0.25 meters *higher* than the upstream water surface.

e. The downstream Froude number,  $F_{r,2}$  is:

$$F_{r,2} = \frac{q}{\sqrt{gy_2^3}} = \frac{3.0}{\sqrt{(9.81)(0.59)^3}} = 2.11$$

Comparing the upstream (2.41) and downstream (2.11) Froude numbers shows that the Froude number remains supercritical but decreases in the downstream direction. This indicates that the effect of the upward step is to drive the flow closer to critical conditions just as was the case in Example 2.2 for subcritical flow conditions.

f. Figure 2.10 shows the  $E$ - $y$  diagram that summarizes the shifts along this curve as the steps were encountered. Notice that regardless of the upstream flow conditions, an upward step drives the flow closer to critical conditions and a downward step drives the flow away from critical conditions. Left as an exercise (see Problem 2.6) to the reader is the case of upstream supercritical conditions encountering a downward step.

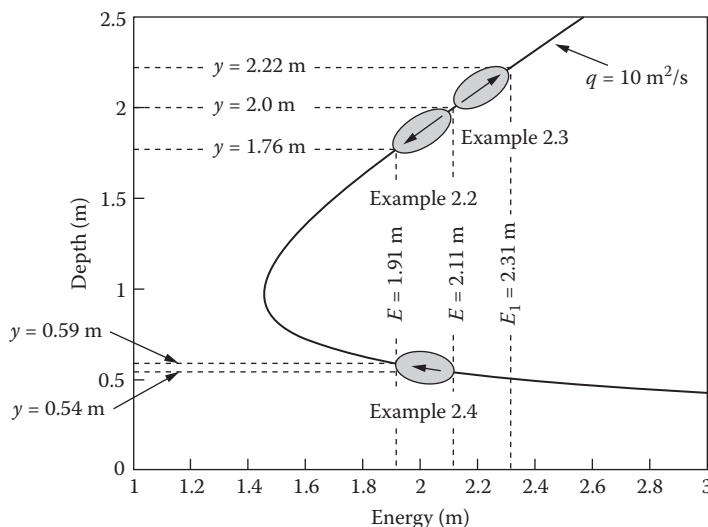


**FIGURE 2.10** Summary of energy shifts on  $E$ - $y$  diagram for Examples 2.2, 2.3, and 2.4.

## Animation: step.avi

Flow conditions:

$$Q = 100 \text{ ft}^3/\text{s}$$

Initial upstream depth is 2.8 ft

Channel is rectangular, width is 10 ft

Channel is frictionless

Apparent movement: step height increases from 0.00 to 1.77 ft

Still image of animation shown in Figure 2.11

This animation shows an upstream subcritical flow as it encounters a brief upward step. The top subplot shows a side view of the channel bottom (thick black line) and water surface (thinner black line). The bottom subplot shows the  $E$ - $y$  diagram that applies to the illustrated flow. As the animation evolves the top plot shows a growing step height and the water surface drawing down at the step. The bottom subplot shows the initial

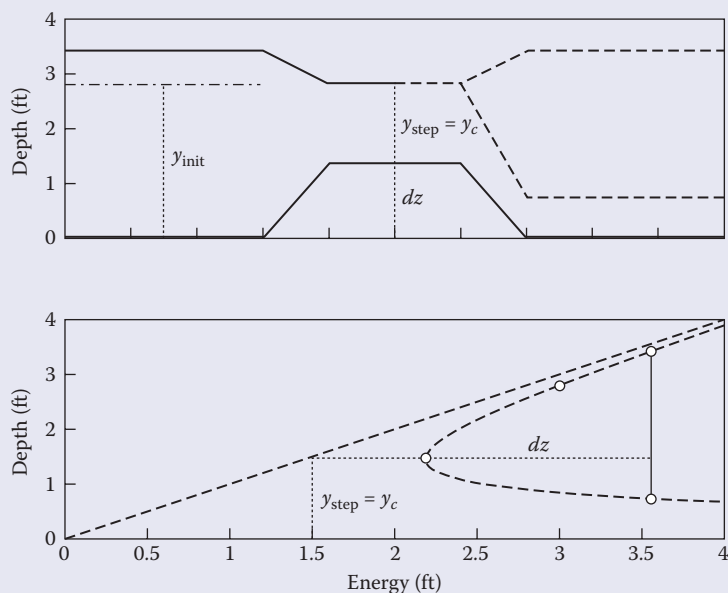


**FIGURE 2.11** Screen capture from step.avi animation. Capture shows a step height  $dz$  that is large enough to act as a choke. Upper subplot shows physical system. Lower subplot shows  $E$ - $y$  diagram.

energy, and the energy over the step that is reduced by the step height  $dz$ . When the step height is great enough that the initial upstream energy is insufficient to pass the entire discharge, a choke results. The animation shows the steady-state result of the flow backing up upstream of the step, and dashed lines in the water surface downstream of the step indicate that the downstream condition after the step may be either subcritical or supercritical. The initially specified depth (a subcritical depth) upstream of the step is shown as a dashed line once the step height is large enough to act as a choke.

## 2.7 ENERGY CONSIDERATIONS IN CONSTRICTIONS AND EXPANSIONS

The final obstruction to flow that we consider is the case of a smooth, energy-conserving constriction or expansion in channel width. Figure 2.12 shows a flow entering from the left in a rectangular channel of width,  $w_1$ , and encountering a constriction to width  $w_2$ . Since the flow is at equilibrium, the total discharge,  $Q$ , is a constant through locations 1 and 2; however, the specific discharge is not. In this case, we have  $q_1 = Q/w_1$  and  $q_2 = Q/w_2$ . Since  $w_1 > w_2$  we know that  $q_1 < q_2$ . Thus, two different “ $q$ -curves” on an  $E-y$  diagram relate to this constriction in the flow. The salient observation for flow entering such a constriction is that energy remains fixed while the flow transitions through a continuum of specific discharge values between  $q_1$  and  $q_2$ . On an  $E-y$  diagram, such a transition corresponds to a simple vertical,  $E$  remains constant, translation from the  $q$ -curve corresponding to  $q_1$  to the curve corresponding to  $q_2$ .

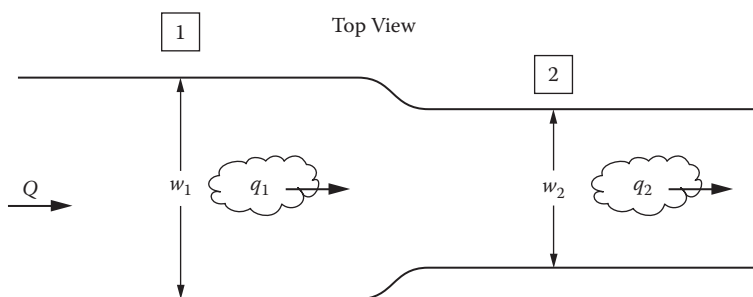


**FIGURE 2.12** Definition sketch for flow encountering a constriction in flow width.

**Example 2.5**

Consider a system with a discharge of  $9 \text{ m}^3/\text{s}$ . The channel is rectangular. The width at location 1 is  $w_1 = 4.5 \text{ m}$ . A constriction is encountered at location 2 downstream such that the width  $w_2 = 3 \text{ m}$ . The depth of flow  $y_2$  at downstream location 2 is 2 meters.

- Determine the specific discharges at locations 1 and 2.
- Determine the downstream specific energy,  $E_2$ .
- Determine the downstream Froude number,  $F_{r,2}$ .
- Determine the upstream specific energy,  $E_1$ .
- Determine the upstream depth,  $y_1$ .
- Determine the upstream Froude number,  $F_{r,1}$ .
- Determine the absolute change in the water surface from location 1 to location 2.
- Sketch the transition of the system from location 1 through the flow constriction to location 2 on an  $E$ -y diagram.

**Solution:**

- The specific discharges are:

$$q_1 = \frac{Q}{w_1} = \frac{9.0}{4.5} = 2.0 \frac{\text{m}^2}{\text{s}}, \quad q_2 = \frac{Q}{w_2} = \frac{9.0}{3.0} = 3.0 \frac{\text{m}^2}{\text{s}}$$

The reader should thus recognize that the conditions at location 2 are as they have been specified in many of the previous examples (at location 1).

- First calculated in Example 2.1(b), the specific energy,  $E_2$ , is the same as the specific energy  $E_1$  from that earlier example. Namely,  $E_2 = 2.11 \text{ m}$ .
- By the same argument as above, the Froude number,  $F_{r,2}$ , is the same as the Froude number  $F_{r,1}$  from Example 2.1(a).  $F_{r,2} = 0.34$ .
- The constriction is energy conserving, thus,

$$E_1 = E_2 = 2.11$$

- The flow depth upstream,  $y_1$ , must satisfy the specific energy equation for the energy calculated above and the specific discharge calculated in Example 2.5(a):

$$E_1 = \frac{q_1^2}{2gy_1^2} + y_1 = \frac{(2.0)^2}{2(9.81)y_1^2} + y_1$$

By trial and error, two positive solutions for  $y_1$  exist: 0.34 m and 2.06 m. These two depths are an alternate depth pair that both produce a specific energy of 2.11 m. By the same reasoning as

earlier, the solution will proceed with the subcritical value for  $y_2 = 2.06 \text{ m}$ .

- f. The upstream Froude number,  $F_{r1}$  is:

$$F_{r1} = \frac{q_1}{\sqrt{gy_1^3}} = \frac{2.0}{\sqrt{(9.81)(2.06)^3}} = 0.22$$

Thus the constriction, as the upward step in Example 2.2, serves to drive the flow from a Froude number of 0.22 to a value of 0.34. In other words, the constriction drives the flow toward critical conditions.

- g. The absolute change in water depth,  $\Delta w_s$ , between locations 1 and 2 is:

$$\Delta w_s = y_2 - y_1 = 2.0 - 2.06 = -0.06 \text{ m}$$

Thus the flow depth has decreased 0.06 m within the constriction.

- h. Figure 2.13 shows an  $E$ - $y$  diagram with  $q$ -curves corresponding to  $q_1 = 2 \text{ m}^2/\text{s}$  (to the left) and  $q_2 = 3 \text{ m}^2/\text{s}$  (to the right). The constriction manifests itself as a vertical transition from the  $q_1 = 2 \text{ m}^2/\text{s}$  curve at an energy of 2.11 m and depth of 2.06 m down to the  $q_2 = 3 \text{ m}^2/\text{s}$  curve at the same energy 2.11 m and a depth of 2.0 m.

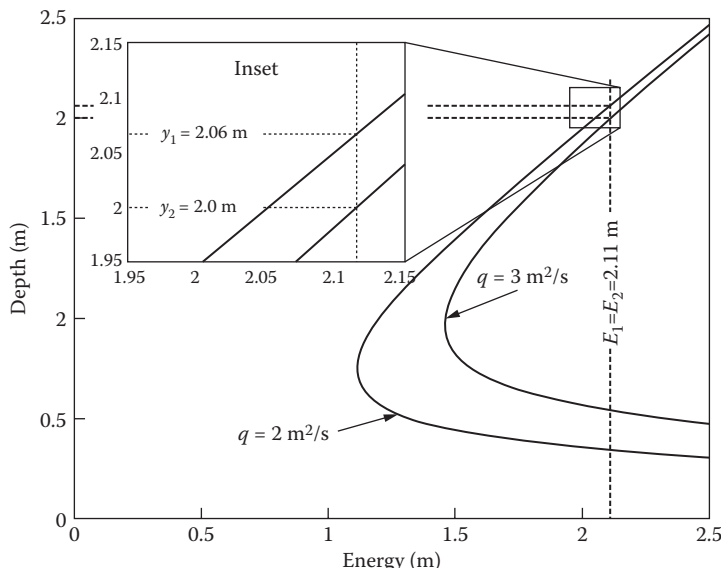


**FIGURE 2.13**  $E$ - $y$  diagram showing solutions to Example 2.5.

Similar to the earlier examination of upward and downward steps encountered by subcritical and supercritical flows, it would be possible to explore several more examples of, for instance, a subcritical flow encountering an expansion, and a supercritical flow encountering both a constriction or expansion. These problems are instead left as exercises (see Problems 2.7–2.9) to the reader.

### Animation: constriction.avi

Flow conditions:

$$Q = 100 \text{ ft}^3/\text{s}$$

Initial depth is 2.8 ft

Channel is rectangular

Channel is frictionless

Apparent movement: channel width decreases from 10 ft to 5 ft

Still image of animation shown in Figure 2.14

This animation shows an upstream subcritical flow as it encounters a constriction in channel width. The top subplot shows a top view of the flume and the growing constriction. The middle subplot shows a side view of the channel and water surface. The bottom row of the figure is divided into left and right subplots. The left bottom subplot is an overall  $E-y$  diagram showing the initial  $q$  curve ( $q = 10 \text{ ft}^2/\text{s}$ , to the left) as well as the  $q$  curve that corresponds to flow in the constriction (curve to the right). A dashed box in this subplot shows the enlarged area in the right bottom subplot. The right bottom subplot shows the  $E-y$  diagram focused on the dashed box in the left bottom subplot. This is the region of the figure that is most closely engaged in the evolution being shown. When the constriction is severe enough that the initial upstream energy is insufficient to pass the entire discharge, a choke results. The animation shows the steady-state result of the flow backing up upstream of the constriction. The dashed lines in the water surface downstream of the constriction indicate that the downstream conditions after the constriction may be either subcritical or supercritical. Critical conditions exist within the constriction if the constriction is a choke. The right-most points on the  $q = 10 \text{ ft}^2/\text{s}$  diagrams indicate the alternate depth pairs that are possible downstream of the critical (choke) condition.

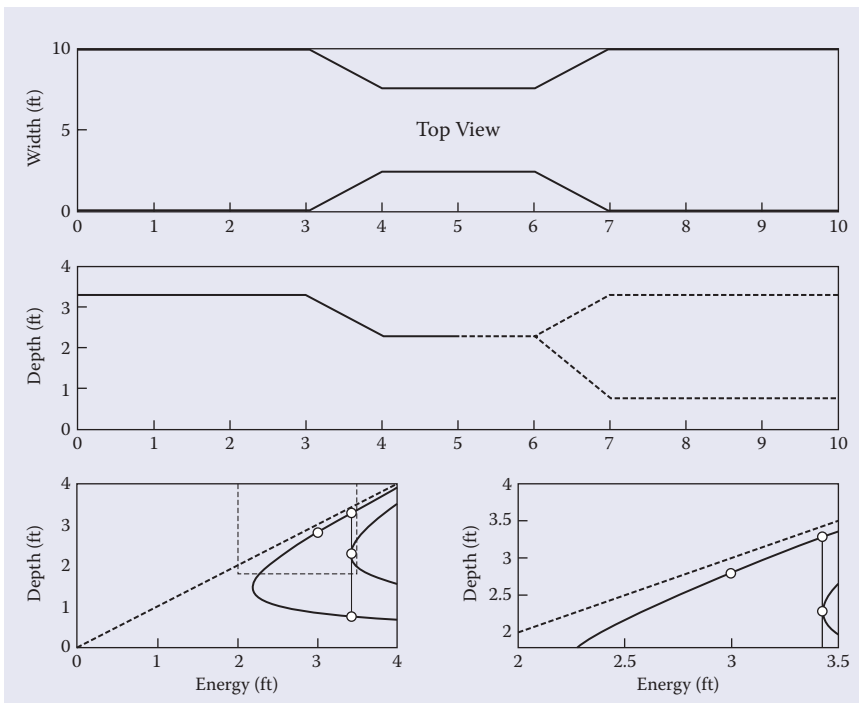


**FIGURE 2.14** Screen capture from constriction.avi animation. Capture shows a constriction in width (top subplot) that is severe enough to act as a choke. Middle subplot shows flow depth upstream of, within, and downstream of the constriction. Lower left subplot shows overall  $E$ - $y$  diagram, while lower right subplot shows enlargement of a portion of the  $E$ - $y$  diagram.

## 2.8 CHOKES, FLOW ACCESSIBILITY, CRITICAL FLOW, AND TRANSIENTS

In several of the previous examples (e.g., Examples 2.2, 2.4, and 2.5), it was calculated that the obstruction encountered by the flow had the effect of driving the Froude number closer to 1. In other words, the obstruction moved the flow conditions closer to critical conditions. Extending the thinking from Example 2.5, the reader should surmise that a downstream width smaller than the 3 m used in the example would be needed to force the flow to critical conditions. From equations 2.13 and 2.14 we can actually determine what width of channel will bring about critical flow. Recall that the

specific energy of the flow at location 1 in Example 2.5 is 2.11 m. Thus using equation 2.14,

$$E_1 = E_2 = E_c = \frac{3}{2}y_c = 2.11 \text{ m} \quad (2.26)$$

so,

$$y_c = \frac{2}{3}(2.11) = 1.41 \text{ m} \quad (2.27)$$

We can rearrange equation 2.13 to give  $q_c$  as a function of  $y_c$  and then solve for  $q_c$ :

$$q_c = \sqrt{gy_c^3} = \sqrt{(9.81)(1.41)^3} = 5.19 \frac{\text{m}^2}{\text{s}} \quad (2.28)$$

Finally, knowing  $q_c$  and total discharge,  $Q = 9 \text{ m}^3/\text{s}$ , we can rearrange equation 2.9 to solve for the critical width,  $w_c$ :

$$w_c = \frac{Q}{q_c} = \frac{9.0}{5.19} = 1.73 \text{ m} \quad (2.29)$$

Thus, returning to Example 2.5, if the width at location 2 is 1.73 m, then this is sufficient to bring the channel to critical flow conditions.

The following is a question that might naturally occur to the reader: What if the width at location 2 is smaller than  $w_c$ ? For instance, what if the width at location 2 were only 1.5 m? Using the specific discharge relationship already established,

$$q_{2,new} = \frac{9.0}{1.5} = 6.0 \frac{\text{m}^2}{\text{s}}$$

From earlier arguments, it is known that the minimum energy associated with this unit discharge occurs at critical conditions:

$$E_{min} = E_c = \frac{3}{2}y_c = \frac{3}{2}\left(\frac{q_{2,new}}{g}\right)^{1/3} = \frac{3}{2}\left(\frac{6.0^2}{9.81}\right)^{1/3} = 2.31 \text{ m} \quad (2.30)$$

So we have arrived at a fundamental impasse between the initial conditions, which provided an energy of 2.11 m and the minimum energy required to pass through a rectangular constriction 1.5 m wide, which is 2.31 m. The upstream flow, as specified, simply does not have enough energy to pass through the

constriction. This is an example of a *choke*. A choke occurs when a flow encounters an obstruction that requires more energy than the flow has. In such cases, there will be a period of transient conditions or unsteady flow during which some fraction of the flow backs up upstream of the obstruction. This accrual of water behind the obstruction will result in an increase in depth and, thus, an increase in specific energy. The transient conditions will cease when the depth has increased to the point that the specific energy upstream of the obstruction is equal to the minimum energy required to flow through the obstruction. As was shown earlier, this minimum energy is realized at critical flow conditions. Example 2.6 further explores this problem in quantitative fashion.

### **Example 2.6**

Returning to the system specified in Example 2.5. The total discharge remains unchanged as  $Q = 9.0 \text{ m}^3/\text{s}$ . Let the upstream depth be as calculated in Example 2.5(e),  $y_1 = 2.06 \text{ m}$ . A constriction is encountered at location 2 downstream such that the width  $w_2 = 1.5 \text{ m}$ .

- Determine the energy initially held by the flow at location 1.
- Determine the minimum energy required to flow through the constriction at location 2.
- Assuming the flow as initially specified instantaneously encounters the constriction at location 2, determine the initial discharge that passes through the constriction.
- Assuming the flow as initially specified instantaneously encounters the constriction at location 2, determine the initial rate of water storage immediately upstream of the constriction.
- Determine the depths and specific energy values at locations 1 and 2 when the system returns to steady state.

#### **Solution:**

- As was determined in Example 2.5 and repeated in the discussion in the text, the specific energy as initially specified in this problem is  $2.11 \text{ m}$ .
- At location 2, the new width of the channel is  $1.5 \text{ m}$ . Thus,  $q_{2,new} = 9.0/1.5 = 6.0 \text{ m}^2/\text{s}$ . Knowing that the minimum energy corresponds to critical conditions, equation 2.30 is repeated here:

$$E_{\min} = E_c = \frac{3}{2} y_c = \frac{3}{2} \left( \frac{(q_{2,new})^2}{g} \right)^{1/3} = \frac{3}{2} \left( \frac{(6.0)^2}{9.81} \right)^{1/3} = 2.31 \text{ m} \quad (2.30)$$

So the specific energy at location 1 is approximately 0.20 m smaller than the required energy to pass location 2. This means location 2 is a choke given the specified initial conditions.

- c. The initial discharge that passes location 2 is the maximum discharge that can be supported by a specific energy of 2.11 m. From Observation 7 presented earlier in this chapter, for a given specific energy, discharge is maximized at critical conditions. Thus,  $E_c = 2.11$  m. Our goal is to determine what  $q_c$  and  $Q_c$  correspond to this critical energy. Using equations 2.27 and 2.28,

$$y_{c,init} = \frac{2}{3}(2.11) = 1.41 \text{ m} \quad (2.27)$$

Equation 2.13 is rearranged to give  $q_c$  as a function of  $y_c$  and then solve for  $q_c$ :

$$q_{c,init} = \sqrt{gy_{c,init}^3} = \sqrt{(9.81)(1.41)^3} = 5.19 \frac{\text{m}^2}{\text{s}} \quad (2.28)$$

Since  $Q = q \cdot w$ ,

$$Q_{c,init} = (5.19)(1.5) = 7.79 \frac{\text{m}^3}{\text{s}}$$

- d. The initial rate of storage upstream of the constriction is the difference between the steady-state flow rate ( $Q_{ss} = 9 \text{ m}^3/\text{s}$ ) and the initial discharge ( $Q_{c,init} = 7.79 \text{ m}^3/\text{s}$ ) calculated immediately above:

$$\frac{\Delta S}{dt} = Q_{ss} - Q_{c,init} = 9.0 - 7.79 = 1.21 \frac{\text{m}^3}{\text{s}}$$

Note that this is the initial rate of storage at the very moment the choke is first encountered. Since this discharge is being stored, the depth will be backing up upstream of the constriction, resulting in increased specific energy upstream of the constriction. So the transient will be characterized by a diminishing storage rate as the specific energy deficit decreases from 0.20 m to 0 when the system returns to steady state.

- e. When the system returns to steady state, the discharge through the constriction in location 2 will be 9 m<sup>3</sup>/s. The system will only accrue the minimum energy to pass this discharge, so location 2 will still be at critical conditions. At location 2, this will

mean that  $q = 9/1.5 = 6 \text{ m}^2/\text{s}$ . The critical depth,  $y_{c,ss}$ , and specific energy,  $E_{c,ss}$ , associated with this specific discharge are:

$$y_{2,ss} = y_{c,ss} = \left( \frac{q_2^2}{g} \right)^{1/3} = \left( \frac{(6.0)^2}{9.81} \right)^{1/3} = 1.54 \text{ m}$$

$$E_{2,ss} = E_{c,ss} = \frac{3}{2} y_{c,ss} = \frac{3}{2}(1.54) = 2.31 \text{ m}$$

To determine the depth and specific energy upstream at location 1, we note that specific energy is conserved between locations 1 and 2 and recall that the width at the upstream location is 4.5 m, so  $q_1 = 2 \text{ m}^2/\text{s}$  and:

$$E_{1,ss} = E_{2,ss} = 2.31 \text{ m}$$

$$E_1 = \frac{q_1^2}{2gy_{1,ss}} + y_{1,ss} = \frac{(2.0)^2}{2(9.81)y_{1,ss}} + y_{1,ss} = 2.31$$

Solving this latter equation for  $y_{1,ss}$  and taking the subcritical root, we get  $y_{1,ss} = 2.27 \text{ m}$ . Compare this final, steady-state depth with the initial depth before the choke was resolved of  $y_{1,init} = 2.06 \text{ m}$ . Thus, the increase in upstream flow depth is about 0.21 m. This increase in depth is by virtue of the choke and the subsequent backup of discharge during the transient recovery and return to a steady-state discharge of 9  $\text{m}^3/\text{s}$ .

### Animation: step\_transient.avi

Flow conditions:

$$Q = 100 \text{ ft}^3/\text{s}$$

Initial depth is 2.8 ft

Channel is rectangular

Channel is frictionless

Depth-volume relationship is approximately:

$$V = 0.045d^3$$

with volume ( $V$ ) in  $\text{ft}^3 \times 10^6$  and depth ( $d$ ) in feet

Apparent movement: Step of height  $\Delta z = 2.0$  feet appears at  $t = 5$  hours  
 Still image of animation shown in Figure 2.15

Animation shows an upstream subcritical flow as it encounters an instantaneous step. The animation shows the transient backup of flow as the system adjusts to the step and returns to steady state. Subplots show growth of storage behind the step over time,  $Q$  versus  $t$ ; and the  $E-y$  diagram illustrates transient behavior.

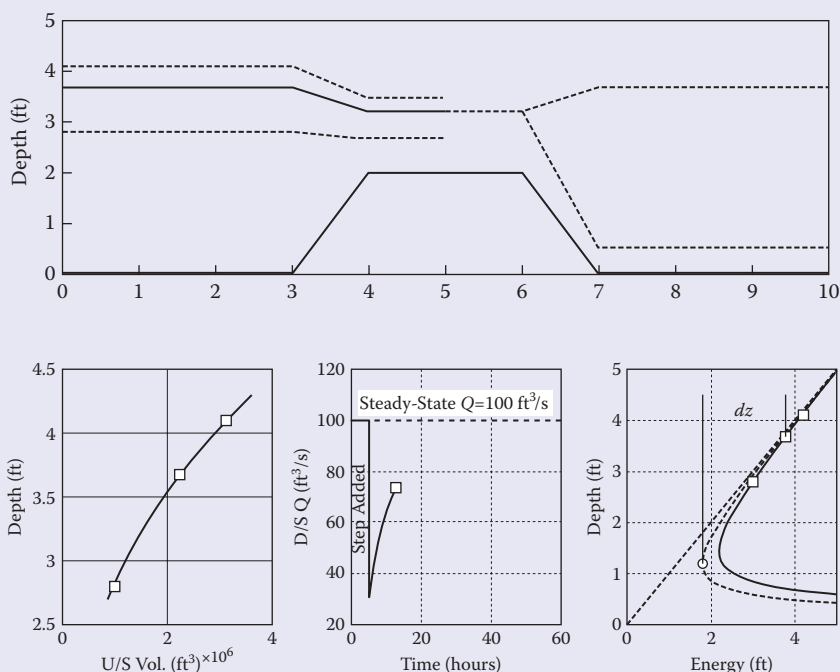


**FIGURE 2.15** Screen capture from *step\_transient.avi* animation. Capture shows a step height of 2 ft, that appears instantaneously at time = 2 hours. Upper subplot shows physical system with the right/lower dashed trace showing the initial water surface at the introduction of the step and right/upper dashed trace shows the final, steady-state water surface. The solid trace shows the water surface at the current place in the evolution. Dashed lines on right side indicate that both subcritical and supercritical flow are accessible downstream. Lower-left subplot shows depth-storage relationship upstream of step with the lowest square marking the initial condition, the middle square marking the current condition, and the highest square marking the ultimate, steady-state condition. Lower-middle subplot shows the discharge passing the step as a function of time. Lower-right subplot shows the transient  $E-y$  diagram in the dashed curve and the ultimate, steady-state  $E-y$  diagram in the solid curve.

Now that choke conditions have been explored, the reasoning behind flow accessibility requires further explanation. Three flow obstructions have been explored: sluice gates, steps, and constrictions. Each obstruction has its own effect on the flow and interpretation on the  $E-y$  diagram. The skill the reader must develop is to envision the available transition pathways on the  $E-y$  diagram that relate to the precise conditions related in any open channel flow problem. Several such pathways have been illustrated in Example 2.6 and in all three animations. In particular, the reader must determine if the obstructions encountered were severe enough to bring the flow to critical conditions. If not, then the upstream and downstream flow regime should both be the same. For instance, Examples 2.2, 2.3, and 2.5 presented conditions that resulted in subcritical flow upstream and downstream; Example 2.4 presented conditions that resulted in flow that was supercritical upstream and downstream.

At this juncture, there is some ambiguity surrounding the concept of flow accessibility. That ambiguity is, if an obstruction is sufficient to drive a system to critical conditions, then which flow regime, supercritical or subcritical, will prevail downstream of that obstruction since both are equally accessible? This question was illustrated graphically in the upper half of Figure 2.11 which shows an upward step of finite length followed by a downward step that returns the channel bottom to its original elevation. The flow upstream of the step is subcritical, and over the course of the animation, the height of the upward step became severe enough to drive the flow over the step to critical conditions. When the flow then undergoes the transition back down the step to the original channel bottom elevation, it could be argued that both subcritical and supercritical flow are equally accessible pathways. To anthropomorphize, which pathway does the flow choose?

I have posed this mental experiment to my students for many years and I liken it to an equally unanswerable question as illustrated in Figure 2.16. In this figure, a perfect ball is placed at the exact top of a perfectly symmetric hill. The ball cannot rest at the top of the hill, but which side will it roll down? My students stare at me blankly not knowing the answer to this

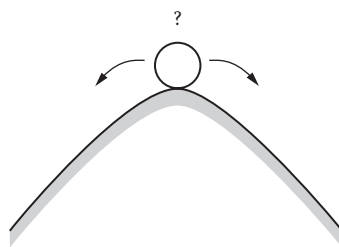


**FIGURE 2.16** Mental experiment: A ball is placed at the exact top of a perfectly symmetrical hill. Which way does it roll down?

question (and perhaps knowing that the wisest course of action is to remain quiet). Eventually, my solution to this latter experiment is to say that the ball will roll according to which way the wind is blowing. A less philosophical response is to say that we cannot answer either question yet because the systems we are studying are idealized. We cannot know what flow regime prevails downstream because we are not yet considering friction and its role in controlling flow. This question of flow over a finite, critical height will be revisited once a few more important, real-world concepts have been introduced. At that time, an analog to the direction of the blowing wind will emerge, and the conundrum suggested by Figure 2.16 will be resolved.

## 2.9 LONGITUDINAL CHANGES IN FLOW CONDITIONS AND THE FROUDE NUMBER

This section revisits the step problem, but with a focus on how the flow shifts in the presence of a change in elevation of the channel bottom. Total head,  $H$ , is defined as the sum of the velocity head, depth, and elevation of the channel above a defined datum. See definition sketch in Figure 2.17 as well as equation 2.31:

$$H = \frac{v^2(x)}{2g} + y(x) + z(x) \quad (2.31)$$

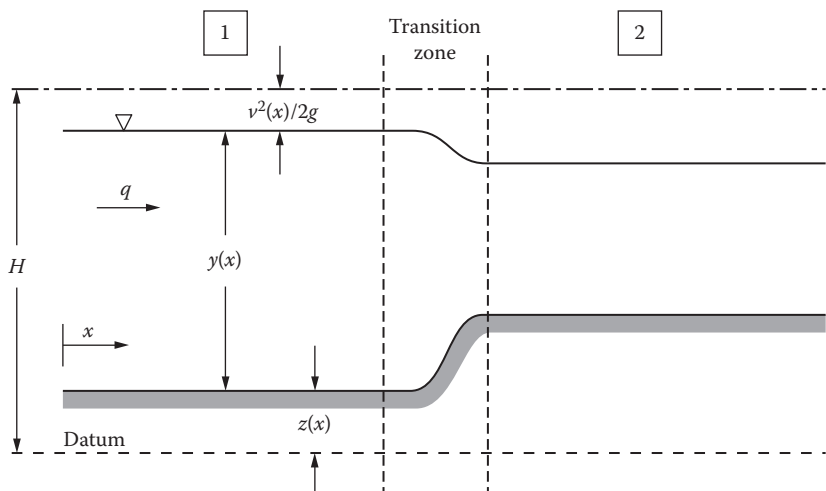


**FIGURE 2.17** Definition sketch for water surface shapes discussion.

Equation 2.31 is simply a generalization of the specific energy equation 2.3, which explicitly introduces a datum that is not necessarily coincident with the channel bottom. The right-hand side of the equation explicitly calls out the dependency of each term on the horizontal position,  $x$ , within the channel. Note that  $H$  is not a function of  $x$  as the system being studied remains idealized as frictionless and therefore energy conserving. In order to characterize the shape of the water surface, we take the derivative of equation 2.31 with respect to position  $x$ :

$$0 = \frac{dH}{dx} = \frac{dE}{dx} + \frac{dz}{dx} \quad (2.32)$$

Using the chain rule to expand on  $dE/dx$ :

$$0 = \frac{dE}{dy} \cdot \frac{dy}{dx} + \frac{dz}{dx} \quad (2.33)$$

Substituting from equation 2.20 into 2.33:

$$0 = (1 - F_r^2) \cdot \frac{dy}{dx} + \frac{dz}{dx} \quad (2.34)$$

Note that the term  $dy/dx$  represents the change in flow depth. Let us return to a few previous examples to examine this further. In Example 2.2 an upward step was encountered under subcritical flow conditions. Since the flow is subcritical we know that the Froude number is less than 1, and the value of  $(1 - F_r^2)$  is positive. Since the step is upward in the direction of flow,  $dz/dx$  is positive. Concerning ourselves only with the sign of terms in equation 2.34 we have:

$$0 = (+) \cdot \frac{dy}{dx} + (+) \quad (2.35)$$

where “(+)” indicates a positive number. For equation 2.35 to hold, it must be the case that the first term in total is a negative number, equal in magnitude to the second term. It follows that  $dy/dx$  is negative. This is what was concluded in Example 2.2 where the depth shifted from 2.0 m to 1.76 m downstream of the step—a negative change in flow depth.

In contrast, Example 2.4 involved supercritical flow encountering an upward step. By similar reasoning, equation 2.34 evaluates as follows:

$$0 = (-) \cdot \frac{dy}{dx} + (+) \quad (2.36)$$

The system still contains an upward step, so for equation 2.36 to hold, it is still true that the second term is positive. Since  $(1 - F_r^2)$  is now negative, it must be the case that  $dy/dx$  is positive. This is what was concluded in Example 2.4 where the depth shifted from 0.54 m to 0.59 m downstream of the step, a positive change in flow depth.

In the context of this discussion, the slope of the channel bottom,  $dz/dx$  can be effectively zero in two different situations. The first situation is the case of a simply flat channel. In that case, equation 2.34 evaluates to:

$$0 = (1 - F_r^2) \cdot (0) + (0) \quad (2.37)$$

This is the uninteresting case because nothing of note is happening. The channel bottom is flat and the flow depth is not changing with distance. Any Froude number will satisfy this equation so the flow can be subcritical, supercritical, or critical.

The more interesting possibility is for  $dz/dx = 0$  to be only locally true at, for instance, the outfall from a lake discharging into a steep channel (a channel that offers small resistance to flow), as shown in Figure 2.18.

For the conditions illustrated in Figure 2.18, equation 2.34 can be simplified to:

$$0 = (1 - F_r^2) \cdot (-) + 0 \quad (2.38)$$

Since  $dy/dx < 0$ , it follows from equation 2.38 that the first term on the right-hand side,  $(1 - F_r^2)$ , must evaluate to zero, and thus it must be that  $F_r^2 = 1$ . In other words, the flow is critical at the outfall from the lake. This statement can be generalized that critical flow will result at locations in the channel with zero slope at the head of a steep reach or free overfall. Such a location is called a *control* because it is known that the flow at this location will be critical.

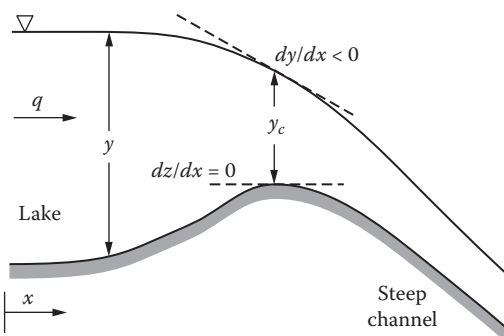


**FIGURE 2.18** Flow depth transitioning through critical depth,  $y_c$ , at the outfall from a lake.

Thus there is a unique depth-discharge relationship that applies at this location. Controls are useful because they allow the engineer to quickly and accurately estimate discharge based on a simple depth measurement. In the United States, the US Geological Survey and other organizations that build and maintain stream gaging sites often seek or build short channel sections that will act as controls to support their gaging activities.

## 2.10 ENERGY IN NON-RECTANGULAR CHANNELS

To this point, the discussion has focused on rectangular channels. This has served to keep the math as straightforward as possible, but the vast majority of open channels are not rectangular. This section presents a generalization of several of the equations discussed earlier along with specific solution techniques for determining alternate and critical depths in trapezoidal and circular channel cross-sections.

Because the channel width varies with depth, the concept of specific or unit discharge,  $q$ , is undefined in non-rectangular channels. We must return to equation 2.8:

$$E = \frac{v^2}{2g} + y \quad (2.8)$$

or recognizing that  $v = Q/A$ , equation 2.8 can be rewritten as:

$$E = \frac{Q^2}{2gA^2} + y \quad (2.39)$$

Equation 2.39 has the advantage of removing velocity from the calculation so that if the cross-sectional shape is known, then the cross-sectional area,  $A$ , is a function of depth and can be rewritten as  $A(y)$  to emphasize this dependency. Consider the case of a trapezoidal section with bottom width,  $b$ , and side slopes  $m$  as shown in Figure 2.19.

From Figure 2.19, the reader should be able to quickly derive the following general equations for a trapezoidal section:

$$A_{trap} = by + my^2 \quad (2.40)$$

$$B_{trap} = b + 2my \quad (2.41)$$

where  $A_{trap}$  is the area of the trapezoidal section, and  $B_{trap}$  is the top width of the trapezoidal section.

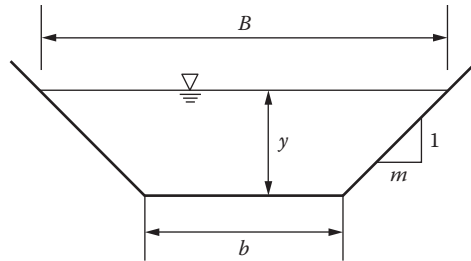


**FIGURE 2.19** Definition sketch for trapezoidal section geometry.

Figure 2.20 shows the definition sketch for a circular cross-section. The equations for area and top-width are dependent on the cross-section radius,  $r$ :

For  $y \leq r$ :

$$\theta = \cos^{-1}\left(\frac{r-y}{r}\right) \quad (2.42)$$

$$A_{circ} = \theta r^2 - r(r-y)\sin(\theta) \quad (2.43)$$

$$B_{circ} = 2r\sin(\theta) \quad (2.44)$$

For  $y > r$ :

$$\theta = \cos^{-1}\left(\frac{y-r}{r}\right) \quad (2.45)$$

$$A_{circ} = \pi r^2 - \theta r^2 + r(r-y)\sin(\theta) \quad (2.46)$$

$$B_{circ} = 2r\sin(\theta) \quad (2.47)$$

where  $A_{circ}$  is the area of the trapezoidal section, and  $B_{circ}$  is the top width of the circular section. For convenience, the Appendix provides a dimensionless tabulation of circular channel properties such as  $A_{circ}$  and  $B_{circ}$  as a function of  $y/D$ .

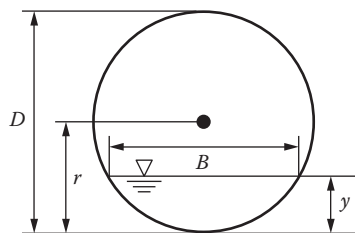


**FIGURE 2.20** Definition sketch for a circular section geometry.

## 2.10.1 Alternate Depths in Non-Rectangular Channels

The calculation of alternate depths in a non-rectangular section is best illustrated through an example.

---

### Example 2.7

Consider a trapezoidal section with side slope parameter  $m = 2$ , and bottom width  $b = 1.5$  m. The discharge is  $Q = 9$  m<sup>3</sup>/s. Let the depth be  $y_1 = 2$  m.

- a. Determine the cross-sectional area,  $A_1$ .
- b. Determine the top width,  $B_1$ .
- c. Determine the specific energy,  $E_1$ .
- d. Determine the alternate depth,  $y_2$ .
- e. Based on your findings, discuss which depth likely corresponds to subcritical and which depth corresponds to supercritical flow conditions.

**Solution:**

- a. Using equation 2.40,

$$A_1 = by + my^2 = (1.5) \cdot (2.0) + 2 \cdot (2.0)^2 = 11.0 \text{ m}^2$$

- b. Using equation 2.41,

$$B_1 = b + 2my = 1.5 + (2) \cdot (2) \cdot (2.0) = 9.5 \text{ m}$$

- c. Using equation 2.39,

$$E_1 = \frac{Q^2}{2gA_1^2} + y = \frac{9^2}{2 \cdot (9.81) \cdot (11.0)^2} + 2.0 = 2.03 \text{ m}$$

- d. The alternate depth,  $y_2$ , can be determined by iteration. Values of  $y_2$  are assumed and entered into equation 2.40. The resulting area is then used in equation 2.39 until the energy produced is equal to  $E_1 = 2.03$  m. Using the Goal Seek (see box below) function in Excel®, we find that  $y_2 = 0.62$  m (resulting in  $A_2 = 1.71$  m<sup>2</sup>,  $B_2 = 3.99$  m).

- e. As with rectangular channels, it should be apparent that the deeper flow (condition 1) is lower velocity and has the majority of its energy in the form of the static depth, while the shallower flow (condition 2) is higher velocity and with its majority of energy from the kinetics of the flow. Therefore, we expect that  $y_1 = 2 \text{ m}$  corresponds to subcritical flow and  $y_2 = 0.62 \text{ m}$  corresponds to supercritical flow.

### Use of Excel Goal Seek Tool for Finding Roots

Many open channel flow problems amount to root-finding exercises. Consider a slight restatement of the problem faced in Example 2.7:

$$2.03 \text{ m} = E_1 = E_2 = \frac{Q^2}{2gA_2^2} + y_2 = \frac{9^2}{2 \cdot (9.81) \cdot (by_2 + my_2^2)^2} + y_2 \quad (2.48)$$

We seek a value of  $y_2$  that produces a specific energy of 2.03 m other than the original specified depth of  $y_1 = 2 \text{ m}$ . Equation 2.45 cannot be solved analytically so some iterative approach must be used to find  $y_2$ . Rather than using a brute-force trial-and-error solution, we make use of a commonly available tool within the Microsoft Excel Program: Goal Seek. Following is a step-by-step approach to setting up and executing a Goal Seek solution:

1. In Excel, set aside several adjacent cells in a spreadsheet for executing the Goal Seek solution.
2. In this case, the depth  $y$  is the value being sought. One cell of the spreadsheet should contain exclusively this quantity. Assume that spreadsheet cell C3 contains this quantity as shown in Figure 2.21. We enter an initial value of  $y_2 = 1 \text{ m}$  in this cell so that cell formulas dependent on this cell are able to calculate as the spreadsheet is being generated.
3. The trapezoidal cross-sectional area is a simple function of depth. Let cell D3 contain this quantity with the cell formula:  $= 1.5*C3+2*C3^2$ . (Note that the use of 1.5 and 2 in this cell formula makes this cell formula exclusively useful for the problem at hand. The reader is encouraged to develop a spreadsheet that uses other cells to contain the bottom width ( $b$ ) and side

	A	B	C	D	E	F
1						
2			Depth, $y_2$ (m)	Area ( $m^2$ )	Specific Energy (m)	
3			1	3.5	1.33702	
4						

**FIGURE 2.21** Initial programming of spreadsheet for Goal Seek root-finding exercise to determine the alternate depth,  $y_2$ , in a trapezoidal section that produces a desired specific energy.

slope ( $m$ ) parameters and then uses a more general cell formula that draws these parameters from the appropriate cell location.)

4. Specific energy is now readily calculated using equation 2.48 in cell E3 with the cell formula: = C3 + (9^2)/(2\*9.81\*D3^2). (The same comment as above applies. The value for discharge,  $Q$ , and gravity,  $g$ , could also be drawn from separate cell locations.) Figure 2.21 shows the calculated trapezoidal area and specific energy for an initial value of  $y_2 = 1$  m.
5. It is a good practice to check the results to confirm that the cell formulas have been programmed correctly. If hand calculations differ from those reported in the spreadsheet, check programmed cell formulas for the possible need of parentheses, missing exponents, and so on. You may find it helpful to break more involved equations into smaller parts, giving each part a unique cell location. For instance, you might give separate terms of an equation or the numerator and denominator individual cell locations. Only proceed when hand-calculated and spreadsheet reported results are consistent.
6. We are now ready to invoke the Goal Seek tool. Choose: “Data: What-If Analysis: Goal Seek....” A dialog box like the one shown in Figure 2.22 will appear. The “Set cell:” entry should be the cell that contains the right-hand side of equation 2.48 in

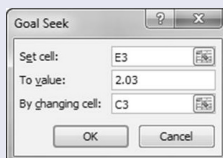


**FIGURE 2.22** The Excel “Goal Seek” dialog with entries populated to solve for the alternate depth to  $y_1 = 2$  m in Example 2.7.

	A	B	C	D	E	F
1						
2			Depth, $y_2$ (m)	Area ( $m^2$ )	Specific Energy (m)	
3			0.62361	1.71321	2.03019	
4						

**FIGURE 2.23** Final programming of spreadsheet for Goal Seek root-finding exercise. Note that the depth indicated for  $y_2$ , approximately 0.62 m, produces an energy of 2.03 m which was the goal indicated in the “Goal Seek” dialog shown in Figure 2.22.

this case. The “To value:” should be the constant desired, the left-hand side of equation 2.48 in this case. The “By changing cell:” should be the quantity whose root value is to be determined,  $y_2$  in this case.

- When each of these entries has been correctly specified, click the “OK” button. The dialog box will update showing a comparison of the optimized value and the target value, and the spreadsheet will update with the optimized value for the “By changing cell:” inserted along with updated calculations for all cells dependent on this cell. Figure 2.23 shows the updated spreadsheet with the approximate depth of  $y_2 = 0.62$  m in cell C3 determined along with revised values for area and specific energy in cells D3 and E3, respectively.
- One last point is important to make. In this example, we chose as our initial guess for  $y_2 = 1$  m. This was done for simplicity and so calculated cell values could be checked for correctness. We could have chosen any value for  $y_2$ . We encourage the reader to change the value of cell C3 to 3 (i.e., initial guess is  $y_2 = 3$  m). With only this change, we find that Goal Seek determines  $y_2 = 1.995$  m (essentially  $y_2 = 2$  m which was our starting value for  $y_1$ ). This shows that the optimized value returned by the Goal Seek tool is path dependent. For Goal Seek to provide useful results, the reader needs to give an appropriate initial guess for the optimized value. In the case of finding an alternate depth, the reader should have an idea of whether the known depth is subcritical or supercritical. Based on this understanding, the initial guess should be considerably bigger/smaller than the known depth so as to force the Goal Seek tool to produce the other root.

The Froude number as originally presented earlier in this chapter appeared by minimizing energy with respect to depth. This derivation was presented in the context of a rectangular channel that produced a solution that was specific to the rectangular channel shape. For a non-rectangular channel, the equation for the Froude number is more general than as presented in equation 2.19. The depth term is replaced by the hydraulic depth, the ratio of the cross-sectional area over the top width:

$$F_r = \frac{v}{\sqrt{g \frac{A}{B}}} = \frac{Q}{A \sqrt{g \frac{A}{B}}} \quad (2.49)$$

Notice that the units of  $A/B$  are length as they were in equation 2.19 and that in the case of a rectangular channel  $A/B = y$ .

Returning to Example 2.7, simply determine the Froude numbers for the alternate depth pair:  $y_1$  and  $y_2$ .

For  $y_1$ ,

$$F_{r,1} = \frac{Q}{A_1 \sqrt{g \frac{A_1}{B_1}}} = \frac{9.0}{11.0 \cdot \sqrt{(9.81) \cdot \frac{11.0}{9.5}}} = 0.24 \text{ (subcritical)}$$

For  $y_2$ ,

$$F_{r,2} = \frac{9.0}{1.71 \cdot \sqrt{(9.81) \cdot \frac{1.71}{3.99}}} = 2.57 \text{ (supercritical)}$$

These values for the Froude numbers for this alternate depth pair confirm the Example 2.7(e) response concerning subcritical and supercritical flow conditions.

## 2.10.2 Critical Depth and Energy in Non-Rectangular Channels

As shown earlier in this chapter, critical depth and critical energy are important concepts because at critical conditions energy is minimized for a given discharge (Observation 3 from Section 2.2), and at critical conditions, discharge is maximized for a given energy (Observation 7 from Section 2.3). These observations apply regardless of the channel shape, so it is useful to be able to determine critical depth and energy in non-rectangular channels. In this section, a general approach will be presented for calculating critical depth and energy in irregular cross-sections. Further, tools for quickly estimating critical

depth in trapezoidal and circular channels will be presented along with methods for more precise calculations of the same quantity.

The provided curves that can be used to solve problems of critical depth (Figure 2.24) and critical energy (Figure 2.25) in trapezoidal and circular channels are the focus of this section. We will examine the use of these figures through the solutions to two example problems.

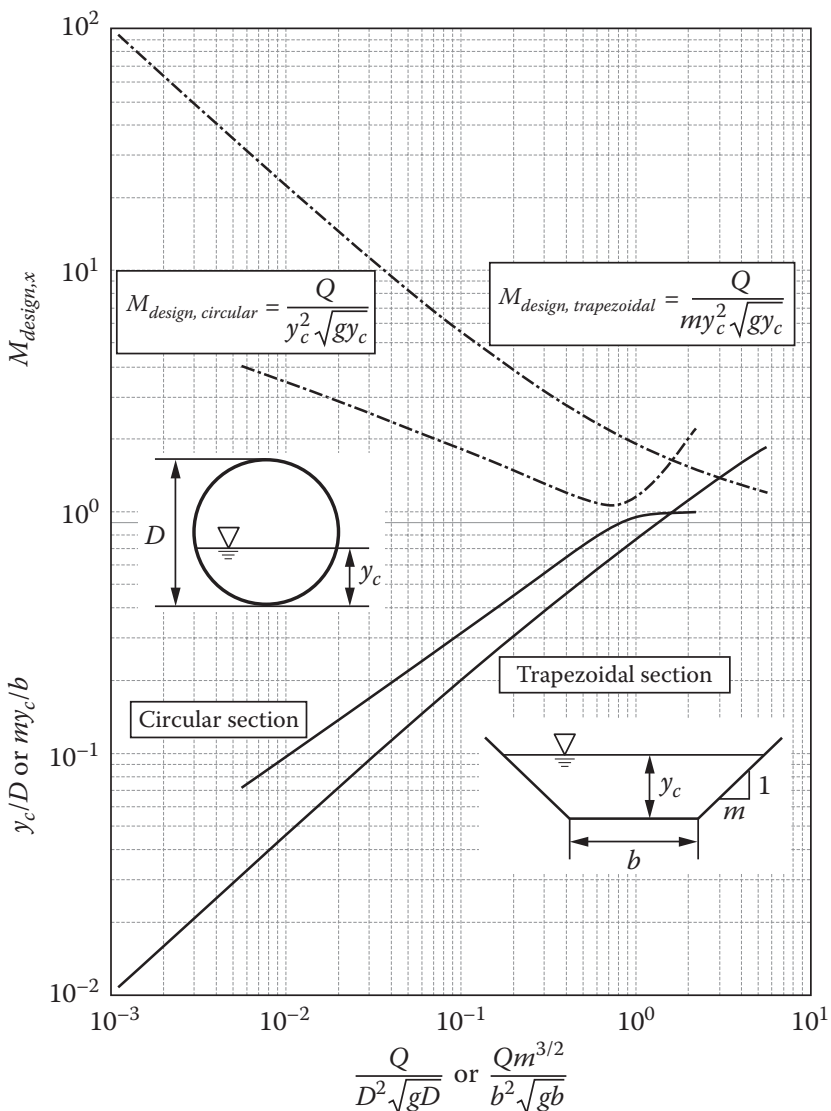


**FIGURE 2.24** Critical depth,  $y_c$ , in trapezoidal and circular cross-sections.

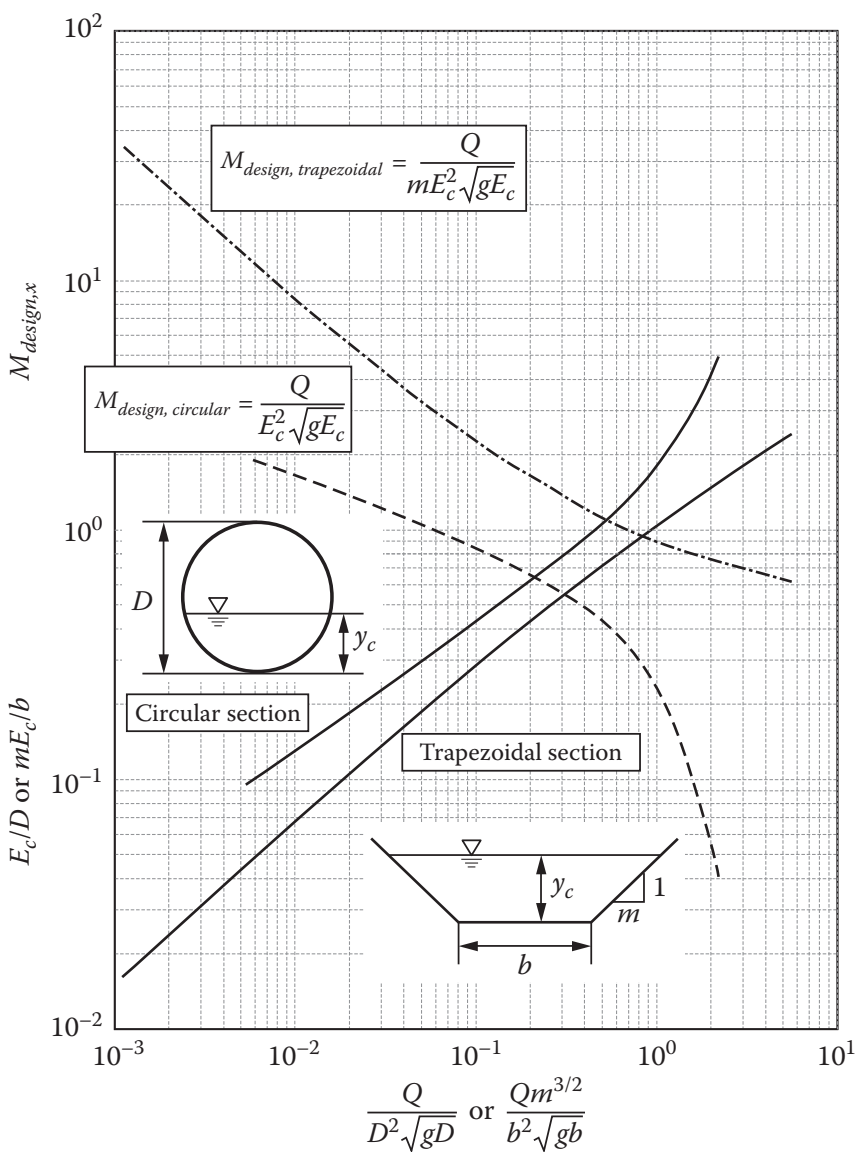


**FIGURE 2.25** Critical energy,  $E_c$ , in trapezoidal and circular cross-sections.

**Example 2.8a**

A trapezoidal channel (bottom width 1.5 m, side slopes  $m = 2$ ) forms the outlet structure of a lake that discharges to a steep channel as shown in Figure 2.26. The lake level far from the outlet is 0.6 m relative to the invert of the outlet structure. What is the discharge from the lake?

**Solution:**

From the reasoning presented in Section 2.9, the flow can be assumed to be critical at the head of the steep channel. From the problem statement the critical energy associated with the flow at the outlet is 0.6 m. The solution will proceed in two steps. First we will make use of Figure 2.25 to make a rough estimate of discharge, and then we will use first principles concerning the energy-depth relationship in the channel to make a more precise determination of the discharge.

**Rough estimate using Figure 2.25:**

Looking at Figure 2.25 the reader should note that the provided information fully defines the parameters necessary to quantify the vertical axis of this figure. The parameters necessary to quantify the horizontal axis are all known except for the discharge,  $Q$ . Thus, entering Figure 2.25 on the vertical axis, translating horizontally to the trapezoidal curve and then translating vertically to the horizontal axis provides a value that can be used to determine  $Q$ .

Vertical axis calculation:

$$\frac{mE_c}{b} = \frac{(2) \cdot (0.6)}{1.5} = 0.8$$

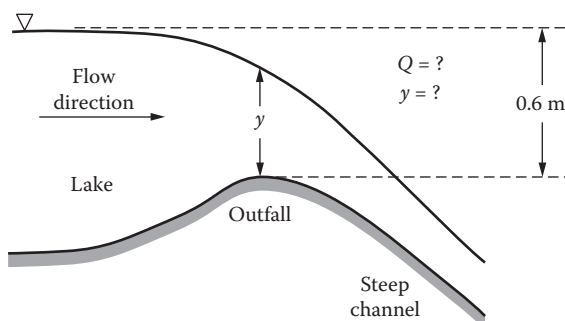


**FIGURE 2.26** Flow conditions at lake outlet structure for Examples 2.8a and 2.8b.

**TABLE 2.3** Variation in Area, Top Width, Froude Number, and Discharge with Depth in Example 2.8a

Depth, $y$ (m)	Area, $A$ ( $m^2$ )	Top Width, $B$ (m)	Froude Number, $F_r$	Discharge, $Q$ ( $m^3/s$ )
0.41	0.951	3.14	1.120	1.837
0.42	0.983	3.18	1.079	1.847
0.43	1.015	3.22	1.039	1.853
0.44	1.047	3.26	0.998 (essentially 1)	1.855 (maximum)
0.45	1.080	3.30	0.957	1.853
0.46	1.113	3.34	0.917	1.845
0.47	1.147	3.38	0.875	1.832

Entering the vertical axis at 0.8, we move to the trapezoidal section curve and down to the horizontal axis where we read approximately 0.6. Thus,

$$0.6 = \frac{Qm^{3/2}}{b^2 \sqrt{gb}}$$

Rearranging and solving for discharge,  $Q$ ,

$$Q = \frac{(0.6) \cdot b^2 \sqrt{gb}}{m^{3/2}} = \frac{(0.6) \cdot (1.5) \cdot \sqrt{(9.81) \cdot (1.5)}}{2^{3/2}} = 1.8 \frac{m^3}{s}$$

*More precise estimate using first principles:*

We start by rearranging equation 2.39 and solving for  $Q$ :

$$Q = \sqrt{2gA^2(E_c - y)}$$

Expanding for  $A$  using the equation for area of a trapezoid,

$$Q = \sqrt{2g \cdot (by + my^2)^2(E_c - y)}$$

gives  $Q$  as a function depth,  $y$ . We draw on Observation 7 that discharge is maximized at critical conditions. Assuming values of  $y$ , we can tabulate the above equation for  $b = 1.5$  m,  $m = 2$ , and  $E_c = 0.6$  m to determine  $Q$ . The value of  $y$  that maximizes  $Q$  corresponds to critical depth and is the solution to this problem (see Table 2.3).

Thus, the more precise method that yields an estimate of  $Q = 1.855 \text{ m}^3/\text{s}$  is consistent with  $Q = 1.8 \text{ m}^3/\text{s}$  derived from Figure 2.25.

**Example 2.8b**

Use the same setup as in Example 2.8a, but now it is given that the discharge is  $Q = 1.86 \text{ m}^3/\text{s}$  (the discharge found in 2.8a reported to two decimal places). The problem now is to determine the depth at the outfall,  $y$ .

**Solution:**

By the same reasoning as before, we know that the depth at the outfall corresponds to critical conditions. Thus,  $y = y_c$  at the outfall.

*Rough estimate using Figure 2.24:*

Since  $y_c$  is known, use of Figure 2.24 is indicated. In contrast to Example 2.8a, it is now the horizontal axis that is fully defined and the vertical axis (which includes  $y$ ) that is to be determined. The solution thus proceeds in the opposite direction to Example 2.8a.

Horizontal axis calculation:

$$\frac{Qm^{3/2}}{b^2\sqrt{gb}} = \frac{(1.86) \cdot (2)^{3/2}}{(1.5)^2 \cdot \sqrt{(9.81) \cdot (1.5)}} = 0.61 \quad (\text{use } 0.6)$$

Entering the horizontal axis at 0.6, we move to the trapezoidal section curve and over to the vertical axis where we read something slightly less than 0.6 (use 0.58). Thus,

$$0.58 = \frac{my_c}{b}$$

Rearranging and solving for critical depth,  $y_c$ ,

$$y_c = \frac{(0.58) \cdot b}{m} = \frac{(0.58) \cdot (1.5)}{2} = 0.44 \text{ m}$$

*More precise estimate using first principles:*

We start with equation 2.39,

$$E = \frac{Q^2}{2gA^2} + y \quad (2.39)$$

Expanding for  $A$  using the equation for area of a trapezoid,

$$E = \frac{Q^2}{2g(by + my^2)^2} + y$$

**TABLE 2.4** Variation in Area, Top Width, Froude Number, and Discharge with Depth in Example 2.8b

Depth, $y$ (m)	Area, $A$ ( $m^2$ )	Top Width, $B$ (m)	Froude Number, $F_r$	Energy, $E$ (m)
0.41	0.951	3.14	1.134	0.6049
0.42	0.983	3.18	1.087	0.6026
0.43	1.015	3.22	1.042	0.6012
0.44	1.047	3.26	1.001 (essentially 1)	0.6008 (minimum)
0.45	1.080	3.30	0.961	0.6012
0.46	1.113	3.34	0.924	0.6023
0.47	1.147	3.38	0.889	0.6041

gives  $E$  as a function depth,  $y$ . We draw on Observation 3 that the  $E$ - $y$  relationship is minimized at critical conditions. Assuming values of  $y$ , we can tabulate the above equation for  $b = 1.5$  m,  $m = 2$ , and  $Q = 1.86$   $m^3/s$  to determine  $E$ . The value of  $y$  that minimizes  $E$  corresponds to critical depth and is the solution to this problem (see Table 2.4).

The two methods are, again, consistent with one another as well as with the earlier findings of Example 2.8a.

This example showed how Figures 2.24 and 2.25 can be used to solve two classes of problems:

- Given  $y_c$  or  $E_c$  and  $m$  and  $b$  or  $D$ , determine  $Q$  (Example 2.8a).
- Given  $Q$  and  $m$  and  $b$  or  $D$ , determine  $y_c$  or  $E_c$  (Example 2.8b).

A third class of problems is the design problem in which both  $Q$  and critical depth or energy are known. In the case of a trapezoidal channel, the channel shape parameter  $m$  is also known. What is not known (to be designed) is the channel size parameter  $b$  or  $D$ . Let us explore how to use these figures to solve this class of problems in Example 2.9.

### Example 2.9

A circular culvert forms the outlet structure of a lake that discharges to a steep channel. Local design codes require that the depth at the outfall from the lake be no more than 0.4 m for a discharge of 0.75  $m^3/s$ . What is the smallest diameter culvert that will satisfy the design codes?

**Solution:**

As in Example 2.8 the problem deals with critical conditions at the outfall from a lake so Figures 2.24 and 2.25 apply. Because the code focuses on depth at the outfall and not energy (i.e., lake level relative to the invert), Figure 2.24 applies. We will use this figure to generate a rough estimate of the culvert diameter as well as a more precise first principles approach.

*Rough estimate using Figure 2.24:*

The solution begins by determining  $M_{design,circular}$ :

$$M_{design,circular} = \frac{Q}{y_c^2 \sqrt{gy_c}} = \frac{0.75}{(0.4)^2 \cdot \sqrt{(9.81) \cdot (0.4)}} = 2.4$$

Entering Figure 2.24 on the vertical axis at 2.4 (the reader will need to visually interpolate liberally), we move horizontally to the dashed line for the circular section shape. We now move vertically from the intersection point down to the solid curve for the circular section. We then project from this intersection point either to the horizontal axis (value is approximately 0.04) or to the vertical axis (value is approximately 0.2).

Using the horizontal axis value, we get

$$0.04 = \frac{Q}{D^2 \sqrt{gD}}$$

Rearranging and solving for pipe diameter,  $D$ ,

$$D = \left( \frac{Q}{(0.04) \cdot \sqrt{g}} \right)^{2/5} = \left( \frac{0.75}{(0.04) \cdot \sqrt{9.81}} \right)^{2/5} = 2.0 \text{ m}$$

Using the vertical axis value, we get

$$0.2 = \frac{y_c}{D}$$

Rearranging and solving for pipe diameter,  $D$ ,

$$D = \frac{y_c}{0.2} = \frac{0.4}{0.2} = 2.0 \text{ m}$$

*More precise estimate using first principles:*

We start with the second form of equation 2.49 for the Froude number in a non-rectangular channel:

$$F_r = \frac{Q}{A \sqrt{g \frac{A}{B}}} \quad (2.49)$$

**TABLE 2.5** Variation in Angle, Area, Top Width, and Froude Number with Pipe Diameter in Example 2.9

Pipe Diameter, <i>D</i> (m)	Angle, $\theta$ (degrees)	Area, <i>A</i> ( $m^2$ )	Top Width, <i>B</i> (m)	Froude Number, $F_r$
1.90	54.6	0.434	1.55	1.041
1.95	53.9	0.441	1.57	1.026
2.00	53.1	0.447	1.60	1.013
2.05	52.4	0.454	1.62	0.999 (essentially 1)
2.10	51.8	0.460	1.65	0.986
2.15	51.1	0.466	1.67	0.974
2.20	50.5	0.472	1.70	0.962

With flow depth known ( $y_c = 0.4$  m), we note that both *A* and *B* become dependent only on the pipe diameter, *D*. The solution thus proceeds by tabulating *A*, *B*, and Froude number for varying assumed values of *D*. The value of *D* that produces a Froude number closest to 1 is the solution we seek (see Table 2.5).

Thus, the more precise method that yields an estimate of *D* = 2.05 m is consistent with *D* = 2 m derived from either axis of Figure 2.24. In general, Figures 2.24 and 2.25 will provide sufficient precision for most problems, given the inherent uncertainty in the other quantities: discharge, critical depth, and critical energy. If greater precision of the inputs is available and greater precision in the unknown to be calculated is needed, the tabular solutions shown as part of Examples 2.8 and 2.9 illustrate how that precision can be achieved.

## 2.11 SUMMARY

This chapter explored the implications of energy on flow in open channels. The concept of critical flow was introduced along with the dimensionless Froude number that quantifies the nature of the flow regime relative to critical flow. The concept of alternate depths—depths that correspond to the same specific energy—was presented and an equation that relates one alternate depth as a function of the other for rectangular channels was presented. Flow through several different channel obstructions—sluice gates, steps, and constrictions/expansions—was discussed. The concept of a choke was presented

in the context of these obstructions and the calculation of both initial and final flow conditions in these settings was presented if a choke and subsequent flow transient was encountered. The conditions that support the occurrence of critical flow were discussed. Finally, flow in non-rectangular cross-sections was presented with a focus on trapezoidal and circular cross-sections. Tools for making good rough estimates for critical flow in non-rectangular sections were presented along with techniques for higher precision solutions in such sections. We conclude this chapter with a simple table that summarizes some useful relationships (see Table 2.6).

**TABLE 2.6** Summary Table of Energy-Related Open Channel Flow Relationships

Quantity	Rectangular Section	Irregular Section (e.g., Trapezoidal, Circular)
Discharge	$q = \frac{Q}{b}$	$Q$
Critical depth	$y_c = \left( \frac{q^2}{g} \right)^{1/3}$	Figure 2.24 or use Goal Seek
Froude number	$F_r = \frac{v}{\sqrt{gy}}$	$F_r = \frac{v}{\sqrt{g\left(\frac{A}{B}\right)}}$
Energy equation	$E = y + \frac{v^2}{2g}$ $E = y + \frac{q^2}{2gy^2}$	$E = y + \frac{v^2}{2g}$ $E = y + \frac{Q^2}{2gA^2}$
Critical energy	$E_c = \frac{3}{2}y_c$	Figure 2.25 or use Goal Seek
Alternate depths	$y_2 = \frac{2y_1}{-1 + \sqrt{1 + \frac{8gy_1^3}{q^2}}}$	Use Goal Seek

## Reference

Bakhmeteff, B.A. (1932). *Hydraulics of Open Channels*, 1st ed., McGraw-Hill, New York.

## Problems

- 2.1. You are given the depth upstream ( $y_1$ ) and downstream ( $y_2$ ) of a sluice gate. Using conservation of energy at the sluice gate, find an equation for the unit discharge,  $q$ , in terms of  $y_1$  and  $y_2$ .
- 2.2. For a fixed specific energy of  $E^* = 0.9$  m and in a rectangular channel, vary depth from 0 to 0.9 meters in increments of 0.01 or 0.05 meters and determine the unit discharge,  $q$ , at each depth. Plot depth versus  $q$  over the range of calculated values. Verify that the maximum specific discharge occurs at  $y = 2/3E^*$ .
- 2.3. You are given a rectangular channel 3.50 feet wide. The flow depth upstream of a sluice gate is 2.15 feet. Downstream of the sluice gate the depth is 1.25 feet.
  - a. Find the unit discharge,  $q$ , and the discharge,  $Q$ .
  - b. What specific energy,  $E$ , does the flow have?
- 2.4. The flow depth upstream of a sluice gate is 0.60 meters. The velocity is 0.9 m/s.
  - a. What is the minimum allowable gate opening for the upstream flow to be possible as specified?
  - b. If the gate opening is instantaneously set to 0.15 meters:
    - i. What is the initial unit discharge,  $q$ , under the gate?
    - ii. What is the final depth at the upstream side of the gate?
- 2.5. Water is flowing at a velocity of 2.6 ft/s and a depth of 1.1 feet in a rectangular channel.
  - a. The flow encounters a smooth upward step of 0.2 feet.
    - i. What is the depth of flow on the step?
    - ii. What is the absolute change in water level compared to the channel bottom before the step?
    - iii. What are the Froude numbers upstream and at the step?
  - b. Find the maximum allowable size of upward step for the upstream flow to be possible as specified.
- 2.6. Consider a system with a specific discharge of  $3 \text{ m}^2/\text{s}$ . The depth,  $y_1$ , upstream of the step is 0.9 meters. The downward step height is 0.2 meters. Determine the following:
  - a. The downstream specific energy,  $E_2$
  - b. The downstream depth,  $y_2$

- c. The absolute change in the water surface from location 1 to location 2
  - d. The downstream Froude number,  $F_{r,2}$
- 2.7. Consider a system with a discharge of  $9 \text{ m}^3/\text{s}$ . The channel is rectangular. The width at location 1 is  $w_1 = 4.5 \text{ m}$ . A constriction is encountered at location 2 downstream such that the width  $w_2 = 3 \text{ m}$ . The depth of flow  $y_2$  at downstream location 2 is 0.7 meters.
- a. Determine the specific discharges at locations 1 and 2.
  - b. Determine the downstream specific energy,  $E_2$ .
  - c. Determine the downstream Froude number,  $F_{r,2}$ .
  - d. Determine the upstream specific energy,  $E_1$ .
  - e. Determine the upstream depth,  $y_1$ .
  - f. Determine the upstream Froude number,  $F_{r,1}$ .
  - g. Determine the absolute change in the water surface from location 1 to location 2.
  - h. Sketch the transition of the system from location 1 through the flow constriction to location 2 on an  $E$ - $y$  diagram.
- 2.8. Re-solve Problem 2.7 except  $w_2 = 6 \text{ m}$  (so the flow encounters an expansion, not a constriction) and  $y_2 = 1 \text{ m}$ .
- 2.9. Re-solve Problem 2.7 except  $w_2 = 6 \text{ m}$  (so the flow encounters an expansion, not a constriction) and  $y_2 = 0.3 \text{ m}$ .
- 2.10. Water flows in a horizontal, rectangular channel initially 10 feet wide and 2 feet deep. The initial velocity is 6 ft/s. This flow encounters downstream a simultaneous downward step and constriction. No energy losses are associated with these changes in channel configuration.
- a. What is the specific discharge,  $q$ :
    - i. Upstream (for  $w = 10 \text{ feet}$ )?
    - ii. Downstream (for  $w = 6 \text{ feet}$ )?
  - b. What specific energy,  $E$ , is associated with the flow as initially specified (at the upstream location)?
  - c. What is the minimum energy needed to pass the full discharge at the downstream location?
  - d. What is the height ( $\Delta z$ ) of the smallest downward step necessary for the upstream flow conditions to remain as specified?
- 2.11. A trapezoidal channel has a bottom width of 20 feet, has side slopes of 2H:1V, and carries a flow of  $750 \text{ ft}^3/\text{s}$ .
- a. Find the flow depth at the head of a steep slope.
  - b. If there is a short but smooth transition to a rectangular section 20 feet wide just before the head of the steep slope, find the depth at the upstream and downstream ends of the transition,

assuming that the specific energy remains unchanged through the transition.

- 2.12. A horizontal, frictionless channel of circular cross-section and diameter equal to 5 feet flows at a depth of 3 feet and a velocity of 2 ft/s.
- Find the discharge in the channel.
  - Determine the specific energy of this flow.
  - Determine the Froude number of this flow.
  - What is the maximum upward step height ( $\Delta z_{max}$ ) that this flow can negotiate without a choke?
- 2.13. A trapezoidal channel with a base width of 20 feet and side slopes of 2H:1V carries a flow of  $2000 \text{ ft}^3/\text{s}$  at a depth of 8 feet. There is a smooth transition to a rectangular section 20 feet wide accompanied by a gradual lowering of the channel bed by 2 feet.
- Find the depth of water within the rectangular section, and the change in the water surface level.
  - What is the minimum amount by which the bed must be lowered for the upstream flow to be possible as specified?



# Momentum

## CHAPTER OBJECTIVES

1. Understand how momentum varies as a function of depth, velocity, and discharge.
2. Introduce the concept of conjugate depths and, by association, the hydraulic jump:
  - a. Discuss loss of energy in hydraulic jump.
  - b. Discuss the fact that energy loss increases as upstream conditions have higher Froude number.
3. Examine dimensionless expression of energy and momentum to explore duality between these concepts.
4. Employ duality to derive alternate depth relationship from conjugate depth equation.
5. Examine momentum in non-rectangular channels.
  - a. Provide and use figures for hydraulic jumps in trapezoidal and circular sections.
  - b. Illustrate use of Excel® Goal Seek to achieve greater precision in non-rectangular sections.

### 3.1 INTRODUCTORY COMMENTS

In physics, we learn of conservation of several quantities: mass, energy, and momentum. In open channel flow, we make use of these conservation laws to analyze a flow. My general observation is that students find conservation of mass (i.e., the continuity equation) obvious; water can neither be

created nor destroyed. Conservation of energy and momentum require a bit more effort to accept, but it has been my observation that conservation of energy is more intuitive than conservation of momentum, perhaps because energy depends only on location; it is a scalar quantity. Conservation of momentum is a bit more challenging because of its directional nature; it is a vector quantity. Further confounding students is the fact that the units of momentum, as classically treated in open channel flow, appear similar to energy. As is the case in this book, momentum is generally introduced after conservation of energy. Students must reconcile these questions: "Why is energy conserved here but not momentum?" and its complement, "Why is momentum conserved here but not energy?"

In truth, both energy (if an energy loss term is included) and momentum (if all forces are considered) are conserved as long as the system is defined appropriately. The correct conservation law to apply depends on the unknown quantity that is to be determined. This can be trickier than it sounds, but it is fairly sound advice that if one conservation law does not address the desired unknown, then the other law is likely to provide the missing information.

A focus of this chapter is the simple hydraulic jump. Such a jump is shown in Figure 3.1. We note the obvious that  $y_1$  and  $y_2$  are alternate depths, both possessing the same specific energy. But what is the energy associated with  $y_3$ ? We can see from the figure that  $y_3$  is greater than critical depth,  $y_c$ , so it therefore corresponds to subcritical flow. Since  $y_3$  is less than  $y_1$ , it follows that the specific energy at a flow depth of  $y_3$  is less than the specific energy corresponding to a depth of  $y_1$ . Some energy loss takes place through the hydraulic jump.

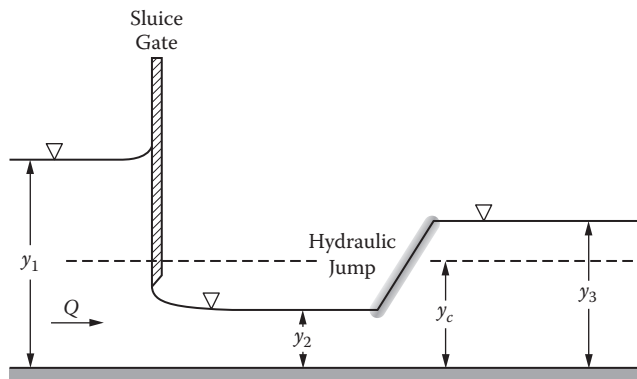


**FIGURE 3.1** A sluice gate followed by a hydraulic jump. The depths  $y_1$  and  $y_2$  are alternate depths, while  $y_2$  and  $y_3$  are conjugate depths. Notice that  $y_3 < y_1$ , indicating an energy loss incurred within the hydraulic jump.

Pertaining to the discussion above, how do we determine this energy loss? Conservation of energy provides us with the following:

$$E_l = E_3 + h_L = y_3 + \frac{q^2}{2gy_3^2} + h_L \quad (3.1)$$

where  $h_L$  is the head loss. Although equation 3.1 holds true, this equation gives us no further insight into how substantial the head loss is. Following the advice above, let us now turn to conservation of momentum to determine the head loss in equation 3.1. Before we can do so, we must define momentum in the context of open channel flow. That is the subject of this chapter.

## 3.2 THE MOMENTUM FUNCTION

In physics, we learn that momentum,  $\vec{p}$ , is:

$$\vec{p} = m\vec{v} \quad (3.2)$$

Momentum has units  $MLT^{-1}$ . Further, momentum is a vector quantity in which both momentum and velocity have the same direction.

In the context of open channel flow, we will focus on one-dimensional flow along the downstream-oriented axis of the channel. With this understanding, we drop the vector notation and choose the downstream direction as the positive direction. Further, we modify the units of analysis from momentum to momentum per unit of time (momentum flux, also simply known as force) with units of  $MLT^{-2}$ .

There are two kinds of forces associated with flow in an open channel: static and dynamic. Consider Figure 3.2 which depicts these two forces in the context of a rectangular open channel of width,  $w$ . The static force ( $F_s$ ) is quantified by the hydrostatic pressure distribution integrated over the depth of flow:

$$F_s = \gamma \cdot w \cdot \frac{y^2}{2} \quad (3.3)$$

The dynamic force ( $F_D$ ) is the product of mass flow rate and the velocity:

$$F_D = \rho \cdot Q \cdot v \quad (3.4)$$

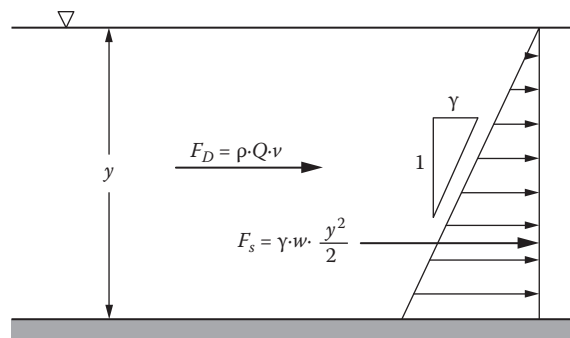


**FIGURE 3.2** Static and dynamic forces associated with a flow.

The total momentum,  $p$ , of a flow is then simply the sum of the static and dynamic forces quantified by equations 3.3 and 3.4:

$$F_s + F_d = \gamma \cdot w \cdot \frac{y^2}{2} + \rho \cdot Q \cdot v \quad (3.5)$$

For simplicity, assume a rectangular channel of unit width ( $w = 1$ ), so equation 3.5 is divided by  $w$ . Also divide equation 3.5 by the density of water,  $\gamma$ . Note that division of  $Q$  by  $w$  produces the unit discharge,  $q$  and that  $\gamma = \rho g$ :

$$\frac{F_s + F_d}{\gamma \cdot w} = \frac{y^2}{2} + \frac{q \cdot v}{g} \quad (3.6)$$

Finally, define  $M$  as the open channel flow *momentum function* which is equal to the left-hand side of equation 3.6. We will also replace  $v$  in the second right-hand-side term of equation 3.6 with the substitution,  $v = q/y$ . The final result is the momentum function (Belanger 1838):

$$M = \frac{y^2}{2} + \frac{q^2}{gy} \quad (3.7)$$

The units of  $M$  in equation 3.7 are  $L^2$ . More appropriately, recalling that equation 3.7 was derived for a channel of unit width, the units of equation 3.7 are thus  $L^3/L$ . In general, the reader should consider the units of the momentum function in the context of open channel flow to be  $L^3$ , reducing to  $L^2$  in the context of a unit width analysis in a rectangular channel.

How does the momentum function vary with depth and discharge? Figure 3.3 shows a family of momentum-depth ( $M$ - $y$ ) curves for  $q = 2, 3, 4$ , and  $5 \text{ m}^2/\text{s}$  over a range of relevant depths. The reader will immediately recognize the similarity of these curves to those shown for specific energy in Figure 2.5. The similarities are obvious: both the  $E$ - $y$  and  $M$ - $y$  relationships have similar shapes with a subcritical and supercritical branch, both curves shift to the right as  $q$  increases and both curves reach a minimum (see Problem 3.3) at critical depth. There are, however, several differences. There is no analog to the  $y = E$  asymptote, and the curve that passes through critical depth is not linear but instead is given by the following (see Problem 3.4):

$$y_c = \sqrt{\frac{2}{3} M_c} \quad (3.8)$$

In Chapter 2, we learned that an alternate depth pair was a pair of depths of flow that both had the same specific energy. One of these flow depths was subcritical and the other supercritical. Because a sluice gate conserves energy and because, under the right conditions, it imposes subcritical conditions upstream and supercritical conditions downstream, the depths observed on opposite sides of the gate are alternate to one another.

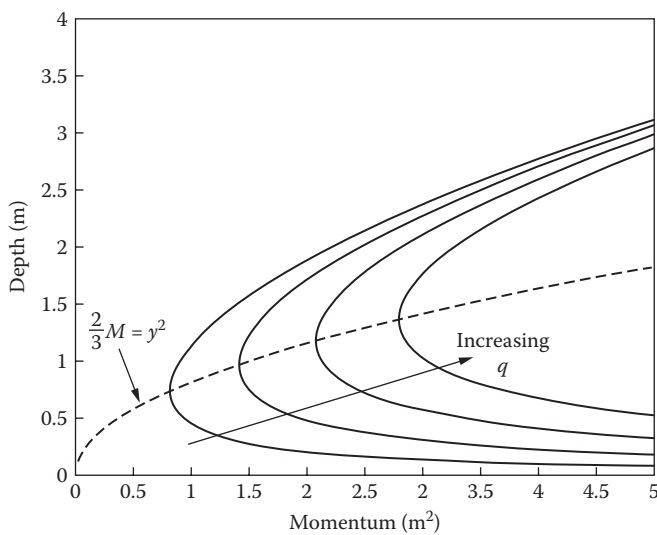


**FIGURE 3.3** A family of  $M$ - $y$  curves for  $q = \{2, 3, 4, 5\} \text{ m}^2/\text{s}$ . Note that the dashed line for  $2/3M = y^2$  crosses each curve at its minimum momentum value.

In an analogous way, a hydraulic jump sets up a pair of depths, supercritical upstream and subcritical downstream, that conserve momentum. These depths are referred to as *conjugate depths*. In the next section, we will derive an analytical relationship between conjugate depths for flows in a rectangular channel.

### 3.3 HYDRAULIC JUMP

Referring back to Figure 3.1, we additionally observe that the hydraulic jump shown is stationary. The jump is translating neither upstream nor downstream. If the jump is stationary then the upstream and downstream sides of the jump depicted in Figure 3.1 are in force balance and it follows that the momentum function on the upstream side of the jump is equal to the momentum function on the downstream side. Thus,  $M_2 = M_3$ , or

$$\frac{y_2^2}{2} + \frac{q^2}{gy_2} - \left( \frac{y_3^2}{2} + \frac{q^2}{gy_3} \right) = 0$$

Our goal is to develop an equation that relates the depth on one side of the hydraulic jump to the depth and flow conditions on the other side of the jump. A bit of algebra is needed:

$$\frac{1}{2}(y_2^2 - y_3^2) - \frac{q^2}{g} \left( \frac{1}{y_3} - \frac{1}{y_2} \right) = 0$$

Factoring the static force term and grouping a common denominator in the dynamic force term, we get:

$$\frac{1}{2}(y_2 + y_3) \cdot (y_2 - y_3) - \frac{q^2}{g} \left( \frac{y_2 - y_3}{y_2 \cdot y_3} \right) = 0$$

Dividing through by  $(y_2 - y_3)$ ,

$$\frac{1}{2}(y_2 + y_3) - \frac{q^2}{g \cdot y_2 \cdot y_3} = 0$$

Multiplying by  $2y_2$ ,

$$y_2^2 + y_2 \cdot y_3 - \frac{2q^2}{g \cdot y_3} = 0$$

This is a quadratic equation for  $y_2$ , with  $a = 1$ ,  $b = y_3$ ,  $c = -2q^2/g y_3$ . Hence,

$$y_2 = \frac{-y_3 \pm \sqrt{y_3^2 - 4 \cdot (1) \cdot \left( \frac{-2q^2}{g \cdot y_3} \right)}}{2}$$

Multiply the second term under the radical by  $y_3^2/y_3^2$  and then factor  $y_3^2$  from both terms under the radical:

$$y_2 = \frac{-y_3 \pm y_3 \sqrt{1 + 8 \cdot \left( \frac{q^2}{g \cdot y_3^3} \right)}}{2}$$

Finally, we observe that  $F_{r,3}^2 = q^2/g \cdot y_3^3$  and take only the positive radical term, so the ultimate result is:

$$y_2 = \frac{y_3}{2} \left( \sqrt{1 + 8 \cdot \frac{q^2}{g \cdot y_3^3}} - 1 \right) = \frac{y_3}{2} \left( \sqrt{1 + 8 \cdot F_{r,3}^2} - 1 \right) \quad (3.9)$$

Notice that the right-hand side of the equation depends only on the conditions at location 3, while the left-hand side depends, obviously, only on the conditions at location 2. Further, since the derivation began from a simple statement of the momentum function value on both the upstream and downstream sides of the jump, the subscripts (2 and 3) can be reversed. In other words, if we know the conditions on one side of the jump, we can use equation 3.9 to solve for the depth on the other side of the jump. In this derivation, the depths  $y_2$  and  $y_3$  are a conjugate depth pair.

### Example 3.1

Consider a system with a specific discharge of  $3 \text{ m}^2/\text{s}$ . The upstream depth,  $y_1$ , is 0.54 meters.

- Determine the upstream Froude number,  $F_{r,1}$ , and specific energy,  $E_1$ .
- If a hydraulic jump spontaneously occurs from this depth, determine the downstream conjugate depth,  $y_2$ , and downstream specific energy,  $E_2$ .

- c. Show that both the upstream and downstream conditions correspond to the same momentum.
- d. On a pair of  $E$ - $y$  and  $M$ - $y$  diagrams, show the conditions at locations 1 and 2.
- e. A smooth, upward step that is just sufficient to force the flow to critical conditions appears in the channel. This upward step is immediately followed by a smooth downward step back to the original channel bottom. Flow downstream of the step is observed to be subcritical. What is the height,  $\Delta z$ , of this smooth, critical step?
- f. For the critical step determined in part (e), determine the downstream depth,  $y'_2$ , and downstream specific energy,  $E'_2$ .
- g. Contrast the downstream conditions from the hydraulic jump and from the critical step. Why do downstream conditions differ? How much energy is lost in the hydraulic jump? If supercritical flow is to give way to subcritical flow downstream, which of the two calculated conditions is more likely to be observed?

**Solution:**

- a. The upstream Froude number was calculated in Example 2.1(e) as 2.41 (i.e., supercritical flow) and in Example 2.1(d) the upstream energy,  $E_1$ , was found to be 2.11 m.
- b. Applying the hydraulic jump equation,

$$y_2 = \frac{y_1}{2} \left( \sqrt{1 + 8 \cdot F_{r,1}^2} - 1 \right) = \frac{0.54}{2} \left( \sqrt{1 + 8 \cdot (2.41)^2} - 1 \right) = 1.59 \text{ m}$$

The downstream specific energy is

$$E_2 = \frac{(3.0)^2}{2 \cdot (9.81) \cdot (1.59)} + 1.59 = 1.77 \text{ m}$$

- c. The momentum function at location 1 ( $y_1 = 0.54$  m) is

$$M_1 = \frac{y_1^2}{2} + \frac{q^2}{gy_1} = \frac{(0.54)^2}{2} + \frac{(3.0)^2}{(9.81) \cdot (0.54)} = 1.84 \text{ m}^2$$

The momentum function at location 2 ( $y_2 = 1.59$  m) is

$$M_2 = \frac{(1.59)^2}{2} + \frac{(3.0)^2}{(9.81) \cdot (1.59)} = 1.84 \text{ m}^2$$

Therefore,

$$M_1 = M_2$$

- d. Figure 3.4 shows flow conditions at locations 1 and 2 (upstream and downstream of the hydraulic jump). Also shown is the energy loss,  $\Delta E$ , in the hydraulic jump. This loss is calculated quantitatively in part (g) of this example.
- e. Critical energy for this specific discharge is

$$E_c = \frac{3}{2} \cdot \sqrt[3]{\frac{(3.0)^2}{9.81}} = 1.46 \text{ m}$$

Therefore,  $\Delta z$  is determined by the difference between  $E_1$  and  $E_c$ :

$$\Delta z = 2.11 - 1.46 = 0.65 \text{ m}$$

- f. The depth and specific energy for the subcritical conditions downstream of the critical step determined in part (e) correspond simply to the alternate depth to  $y_1 = 0.54$  determined in Example 2.1,

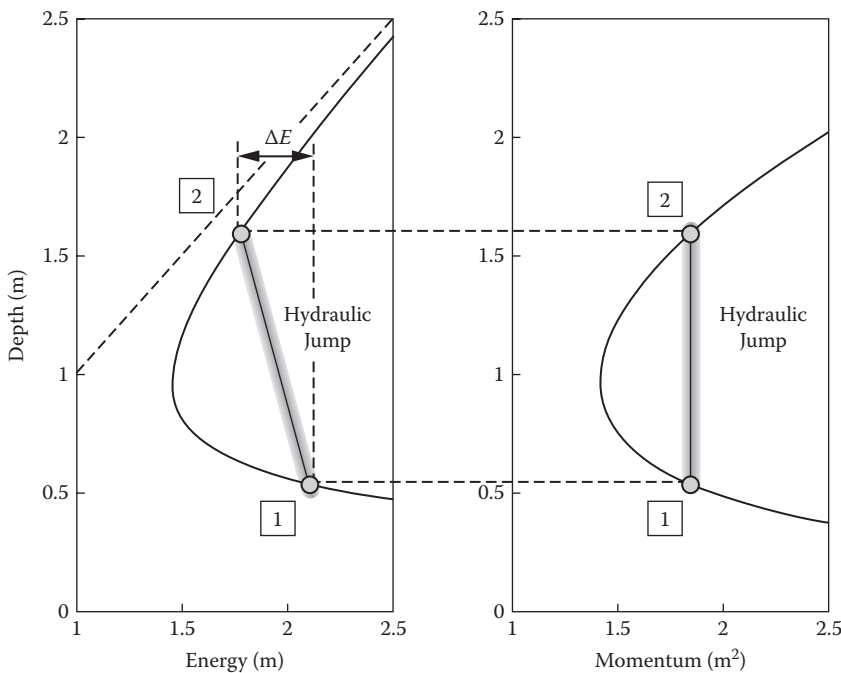


**FIGURE 3.4**  $E$ - $y$  and  $M$ - $y$  curves for  $q = 3 \text{ m}^2/\text{s}$  and the graphical solution to Example 3.1. The energy lost in the hydraulic jump is indicated by  $\Delta E$ .

so  $y'_2 = 2$  m, and since energy is conserved in this case, the specific energy,  $E'_2 = 2.11$  m.

- g. Although both the hydraulic jump and critical step problems start with the same upstream conditions, energy is lost in the jump but is conserved in the flow over the step. The pair of depths calculated in part (b) are conjugate to one another. The pair of depths presented in part (f) are alternate to one another.

The conditions downstream of the jump have less energy relative to the conditions downstream of the step. We can calculate the energy lost in the jump by subtracting the specific energy downstream of the jump from that upstream of the jump:

$$\Delta E = 2.11 - 1.77 = 0.34 \text{ m}$$

The likelihood of encountering a smooth upward step that is just high enough to force critical flow (making subcritical flow accessible downstream) but not serve as a choke is very small. In contrast the hydraulic jump requires no unusual conditions, only that supercritical flow exists upstream and conditions downstream favor subcritical flow.

### 3.4 ENERGY AND MOMENTUM LOSSES

In Example 3.1 the reader sees the computation of the downstream (subcritical) conjugate depth to the given upstream (supercritical) depth. The reader also learns that energy is lost in the hydraulic jump. In this section we explore how energy losses relate to the flow conditions. Symmetrically, we explore momentum losses in the context of flow through a sluice gate.

As discussed in the introductory section of this chapter, the statement was made that if one conservation law does not address the desired unknown, then the other law is likely to provide the missing information. This is the case with determining the energy loss in the hydraulic jump. Based on the specific energy equation alone, we cannot determine the loss of energy in the jump because this equation provides no guidance on how to determine the depth on one side of the jump given the depth on the other side. But as we found in the previous section, conservation of momentum allows us to do precisely this calculation. Once we know the depths, specific energy can be calculated using either Equation 2.8 or 2.12. Considering Figure 3.1, the energy is lost by the flow as it jumps from the upstream location 2 (with energy,  $E_2$ ) to the

downstream location 3 (with energy  $E_3$ ). The energy lost in the jump is simply  $E_2 - E_3$ . More generally, Figure 3.5 shows relative energy loss,  $E_L$ :

$$E_L = 100 \cdot \frac{E_2 - E_3}{E_3} \quad (3.10)$$

where  $E_L$  is in units of percent as a function of the upstream Froude number. The figure shows the positive relationship between these two quantities. In other words, the more supercritical the upstream flow, the more energy that is dissipated in the jump. Returning to Figure 3.3, it should be clear that the more supercritical the flow upstream of the jump, the more subcritical will be the flow downstream of the jump.

In Chapter 2 when the sluice gate problem was first presented, you may have wondered how energy could be conserved across the gate. In truth, energy is conserved, but the flowing water impinges upon the gate with the gate imparting an equal force back upon the flowing water. This force that the gate imparts back upon the flow results in a loss of momentum possessed by the flow. That loss of momentum can be calculated by applying equation 3.7 for the depths observed just upstream (at location 1 in Figure 3.1) and downstream (at location 2) of the sluice gate. We illustrate this momentum loss calculation in Example 3.2.

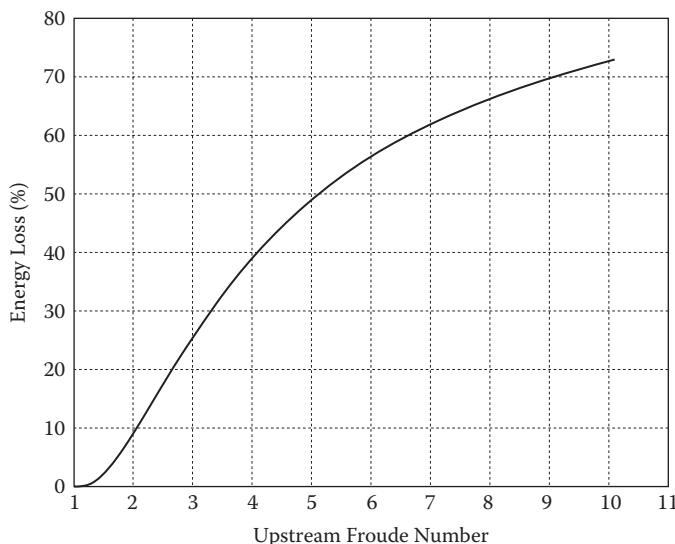


**FIGURE 3.5** Relative energy loss as a function of upstream Froude number. This was generated based on a rectangular cross-section with  $q = 1 \text{ m}^2/\text{s}$ .

**Example 3.2**

We return to the system studied in Example 3.1. A sluice gate is placed upstream of the supercritical depth specified ( $y_1$  is 0.54 meters). Recall that the specific discharge is  $3 \text{ m}^2/\text{s}$ .

- Assuming energy conservation across the sluice gate, determine the depth,  $y_0$ , upstream of the gate.
- Determine the momentum corresponding to the flow upstream of the gate.
- Determine the momentum corresponding to the flow downstream of the gate.
- Determine the momentum loss as indicated by the results in parts (b) and (c), and use this momentum loss to determine the thrust imparted by the gate on the flow.

**Solution:**

- Using the alternate depth equation,

$$y_0 = \frac{2y_1}{-1 + \sqrt{1 + \frac{8gy_1^3}{q^2}}} = \frac{2 \cdot (0.54)}{-1 + \sqrt{1 + \frac{8 \cdot (9.81) \cdot (0.54)^3}{(3.0)^2}}} = 2.0 \text{ m}$$

- The momentum function for  $y_0 = 2 \text{ m}$  gives

$$M_0 = \frac{y_0^2}{2} + \frac{q^2}{gy_0} = \frac{(2.0)^2}{2} + \frac{(3.0)^2}{(9.81) \cdot (2.0)} = 2.46 \text{ m}^2$$

- The momentum function for  $y_1 = 0.54 \text{ m}$  was determined in Example 3.1 as  $M_1 = 1.84 \text{ m}^2$ .
- The momentum loss is shown in Figure 3.6 and is calculated as

$$\Delta M = M_0 - M_1 = 2.46 - 1.84 = 0.62 \text{ m}^2$$

The “thrust” is simply the net force,  $F$ , imparted by the gate on the flowing water. It is calculated as

$$\begin{aligned} \frac{F}{b} &= \rho g \Delta M = \left( 1000 \frac{\text{kg}}{\text{m}^3} \right) \cdot \left( 9.81 \frac{\text{m}}{\text{s}^2} \right) \cdot (0.62 \text{ m}^2) \\ &= 6.1 \frac{\text{kN}}{\text{m}} \end{aligned}$$

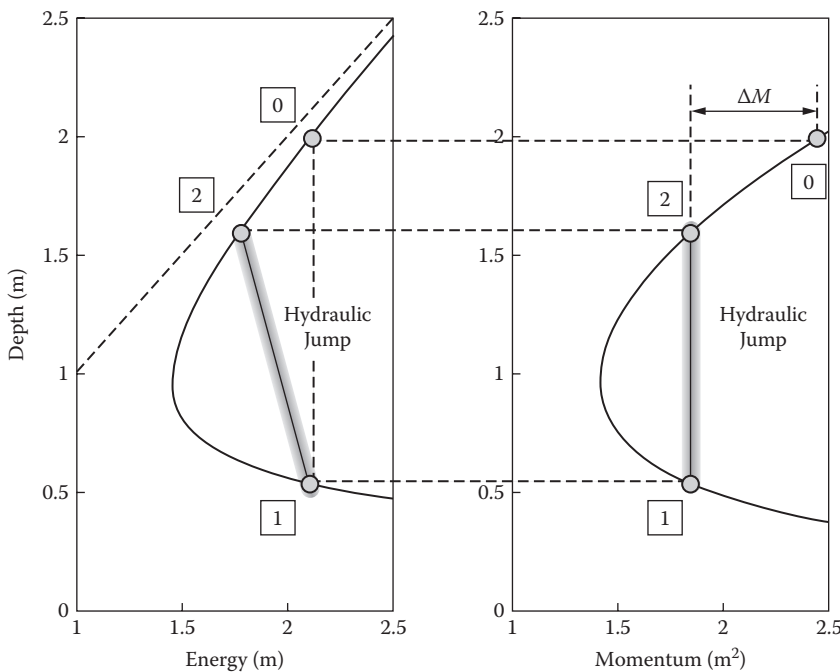


**FIGURE 3.6**  $E-y$  and  $M-y$  curves for  $q = 3 \text{ m}^2/\text{s}$  and the graphical solution to Example 3.2. The momentum lost across the gate (from position 0 to position 1) is indicated by  $\Delta M$ .

Note that this force has been calculated per unit width of the channel since the overall width of the system was not provided in the problem statement.

### Animation: gatejump.avi

Flow conditions:

$$q = 20 \text{ ft}^2/\text{s}$$

Initial upstream depth is 3 ft

Channel is rectangular

Channel is frictionless

Apparent movement: Sluice gate lowers starting from  $y_1 = 3 \text{ ft}$  and passes through critical depth, alternate to  $y_1$ , and ultimately

becomes a choke as it closes down to a minimum depth of 1 ft. When it becomes a choke the animation shows the flow backing up behind the gate and leading to more dramatic hydraulic jumps downstream of the gate.

Still image of animation is shown in Figure 3.7

This animation shows a gate lowering into a subcritical flow in a horizontal, frictionless, rectangular flume. There are three depths of interest: upstream of the gate, immediately downstream of the gate (alternate to upstream gate depth), and downstream of the hydraulic jump (if present).

The top subplot shows the water surface and an animation of the effect of the sluice gate on the downstream depth and ultimately on the

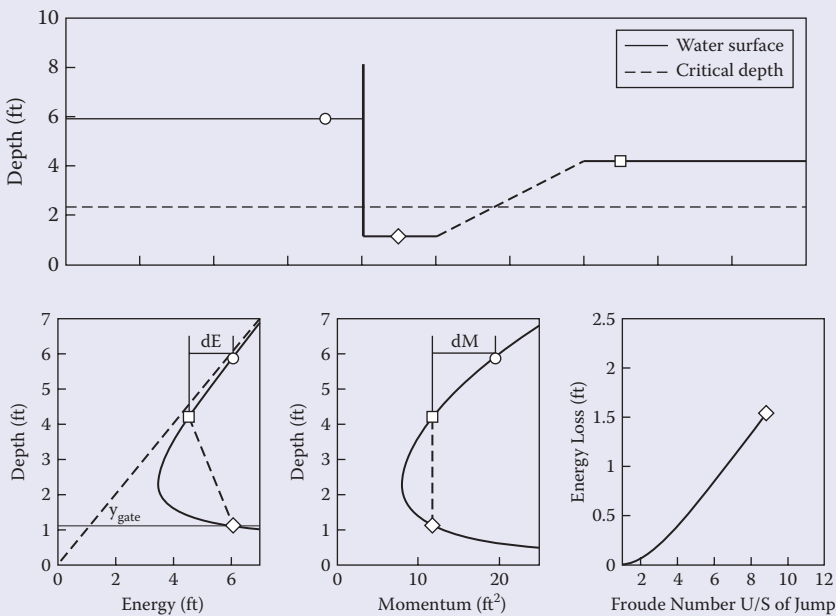


**FIGURE 3.7** Screen capture from *gatejump.avi* animation. The capture shows a sluice gate followed by a hydraulic jump. In the lower plots, the circle shows flow conditions upstream of the gate, the diamond shows conditions immediately downstream of the gate, and the square shows conditions downstream of the hydraulic jump. Energy loss ( $\Delta E$ ) in the jump and momentum loss ( $\Delta M$ ) at the gate are indicated in the lower left and lower middle subplots, respectively. The energy loss as a function of the upstream Froude number is shown in the lower right subplot.

hydraulic jump that occurs downstream. The bottom subplot is divided in three. The bottom left subplot shows the  $E$ - $y$  diagram with the depths at the three locations indicated (if appropriate). The gate opening is indicated on the  $E$ - $y$  diagram by a thin horizontal line marked  $y_{gate}$ . The  $E$ - $y$  diagram is useful for seeing the following:

1. Alternate depth
2. The effect of a choke when the gate depth decreases to less than the alternate depth to the initial upstream depth
3. The energy loss in a hydraulic jump

The bottom middle subplot shows the  $M$ - $y$  diagram with the depths at the three locations indicated (if appropriate). The  $M$ - $y$  diagram is useful for seeing the following:

1. Conjugate depths
2. Loss in momentum at the sluice gate

The bottom right subplot, similar to Figure 3.5, shows the loss of energy in the hydraulic jump as a function of the Froude number upstream of the jump.

### 3.5 DIMENSIONLESS ENERGY AND MOMENTUM

In Chapter 2 an analytical relationship was presented for calculating one alternate depth as a function of the flow characteristics and the other alternate depth in a rectangular channel. The derivation for that relationship is presented here in the larger context of a study of dimensionless versions of both the specific energy equation and the momentum function.

We can develop a dimensionless form of the energy equation (Henderson 1966) in a rectangular channel by dividing equation 2.12 by  $y_c$  and noting from equation 2.13 that  $q^2$  can be replaced with  $gy_c^3$ . The result gives

$$E' = \frac{E}{y_c} = \frac{y}{y_c} + \frac{gy_c^3}{2gy_c y^2} = y' + \frac{1}{2(y')^2} \quad (3.11)$$

where  $E'$  is defined as  $E/y_c$ , and  $y'$  is defined as  $y/y_c$ .

In an analogous way, dividing equation 3.7 by  $y_c^2$  produces a dimensionless version of the momentum equation (Henderson 1966):

$$M' = \frac{M}{y_c^2} = \frac{q^2}{g y y_c^2} + \frac{y^2}{2 y_c^2} = \frac{1}{y'} + \frac{(y')^2}{2} \quad (3.12)$$

Henderson (1966) points out that a duality of the energy and momentum equations can be obtained by observing that the extreme right-hand sides of equations 3.11 and 3.12 take on the same functional form if we define a new term:

$$y'' = \frac{1}{y'} = \frac{y_c}{y} \quad (3.13)$$

For instance, substituting equation 3.13 into equation 3.11 results in

$$E'' = \frac{y_c}{E} = \frac{1}{y''} + \frac{(y'')^2}{2} \quad (3.14)$$

which is the identical functional relationship as was determined for the dimensionless momentum function in equation 3.12. Therefore, any result that applies to the dimensionless momentum function would likewise apply to the dimensionless energy equation, provided the  $y''$  transform from equation 3.13 is used. We use this observation to develop an analytical expression for alternate depths in a rectangular channel, starting from the analytical expression for conjugate depths in a rectangular channel.

The conjugate depth relationship was derived earlier with the final forms of this relationship presented in equation 3.9, repeated below with only the subscripts altered:

$$y_2 = \frac{y_1}{2} \left( \sqrt{1 + 8 \cdot \frac{q^2}{g \cdot y_1^3}} - 1 \right) = \frac{y_1}{2} \left( \sqrt{1 + 8 \cdot F_{r,1}^2} - 1 \right) \quad (3.9)$$

where  $F_{r,1}$  is the Froude number at location 1 (which can be chosen to be either the head or toe of the hydraulic jump). We can take advantage of the duality between the energy and momentum equations by determining the analog

to equation 3.9 for the energy equation. Such an analog would produce an analytical relationship between alternate depths  $y_1$  and  $y_2$ .

The first step is to determine the analog to  $F_{r,1}$  for such a relationship. We observe that the dimensionless momentum equation has a value of  $y'$  equal to unity at critical depth. If we choose\*

$$q = \sqrt{g}$$

then the resulting  $M$ - $y$  relationship will be numerically identical to the  $M$ - $y'$  relationship since  $y_c$  is unity. For this unit discharge,  $q$ , the Froude number simplifies to:

$$F_r(q = \sqrt{g}) = \frac{v}{\sqrt{gy}} = \frac{q}{\sqrt{gy^3}} = \frac{\sqrt{g}}{\sqrt{gy^3}} = \frac{1}{\sqrt{y^3}}$$

We can express the analog of the  $F_{r,1}$  in equation 3.9 as

$$\tilde{F}_{r,1} = \frac{1}{\sqrt{(y''_1)^3}}$$

where the tilde in the  $\tilde{F}_{r,1}$  symbol indicates that this is simply the energy equation analog to the Froude number in this analysis. The remainder of the solution follows naturally from substitution in equation 3.9:

$$y''_2 = \frac{y''_1}{2} \left[ -1 + \sqrt{1 + \frac{8}{(y''_1)^3}} \right] \quad (3.15)$$

Observing that  $y_2 = y_c/y''_2$ , and replacing  $(y''_1)^3$  with  $q^2/gy_1^3$ , equation 3.15 can be simplified to

$$y_2 = \frac{2y_1}{-1 + \sqrt{1 + \frac{8gy_1^3}{q^2}}} = \frac{2y_1}{-1 + \sqrt{1 + \frac{8}{F_{r,1}^2}}} \quad (2.23)$$

---

\* Please note that this relationship is used for mathematical convenience and that we are equating only the numerical magnitudes. The units of  $q$  and  $g$  are not dimensionally consistent with this relationship.

which is the final result presented earlier in Chapter 2. Notice that because of the symmetry of the original equation 3.9 for conjugate depths, the result in 2.23 applies regardless of the Froude number at location 1. That is,  $y_1$  may correspond to either supercritical or subcritical flow conditions. Equation 2.23 will yield the alternate depth to  $y_1$  corresponding to the opposite flow regime in either case.

### 3.6 MOMENTUM IN NON-RECTANGULAR CHANNELS

We are now ready to generalize the discussion of the momentum function to apply to non-rectangular channel cross-sections. Equation 3.7, derived earlier in this chapter, described the momentum function in a rectangular cross-section. We now generalize from equation 3.7 by stating that the momentum function for any cross-sectional shape is quantified as

$$M = A\bar{y} + \frac{Q^2}{gA} \quad (3.16)$$

The reader may recall that the units of equation 3.7 were  $L^2$  or, more appropriately,  $L^3/L$ . Thus, the units of  $M$  in equation 3.16 are  $L^3$ , as the concept of unit width is undefined in non-rectangular sections. As in equation 3.7, the left term on the right-hand side of equation 3.16 represents the hydrostatic force component of momentum while the right term represents the dynamic force component. The term,  $\bar{y}$ , represents the depth of the centroid of the cross-sectional area *as measured from the top of the water surface*.

We will again focus on specific characteristics of the trapezoidal and circular channel cross-sections. We remind the reader that the centroid of a rectangular channel flowing at depth,  $y$ , is located at  $y/2$ . The centroid of a triangular area (see Figure 3.8) is located at a distance of  $y/3$  from the water surface. Given these geometric facts, the reader should be able to derive (see Problem 3.9) that the hydrostatic term of the momentum function for a trapezoidal cross-section becomes

$$[A\bar{y}]_{trapezoid} = \frac{y^2}{6}(2my + 3b) \quad (3.17)$$

In the case of a circular cross-section, the calculation of  $A\bar{y}$  depends on the simple geometry of a circle, as presented in Figure 3.9. Assuming the depth of

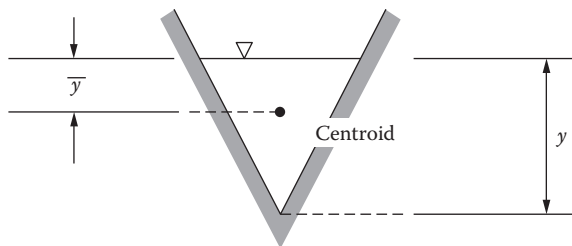


**FIGURE 3.8** The quantity,  $\bar{y}$ , is the distance from the water surface to the centroid of the channel cross-section.

flow,  $y$ , is less than the radius of the circular cross-section the following equations apply:

$$\theta = 2 \cos^{-1} \left( \frac{r - y}{r} \right) \quad (3.18)$$

$$\bar{y} = \frac{4r \sin^3 \left( \frac{\theta}{2} \right)}{3(\theta - \sin \theta)} - r \cos \left( \frac{\theta}{2} \right) \quad (3.19)$$

$$A = \frac{r^2}{2} (\theta - \sin \theta) \quad (3.20)$$

Remember that  $\theta$  in equations 3.18 through 3.20 is in units of radians, not degrees. (In Problem 3.12, equations 3.18 through 3.20 are used and some basic geometric principles are applied to modify the above equations if the flow depth exceeds the radius of the circular section.) Owing to the tediousness of the application of these equations, the Appendix of this book presents several circular section properties (e.g. area, wetted perimeter, hydraulic radius, top width, hydraulic depth, centroid depth) in dimensionless form. This reduces

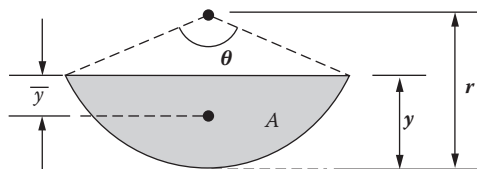


**FIGURE 3.9** Definition sketch for flow in a circular cross-section flowing less than half full. Refer to equations 3.18 through 3.20 to determine  $\bar{y}$  and  $A$ .

the tedium and potential for error to a minimum. Before going forward, let's briefly explore the mechanics of calculation of the momentum function in non-rectangular sections.

### **Example 3.3**

Determine the momentum function for the following three non-rectangular settings:

- A trapezoidal cross-section with  $b = 5.0 \text{ m}$ ,  $m = 2$ ,  $Q = 10 \text{ m}^3/\text{s}$ , and  $y = 0.5 \text{ m}$ .
- A trapezoidal cross-section with  $b = 5.0 \text{ m}$ ,  $m = 2$ ,  $Q = 10 \text{ m}^3/\text{s}$ , and  $y = 2.0 \text{ m}$ .
- A circular cross-section with  $D = 5.0 \text{ m}$ ,  $Q = 10 \text{ m}^3/\text{s}$ , and  $y = 0.5 \text{ m}$ .

#### **Solution:**

- The cross-sectional area of a trapezoidal cross-section for the geometry given is calculated as

$$A = by + my^2 = 5 \cdot (0.5) + 2 \cdot (0.5)^2 = 3.0 \text{ m}^2$$

The momentum function then gives

$$\begin{aligned} M &= A\bar{y} + \frac{Q^2}{gA} = \frac{y^2}{6}(2my + 3b) + \frac{Q^2}{gA} \\ &= \frac{(0.5)^2}{6}(2 \cdot 2 \cdot (0.5) + 3 \cdot 5) + \frac{(10)^2}{(9.81) \cdot (3.0)} = 4.11 \text{ m}^3 \end{aligned}$$

- Similar to part (a), the cross-sectional area is

$$A = 5 \cdot (2.0) + 2 \cdot (2.0)^2 = 18.0 \text{ m}^2$$

The momentum function then gives

$$M = \frac{(2.0)^2}{6}(2 \cdot 2 \cdot (2.0) + 3 \cdot 5) + \frac{(10)^2}{(9.81) \cdot (18.0)} = 15.9 \text{ m}^3$$

- The area of a circular cross-section for the geometry given is calculated using the Appendix of this book. For the given problem we have

$$\frac{y}{D} = \frac{0.5}{5.0} = 0.1$$

Entering the Appendix for  $y/D = 0.1$ , we find that  $A/D^2 = 0.0409$ , and  $\bar{y}/D = 0.0404$ . Thus,

$$A = \frac{A}{D^2} \cdot D^2 = 0.0409 \cdot (5.0)^2 = 1.0225 \text{ m}^2$$

and

$$\bar{y} = \frac{\bar{y}}{D} \cdot D = 0.0404 \cdot (5.0) = 0.202 \text{ m}$$

Thus, the momentum function becomes

$$M = A\bar{y} + \frac{Q^2}{gA} = (1.0225) \cdot (0.202) + \frac{(10)^2}{(9.81) \cdot (1.0225)} = 10.2 \text{ m}^3$$


---

With the application of the general equation for the momentum function under control, the natural next question is how to determine conjugate depths in non-rectangular settings. Two papers published in the early 1960s developed the mathematics to graphically depict the relationship between upstream and downstream conjugate depths as a function of discharge, channel geometry, and flow conditions upstream of the jump.

For trapezoidal cross-sections, Massey (1961) developed the expression:

$$\frac{Q}{my_1^2 \sqrt{gy_1}} = \sqrt{\frac{\left(\frac{y_2}{y_1}\right)^4 + [(2.5)k+1]\left(\frac{y_2}{y_1}\right)^3 + (1.5k+1)(k+1)\left(\frac{y_2}{y_1}\right)^2 + (1.5k+1)k\left(\frac{y_2}{y_1}\right)}{3\left[\frac{y_2}{y_1(k+1)} + 1\right]}} \quad (3.21)$$

where  $k$  is the channel geometry form factor:

$$k = \frac{b}{my_1} \quad (3.22)$$

As a practical matter, the above mathematics are of limited value. More useful is to explore equation 3.21 for a number of trapezoidal cross-section geometry

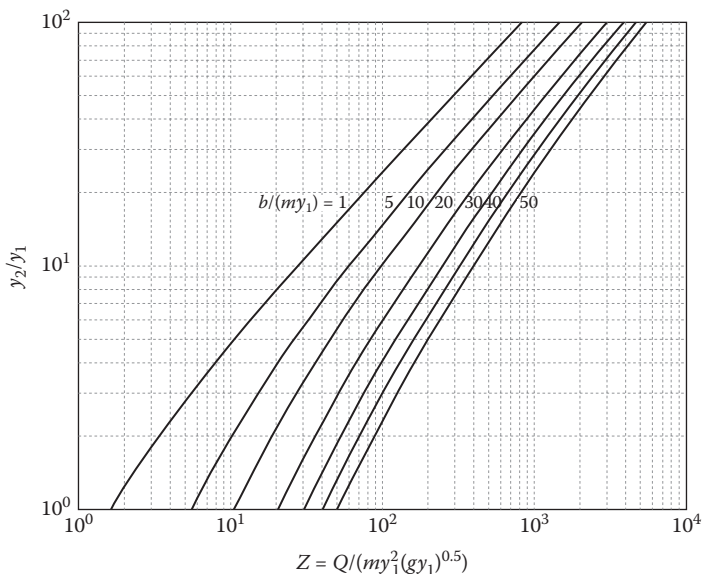


**FIGURE 3.10** Hydraulic jump characteristics in a trapezoidal channel.

ratios ( $k$ ) and for a range of jump depth ratios ( $y_2/y_1$ ). Figure 3.10 presents exactly this exploration of equation 3.21 and provides a more readily usable tool when working with hydraulic jumps in a trapezoidal cross-section.

Similarly, for circular cross-sections, Thiruvengadam (1961) developed the following expression:

$$\frac{Q^2}{gy_1^5} = \frac{\lambda_1 \lambda_2 \frac{D^2}{y_1^2} \left[ \left( \frac{y_2}{y_1} \right)^3 \frac{\theta_2}{\lambda_2} - 1 \right]}{1 - \frac{\lambda_1}{\theta_1}} \quad (3.23)$$

where

$$\lambda_1 = \frac{1}{4} \cos^{-1} \left( 1 - 2 \frac{y_1}{D} \right) - \frac{1}{2} \left( 1 - 2 \frac{y_1}{D} \right) \sqrt{\frac{y_1}{D} - \left( \frac{y_1}{D} \right)^2} \quad (3.24)$$

$$\lambda_2 = \frac{2}{3} \left( \frac{D}{y_1} - 1 \right)^{\frac{3}{2}} - \left( \frac{D}{y_1} \right)^2 \lambda_1 \left( \frac{D}{2y_1} - 1 \right) \quad (3.25)$$

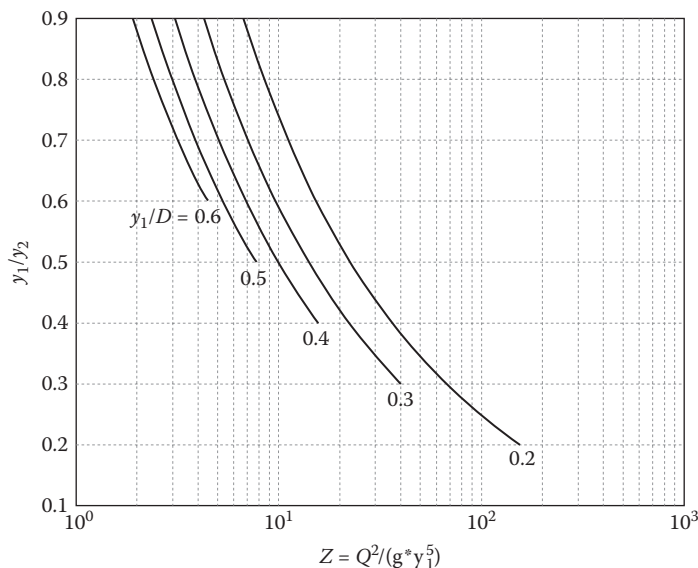


**FIGURE 3.11** Hydraulic jump characteristics in a circular channel.

$$\theta_1 = \frac{1}{4} \cos^{-1} \left( 1 - 2 \frac{y_1}{D} \frac{y_2}{y_1} \right) - \frac{1}{2} \left( 1 - 2 \frac{y_1}{D} \frac{y_2}{y_1} \right) \sqrt{\frac{y_1}{D} \frac{y_2}{y_1} - \left( \frac{y_1}{D} \right)^2 \left( \frac{y_2}{y_1} \right)^2} \quad (3.26)$$

$$\theta_2 = \frac{2}{3} \left( \frac{D}{y_1} \frac{y_2}{y_1} - 1 \right)^{3/2} - \left( \frac{D}{y_1} \right)^2 \left( \frac{y_2}{y_1} \right)^2 \lambda_1 \left( \frac{D}{2y_1} \frac{y_2}{y_1} - 1 \right) \quad (3.27)$$

Similar to the trapezoidal case, Figure 3.11 presents equation 3.23 for a range of upstream depth ratios ( $y_1/D$ ).

#### Example 3.4

Use Figures 3.10 and 3.11 to determine the conjugate depths to the trapezoidal and circular cross-sections and flows examined in Example 3.3. In all cases, be sure to first calculate the Froude number. Once a solution has been reached, check the solution and estimate the error in reading the appropriate figure and use the sign of the error to determine the direction of revision (up or down) for the estimate of  $y_2$ .

- a. Recall that in Example 3.3a we were given a trapezoidal cross-section with  $b = 5.0 \text{ m}$ ,  $m = 2$ ,  $Q = 10 \text{ m}^3/\text{s}$ , and  $y = 0.5 \text{ m}$ . The momentum function was determined to be  $4.11 \text{ m}^3$ .
- b. In Example 3.3b, we were given the same cross-section as in 3.3a but with the depth shifted to  $y = 2.0 \text{ m}$ . The momentum function was determined to be  $15.9 \text{ m}^3$ .
- c. In Example 3.3c, we were given a circular cross-section with  $D = 5.0 \text{ m}$ ,  $Q = 10 \text{ m}^3/\text{s}$ , and  $y = 0.5 \text{ m}$ . The momentum function was determined to be  $10.2 \text{ m}^3$ .

**Solution:**

- a. First we calculate the Froude number:

$$F_r = \frac{Q}{A\sqrt{g\left(\frac{A}{B}\right)}} = \frac{10}{3.0\sqrt{9.81\left(\frac{3.0}{7.0}\right)}} = 1.63$$

Since the Froude number is greater than 1, the flow is super-critical so the depth provided must be the upstream depth,  $y_1$ . Using Figure 3.10, we note that we have all the values to calculate the horizontal axis quantity,  $Z$ :

$$Z = \frac{Q}{my_1^2\sqrt{gy_1}} = \frac{10}{2 \cdot (0.5)^2\sqrt{(9.81) \cdot (0.5)}} = 9.03$$

In addition, we need to calculate the channel geometry factor:

$$\frac{b}{my_1} = \frac{5}{2 \cdot 0.5} = 5.0$$

Entering Figure 3.10 on the horizontal axis at  $Z = 9.03$  (use 9), we trace vertically up to the channel geometry curve corresponding to  $b/my_1 = 5$  and then move horizontally, pulling off the value  $y_2/y_1 = 1.9$ . (This is an approximate estimate.) Solving for  $y_2$ , we get

$$y_2 = \frac{y_2}{y_1} \cdot y_1 = (1.9) \cdot (0.5) = 0.95 \text{ m}$$

Using  $y_2 = 0.95$ , we first calculate the area:

$$A = by + my^2 = 5 \cdot (0.95) + 2 \cdot (0.95)^2 = 6.555 \text{ m}^2$$

The momentum function then gives

$$M = \frac{y^2}{6}(2my + 3b) + \frac{Q^2}{gA} = \frac{(0.95)^2}{6}(2 \cdot 2 \cdot (0.95) + 3 \cdot 5) + \frac{(10)^2}{(9.81) \cdot (6.555)} = 4.38 \text{ m}^3$$

The percent error,  $E$ , in estimating the momentum function is thus,

$$E = \frac{(4.38 - 4.11)}{4.11} \cdot 100\% = 6.6\%$$

Since  $E$  is positive it must be the case that the true value of  $y_2$  is a depth slightly less than 0.95 m. We will find (see Goal Seek toolbox below) that the true value of  $y_2$  is 0.88 m.

b. First we calculate the Froude number:

$$F_r = \frac{Q}{A\sqrt{g \cdot \left(\frac{A}{B}\right)}} = \frac{10}{18.0\sqrt{9.81 \cdot \left(\frac{18.0}{13.0}\right)}} = 0.15$$

Since the Froude number is less than 1, the flow is *subcritical*, so the depth provided must be the *downstream* depth,  $y_2$ . Note that Figures 3.10 and 3.11 are structured in terms of the upstream depth,  $y_1$ , being known. That is not the case with this example. In order to use Figure 3.10, we need to guess a value for  $y_1$ , solve for  $y_2$ , and then see how the actual value of  $y_2$  compares with the calculated value. If necessary, iteration of this approach is indicated until the actual and calculated values of  $y_2$  are essentially equal. Looking at part (a) for guidance, we see that the conjugate depth pair is (0.5 m, 0.95 m). Since  $y_2$  in part (b) is more than twice as big as in part (a), we guess an initial  $y_1$  that is only half as big as  $y_1$  in part (a), thus we guess  $y_1 = 0.25$  m. So,

$$Z = \frac{10}{2 \cdot (0.25)^2 \sqrt{(9.81) \cdot (0.25)}} = 51.1$$

The channel geometry factor is

$$\frac{b}{my_1} = \frac{5}{2 \cdot (0.25)} = 10$$

Entering Figure 3.10 on the horizontal axis at  $Z = 51.1$  (use approximately 50), we trace vertically up to the channel geometry curve corresponding to  $b/m y_1 = 10$ , and then move horizontally, pulling off the value  $y_2/y_1 = 5.7$ . (This is an approximate estimate.) Solving for  $y_2$ , we get

$$y_2 = \frac{y_2}{y_1} \cdot y_1 = (5.7) \cdot (0.25) = 1.42 \text{ m}$$

Since  $1.42 \text{ m} < 2.0 \text{ m}$ , we know that our initial guess for  $y_1$  was too deep. We need to make a new estimate of  $y_1$  smaller than the original guess of 0.25 m. Try  $y_1 = 0.10 \text{ m}$ . Thus  $Z = 504$ , the channel geometry factor is 25, and  $y_2/y_1 = 24$  (approximately), leading to a  $y_2$  estimate of 2.4 m. So our second guess was too shallow, but now we have the solution bounded. Iteration continues in this fashion. Make a final guess for  $y_1$  of 0.12. Thus,  $Z = 320$ , and the channel geometry factor is 20.8, leading to  $y_2/y_1 = 17$  (approximately), leading to a  $y_2$  estimate of 2.04 m (close enough to 2.0 m).

The momentum function then gives

$$M = \frac{(2.04)^2}{6} (2 \cdot 2 \cdot (2.04) + 3 \cdot 5) + \frac{(10)^2}{(9.81) \cdot (18.523)} = 16.6 \text{ m}^3$$

The percent error,  $E$ , is thus

$$E = \frac{(16.6 - 15.9)}{15.9} \cdot 100\% = 4.4\%$$

Since  $E$  is positive, it must be the case that the true value of  $y_1$  is a depth slightly greater than 0.12 m. However, within the confines of using Figure 3.10, it might be difficult to make a more precise estimate of  $y_1$ . Figure 3.10 is tedious to work with when the upstream depth,  $y_1$ , is not known.

- c. Using Figure 3.11, we calculate the horizontal axis quantity:

$$Z = \frac{Q^2}{g y_1^5} = \frac{(10)^2}{(9.81) \cdot (0.5)^5} = 326$$

The channel geometry factor is

$$\frac{y_1}{D} = \frac{0.5}{5.0} = 0.1$$

Entering Figure 3.11 on the horizontal axis at  $Z = 326$  (use best visual approximation of  $Z = 326$ ), we trace vertically up to the channel geometry curve corresponding to  $y_1/D = 0.1$ , and then move horizontally, pulling off the value  $y_1/y_2 = 0.21$ . (This is an approximate estimate.) Solving for  $y_2$ , we get

$$y_2 = \frac{1}{y_1} \cdot y_1 = \frac{0.5}{0.21} = 2.38 \text{ m}$$

The Appendix is used to estimate both  $A$  and  $\bar{y}$ . The depth ratio  $y/D$  is  $2.38/5 = 0.476$ . So as to minimize table errors, we will interpolate values of both  $A$  and  $\bar{y}$  for depths of 0.47 and 0.48. We build a small table to manage this process:

$y/D$	$A/D^2$	$A (m^2)$	$\bar{y}/D$	$\bar{y} (m)$	$A\bar{y}(m^3)$
0.47	0.3627	N/A	0.1985	N/A	N/A
<b>0.476</b>	<b>0.3667</b>	<b>9.1675</b>	<b>0.20126</b>	<b>1.0063</b>	<b>9.225</b>
0.48	0.3727	N/A	0.2031	N/A	N/A

$$M = A\bar{y} + \frac{Q^2}{gA} = (9.225) + \frac{(10)^2}{(9.81) \cdot (9.1675)} = 10.34 \text{ m}^3$$

The percent error,  $E$ , is thus

$$E = \frac{(10.34 - 10.2)}{10.2} \cdot 100\% = 1.4\%$$

As in part (a),  $E$  is positive, so the true value of  $y_2$  is a depth slightly less than 2.38 m. Through the use of the Goal Seek tool, we learn that the true value of  $y_2$  is 2.36 m (very close to our estimate from Figure 3.11).

## Return to Use of Excel Goal Seek Tool

The Goal Seek tool is useful for determining a depth that produces a particular value of specific energy. The same is true for determining a depth that produces a particular value of the momentum function. Consider Example 3.3a in which the momentum function was determined to equal  $4.11 \text{ m}^3$ . We now seek to find the depth  $y_2$  that produces the same value of the momentum function as determined in Example 3.3a:

$$4.11 = \frac{y_2^2}{6} (2my_2^2 + 3b) + \frac{Q^2}{g(by_2 + my_2^2)} \quad (3.28)$$

The value for  $y_2$  that satisfies the momentum function and corresponds to subcritical flow conditions will be the conjugate depth to the original  $y_1 = 0.5 \text{ m}$  specified in Example 3.3a. We again turn to the Excel Goal Seek tool.

1. In Excel set aside several adjacent cells in a spreadsheet for executing the Goal Seek solution.
2. In this case, the depth  $y$  is the value being sought. One cell of the spreadsheet should contain exclusively this quantity. Let us assume that spreadsheet cell C3 contains this quantity. We enter a large initial value of  $y_2 = 100 \text{ m}$  in this cell. We do this for two reasons: (1) so that cell formulas dependent on this cell are able to calculate as the spreadsheet is being generated, and (2) a large value is chosen so that the root searching process will be biased toward selecting the large value of  $y$  that satisfies the momentum function. The large value for depth will correspond to subcritical conditions.
3. Following an analogous approach to the Goal Seek demonstration in Chapter 2, we program equation 3.28 into the spreadsheet, say in cell D3. We then use the Goal Seek function to adjust the value in cell C3 until the value in cell D3 is equal to  $4.11 \text{ m}^3$ . Goal Seek returns that desired value of  $y_2 = 0.88 \text{ m}$ .

To summarize this discussion on momentum in non-rectangular cross-sections, there are several take-away messages regarding determination of one conjugate depth value given the other value:

- For a trapezoidal or circular cross-section, if the upstream conjugate depth,  $y_1$ , is known, then the use of either Figure 3.10 or Figure 3.11 to determine the downstream depth,  $y_2$ , is straightforward and reasonably accurate.
- Because of the presence of logarithmic scales and because channel geometry curves are provided for only a limited number of values, answer precision degrades if the analyst must interpolate between channel geometry curves or widely spaced logarithmic grid lines.
- If the downstream depth is known and upstream depth is sought, Figures 3.10 and 3.11 can be used, but an iterative process is required that can be tedious.
- A “brute force” approach of simply iterating on estimated depth until a desired value of the momentum function is obtained will always work, but is tedious.
- The use of Excel’s Goal Seek program automates the brute force technique and is easy to employ as long as the channel geometry (area and depth of centroid) is readily programmed into the spreadsheet. (Such spreadsheet programming is the subject of Problems 3.10, 3.11, and 3.13.)

### 3.7 SUMMARY

This chapter explored the implications of momentum on flow in open channels. The simple, momentum-conserving hydraulic jump was explored throughout this chapter. The momentum function was derived for flow in rectangular channels and also provided for flow in non-rectangular channels. Analogous to the concept of alternate depths, the concept of conjugate depths was introduced. Conjugate depths are a pair of depths that correspond to the same value of the momentum function and are the depths that appear immediately upstream and downstream of a simple hydraulic jump. An analytical expression for conjugate depth pairs in a rectangular channel was derived. By applying the specific energy equation to the depths on opposite sides of a hydraulic jump, we were able to quantify the energy loss across a hydraulic jump. In a similar way, we returned to the sluice gate problem of Chapter 2 and determined the value of the momentum function upstream and downstream of

the sluice gate to determine the momentum loss and the net force (or thrust) exerted by the gate on the flow.

Following Henderson's (1966) approach, dimensionless versions of the specific energy and momentum function equations in rectangular channels were derived and it was shown that a simple transformation could be employed that rendered the dimensionless versions of these equations identical. Using this dimensionless relationship and the previously derived analytical relationship between conjugate depths in a rectangular channel, the analytical relationship between alternate depths (previously presented without proof in Chapter 2) was derived.

Finally, a general momentum function equation for flow in non-rectangular channels was explored along with specific approaches for applying momentum concepts in trapezoidal and circular cross-sections. Two figures were presented that allow for relatively rapid and easy calculation of the downstream conjugate depth in trapezoidal and circular cross-sections, given the upstream conjugate. Similar to Chapter 2 for the determination of an alternate depth given a known specific energy, the Excel "Goal Seek" function was again presented as a useful tool for determination of a conjugate depth given a known value of the momentum function. We conclude with Table 3.1 which summarizes some additional useful relationships developed in this chapter.

**TABLE 3.1** Summary Table of Momentum-Related Open Channel Flow Relationships

Quantity	Rectangular Section	Irregular Section (e.g., Trapezoidal, Circular)
Momentum function	$M = \frac{y^2}{2} + \frac{q^2}{gy}$	$M = A\bar{y} + \frac{Q^2}{gA}$ (general) $M = \frac{y^2}{6}(2my + 3b) + \frac{Q^2}{gA}$ (trapezoidal)
Conjugate depths	$y_2 = \frac{y_1}{2} \left( \sqrt{1 + 8 \cdot \frac{q^2}{g \cdot y_1^3}} - 1 \right)$	Use Figure 3.10 (trapezoidal), Figure 3.11 (circular), or Goal Seek
Force (or net thrust)	$F = \gamma \cdot \Delta M \cdot b$	$F = \gamma \cdot \Delta M$

## References

- Belanger, J.B. (1838). *Summary of Lectures*, Paris, France.
- Henderson, F.M. (1966). *Open Channel Flow*, Macmillan, New York, NY.
- Massey, B.S. (1961). Hydraulic jump in trapezoidal channels—an improved method. *Water Power*, 13(June), 232 and 237.
- Thiruvengadam, A. (1961). Hydraulic jump in circular channels. *Water Power*, 13(December), 496–497.

## Problems

- 3.1. Given a rectangular channel with  $q = 10, 20$ , and  $30 \text{ ft}^2/\text{s}$ , calculate the momentum function over a range of depths,  $y$ , from 0 to 8 feet. Make a plot with the momentum function on the horizontal axis and  $y$  on the vertical axis. To make the graph easily viewable, please limit the horizontal axis so it covers only  $0 \leq M \leq 30 \text{ ft}^2$ . Please be sure to label your axes and clearly indicate the  $q$  value for each of the three curves.
- 3.2. Using  $Q = 400 \text{ ft}^3/\text{s}$ , calculate the momentum function over a range of depths,  $y$ , from 0 to 8 feet. The flow is in a trapezoidal section with a bottom width,  $b = 4$  feet, and side-slope parameter,  $m = 2$ . Make a plot with the momentum function on the horizontal axis and  $y$  on the vertical axis.
- 3.3. Consider flow in a rectangular channel. Set  $dM/dy = 0$ . Show that this leads to the same value of critical depth,  $y_c$ , as we determined based on specific energy. Namely, that  $y_c = (q^2/g)^{1/3}$ , and thus critical depth is the same from both standpoints of energy and momentum.
- 3.4. Consider equation 3.7 at critical flow conditions:  $y$  becomes  $y_c$  and  $M$  becomes  $M_c$ . Use this modified form of equation 3.7 and the old result for critical depth [namely that  $y_c = (q^2/g)^{1/3}$ ] to derive equation 3.8.
- 3.5. A hydraulic jump is formed in a 5 meter wide outlet at a short distance downstream of a control (sluice) gate. If the flow depth upstream of the gate is 9 meters and the discharge is  $150 \text{ m}^3/\text{s}$ , find (1) the flow depth just downstream of the gate, (2) the flow depth downstream of the jump, 3) the thrust on the gate, and 4) the head losses in the jump.
- 3.6. Given a  $q$  of  $25 \text{ ft}^2/\text{s}$  and a sluice gage/jump configuration. What depth upstream of the sluice gate is necessary to dissipate 30% of the original (upstream of the sluice gate) energy? What are the Froude numbers just upstream and downstream of the jump?

- 3.7. A hydraulic jump occurs in a trapezoidal channel with a base width  $b = 20$  feet and side-slope parameter,  $m = 2$ . The downstream depth is 8 feet, and the discharge is 1000 ft<sup>3</sup>/s. Find the upstream depth, the head loss, and the horsepower dissipated in the jump. (Note that Figure 3.10 assumes that the upstream depth,  $y_1$ , is known.) Since  $y_1$  is unknown in this problem, your solution will need to be iterative if using the figure. Alternatively, you can approach the problem using  $M_1 = M_2$  and the Goal Seek function. Reminder: Horsepower ( $hp$ ) is calculated as

$$hp = \frac{\gamma \cdot Q \cdot \Delta h}{550}$$

that is, 1  $hp = 550$  ft-lb/s.

- 3.8. A pipe is 5 meters in diameter and has an upstream depth of  $y_1 = 1.5$  meters. If  $y_2$  is 2.5 meters, what is the discharge in the pipe? What are the upstream and downstream Froude numbers?
- 3.9. Derive the expression for the  $A\bar{y}$  term of a trapezoidal cross-section given a depth,  $y$ , a bottom width  $b$ , and a side-slope parameter,  $m$ .

*Problems 3.10, 3.11, and 3.13 involve modest programming in Excel or a similar spreadsheet application. Once programmed, this spreadsheet can be coupled with the Goal Seek function to determine a conjugate depth once the momentum function value is known.*

- 3.10. Develop a rectangular channel conjugate depth tool. Using Excel, program a spreadsheet that takes as input discharge, depth, channel width, and value for  $g$  (9.81 m/s<sup>2</sup> indicates metric, 32.2 ft/s<sup>2</sup> indicates English units). The spreadsheet calculates the following: area, velocity, Froude number, momentum function, and specific energy.
- 3.11. Develop a trapezoidal channel conjugate depth tool. Using Excel, program a spreadsheet that takes as input discharge, depth, channel bottom width, side-slope parameter, and value for  $g$  (9.81 m/s<sup>2</sup> indicates metric, 32.2 ft/s<sup>2</sup> indicates English units). The spreadsheet calculates the following: area, velocity, top width, Froude number, depth of centroid ( $\bar{y}$ ), momentum function, and specific energy.
- 3.12. Equations 3.18 through 3.20 apply to flow in a circular cross-section flowing at a depth less than the radius of the section. Develop three new equations for  $\theta$ ,  $\bar{y}$ , and  $A$  that apply in a circular cross-section flowing at a depth greater than the radius of the section.
- 3.13. Develop a circular channel conjugate depth tool. Using Excel, program a spreadsheet that takes as input discharge, depth, channel

diameter, and value for  $g$  (9.81 m/s<sup>2</sup> indicates metric, 32.2 ft/s<sup>2</sup> indicates English units). The spreadsheet calculates the following: area, velocity, top width, Froude number, depth of centroid ( $\bar{y}$ ), momentum function, and specific energy. You may choose to divide your spreadsheet tool into two sections:

- a. Section 1 applies when  $y \leq r$ . Refer to Figure 3.9 and equations 3.18 through 3.20 to calculate the centroid depth,  $\bar{y}$ , and cross-sectional area,  $A$ .
- b. Section 2 applies when  $y > r$ . To calculate the centroid depth,  $\bar{y}$ , and cross-sectional area,  $A$ , keep in mind that you will need to program the equations derived in Problem 3.12, rather than using equations 3.18 through 3.20 directly.



# Friction and Uniform Flow

## CHAPTER OBJECTIVES

1. Introduce the concept of friction.
2. Derive Chézy's equation and compare it to Manning's equation.
3. Define concepts of uniform flow and normal depth.
4. Examine how normal depth varies as a function of discharge, roughness, channel geometry, and channel slope.
5. Develop a reach classification scheme that distinguishes between channel conditions that favor normal depth that is supercritical, subcritical, or critical.

### 4.1 INTRODUCTORY COMMENTS

In Chapter 2 we studied specific energy from the idealized perspective of a frictionless, horizontal channel. In Chapter 3, we continued to analyze frictionless systems except that we found that energy was lost within a hydraulic jump. In this chapter, we finally relax the assumption of a frictionless channel and explore two commonly used friction equations—Chézy's and Manning's equations. The fundamental concept of *normal depth* is introduced, and how it arises in open channel flow analogously to the concept of terminal velocity in projectile motion is examined. We explore how normal depth varies as a function of the conditions in the channel: discharge, roughness, channel size and shape, and channel slope. To conclude the chapter, a reach classification system is developed that is largely dependent on the relative magnitudes of normal and critical depth.

## 4.2 UNIFORM FLOW

Uniform flow, as its name implies, is flow that is unchanging. Specifically, it is flow that does not change in depth along the direction of flow in an open channel. Also implied is that all the other characteristics affecting flow in an open channel (e.g., discharge, roughness, channel size and shape, and channel slope) are also unchanging along the direction of flow. Under such conditions, we can write:

$$\frac{dy}{dx} = 0 \text{ (uniform flow)} \quad (4.1)$$

where  $y$  is the depth of flow and  $x$  is distance measured in the horizontal plain along the direction of flow. Since  $y$  is constant, it follows that energy,  $E$ , is constant, and we can write that under uniform flow:

$$\frac{dE}{dx} = 0 \text{ (uniform flow)} \quad (4.2)$$

Uniform flow is a concept—an idealization. In the natural world, channel geometry, slope, sediment size, and vegetation are changing constantly. Lateral flows into or out of the channel are also generally present. Uniform flow might actually be realized in engineered channels of sufficient length. In such cases the channel is likely impermeable, so discharge is constant while the geometry and roughness are fixed. Figure 4.1 shows such a case. One might imagine the situation shown in Figure 4.1 occurring in a canal or aqueduct. However, such

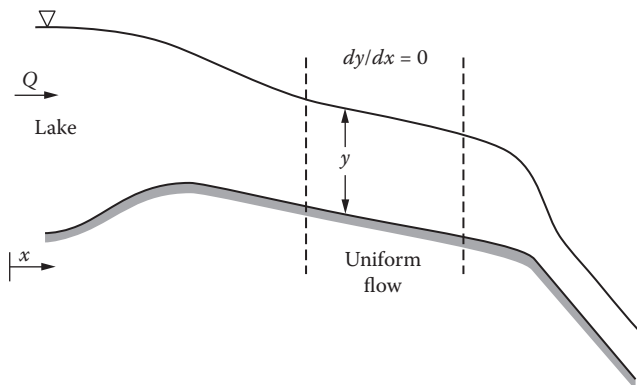


**FIGURE 4.1** Region of uniform flow for reach downstream of a lake and upstream of a break in reach slope. Within the region of uniform flow, the flow depth,  $y$ , does not change with distance,  $x$ .

a case might appear in a more commonplace location, for instance, flow along curb and gutter infrastructure. Uniform flow in this latter setting might occur, for instance, when a homeowner is watering his lawn over a protracted period of time and the lawn drains to the nearby gutter at a constant rate. The gutter is of fixed geometry and material and the slope of the gutter is effectively constant.

Having now exhaustively described the rare setting where uniform flow occurs in actuality, recognize that, in an approximate sense, the factors that control flow are often effectively constant over short distances. In such regions the flow tends toward uniform conditions. The concept of uniform flow provides a useful and powerful framework from which we can describe departures from uniform flow in the following chapters.

Why does uniform flow occur? Uniform flow occurs because a dynamic equilibrium between forces is realized. The force driving the flow, gravity, is balanced by the resisting force, friction. This balance is exactly analogous to the concept of terminal velocity, generally covered in basic mechanics in physics. An object in vertical free fall will undergo gravitational acceleration from an initial velocity of zero. If the vertical fall is long enough, the object will eventually be observed to be falling at a constant velocity, its terminal velocity. When this happens, the drag force on the object is acting with equal magnitude but opposite direction to gravity. As shown in Figure 4.2, an object moving at a constant velocity is in a force balance. The sum of all forces acting on it is zero. This is not to say that it is not moving. It may be moving quite fast. The object is no longer accelerating. This is an equilibrium. We refer to it as a dynamic equilibrium because the object is moving with terminal velocity,  $v_T$ .

Turning back to open channel flow, Figure 4.3 is akin to Figure 4.2, except now the gravitational force is limited by the slope of the channel, and the drag

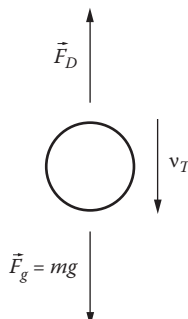


**FIGURE 4.2** An object in free fall with mass,  $m$ , reaches its terminal velocity,  $v_T$ , when the force due to gravity,  $F_g$ , acting downward is balanced by the drag force,  $F_D$ , acting upward.

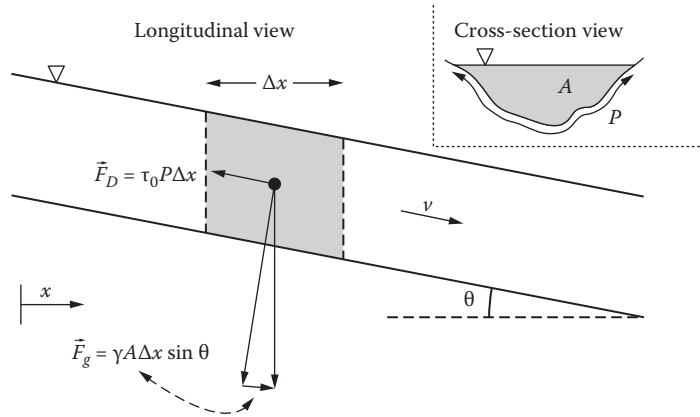


**FIGURE 4.3** Shaded regions give longitudinal and cross-sectional views of a parcel of water flowing in an open channel. As with the object in free fall, when the gravitational force,  $F_g$ , is balanced by the drag force,  $F_D$ , the flow is balanced and uniform flow occurs. Unlike the object in free fall, forces are now resolved along the longitudinal direction of flow indicated by bulk velocity,  $v$ .

force is now a consequence of friction between the flowing water and the channel surfaces. If the channel slope is  $\theta$ , then we can write the force balance as:

$$\text{driving force} = \text{resisting force}$$

$$\rho g \sin(\theta) = F_D \quad (4.3)$$

where  $\rho$  is the mass density of water and  $F_D$  is the drag force due to friction between the flowing water and channel surfaces. Note that the product,  $\rho g$ , is equal to  $\gamma$ . The weight,  $w$ , of the parcel of water is the product of  $\gamma$  and the volume of the parcel. Thus,

$$w = \gamma \cdot (A \cdot \Delta x) \quad (4.4)$$

## 4.3 SHEAR STRESS IN OPEN CHANNEL FLOW

In open channel flow, friction manifests itself as a shear stress,  $\tau_0$ , between the flowing water and the wetted surface of the channel. Referring to Figure 4.3, the drag force acting on the parcel of water is equal to the product of the shear stress and the area of the wetted surface:

$$F_D = \tau_0 \cdot (P \cdot \Delta x) \quad (4.5)$$

where  $P$  is the wetted perimeter of the channel cross-section, and  $F_D$  is understood to act opposite to the direction of flow. Substituting equations 4.4 and 4.5 into 4.3, we get

$$\gamma \cdot A \cdot \Delta x \cdot \sin(\theta) = \tau_0 \cdot P \cdot \Delta x \quad (4.6)$$

Dividing both sides by the wetted surface area of the channel,  $P\Delta x$ ,

$$\gamma \cdot \frac{A}{P} \cdot \sin(\theta) = \gamma \cdot R \cdot \sin(\theta) = \tau_0 \quad (4.7)$$

where we have defined the hydraulic radius,  $R$ , as the cross-sectional area of the channel divided by its wetted perimeter. For small values of  $\theta$ ,  $\sin(\theta)$  and  $\tan(\theta)$  are essentially the same. For instance, at  $10^\circ$ ,  $\sin(10^\circ)/\tan(10^\circ) = 98.5\%$  even as a  $10^\circ$  slope is extremely steep for a flowing channel. Using  $\tan(\theta)$  as an approximation of  $\sin(\theta)$ , equation 4.7 becomes

$$\gamma \cdot R \cdot \tan(\theta) = \tau_0 \quad (4.8)$$

and we note that  $\tan(\theta)$  is simply the slope,  $S$  (rise/run) of the channel arriving at the final result:

$$\gamma \cdot R \cdot S = \tau_0 \quad (4.9)$$

In Figure 4.3, the parameter  $\theta$  is used to quantify the slope of the channel bottom. In truth, there are actually three slopes one might measure in the context of a flowing channel as shown in Figure 4.4. These slopes are the physical slope

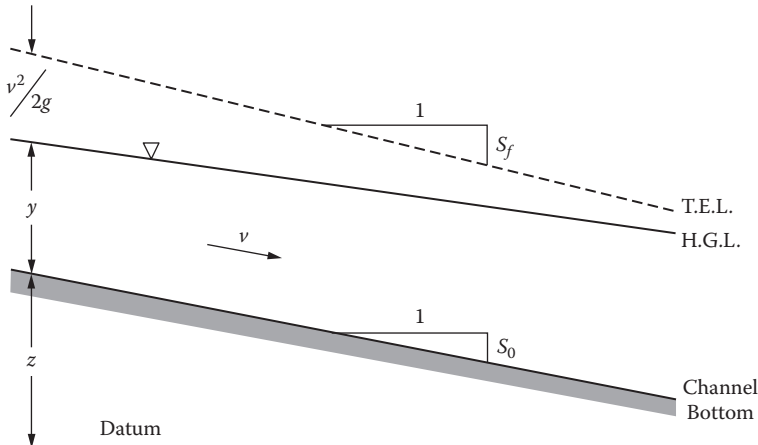


**FIGURE 4.4** Definition sketch for channel slope,  $S_0$ , and friction slope,  $S_f$ . “T.E.L.” is the total energy line; “H.G.L.” is the hydraulic grade line.

of the channel bottom,  $S_0$ ; the slope of the water surface (also known as the slope of the hydraulic grade line, H.G.L.); and the friction slope,  $S_f$  (also known as the slope of the total energy line, T.E.L.). Which slope is meant by  $S$  in equation 4.9? As derived, for uniform flow, all three slopes are equal. However, when flow depth is non-uniform then the friction slope,  $S_f$ , is the relevant slope. Thus the reader can simply always consider the  $S$  in equation 4.9 to represent the friction slope,  $S_f$ , with the understanding that under uniform flow conditions  $S_f$  equals  $S_0$ .

The appearance of  $S_f$  is important, because now our analyses can realistically portray energy loss by water flowing in a channel. We now have friction. Further, from the preceding discussions and from Figure 4.4 it should be intuitive that the change in energy possessed by the flow is equal to the difference between  $S_0$  and  $S_f$ . A more general expression for equation 4.2 is:

$$\frac{dE}{dx} = S_0 - S_f \quad (4.10)$$

We return to equation 4.10 in Chapters 5 and 6 as we explore non-uniform flow.

## 4.4 CHÉZY AND MANNING'S EQUATIONS

Chézy's equation emerges from equation 4.9 using the assertion that shear stress is directly proportional to the velocity head:

$$\tau_0 \propto \frac{v^2}{2g} \quad (4.11)$$

Combining equations 4.9 and 4.11 gives:

$$v^2 = C_1 \cdot 2g \cdot \gamma \cdot R \cdot S_f \quad (4.12)$$

where  $C_1$  is the constant of proportionality needed to make equation 4.11 an equality. Note that for generality, the friction slope,  $S_f$ , is indicated explicitly. Taking the square root of equation 4.12 and combining all the constants from the right-hand side of equation 4.12 into a single constant, we arrive at:

$$v = C \sqrt{R \cdot S_f} \quad (4.13)$$

which is the Chézy equation. Since  $R$  has units of length and  $S_f$  is dimensionless, the Chézy constant,  $C$ , must have units of  $L^{0.5}/T$ .

Tabulated values of  $C$  are not presented in this book, though such tables can readily be found in other texts or online. However, we present here a brief analysis that relates the Chézy  $C$  to the Darcy-Weisbach friction factor,  $f$ , for head loss in pipe flow. The Darcy-Weisbach formula is:

$$h_L = f \cdot \frac{l}{D} \cdot \frac{v^2}{2g} \quad (4.14)$$

where  $h_L$  is the head loss in a pipe of diameter,  $D$ , and length,  $l$ . For a pipe flowing full or half full, the reader should be able to quickly verify that the hydraulic radius,  $R = D/4$ . Rearranging equation 4.14 and substituting  $4R$  for  $D$ , we get

$$v^2 = \frac{2g}{f} \cdot 4R \cdot \frac{h_L}{l}. \quad (4.15)$$

Noting that  $h_L/l$  is the friction slope,  $S_f$ , and taking the square root of equation 4.15, we get

$$v = \sqrt{\frac{8g}{f}} \cdot \sqrt{R \cdot S_f}. \quad (4.16)$$

which implies that

$$C = \sqrt{\frac{8g}{f}} \quad (4.17)$$

Assuming that the circumstances do not stray too far from those for which the Darcy-Weisbach equation is appropriate (i.e., the channel is relatively small and smooth), the Moody diagram (Moody 1944) can be used to estimate  $f$ . The Chézy  $C$  value is then readily determined using equation 4.17.

We turn now to Manning's equation. Manning's equation is similar to Chézy's equation with a slight additional dependency on the hydraulic radius and a different presentation of the roughness coefficient:

$$C = \frac{k}{n} \cdot R^{1/6} \quad (4.18)$$

where  $C$  is Chézy's roughness coefficient,  $n$  is Manning's roughness coefficient, and  $k$  is either 1 if velocity is reported in m/s or 1.48592... (see Problem 4.1) if velocity is reported in ft/s. As a practical matter,  $k = 1.49$  is quite sufficient for

English units given the lack of precision in the fundamental roughness coefficient,  $n$ . Thus, Manning's equation is

$$v = \frac{k}{n} \cdot R^{2/3} S_f^{1/2} \quad (4.19)$$

In the author's experience, Manning's equation is more widely used than Chézy's equation, perhaps for the simple reason that Manning's  $n$  is apparently independent of units (with  $k$  doing the work of units conversion) while tables of Chézy's  $C$  must indicate if the tabulated values are for English or metric units. An extensive listing of values of Manning's  $n$  appears in Table 4.1.

A brief discussion on the friction slope,  $S_f$ , is merited. Channel slope,  $S_0$ , is easy to visualize, but the friction slope can be more elusive, despite its visual depiction as the slope of the T.E.L., in Figure 4.4. Specifically, the reader

**TABLE 4.1** Values of Manning's Roughness Coefficient,  $n$ , for Various Surfaces

Major Category	Surface Description	Range
Pipe	Cast-iron, coated	0.010–0.014
	Cast-iron, uncoated	0.011–0.015
	Wrought iron, galvanized	0.013–0.017
	Wrought iron, black	0.012–0.015
	Steel, riveted and spiral	0.013–0.017
	Corrugated	0.021–0.0255
	Wood stave	0.010–0.014
	Neat cement surface	0.010–0.013
	Concrete	0.010–0.017
	Vitrified sewer pipe	0.010–0.017
Lined channels	Clay, common drainage tile	0.011–0.017
	Metal, smooth semicircular	0.011–0.015
	Metal, corrugated	0.0228–0.0244
	Wood, planed	0.010–0.015

(continued)

**TABLE 4.1** Values of Manning's Roughness Coefficient,  $n$ , for Various Surfaces (Continued)

Major Category	Surface Description	Range
Lined channels	Wood, unplanned	0.011–0.015
	Neat, cement lined	0.010–0.013
	Concrete	0.012–0.018
	Cement rubble	0.017–0.030
	Vegetated, small channels, shallow depths, Bermuda grass, short	0.034 (min)
	Vegetated, small channels, shallow depths, Bermuda grass, long	0.035–0.28
	Sericea Lespedeza, short	0.033–0.034
	Sericea Lespedeza, long	0.050–0.22
Unlined channels	Earth, straight and uniform	0.017–0.025
	Earth, winding and sluggish	0.0225–0.030
	Earth, stony bed, weeds on bank	0.025–0.040
	Earth bottom, rubble sides	0.028–0.035
	Rock cuts, smooth and uniform	0.025–0.035
	Rock cuts, jagged and irregular	0.035–0.045
Natural streams	(1) Clean, straight banks, full stage no rifts or deep pools	0.025–0.033
	(2) Same as (1) but more weeds and stones	0.030–0.040
	(3) Winding, some pools, shoals, clean	0.033–0.045
	(4) Same as (3), lower stages, more ineffective slopes and sections	0.040–0.055
	(5) Same as (3), some weeds and stones	0.035–0.050
	(6) Same as (4), stony sections	0.045–0.060
	(7) Sluggish reaches, rather weedy, very deep pools	0.050–0.080
	(8) Very weedy reaches	0.075–0.15

Source: From compilation in Soil Conservation Service (1974).

may wonder how the friction slope varies with flow depth. We leave it to the reader (see Problem 4.6) to show that for a fixed discharge, the friction slope is a strictly decreasing function of flow depth. It thus follows that there is some depth,  $y_0$ , at which  $S_0 = S_f$ . Normal depth is the depth that separates the regions of dominance between the friction and channel slopes. For  $y < y_0$ ,  $S_f > S_0$ . For  $y > y_0$ ,  $S_0 > S_f$ .

## 4.5 UNIFORM FLOW AND NORMAL DEPTH

Combining Manning's equation with the continuity equation yields:

$$Q = \frac{k}{n} \cdot A \cdot R^{2/3} S_f^{1/2} \quad (4.20)$$

If the channel geometry is regular (e.g., rectangular, trapezoidal, or circular) note that both  $A$  and  $R$  are straightforward functions of depth. Normal depth,  $y_0$ , is the depth that is observed under uniform flow conditions. The depths employed in equation 4.20 are trial normal depths, and since we are assuming uniform flow, we can substitute the known channel slope,  $S_0$ , for the friction slope,  $S_f$ . It follows that the discharge calculated in equation 4.20 is the discharge corresponding to uniform flow conditions. The trial normal depth value that corresponds to a particular discharge,  $Q_0$ , is the normal depth for that discharge. We can write:

$$\frac{k}{n} \cdot A(y_0) \cdot R(y_0)^{2/3} S_0^{1/2} - Q_0 = 0 \quad (4.21)$$

where we have written  $A(y_0)$  and  $R(y_0)$  to emphasize that area and hydraulic radius are explicit functions of the normal depth, and we have replaced  $S_f$  with  $S_0$ , consistent with the assumption of uniform flow.

### **Example 4.1**

Given a trapezoidal channel, 3 meters wide with side slope parameter,  $m = 2$ . The channel has a bottom slope  $S_0 = 0.004 \text{ m/m}$ , and Manning's roughness coefficient,  $n = 0.030$ . Determine the normal depth,  $y_0$ , that produces a discharge of  $Q_0 = 20 \text{ m}^3/\text{s}$ .

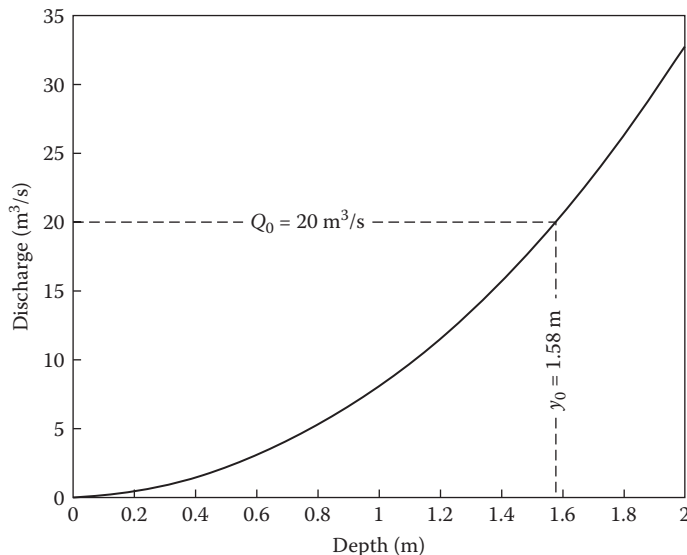


**FIGURE 4.5** Discharge-depth relationship for conditions in Example 4.1. Normal depth of 1.58 m for  $Q_0 = 20 \text{ m}^3/\text{s}$  is indicated.

**Solution:**

Substituting in equation 4.21 for the specific values indicated in the problem statement, we seek the value of  $y_0$  that satisfies

$$\frac{1}{0.030} \cdot A(y_0) \cdot R(y_0)^{\frac{2}{3}} (0.004)^{\frac{1}{2}} - 20 = 0 \quad (4.22)$$

Figure 4.5 provides a graphical depiction of  $Q$  versus  $y$  of equation 4.22 over a range of trial normal depths. The nonlinearity observed in Figure 4.5 follows from the structure of equation 4.22, the shape of the channel, the definition of the hydraulic radius, and the exponent of  $2/3$  placed on the hydraulic radius. By inspection of the figure, a depth of  $y = 1.6 \text{ m}$  is close to the normal depth we are seeking. Let's explicitly work out equation 4.22 for this trial depth.

Area:

$$A = by + my^2 = (3) \cdot (1.6) + (2) \cdot (1.6)^2 = 9.92 \text{ m}^2$$

Wetted perimeter:

$$P = b + 2\sqrt{y^2 + (my)^2} = (3) + (2)\cdot\sqrt{(1.6)^2 + [(2)\cdot(1.6)]^2} = 10.16 \text{ m}$$

Hydraulic radius:

$$R = \frac{A}{P} = \frac{9.92 \text{ m}^2}{10.16 \text{ m}} = 0.98 \text{ m}$$

Discharge:

$$\begin{aligned} & \frac{1}{0.030} \cdot A(y_0) \cdot R(y_0)^{2/3} (0.004)^{1/2} - 20 \\ &= \frac{1}{0.030} \cdot (9.92) \cdot (0.98)^{2/3} (0.004)^{1/2} - 20 = 0.63 \text{ m}^3/\text{s} \end{aligned}$$

The calculated discharge for  $y_0 = 1.6 \text{ m}$  is thus  $0.63 \text{ m}^3/\text{s}$  too large. Examining Figure 4.5, it is clear that a revised estimate of  $y_0$  should be slightly less than  $1.6 \text{ m}$ . By iteration, a value of  $y_0 = 1.58 \text{ m}$  is found to be a good approximation of the root to equation 4.22.

As explored in Chapters 2 and 3, the reader should quickly recognize that the Excel® Goal Seek tool is an excellent resource that can be easily programmed to automate the general determination of  $y_0$  in equation 4.21 for rectangular, trapezoidal, and circular channels (see Problems 4.2 and 4.3).

## 4.6 REACH CLASSIFICATION

In Chapters 2 and 3, the concept of critical depth was found to often be central to consideration in approaching a problem. In the context of friction and uniform flow, we have not yet needed to invoke any such role for critical depth. We now assert that the magnitude of normal depth relative to critical depth is of fundamental importance when analyzing non-uniform flow.

There are three possible relative magnitudes between normal and critical depth. If  $y_0 < y_c$ , then the reach is classified as *steep*. We will henceforth use the symbol *S* to classify such a reach. If  $y_0 > y_c$ , then the reach is classified as *mild* (symbol is *M*). If  $y_0 = y_c$ , then the reach is classified as *critical* (symbol is *C*). This

last case, when normal and critical depth are equal, is a mathematical possibility; however, the real-world likelihood of encountering exactly this condition is small. An alternative approach to these comparative depth assessments would be to simply determine the Froude number associated with normal depth on a reach. If the Froude number is greater than one, the reach is steep, if less than one, the reach is mild, and if equal to one, the reach is critical.

For completeness, there are two other reach classifications that merit brief discussion: horizontal and adverse. A *horizontal* reach, as implied by its name, is a reach in which the channel slope is zero (symbol is  $H$ ). A quick examination of equation 4.19 shows that on such a reach normal depth is infinite. The same is true for an *adverse* reach (symbol is  $A$ ). On an adverse reach, the channel is actually sloping uphill relative to the overall direction of flow. Horizontal and adverse reaches can and do occur both in man-made channel structures and in the natural environment. However, owing to their lack of gravity to support the flow of water, such reaches can only exist over relatively short distances.

A note on terminology is in order. Many older texts (e.g., Chow 1959; Henderson 1966) and even newer texts (e.g., Sturm 2001; Chaudhry 2008) tend to use the terminology *steep slope*, *mild slope*, or *critical slope*. The inclusion of *slope* in these classifications is a misnomer as it could be construed to mean that the slope of the channel determines whether that channel is steep, mild, or critical. In truth the steep, mild, and critical classifications are dependent on the particular blend of flow and channel properties. In contrast, the horizontal and adverse reach classifications depend only on the channel slope. For consistency and clarity, we will use the term *reach*, rather than *slope*, following all five possible classifications.

## Normal Depth Animations

In this section we examine normal depth as a function of discharge, roughness, geometry, and slope. Still images from a series of animations are used to illustrate this dependency. Five animations are provided and are summarized in Table 4.2. In all cases the channel is rectangular. One parameter of the set of discharge, roughness, width, and slope is varied while all other parameters remain constant. The apparent movement in each animation is caused by a simulated instantaneous adjustment of the flow to uniform conditions for the parameter set used. A description of the contents of Figures 4.6 through 4.10 follows.

**TABLE 4.2** Discharge and Channel Properties for the Provided Normal Depth Animations

Animation Name (.avi)	Source of "Movement"	Discharge ( $\text{ft}^3/\text{s}$ )	Manning's $n$	Width (ft)	Channel Slope (ft/ft)
ynorm_discharge	$2.5 \leq Q \leq 240 \text{ ft}^3/\text{s}$	See "movement"	0.03	10	0.02
ynorm_n	$0.01 \leq n \leq 0.04$	100	See "movement"	10	0.005
ynorm_width_mild	$10 \leq w \leq 49.6 \text{ ft}$	100	0.03	See "movement"	0.005
ynorm_width_stEEP	$10 \leq w \leq 49.6 \text{ ft}$	100	0.03	See "movement"	0.04
ynorm_slope	$0.001 \leq S_0 \leq 0.04 \text{ ft/ft}$	100	0.03	10	See "movement"

In each figure, the upper right subplot shows three quantities—normal depth, hydraulic radius, and Froude number—as they evolve with the parameter that is varied in the animation. Note that in the discharge, roughness, and slope animations, the parameter that is varied is sufficient to cause the Froude number to vary between subcritical and supercritical conditions. In other words, depending on the value of the varying parameter, the reach crosses through critical conditions as it transitions between mild and steep (or vice versa) conditions.

The upper left subplot shows either an elevation or a cross-sectional view of the channel with critical depth indicated by a dashed line and normal depth shown directly in the animation. The value of the varying parameter is also indicated within this subplot.

The lower left subplot shows the range of depths over which the following surface water profiles will occur:  $M_1, M_2, M_3$  and  $S_1, S_2, S_3$ . These profiles are defined and discussed further in Chapter 5. Note that in the discharge, roughness, and slope animations a vertical line appears in this subplot at the value of the varying parameter that

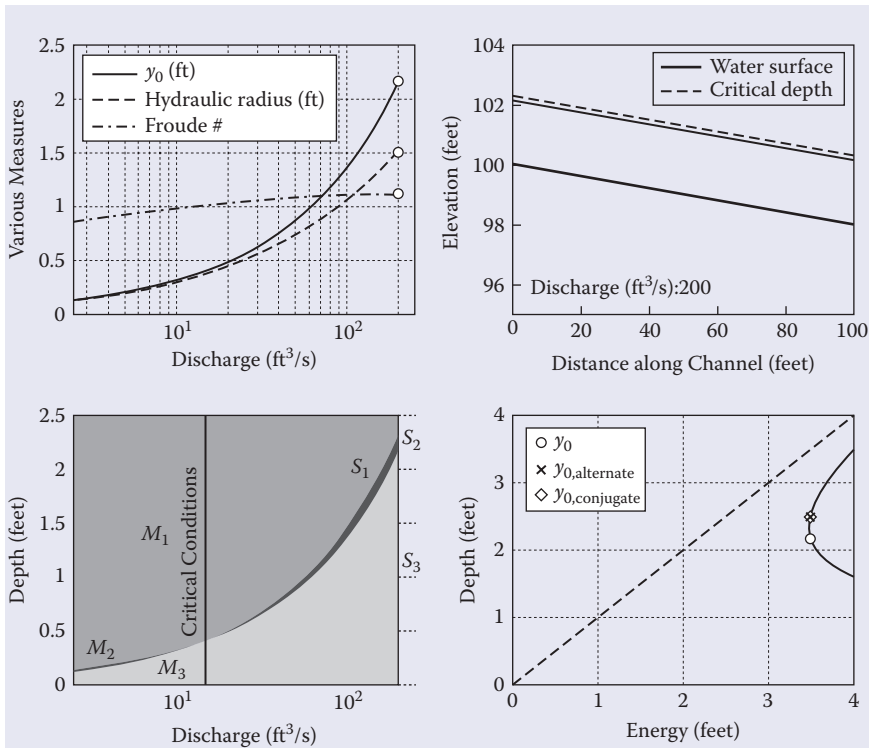


**FIGURE 4.6** Screen capture from *ynorm\_discharge.avi* animation. The capture shows the effect of varying discharge on normal depth. The upper left subplot shows normal depth, hydraulic radius, and the Froude number as a function of discharge. Note that as discharge increases the Froude number increases from subcritical to supercritical conditions. The upper right subplot shows the flow and its depth relative to critical conditions. The lower left subplot shows the depth range for various surface water profiles as a function of discharge. (This is explored in more detail in Chapter 5.) The lower right subplot shows the  $E$ - $y$  diagram for the given discharge with the normal, alternate, and conjugate depths indicated.

causes critical flow (Froude number is 1) conditions. This vertical line separates the mild and steep flow profiles.

The lower right subplot shows the  $E$ - $y$  diagram for the discharge simulated and places an  $\circ$  on this diagram at normal depth, an  $\times$  at alternate depth to normal depth, and a  $\diamond$  at conjugate to normal depth.

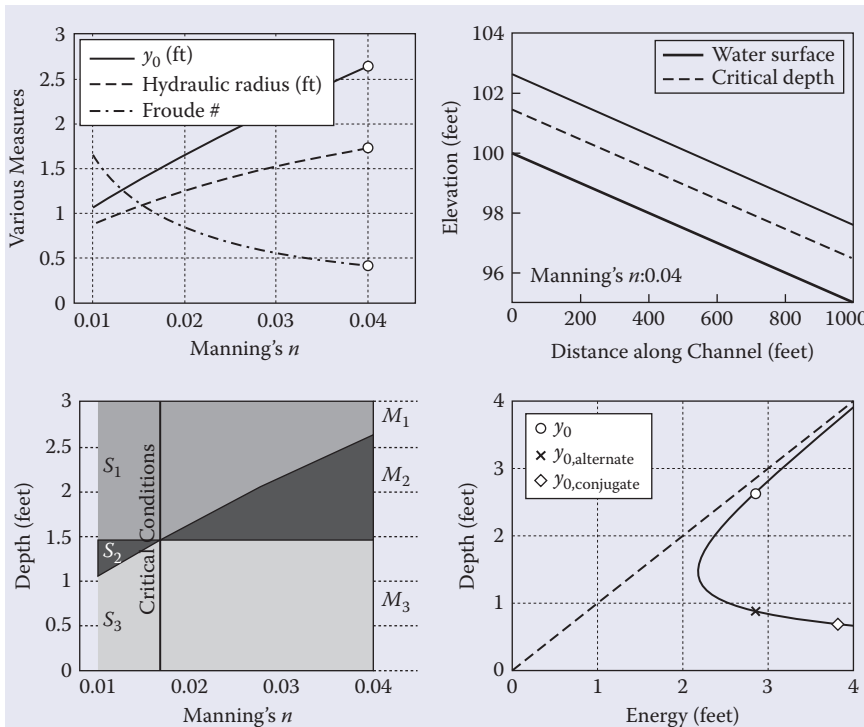


**FIGURE 4.7** Screen capture from *ynorm\_n.avi* animation. The capture shows the effect of varying channel roughness on normal depth. The upper left subplot shows normal depth, hydraulic radius, and the Froude number as a function of Manning's  $n$ . Note that as Manning's  $n$  increases, the Froude number decreases from supercritical to subcritical conditions. The upper right subplot shows the flow and its depth relative to critical conditions. The lower left subplot shows the depth range for various surface water profiles as a function of discharge. (This is explored in more detail in Chapter 5.) The lower right subplot shows the  $E$ - $y$  diagram for the given value of Manning's  $n$  with the normal, alternate, and conjugate depths indicated.

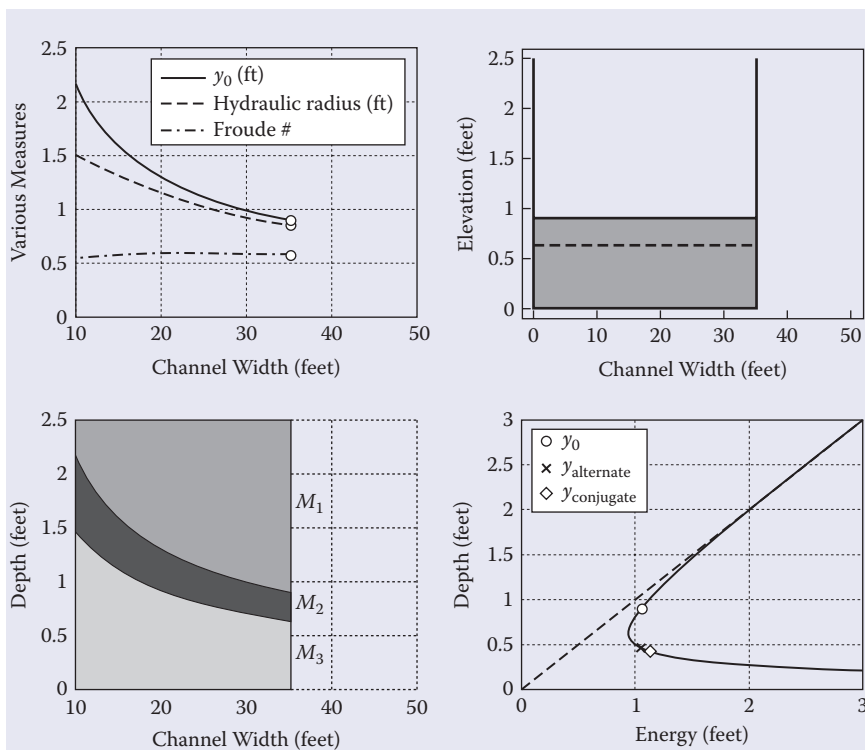


**FIGURE 4.8** Screen capture from *ynorm\_width\_mild.avi* animation. The capture shows the effect of varying channel width on normal depth (mild conditions dominate). The upper left subplot shows normal depth, hydraulic radius, and the Froude number as a function of channel width. The Froude number remains subcritical over the course of this entire animation. The upper right subplot shows the channel in cross-sectional view with the flow shaded and critical conditions indicated. The lower left subplot shows the depth range for various surface water profiles as a function of channel width. (This is explored in more detail in Chapter 5.) The lower right subplot shows the  $E-y$  diagram for the given channel width with the normal, alternate, and conjugate depths indicated.

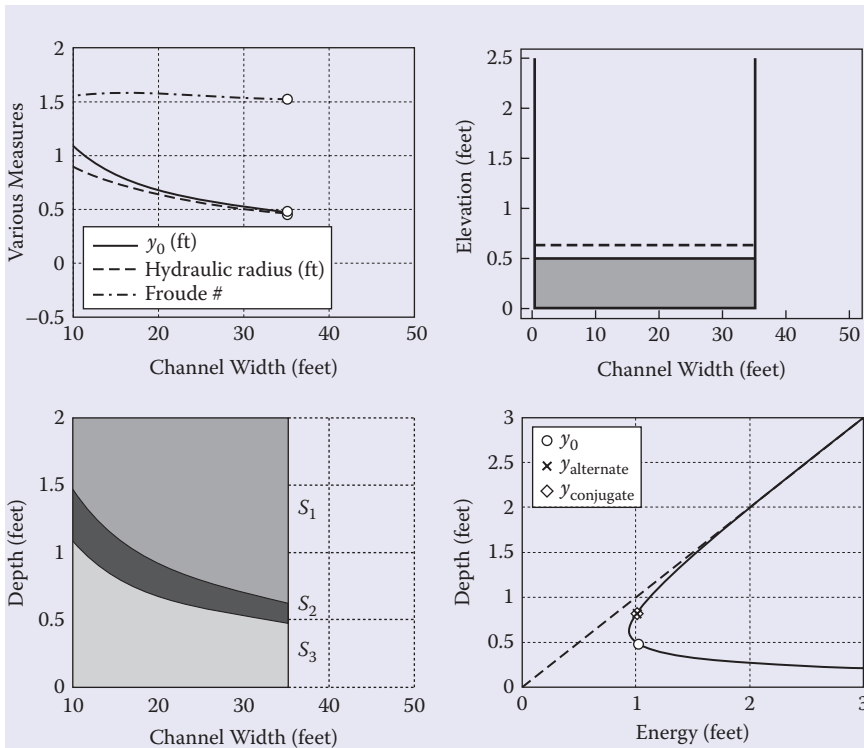


**FIGURE 4.9** Screen capture from *ynorm\_width\_steepl.avi* animation. The capture shows the effect of varying channel width on normal depth (steep conditions dominate). The upper left subplot shows normal depth, hydraulic radius, and the Froude number as a function of channel width. The Froude number remains supercritical over the course of this entire animation. The upper right subplot shows the channel in cross-sectional view with the flow shaded and critical conditions indicated. The lower left subplot shows the depth range for various surface water profiles as a function of channel width. (This is explored in more detail in Chapter 5.) The lower right subplot shows the  $E$ - $y$  diagram for the given channel width with the normal, alternate, and conjugate depths indicated.

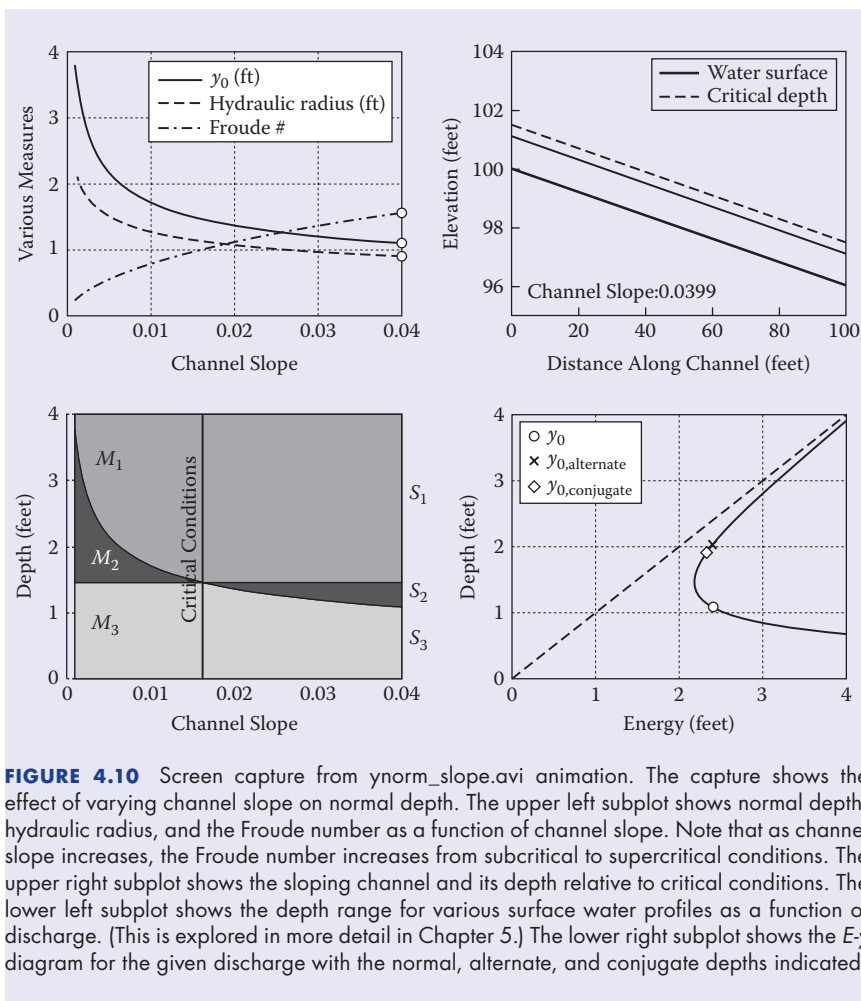


**FIGURE 4.10** Screen capture from *ynorm\_slope.avi* animation. The capture shows the effect of varying channel slope on normal depth. The upper left subplot shows normal depth, hydraulic radius, and the Froude number as a function of channel slope. Note that as channel slope increases, the Froude number increases from subcritical to supercritical conditions. The upper right subplot shows the sloping channel and its depth relative to critical conditions. The lower left subplot shows the depth range for various surface water profiles as a function of discharge. (This is explored in more detail in Chapter 5.) The lower right subplot shows the *E-y* diagram for the given discharge with the normal, alternate, and conjugate depths indicated.

## 4.7 SUMMARY

The focus of this chapter is on the idealized concept of a channel in which the discharge, channel roughness, channel geometry, and channel slope are constant along the direction of flow. The flow that occurs in such an idealized system is observed to have a constant depth as it moves along the channel. This is the definition of uniform flow. Under uniform flow conditions, the gravity force driving the flow downstream is exactly balanced by the friction force holding the flow back. This situation is analogous to the concept of terminal velocity for a free-falling object.

Chézy's and Manning's formulas were presented as the most common examples of equations that relate velocity to channel characteristics. At their core, these equations characterize friction and the loss of energy as a flow moves downstream. Exactly so for the Chézy equation, and approximately so for Manning's equation is that shear stress between the flow and channel interface is proportional to the velocity head. These equations both depend on the friction slope,  $S_f$ , which is the slope of the total energy line measured along the direction of flow. Under conditions of uniform flow, the friction slope, the slope of the water surface, and the channel slope,  $S_0$ , are all equal.

If uniform flow is assumed, either Chézy's or Manning's equation can be coupled with a known discharge, roughness, channel geometry, channel slope, and a root-finding algorithm to solve for the depth that is internally consistent with these knowns. This depth is referred to as the normal depth,  $y_0$ . An example of the calculation of normal depth was provided, and we observed that the Excel Goal Seek tool can be readily used to automate normal depth calculation. Perhaps obvious, but worth emphasizing here is that normal depth is dependent on all the knowns indicated above: discharge, roughness, channel geometry, and channel slope.

A reach classification scheme was introduced that involved comparison between the magnitudes of normal depth and critical depth. A steep reach occurs when the normal depth is less than critical depth. A mild reach is a reach in which the normal depth is greater than critical depth. If normal and critical depths are equal (a mathematical but unlikely possibility), the reach is critical. Finally, there are two other reach classifications that depend only on the channel slope. A horizontal reach is a reach in which the channel slope is zero, while an adverse reach is a reach in which the channel slope is uphill relative to the overall direction of flow. Normal depth on both horizontal and adverse reaches is infinite. The five possible reach classifications are therefore steep (S), mild (M), critical (C), horizontal (H), and adverse (A). These classifications and subcategories associated with them are explored in Chapter 5.

## References

- Chaudhry, M.H. (2008). *Open Channel Flow* (2nd Edition), Springer, New York.
- Chow, V.T. (1959). *Open-Channel Hydraulics*, McGraw-Hill, New York.
- Henderson, F.M. (1966). *Open Channel Flow*, Macmillan, New York.
- Herschel, C. (1897). On the origin of the Chézy formula. *Journal of the Association of Engineering Societies*, 18: 363–368.
- Manning, R. (1891). On the flow of water in open channels and pipes. *Transactions of the Institution of Civil Engineers of Ireland*, 20: 161–207.
- Moody, L.F. (1944). Friction Factors for Pipe Flow. *Transactions of the ASME*, 66 (8): 671–684.

Soil Conservation Service. (1974). *SCS National Engineering Handbook*. US Department of Agriculture.

Sturm, T.W. (2001). *Open Channel Hydraulics*, McGraw-Hill, New York.

## Problems

- 4.1. Management of unit conversion for Manning's and Chézy's equations:
- Considering that  $k$  in equations 4.18 and 4.19 is precisely 1 for the determination of velocity in units of m/s, derive  $k$  if velocity is in units of ft/s.
  - Given that Manning's  $n = 0.030$  (ranging from 0.025 to 0.033), what is an appropriate value for  $k$  when using English units?
  - Imagine that Chézy's equation was presented similarly to Manning's equation with a flexible parameter,  $k_c$ , that is precisely 1 if velocity is in units of m/s. That is,

$$v = k_c \cdot C \sqrt{R \cdot S}$$

What is the value of  $k_c$  if velocity is in units of ft/s?

- 4.2. Develop a rectangular and trapezoidal channel normal depth tool. Using Excel, program a spreadsheet that takes as input discharge, Manning's roughness, channel bottom width, side-slope parameter, channel slope, and value for  $g$  (9.81 m/s<sup>2</sup> indicates metric, 32.2 ft/s<sup>2</sup> indicates English units). The spreadsheet calculates the following: normal depth, area, wetted perimeter, hydraulic radius, velocity, top width, Froude number, depth of centroid ( $\bar{y}$ ), momentum function, specific energy, and reach classification (steep, mild, or critical). Note that the tool developed in Problem 3.11 (Chapter 3) is a good starting point for this tool.
- 4.3. Develop a circular channel normal depth tool. Using Excel, program a spreadsheet that takes as input discharge, Manning's roughness, channel diameter, channel slope, and value for  $g$  (9.81 m/s<sup>2</sup> indicates metric, 32.2 ft/s<sup>2</sup> indicates English units). The spreadsheet calculates the following: normal depth, area, wetted perimeter, hydraulic radius, velocity, top width, Froude number, depth of centroid ( $\bar{y}$ ), momentum function, specific energy, and reach classification (steep, mild, or critical). Note that the tool developed in Problem 3.13 is a good starting point for this tool. As in that problem, you may choose to divide your spreadsheet tool into two sections:
- Section 1 applies when  $y \leq r$ .
  - Section 2 applies when  $y > r$ .

4.4. Given:

$$Q = 50 \text{ ft}^3/\text{s.}$$

$$S = 0.01 \text{ ft/ft.}$$

$$b = 20 \text{ ft.}$$

$$\text{Manning's } n = 0.02.$$

Find:

Critical depth:  $y_c$

Normal depth:  $y_0$

Classify reach: (steep, mild or critical?)

Examine how modest changes in the “givens” affect normal depth and the Froude number. Let each of the parameters shown below change by a modest amount (suggest  $\sim 1$  to  $-2\%$ ). Fill out the following influence chart:

Influence Chart		
Increase in This Parameter	Effect on Normal Depth	Effect on Froude Number
Q		
S		
b		
Manning's $n$		

- 4.5. Design a rectangular channel. The discharge is  $50 \text{ ft}^3/\text{s}$ , slope is  $0.01 \text{ ft/ft}$ , Manning's  $n$  is  $0.02$  (i.e., like in Problem 4.4). Your design is defined as most *efficient* if the cross-sectional area is minimized. What channel width,  $b$ , will produce the most *efficient* channel for these conditions?
- 4.6. Use the wide channel assumption ( $R = y$ ), and either Chézy's or Manning's equation to show that for a given discharge, as depth increases the friction slope decreases.
- 4.7. Using the channel roughness, geometry, and slope from Example 4.1,
  - a. Repeat this problem for discharges of  $Q_0 = 10 \text{ m}^3/\text{s}$  and  $30 \text{ m}^3/\text{s}$ .
  - b. Using the result directly from Example 4.1 and from (a), determine the Chézy C value for each of the three discharges.
  - c. Calculate the Froude number for each of the three discharges and determine if the reach is steep, mild, or critical.
- 4.8. Repeat Problem 4.7, changing Manning's  $n$  from  $0.030$  to  $0.015$ .
- 4.9. Repeat Problem 4.7, changing the channel slope,  $S_0$ , to  $0.01 \text{ m/m}$ . For the conditions in this problem approximately what discharge will result in a critical slope?

# **Qualitative Gradually Varied Flow**

## **CHAPTER OBJECTIVES**

1. Present classification system for gradually varied flow profiles.
2. Present and discuss rules for the translation of information upstream and downstream within a channel.
3. Sketch gradually varied flow profiles in the context of classic flow problems.
4. Examine how surface water profiles blend with both upstream and downstream boundary conditions.
5. Present concept of the conjugate curve and explore how this concept couples with surface water profiles to explain the direction of translation of a hydraulic jump.

### **5.1 INTRODUCTORY COMMENTS**

In Chapters 2 through 4 we have accumulated a handful of fundamental concepts and quantities. We know about specific energy, the momentum function, friction, uniform flow, critical depth, chokes, hydraulic jumps, and normal depth. We have learned how information can only propagate downstream in a supercritical flow, but can propagate both upstream and downstream in a subcritical flow. We have a classification scheme for categorizing stream reaches.

Finally, we have also accumulated a few unanswered questions. What controls where a hydraulic jump is located? How do we make use of the concept of information propagation? Which flow regime prevails downstream of a choke

condition induced by a step or constriction? (This last question was somehow tied to Figure 2.16 and which way the ball would roll downhill.)

In this chapter, we begin to assemble these concepts and quantities, and we leave this chapter with the answers to the questions posed above. This chapter explores gradually varied flow which, in contrast to hydraulic jumps, is the case of slowly changing (with distance) non-uniform flow. The term *water surface profile* is used here to generically refer to the shape of the water surface (how depth changes with distance) over a segment of stream reach. We build upon the classification scheme from Chapter 4 by enumerating water surface profiles that are observed in specific settings, with an emphasis on profiles on steep and mild reaches. The word *qualitative* in the chapter title is meant to emphasize that the goal of the chapter is to present a broad, non-quantitative approach to anticipating how non-uniform flow will behave along one or more connected stream reaches. The computation of the physical shape and length of the water surface profile will be the concern of Chapter 6.

## 5.2 NON-UNIFORM FLOW

Non-uniform flow changes with depth as it moves along the channel. Consider Figure 5.1, which shows a non-uniform flow. Lines A and B are both parallel to the channel bottom. These lines bound the surface water profile shown in the figure.

What can we say about the profile that is shown? Clearly, the flow depth decreases in the downstream direction. Mathematically, we can write:

$$\frac{dy}{dx} < 0 \quad (5.1)$$

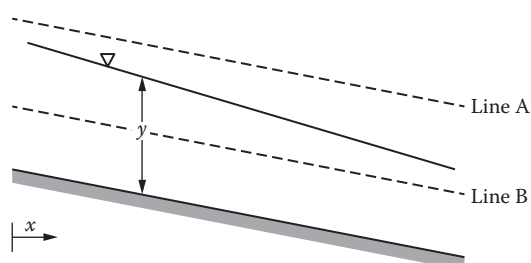


**FIGURE 5.1** Hypothetical surface water profile for Scenarios 1 and 2 discussion. The profile is bounded by lines A and B, which are parallel to the channel bottom.

Is the flow gaining energy? Losing energy? Is the reach shown steep or mild or critical? We do not know. We need more information.

### **5.2.1 Scenario 1**

Assume that lines A and B represent normal and critical depth, respectively, on this reach. Since normal depth (Line A) is greater than critical depth (Line B), we can state the reach is mild (*M*). The profile shown is everywhere greater than critical depth. Considering the shape of an *E-y* diagram, the fact that the depth along the profile diminishes subcritically means that specific energy is decreasing in the downstream direction:

$$\frac{dE}{dx} < 0 \quad (5.2)$$

The reasoning behind the statement in equation 5.2 is also consistent with the assessment that the friction slope is greater than the channel slope:

$$S_f > S_0 \quad (5.3)$$

### **5.2.2 Scenario 2**

Now assume the opposite of Scenario 1. Lines A and B represent critical and normal depth, respectively. Now all the interpretations are flipped. Since normal depth (Line B) is less than critical depth (Line A), the reach is steep (*S*). The profile is now everywhere less than critical depth. The diminishing depth along the profile means that specific energy is increasing in the downstream direction:

$$\frac{dE}{dx} > 0 \quad (5.4)$$

Finally, if energy is increasing along the direction of flow, then it must be the case that

$$S_0 > S_f \quad (5.5)$$

This discussion surrounding Figure 5.1 should emphasize to the reader that the context of a flow profile (whether it appears on a mild or steep reach) is

important to the sign of energy changes along the profile. This discussion is also a bit of a clumsy exploration of an equation we can assemble from an earlier finding in Chapter 2. Let's repeat equations 2.32 and 2.34:

$$0 = \frac{dH}{dx} = \frac{dE}{dx} + \frac{dz}{dx} \quad (2.32)$$

$$0 = (1 - F_r^2) \cdot \frac{dy}{dx} + \frac{dz}{dx} \quad (2.34)$$

Combining parts of each of these equations we get:

$$\frac{dH}{dx} = (1 - F_r^2) \cdot \frac{dy}{dx} + \frac{dz}{dx} \quad (5.6)$$

We note that  $dH/dx$  is the negative of the friction slope,  $-S_f$ , and  $dz/dx$  is the negative of the channel slope,  $-S_0$ . Thus, we can write:

$$-S_f = (1 - F_r^2) \cdot \frac{dy}{dx} - S_0 \quad (5.7)$$

Solving for and placing  $dy/dx$  on the left-hand side of the equation,

$$\frac{dy}{dx} = \frac{S_0 - S_f}{1 - F_r^2} \quad (5.8)$$

With equation 5.8 in hand, we can re-explore Scenarios 1 and 2 above. Consider Scenario 1. The profile is one of decreasing depth, so  $dy/dx$  is negative. Further, the profile is subcritical, so  $1 - F_r^2$  is positive. It follows then that:

$$(-) = \frac{S_0 - S_f}{(+)} \quad (5.9)$$

and thus,  $S_0 < S_f$ , for equation 5.9 to be true, consistent with the earlier determination in equation 5.3. In Scenario 2, the profile is supercritical, so  $1 - F_r^2$  is negative. Therefore,

$$(-) = \frac{S_0 - S_f}{(-)} \quad (5.10)$$

and thus  $S_0 > S_f$  for equation 5.10 to be true, consistent with the earlier determination in equation 5.5.

### 5.3 PROFILE TAXONOMY

We now introduce a naming scheme, or taxonomy, that classifies all possible flow profiles. Figure 5.2 shows three depth ranges on steep and mild reaches separated by normal and critical depths. The taxonomy combines a letter followed by a number (e.g.,  $X_3$ ) to uniquely define a given profile. The leading letter comes from the nomenclature introduced in Chapter 4. The subscript number follows from the depth ranges indicated in Figure 5.2. For instance, the profile from Scenario 1 is an  $M_2$  profile because it is the profile that exists on a mild reach in the depth range bounded by normal depth above and critical depth below. By the same reasoning, the profile from Scenario 2 is an  $S_2$  profile.

Figure 5.3 presents the complete taxonomy of flow profiles for mild, steep, critical, horizontal, and adverse reaches. Coupled with hydraulic jumps, the profiles shown in Figure 5.3 encompass the full range of potential surface water profiles through a system. More complicated composite surface water profiles can be assembled from the fundamental “building blocks” enumerated in Figure 5.3. We will explore single-transition composites in the next section.

It is important to understand that the profiles provided are an exhaustive set; no other profiles are possible. It has been my experience that students can be quite creative, inventing alternative flow profiles that cannot exist. For instance, consider the hypothetical case of a surface water profile that *increases* (rather than decreases as on an  $M_2$  profile) in depth on a mild reach between  $y_c$

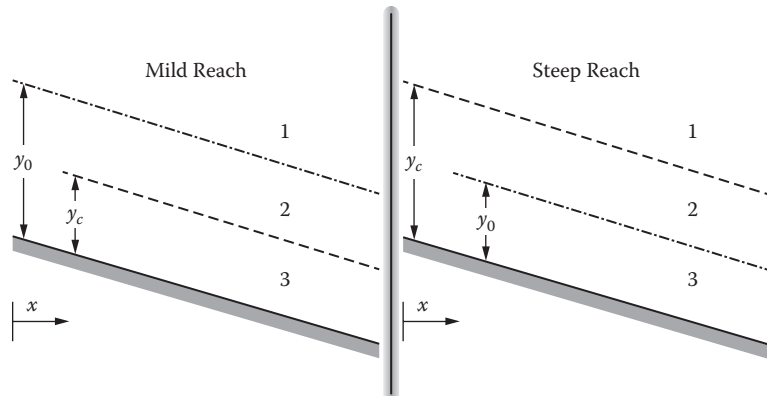


**FIGURE 5.2** Flow depth ranges on mild and steep reaches.

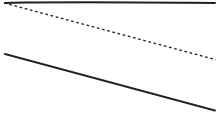
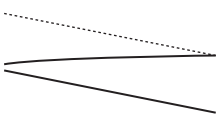
Profile Name	Depth Range	$dy/dx$	$dE/dx$	Froude Number	Profile Image
$M_1$	$y_c < y_0 < y$	+	+	<1	
$M_2$	$y_c < y < y_0$	-	-	<1	
$M_3$	$y < y_c < y_0$	+	-	>1	

(a)

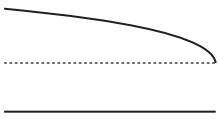
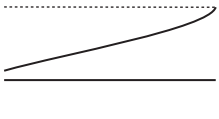
Profile Name	Depth Range	$dy/dx$	$dE/dx$	Froude Number	Profile Image
$S_1$	$y_0 < y_c < y$	+	+	<1	
$S_2$	$y_0 < y < y_c$	-	+	>1	
$S_3$	$y < y_0 < y_c$	+	-	>1	

(b)

**FIGURE 5.3** (a) Table of surface water profiles: mild profiles. (b) Table of surface water profiles: steep profiles. *(continued)*

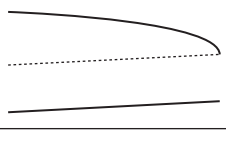
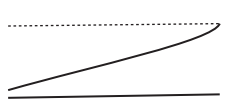
Profile Name	Depth Range	$dy/dx$	$dE/dx$	Froude Number	Profile Image
$C_1$	$y_c = y_0 < y$	+	+	<1	
$C_2$	$y = y_c = y_0$	0	0	1	No profile, uniform flow
$C_3$	$y < y_0 = y_c$	+	-	>1	

(c)

Profile Name	Depth Range	$dy/dx$	$dE/dx$	Froude Number	Profile Image
$H_1$					Because normal depth is infinite, this profile does not exist.
$H_2$	$y_c < y$	-	-	<1	
$H_3$	$y < y_c$	+	-	>1	

(d)

**FIGURE 5.3** (continued) (c) Table of surface water profiles: critical profiles. (d) Table of surface water profiles: horizontal profiles. (continued)

Profile Name	Depth Range	$dy/dx$	$dE/dx$	Froude Number	Profile Image
$A_1$					Because normal depth is infinite, this profile does not exist.
$A_2$	$y_c < y$	-	-	<1	
$A_3$	$y < y_c$	+	-	>1	

(e)

**FIGURE 5.3** (continued) (e) Table of surface water profiles: adverse profiles.

and  $y_0$  (Region 2) of Figure 5.2. Why is such a profile not possible? The answer follows from equation 5.8. Putting signs of terms into this equation, we get

$$(+)=\frac{S_0-S_f}{(+)} \quad (5.11)$$

For equation 5.11 to be true, the numerator of the right-hand side of the equation must be positive. In other words  $S_0 > S_f$ . But this assertion contradicts the statement in Section 4.4 that for  $y < y_0$ , then  $S_f > S_0$ . Therefore, there is no possibility of a surface water profile that increases in depth on a mild reach in the region between  $y_c$  and  $y_0$ .

## 5.4 IN-STREAM OBSTRUCTIONS

In this section we explore a single reach with upstream and downstream boundary conditions of normal depth. Within the reach we place one of the obstructions—sluice gate, step, constriction—that we originally explored in Chapter 2. The same energy and momentum rules learned earlier still apply, but now we have the added realism that the inclusion of friction and surface water profiles contributes to the analysis. The mysteries that may have surrounded the phenomenon of a choked flow will also, hopefully, be solved. These explorations will take the form of a number of example problems.

**Example 5.1**

A 10 m wide rectangular channel carries a discharge of 30 m<sup>3</sup>/s. The gate opening is 0.50 m. The slope of the channel is 0.0050 m/m, and Manning's roughness is 0.030. The upstream and downstream boundary conditions are normal depth,  $y_0$ . Assuming the system has reached steady-state conditions,

- Determine the normal depth,  $y_0$ .
- Determine the energy,  $E_0$ , associated with normal depth.
- Determine the classification (steep, mild, critical) for this reach.
- Determine the depth and specific energy immediately upstream of the sluice gate.
- If there is a hydraulic jump, determine the depths on both sides of the jump.
- Sketch any flow profiles that exist.
- On an  $E$ - $y$  diagram, plot all the relevant profiles and energy-depth combinations for this problem. Show that the system analyzed amounts to an energy-conserving loop.

**Solution:**

- Using the Excel® Goal Seek tool, we readily find that  $y_0 = 1.26$  m.
- Using the specific energy equation,

$$E_0 = y_0 + \frac{q^2}{2gy_0^2} = 1.26 + \frac{\left(\frac{30}{10}\right)^2}{(2) \cdot (9.81) \cdot (1.26)^2} = 1.55 \text{ m}$$

- Critical depth for this problem is:

$$y_c = \left( \frac{q^2}{g} \right)^{1/3} = \left( \frac{\left(\frac{30}{10}\right)^2}{9.81} \right)^{1/3} = 0.97 \text{ m}$$

- Since  $y_0 > y_c$ , the reach is mild. We expect any profiles to be  $M_x$ .
- The gate conserves energy, so the energy associated with the gate opening is also the energy immediately upstream of the sluice gate:

$$E_{gate} = y_{gate} + \frac{q^2}{2gy_{gate}^2} = 0.50 + \frac{\left(\frac{30}{10}\right)^2}{(2) \cdot (9.81) \cdot (0.50)^2} = 2.34 \text{ m}$$

This is greater than the energy associated with normal depth; thus, the gate is a choke. The alternate depth to  $y_{gate} = 0.50$  m is:

$$y = \frac{2y_{gate}}{-1 + \sqrt{1 + \frac{8g y_{gate}^3}{q^2}}} = \frac{2 \cdot (0.50)}{-1 + \sqrt{1 + \frac{8 \cdot (9.81) \cdot (0.50)^3}{3^2}}} = 2.24 \text{ m}$$

We expect an  $M_1$  profile upstream of the gate beginning from normal depth,  $y_0 = 1.26$  m and ending at the gate at a depth of 2.24 m. This  $M_1$  profile provides the required gain in energy upstream of the gate to meet the energy required to pass the discharge for a gate opening of 0.50 m.

- e. Since the downstream boundary condition is  $y_0 = 1.26$  m, we expect a hydraulic jump to this depth. The conjugate depth to normal depth is thus,

$$y_{conj} = \frac{y_0}{2} \left( \sqrt{1 + 8 \cdot \frac{q^2}{g \cdot y_0^3}} - 1 \right) = \frac{1.26}{2} \left( \sqrt{1 + 8 \cdot \frac{(3)^2}{(9.81) \cdot (1.26)^3}} - 1 \right) = 0.73 \text{ m}$$

We expect an  $M_3$  profile downstream of the gate starting at a depth of  $y_{gate} = 0.50$  m and increasing to the conjugate depth,  $y_{conj} = 0.73$  m, calculated above.

- f. Figure 5.4 provides a sketch of the profiles for this system with all relevant depths indicated.

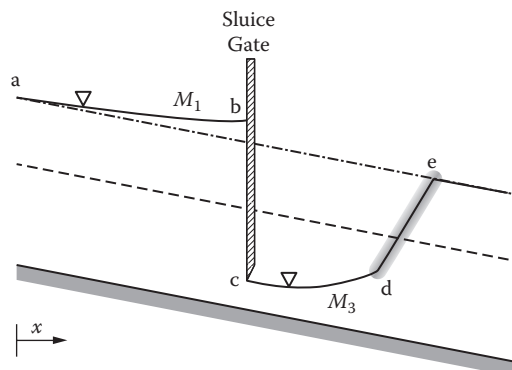


**FIGURE 5.4** Flow profiles for Example 5.1: a sluice gate on a mild reach.

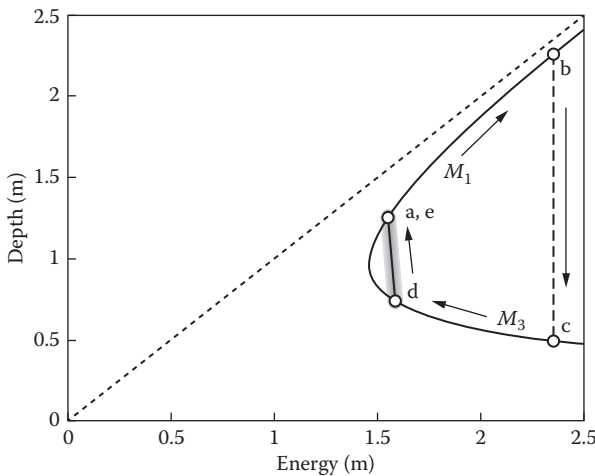


**FIGURE 5.5** E-y cycle for Example 5.1. Since flow begins and ends at same location (a, e), energy is conserved.

g. Likewise, Figure 5.5 shows the E-y diagram for this system.

Notice that because the flow begins and ends at the same depth,  $y_0$ , the flow thus begins and ends with the same energy. This means that the energy gained on the  $M_1$  curve is equal to the energy lost in the combination of the  $M_3$  curve and the hydraulic jump. We can check this:

- Energy gained on  $M_1$ :  $\Delta E = E(y = 2.24 \text{ m}) - E(y_0 = 1.26 \text{ m}) = 2.34 - 1.55 = +0.79 \text{ m}$
- Energy lost on  $M_3$ :  $\Delta E = E(y_{conj} = 0.73 \text{ m}) - E(y_{gate} = 0.50 \text{ m}) = 1.59 - 2.34 = -0.75 \text{ m}$
- Energy lost in hydraulic jump:  $\Delta E = E(y_0 = 1.26 \text{ m}) - E(y_{conj} = 0.73 \text{ m}) = 1.55 - 1.59 = -0.04 \text{ m}$

In this specific case, the vast majority of energy lost by the flow is on the  $M_3$  curve, rather than within the hydraulic jump.

### Example 5.2

Let's remain with the system analyzed in Example 5.1, changing only the roughness of the channel. The new, much smaller, roughness is 0.015. Repeat the analysis in Example 5.1 with this one change.

**Solution:**

- a. Using the Excel Goal Seek tool, we readily find that  $y_0 = 0.81$  m.  
 b. Using the specific energy equation,

$$E_0 = y_0 + \frac{q^2}{2gy_0^2} = 0.81 + \frac{\left(\frac{30}{10}\right)^2}{(2) \cdot (9.81) \cdot (0.81)^2} = 1.51 \text{ m}$$

- c. As we found previously,  $y_c = 0.97$  m, so now  $y_0 < y_c$ . The reach is steep. We expect any profiles to be  $S_x$ .  
 d. The energy associated with the gate is unchanged from Example 5.1. The gate conserves energy, so the energy associated with the gate opening is also the energy immediately upstream of the sluice gate, which was previously calculated in Example 5.1 as  $E_{gate} = 2.34$  m:

$$E_{gate} = y_{gate} + \frac{q^2}{2gy_{gate}^2} = 0.50 + \frac{\left(\frac{30}{10}\right)^2}{(2) \cdot (9.81) \cdot (0.50)^2} = 2.34 \text{ m}$$

This is greater than the energy associated with normal depth; thus, the gate is a choke. The alternate depth to  $y_{gate} = 0.50$  m is 2.24 m as we calculated in Example 5.1. We expect an  $S_1$  profile upstream of the gate. The ending, downstream, depth of the  $S_1$  profile will be 2.24 m, just upstream of the gate.

- e. Since  $y_0 = 0.81$  m and corresponds to supercritical conditions, the upstream end of the  $S_1$  curve anticipated in part (d) must also correspond to the downstream end of a hydraulic jump starting from a depth of 0.81 m. Using the conjugate depth equation we solve for that depth:

$$y_{conj} = \frac{y_0}{2} \left( \sqrt{1 + 8 \cdot \frac{q^2}{g \cdot y_0^3}} - 1 \right) = \frac{0.81}{2} \left( \sqrt{1 + 8 \cdot \frac{(3)^2}{(9.81) \cdot (0.81)^3}} - 1 \right) = 1.15 \text{ m}$$

Thus there is a hydraulic jump from  $y_0 = 0.81$  m to the conjugate of this depth at 1.15 m. An  $S_1$  curve from 1.15 m to 2.24 follows to the gate. Downstream of the gate we anticipate an  $S_3$  curve from  $y_{gate} = 0.50$  m back to  $y_0 = 0.81$  m.

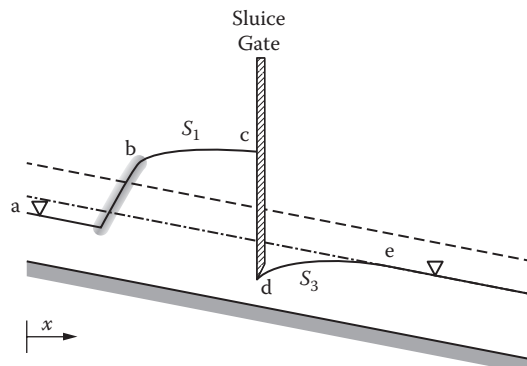


**FIGURE 5.6** Flow profiles for Example 5.2: a sluice gate on a steep reach.

- f. Figure 5.6 provides a sketch of the profiles for this system with all relevant depths indicated.
- g. Likewise, Figure 5.7 shows the  $E-y$  diagram for this system. As before, the flow begins and ends at the same depth,  $y_0$ ; the flow thus begins and ends with the same energy. Checking conservation of energy,

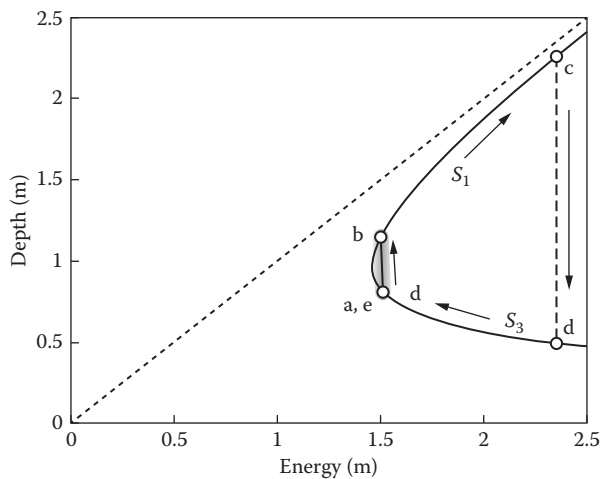


**FIGURE 5.7**  $E-y$  cycle for Example 5.2. Since flow begins and ends at same location (a, e), energy is conserved.

- Energy lost in hydraulic jump:  $\Delta E = E(y_{conj} = 1.15 \text{ m}) - E(y_0 = 0.81 \text{ m}) = 1.50 - 1.51 = -0.01 \text{ m}$
- Energy gained on  $S_1$ :  $\Delta E = E(y = 2.24 \text{ m}) - E(y_{conj} = 1.15 \text{ m}) = 2.34 - 1.50 = +0.84 \text{ m}$
- Energy lost in  $S_3$ :  $\Delta E = E(y_0 = 0.81 \text{ m}) - E(y_{gate} = 0.50 \text{ m}) = 1.51 - 2.34 = -0.83 \text{ m}$
- As in Example 5.1, the vast majority of energy lost by the flow is on a flow profile, this time the  $S_3$  curve, rather than within the hydraulic jump.

Notice that in order for the flow to gain energy on the  $S_1$  curve, it first must counterintuitively lose energy in a hydraulic jump so as to transition to subcritical flow.

We now discuss the concept of the *equivalent in-stream obstruction*. Examples 5.1 and 5.2 show the effect of a sluice gate on flow profiles upstream and downstream of the gate. Viewed at the scale of the entire reach, a step or constriction in flow can be designed to induce these same flow profiles. In this manner, a sluice gate, upward step, or flow constriction can be considered equivalent, if they set up the same profiles upstream and downstream within the reach.

We understand that at the local scale (the scale of the obstruction), both a step and a constriction have some finite length over which they act. This differs from the sluice gate which occupies an essentially negligible length along the direction of flow. At the local scale, the geometry of the step or constriction will control the specifics of flow depth and velocity. We choose to ignore these details at the local scale. We can treat these other obstructions as black-box, energy-conserving devices just like the sluice gate. Example 5.3 illustrates this concept.

### **Example 5.3**

Return to the general conditions provided in Example 5.1. What height of upward step would represent an equivalent in-stream obstruction to the sluice gate specified in Example 5.1?

#### **Solution:**

An upward step, acting as an equivalent in-stream obstruction would set up alternate depths upstream and downstream equal to 2.24 m and

0.50 m, respectively. In Example 5.1, we calculated that these depths both correspond to a specific energy of 2.34 m.

We previously calculated the critical depth in the reach to be 0.97 m. Since the channel is rectangular, the critical energy is

$$E_c = \frac{3}{2} \cdot y_c = \frac{3}{2} \cdot (0.97) = 1.46 \text{ m}$$

The step height needed to produce a specific energy of 2.34 m is, therefore,

$$\Delta z = E_{step} - E_c = 2.34 - 1.46 = 0.88 \text{ m}$$

This step height,  $\Delta z = 0.88 \text{ m}$ , will produce equivalent profiles to the ones determined in Example 5.1. Further, notice that because the normal depth flow conditions are not needed to calculate this solution, this solution is equally applicable to Example 5.2. Problems 5.4 through 5.6 provide additional practice with this concept.

---

The above example quietly addresses the conundrum posed in Figure 2.16. That figure drew the analogy between a ball placed exactly at the top of a perfectly symmetrical hill and the flow regime that prevails downstream of a choke. Which way will the ball roll? My response then was it depended which way the “wind” was blowing. With regard to the prevailing flow regime, we see that the flow must follow the rules associated with the suite of surface water profiles shown in Figure 5.3.

In Example 5.3, the flow reaches critical conditions within the constriction and thus both subcritical and supercritical pathways are accessible downstream. This is a mild reach; thus the flow should seek the subcritical pathway. One might figuratively say that the “wind” is blowing subcritically. However, the flow leaves the constriction with excess energy relative to normal flow conditions. This excess energy must somehow be dissipated. There is no viable subcritical profile to lose energy, and thus the flow immediately downstream of the obstruction must be supercritical. The  $M_3$  profile loses energy until the flow depth reaches the conjugate depth to the subcritical normal depth for this reach. At that point a hydraulic jump returns the flow to normal depth conditions. In this example, as in all cases, flow leaving critical conditions must follow a viable pathway from among those shown in Figure 5.3 in returning to normal flow conditions.

## 5.5 COMPOSITE PROFILES

In this section, we explore a number of paired stream reaches that set up gradually varied surface water profiles. Unless otherwise stated, we assume the boundary conditions such that the flow enters the top of the upper reach (Reach A) at normal depth for the upper reach,  $y_{0,A}$ , and leaves the bottom of the lower reach (Reach B) at normal depth for the lower reach,  $y_{0,B}$ . These explorations will take the form of a number of example problems. The channel slope will be varied to alter normal depth in these problems. This is done for visual purposes, but keep in mind that other elements might also serve to change the normal depth, for instance channel roughness or cross-sectional geometry.

Focusing exclusively on steep and mild reaches, there are six possible paired reach scenarios.

### **Example 5.4: Mild Reach Flowing into a Steep Reach**

Figure 5.8 shows the profiles that result from flow on a mild upstream reach transitioning to a steep downstream reach. The boundary conditions both upstream and downstream are normal depth for the respective reaches. The figure shows an  $M_2$  profile transitioning from  $y_{0,A}$  to  $y_c$  at the interface between Reaches A and B. From there an  $S_2$  profile transitions the flow from  $y_c$  to  $y_{0,B}$ . This case should reinforce understanding of our terminology earlier in the book concerning the occurrence of critical depth at the outfall from a lake (see discussion concerning

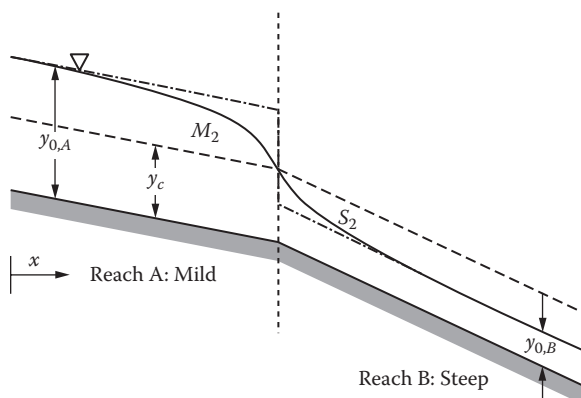


**FIGURE 5.8** Composite surface water profile for a mild reach flowing into a steep reach.

Figure 2.18). The reason for specifying that the discharge was to a steep reach in that example, was to ensure that the flow is not restrained by conditions on the downstream reach. With steep conditions prevailing downstream, the flow necessarily seeks critical depth at the interface between Reaches A and B. We return to this lake discharge discussion later in this chapter, when we examine the possibility of a lake discharging to a mild reach.

Consider how specific energy varies along the  $M_2$  and  $S_2$  profiles. From Figure 5.3, we learn than an  $M_2$  profile loses energy, in this case from the energy associated with  $y_{0,A}$  on Reach A down to critical energy,  $E_c$ . In contrast an  $S_2$  profile gains energy as the depth continues to decrease down to  $y_{0,B}$ . Viewed from the perspective of the  $E$ - $y$  diagram, this pairing of flow profiles amounts to a trip from high depth to low depth along the  $E$ - $y$  curve, passing through critical depth and energy at the interface between Reaches A and B. Due to the qualitative nature of this discussion, the net energy gain or loss cannot be determined. The net energy gain or loss depends on which normal depth,  $y_{0,A}$  or  $y_{0,B}$ , corresponds to the greater specific energy.

Considering past discussions on information propagation, we can see how that concept meshes with this pair of profiles. In the case of the  $M_2$  profile, the fact that Reach B is steep is able to propagate upstream to Reach A. This is reflected in the mere existence of the  $M_2$  profile. This is to be expected given that flow is subcritical on Reach A. In contrast, the  $S_2$  profile on Reach B reflects flow conditions on Reach B, rather than flow conditions downstream. This is also to be expected since the flow is supercritical on Reach B.

---

### ***Example 5.5: Mild Reach Flowing into a Less Mild Reach***

Figure 5.9 shows the profile that results from flow on a mild upstream reach transitioning to a downstream reach on which the flow is less mild (i.e., the normal depth on Reach B is less than the normal depth on Reach A, but is still greater than critical depth). As before, the boundary conditions both upstream and downstream are normal depth for the respective reaches. The figure shows an  $M_2$  profile transitioning from  $y_{0,A}$  to  $y_{0,B}$  at the interface between Reaches A and B. From there uniform flow at a depth of  $y_{0,B}$  persists. As in Example 5.3, an  $M_2$  profile exists on Reach A. The difference is that the  $M_2$  profile does not diminish to all the way down to critical depth,  $y_c$ . In this case, the  $M_2$  profile only needs to diminish to  $y_{0,B}$ . This example illustrates more generally

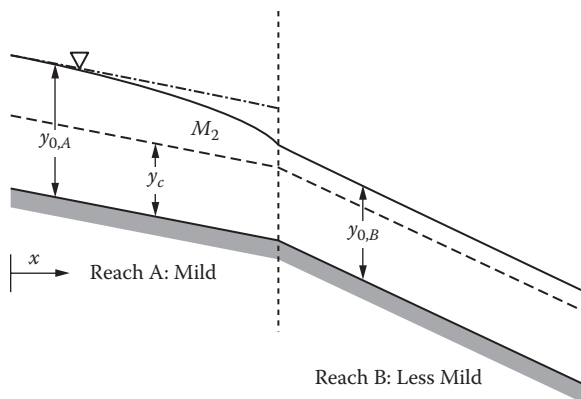


**FIGURE 5.9** Composite surface water profile for a mild reach flowing into a less mild reach.

that while an  $M_2$  profile exists over a depth range between  $y_c$  and  $y_0$ , this does not mean the profile must span this *entire* range. In this case, the  $M_2$  profile only needs to diminish to  $y_{0,B}$ , but no shallower. Since the depth is  $y_{0,B}$  at the head of Reach B, there is no need for any profile on this reach. Instead, uniform flow prevails throughout Reach B at depth,  $y_{0,B}$ .

From the perspective of specific energy, the  $M_2$  loses energy over the course of flow on Reach A. Energy remains constant on Reach B at the specific energy associated with  $y_{0,B}$ . In the net, energy is lost over Reach A and throughout the paired reach system.

As was the case in Example 5.3, conditions on Reach B favor a smaller normal depth than on Reach A. This information is able to propagate upstream with the subcritical flow on Reach A. But why does the profile exist on Reach A? Why can't the flow diminish from  $y_{0,A}$  to  $y_{0,B}$  on Reach B? The reason this is not the case goes back to the discussion presented at the end of Section 5.3. A more practical way to look at this is to assume the profile is on Reach B and then identify the inconsistency with this assumption. Since Reach B is mild, we would expect an  $M_x$  profile. Since the flow is subcritical, that profile must be either an  $M_1$  or  $M_2$ . But an  $M_1$  gains depth so that profile cannot work. Why not an  $M_2$ ? We see that if an  $M_2$  profile were on Reach B, this profile would represent a transition in depth from *greater* than normal depth down to  $y_{0,B}$ . But Figure 5.3 shows that the only profile that can exist at depths greater than normal depth is an  $M_1$ , which we have already ruled out. Hence, there is no profile—no pathway—for the flow to transition from  $y_{0,A}$  to  $y_{0,B}$  on Reach B. The profile must exist exclusively on Reach A.

### Animation: `mild_vary.avi`

Flow conditions:

$$Q = 100 \text{ ft}^3/\text{s}$$

$$n = 0.03$$

$$b = 10 \text{ ft}$$

$$S_{0,A} = 0.005 \text{ ft/ft}$$

Apparent movement:

$$S_{0,B} = \text{varies from } 0.0025 \text{ to } 0.0515 \text{ ft/ft}$$

Rectangular cross-section

Still image of animation shown in Figure 5.10

This animation shows a mild upstream reach and downstream reach that varies from two times milder than the upstream reach to a steep reach. Upstream and downstream boundary conditions are normal depth at all

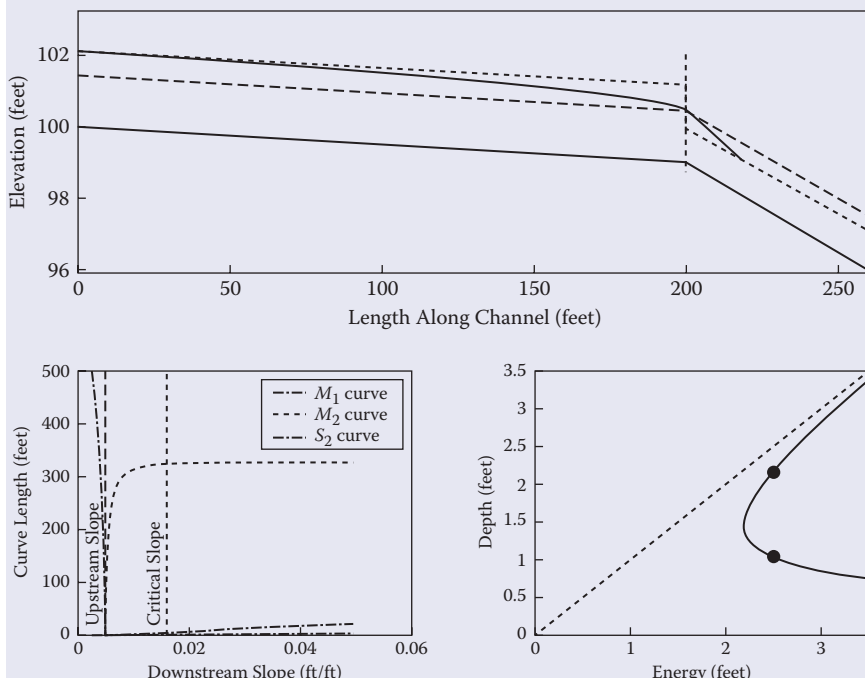


**FIGURE 5.10** Screen capture from `mild_vary.avi` animation. The capture shows the effect of varying downstream reach slope on surface water profiles both upstream and downstream of the break in slope. (See text for further explanation of subplots.)

times. Surface water profiles evolve accordingly. The lower right subplot shows the  $E$ - $y$  diagram with normal depths indicated by the plotted circles. The water surface is shown in the upper subplot with critical and normal depths indicated as dashed lines. The lower left subplot shows lengths of  $M_1$ ,  $M_2$ , and  $S_2$  curves as they evolve with changing downstream slope. The vertical dashed lines in this subplot show the slope of the upstream reach and the slope that corresponds to critical conditions in the downstream reach. These vertical lines form boundaries on the evolution of the different surface water curves. The method for calculation of the lengths of the various profiles shown here will be presented in Chapter 6.

The reader may notice that the remaining two-reach pairing of a mild reach upstream flowing into a more mild reach downstream has not been addressed as an example. Solving the profiles for this pairing is left as an exercise (Problem 5.10).

### **Example 5.6: Steep Reach Flowing into a More Steep Reach**

Figure 5.11 shows the profile that results from flow on a steep upstream reach transitioning to a downstream reach on which the flow is more steep (i.e., the normal depth on Reach B is less than the normal depth on Reach A). The reader should notice that the relative magnitudes of the normal depths on Reaches A and B are the same as in Example 5.5 (compare Figure 5.11 here with Figure 5.9 corresponding to

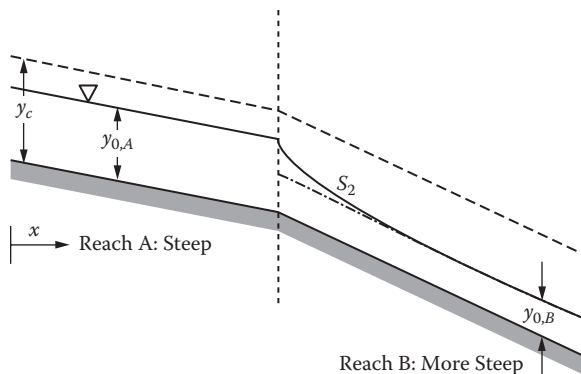


**FIGURE 5.11** Composite surface water profile for a steep reach flowing into a more steep reach.

Example 5.5). The difference in this example is that both reaches are steep, not mild. This difference is important and leads to uniform flow at normal depth,  $y_{0,A}$ , on Reach A followed by an  $S_2$  profile transitioning the depth from  $y_{0,A}$  to  $y_{0,B}$  on Reach B. This concept of information propagation and flow regime, first presented in the discussion of Figure 2.5, is illustrated well in Example 5.6. The information that  $y_{0,B} < y_{0,A}$  is unable to propagate upstream against the supercritical flow. Thus, Reach A flows at uniform conditions throughout, while Reach B contains the  $S_2$  profile.

---

### ***Example 5.7: Steep Reach Flowing into a Mild Reach***

The case of a steep reach flowing into a mild reach is a bit more complicated than the other two reach profile cases we have examined through example thus far. Since the flow enters Reach A at a normal depth corresponding to supercritical conditions and leaves Reach B at a normal depth corresponding to subcritical conditions, there must be a transition from supercritical to subcritical flow. In general, there is no reason to expect the existence of a step or constriction that will mediate this transition perfectly as we examined in Example 3.1(e). In general, we expect a hydraulic jump to move the flow from supercritical to subcritical conditions. So the first question is, On which reach does the jump occur—Reach A or Reach B? The answer is ... it depends. It depends on a comparison of normal depths on each reach and the conjugate to these normal depths on each reach. Ultimately, it depends on the issue of flow accessibility as was originally discussed in Chapter 2. Unlike the other two reach profiles just discussed, we will examine this example quantitatively so that the contrast between the two possibilities is as clear as possible.

---

#### ***Example 5.7a***

Flow conditions:

- Discharge,  $Q = 30 \text{ m}^3/\text{s}$
- Channel is rectangular with width,  $b = 10 \text{ m}$
- Manning's roughness,  $n = 0.030$
- Reach A slope,  $S_A = 0.0927 \text{ m/m}$
- Reach B slope,  $S_B = 0.0050 \text{ m/m}$

Perform the following:

- Determine normal depth,  $y_{0,A}$  and the conjugate depth,  $y_{0,A,conj}$ .
- Determine normal depth,  $y_{0,B}$  and the conjugate depth,  $y_{0,B,conj}$ .
- Determine if the hydraulic jump is located on Reach A or B.
- Sketch the expected flow profiles on Reaches A and B indicating depths at the upstream and downstream ends of these profiles.
- Discuss similarities between the results from this example and those in Example 5.1.

**Solution:**

- Using the Excel Goal Seek tool, we find that  $y_{0,A} = 0.50$  m. The conjugate to this normal depth is

$$y_{0,A,conj} = \frac{y_{0,A}}{2} \left( \sqrt{1 + 8 \cdot \frac{q^2}{g \cdot y_0^3}} - 1 \right) = \frac{0.50}{2} \left( \sqrt{1 + 8 \cdot \frac{(30/10)^2}{(9.81) \cdot (0.50)^3}} - 1 \right) = 1.68 \text{ m}$$

- For Reach B we note that the discharge, roughness, and slope are the same as in Example 5.1, so  $y_{0,B}$  is 1.26 m. The conjugate to this depth was also determined in Example 5.1, so  $y_{0,B,conj}$  is 0.73 m.
- Given the results from parts (a) and (b), we find that the hydraulic jump occurs on Reach B. This is because  $y_{0,A} < y_{0,B,conj}$  allowing simply for an  $M_3$  profile to move the flow from normal depth on Reach A, up to the deeper conjugate depth to normal depth on Reach B. From there we expect a hydraulic jump back to normal depth on Reach B. Reach A exhibits uniform flow at  $y_{0,A} = 0.50$  m along its entire length.
- Figure 5.12 shows the expected flow profiles on Reaches A and B. Reach A flows at normal depth,  $y_{0,A} = 0.50$  m for its entire

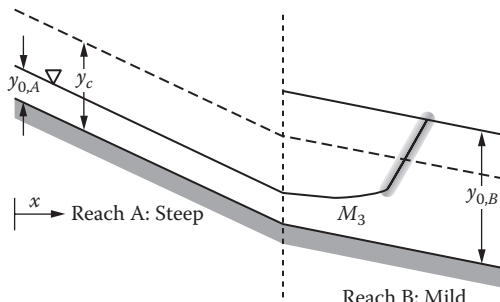


**FIGURE 5.12** Composite surface water profile for a steep reach flowing into a mild reach with the hydraulic jump occurring on the mild reach.

length. At the transition to Reach B, an  $M_3$  profile ensues. This profile begins from a depth of  $y_{0,A} = 0.50$  m and increases to a depth of  $0.73 \text{ m} = y_{0,B,conj}$ . The hydraulic jump returns the flow to normal depth,  $y_{0,B} = 1.26$  m on Reach B.

- e. The sequences of profiles on Reach B in this example are the same as those that were determined to occur downstream of the sluice gate in Example 5.1. In effect, Reach A takes the place of the sluice gate, setting up a flow depth of 0.50 m to be followed by the same  $M_3$  profile and hydraulic jump as in Example 5.1.
- 

### **Example 5.7b**

Flow conditions:

- Discharge,  $Q_r = 30 \text{ m}^3/\text{s}$
- Channel is rectangular with width,  $b = 10 \text{ m}$
- Manning's roughness,  $n = 0.015$
- Reach A slope,  $S_A = 0.0050 \text{ m/m}$
- Reach B slope,  $S_B = 0.000226 \text{ m/m}$

Perform the following:

- a. Determine normal depth,  $y_{0,A}$  and the conjugate depth,  $y_{0,A,conj}$ .
- b. Determine normal depth,  $y_{0,B}$  and the conjugate depth,  $y_{0,B,conj}$ .
- c. Determine if the hydraulic jump is located on Reach A or B.
- d. Sketch the expected flow profiles on Reaches A and B indicating depths at the upstream and downstream ends of these profiles.
- e. Discuss similarities between the results from this example and those in Example 5.2.

### **Solution:**

- a. In Reach A we note that the discharge, roughness, and slope are the same as in Example 5.2, so  $y_{0,A}$  is 0.81 m. The conjugate to this depth was also determined in Example 5.2, so  $y_{0,A,conj}$  is 1.15 m.
- b. Using the Excel Goal Seek tool, we find that  $y_{0,B} = 2.24$  m. The conjugate to this normal depth is

$$y_{0,B,conj} = \frac{y_{0,B}}{2} \left( \sqrt{1 + 8 \cdot \frac{q^2}{g \cdot y_0^3}} - 1 \right) = \frac{2.24}{2} \left( \sqrt{1 + 8 \cdot \frac{(30/10)^2}{(9.81) \cdot (2.24)^3}} - 1 \right) = 0.32 \text{ m}$$

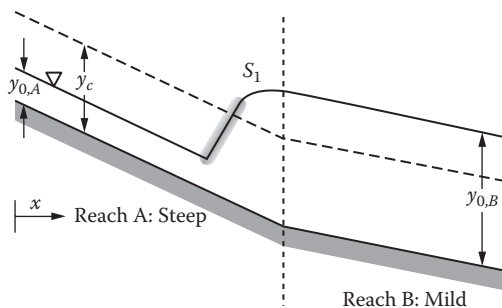


**FIGURE 5.13** Composite surface water profile for a steep reach flowing into a mild reach with the hydraulic jump occurring on the steep reach.

- c. Given the results from parts (a) and (b), we find in this case that the hydraulic jump occurs on Reach A. This is because  $y_{0,A} > y_{0,B,conj}$ , so we expect a hydraulic jump on Reach A, followed by an  $S_1$  profile to move the flow from the conjugate to normal depth on Reach A to a depth of 2.24 m, equal to the normal depth on Reach B. Reach B exhibits uniform flow at  $y_{0,B} = 2.24$  m along its entire length.
- d. Figure 5.13 shows the expected flow profiles on Reaches A and B. Reach A flows first at normal depth,  $y_{0,A} = 0.81$  m. A hydraulic jump occurs, ending at a depth of  $y_{0,A,conj} = 1.15$  m. After the hydraulic jump, there is an  $S_1$  curve on Reach A from an upstream depth of 1.15 m to a depth of 2.24 m at the downstream Reach A-Reach B interface. Reach B flows at normal depth of  $y_{0,B} = 2.24$  m for its entire length.
- e. The sequences of profiles on Reach A in this example are exactly as those that were determined to occur upstream of the sluice gate in Example 5.2. In effect, Reach B mandates a specific energy identical to the specific energy at the sluice gate in Example 5.2, so the profiles observed on Reach A are identical to those observed upstream of the gate in Example 5.2.

It is worth summarizing the findings from Examples 5.7a and 5.7b. Because of the upstream and downstream boundary conditions of normal depth and because Reach A is steep and Reach B is mild, a hydraulic jump must take place somewhere in between. In these examples, we learned that the

**TABLE 5.1** Location of Reach Containing Hydraulic Jump when a Steep Reach (Reach A) Flows into a Mild Reach (Reach B)

Example	Depth Comparison	Reach Containing Hydraulic Jump
Example 5.7a	Normal depth on Reach A is less than conjugate depth on Reach B	Reach B
Example 5.7b	Normal depth on Reach A is greater than conjugate depth on Reach B	Reach A

important comparison to make is between the normal depth on Reach A and the conjugate depth to normal depth on Reach B. The relative magnitude of these two depths will determine the reach that contains the hydraulic jump. This is summarized in Table 5.1.

Table 5.2 summarizes the six possible paired reach scenarios. Some were presented in Examples 5.4 through 5.7. The remainder are left as exercises to the reader in Problem 5.10. All possibilities are covered in either the `mild_vary.avi` or `steep_vary.avi` animations.

**TABLE 5.2** Possible Pairings of Two Reach Profile Scenarios

Upstream Reach (Reach A)	Downstream Reach (Reach B)	Scenario Discussion	Relevant Animation
Mild	Less mild	Example 5.5	<code>mild_vary.avi</code>
	More mild	Problem 5.10	
	Steep	Example 5.4	
Steep	Less steep	Problem 5.10	<code>steep_vary.avi</code>
	More steep	Example 5.6	
	Mild	Examples 5.7a, 5.7b	

### Animation: steep\_vary.avi

Flow conditions:

$$Q = 100 \text{ ft}^3/\text{s}$$

$$n = 0.03$$

$$b = 10 \text{ ft}$$

$$S_{0,A} = 0.000223 \text{ ft/ft}$$

$$S_{0,B} = \text{varies from } 9.7 \times 10^{-6} \text{ ft/ft to } 0.00436 \text{ ft/ft}$$

Apparent movement:

Rectangular cross-section

Still image of animation shown in Figure 5.14

This animation shows a steep upstream reach and a downstream reach that varies from a slope about 20 times smaller than the upstream reach

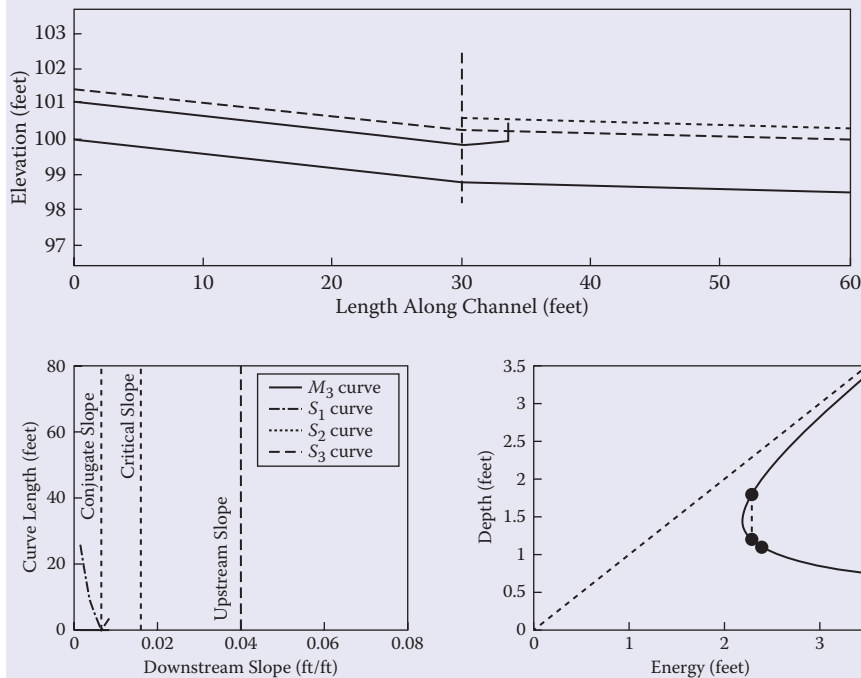


**FIGURE 5.14** Screen capture from *steep\_vary.avi* animation. The capture shows the effect of varying downstream reach slope on surface water profiles both upstream and downstream of the break in slope. The screen capture shown corresponds to conditions early in the simulation when the downstream reach is mild and the hydraulic jump is located on the downstream reach. (See the text for further explanation of the subplots shown.)

to about 20 times steeper than the upstream reach. Upstream and downstream boundary conditions are normal depth at all times. Surface water profiles evolve accordingly. The lower right subplot shows the  $E$ - $y$  diagram with normal depths indicated by the plotted squares. Shaded regions of the  $E$ - $y$  diagram indicate where surface water profiles engage. The water surface is shown in the upper subplot with critical and normal depths indicated as dashed lines. The lower left subplot shows lengths of the  $S_1$  (on upstream reach),  $M_3$  (on downstream reach),  $S_3$  (on downstream reach), and  $S_2$  (on downstream reach) curves, respectively, as they evolve with increasing downstream slope. The vertical dashed lines in this subplot show the slope of the upstream reach and the slope that corresponds to critical conditions in the downstream reach. These vertical lines form boundaries on the evolution of the different surface water curves. The method for calculation of the lengths of the various profiles shown here will be presented in Chapter 6.

## 5.6 DROWNED HYDRAULIC JUMP

In Example 5.1, we observed an  $M_3$  curve downstream of the gate, followed by a hydraulic jump which returned the flow to normal depth. In that example, the gate was set to a depth of 0.50 m and the  $M_3$  curve eventually reached 0.73 m at the toe of the hydraulic jump. Obviously, if the sluice gate were set to a depth of 0.73 m, the  $M_3$  curve would reduce to zero length, and the hydraulic jump would occur immediately downstream of the gate. What, then, if the gate is set to some depth less than  $y_c = 0.97$  m but greater than 0.73 m?

This is a tricky situation. The flow accessibility argument presented in Chapter 2 would suggest that the flow downstream of the gate, since it is set to a depth less than critical depth, would be supercritical. But, if the gate depth is greater than the conjugate to normal depth, how can the flow return to subcritical conditions? The conclusion must be that something other than a momentum-conserving hydraulic jump must occur. This is the case of the *drowned jump*.

---

### Example 5.8

We return to the conditions first explored in Example 5.1:

- a. Determine the smallest gate opening such that no  $M_1$  curve is created upstream of the sluice gate. What surface water profiles would be expected for gate openings greater than this value?

- b. Determine the range of gate openings that result in some energy shifts upstream and/or downstream of the gate, but not a true hydraulic jump?
- c. Determine the range of energy that is dissipated by the gate openings identified in part (b).

**Solution:**

- a. If there is no  $M_1$  curve upstream of the gate, this is just a fancy way of saying that the gate is not a choke. Therefore, the smallest gate opening where this is true is the supercritical alternate depth to the normal depth of 1.26 m. Using the alternate depth equation, we find that this depth (and gate opening) is 0.76 m. Any supercritical gate opening greater than this depth would correspond to less energy than the flow possesses. These openings would result in no  $M_1$  curve upstream of the gate and correspond to the case of a pure drowned jump. No profiles or energy changes will be present immediately upstream or downstream of the gate.
- b. From the result in part (a), we see that there is a relatively narrow range of flow depths  $0.73 \text{ m} < y_{gate} < 0.76 \text{ m}$  over which the gate acts as a choke and thus results in an energy shift. Any gate opening greater than 0.76 m is not a choke, while any gate opening smaller than 0.73 m will result in a true hydraulic jump.
- c. We need only calculate the specific energy associated with depths of 0.73 m and 0.76 m, and this will determine the range of energy dissipated:

$$E(y_{gate} = 0.76 \text{ m}) = y_{gate} + \frac{q^2}{2gy_{gate}^2} = 0.76 + \frac{\left(\frac{30}{10}\right)^2}{(2) \cdot (9.81) \cdot (0.76)^2} = 1.55 \text{ m}$$

$$E(y_{gate} = 0.73 \text{ m}) = 0.73 + \frac{\left(\frac{30}{10}\right)^2}{(2) \cdot (9.81) \cdot (0.73)^2} = 1.59 \text{ m}$$

From this analysis, we see that the range of energy dissipated is a meager 0.04 m at most. Drowned jumps can potentially result in much greater energy dissipation, depending on how far normal depth is from critical flow conditions. Problem 5.13 examines this idea more thoroughly.

## 5.7 GENERALIZED BOUNDARY CONDITIONS

To this point in this chapter, we have almost exclusively limited our discussions of surface water profiles that transition the flow depth to and from either normal depth or the conjugate to normal depth depending on whether a reach is steep or mild and whether the flow is supercritical or subcritical. This has made the discussion simpler, but may have given the mistaken impression that profiles are limited to begin and end at these unique depths. This is not the case. There are myriad reasons why conditions upstream or downstream may differ from normal, critical, or conjugate depth. This section will explore the more general case of any arbitrary depth serving as an upstream or downstream boundary condition.

### 5.7.1 Downstream Boundary Conditions

In large measure, we have already encountered downstream boundary conditions in Section 5.5. There, for instance, we saw how information about downstream conditions cannot propagate upstream in a supercritical flow, only in a subcritical flow. That idea is central again here. Consider the case shown in Figure 5.15. The primary difference now being considered is that the downstream boundary condition is still water (i.e., a lake) rather than flowing water. In this case, the lake represents a boundary condition solely through its water surface elevation and the static energy it implies.

The main consideration in addressing this kind of problem is to balance the specific energy of the flow in the reach with the specific energy indicated by the downstream boundary condition. The same rules we have discussed in earlier chapters and in earlier sections of this chapter still apply. If the downstream

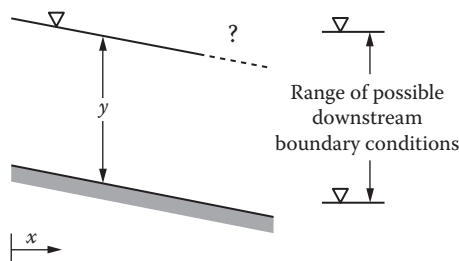


**FIGURE 5.15** River reach flowing into a downstream boundary condition, such as a lake, that can vary in elevation.

water surface elevation implies more specific energy than the flow possesses at normal depth, it represents a choke, and the flow must back up as we have previously examined in the context of in-stream obstructions, to gain the energy necessary to seamlessly merge with the downstream boundary condition. If the reach draining to the lake is steep, a hydraulic jump upstream of the lake will be necessary to first transition to subcritical flow so that it is possible to gain the appropriate specific energy.

One complicating feature with the case of a lake serving as a downstream boundary condition is the velocity in the reach being finite while the lake velocity is zero. How is this reconciled? In truth, a short transitional zone exists over which the flow decelerates to a velocity of zero. We will not elaborate on this zone except to recognize that the specific energy within this zone is conserved. The following example helps illustrate this concept.

### **Example 5.9**

The following flow conditions exist in a reach discharging to a lake at the downstream end:

- Discharge,  $Q = 30 \text{ m}^3/\text{s}$
- Channel is rectangular with width,  $b = 10 \text{ m}$
- Manning's roughness,  $n = 0.03$
- Reach slope,  $S_0 = 0.0050 \text{ m/m}$
- The elevation of the channel bottom where the reach meets the lake is 100 m. For simplicity here, the region where the reach and lake join is such that the channel shape and slope can be assumed to extend into the lake.
- The level of the lake varies over the year from a low of 100 m to a high of 103 m.

Perform the following:

- a. Determine the normal and critical depth for the reach and whether the reach is steep or mild.
- b. Sketch the flow profiles that will be observed over the range of lake levels.

### **Solution:**

- a. The normal and critical depths were previously calculated in Example 5.1 as 1.26 m and 0.97 m, respectively. Since normal depth is greater than critical depth, the reach is mild.

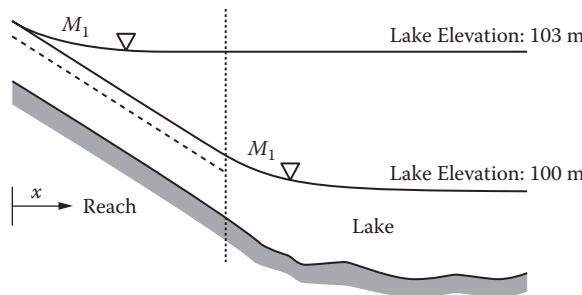


**FIGURE 5.16** Range in  $M_1$  curves joining the reach with the lake in Example 5.9.

- b. Figure 5.16 shows the flow in the reach merging with the lake over the limits of the downstream lake level variation. The reach transitions into the lake through a family of  $M_1$  curves that differ only in how far upstream these profiles propagate over the range of observed lake levels. In this example, that distance of propagation can be approximated by

$$\frac{\Delta y}{S_0} = \frac{103 - 100}{0.005} = 600 \text{ m}$$

where  $\Delta x$  is the propagation distance and  $\Delta y$  is the range in lake level variation.

---

The problem addressed in Example 5.9 concerned a mild reach with a variable downstream boundary condition. Problem 5.11 is similar but concerns a steep reach discharging to a variable downstream condition.

## 5.7.2 Upstream Boundary Conditions

The next consideration is of a variable upstream boundary condition. This possibility is perhaps a little trickier because the behavior of the upstream boundary differs depending on whether it corresponds to incoming supercritical or subcritical conditions. We examine both cases.

### 5.7.2.1 Case 1: Incoming Supercritical Flow

Information does not propagate upstream in a supercritical flow. Thus, if the

incoming flow is supercritical, it brings with it both an incoming water surface elevation and an incoming discharge. This case was examined in the context of the flow conditions downstream of a sluice gate—for example, see the discussion about the  $M_3$  profile downstream of the gate in Example 5.1 or the  $S_3$  profile downstream of the gate in Example 5.2. Please see Problem 5.14 which deals with this case.

### 5.7.2.2 Case 2: Incoming Subcritical Flow

An incoming subcritical flow is sensitive to the reach conditions it encounters downstream; that information will propagate upstream beyond the boundary condition. In this complement to Case 1, the discharge from the upstream boundary depends on the conditions encountered by the incoming flow. There are two possibilities. The first possibility was examined in Chapter 2 for the case of a lake discharging into a steep reach. In this case, the upstream boundary condition specifies the energy or depth, which corresponds to the critical energy or depth, for the discharge entering the reach. Since the downstream reach is steep, we expect an  $S_2$  profile to follow downstream until normal depth is reached. This is the simpler of the two possibilities.

The other possibility results in what is referred to as the *lake discharge problem*. In this case, the downstream reach is mild and thus the flow entering at the top of the reach is subcritical rather than critical. An energy balance between the upstream boundary condition and the flow in the reach must be achieved. The discharge that enters the reach mediates this energy balance, as examined in Example 5.10.

#### **Example 5.10: The Lake Discharge Problem**

A lake has an elevation 2 m greater than the invert at the head of a downstream reach. The downstream reach has a rectangular cross-section, 5 m in width, a Manning's roughness of 0.040, and a channel slope of 0.0025 m/m.

- Show that the downstream reach is mild.
- Find the discharge in the downstream reach.

#### **Solution:**

- Assume that the reach is, in fact, steep. If this is the case, then lake elevation of 2 m corresponds to the critical energy at the

entrance to the downstream reach, and the discharge can thus be calculated:

$$Q = b \sqrt{g \cdot \left(\frac{2}{3} E_c\right)^3} = 5 \sqrt{9.81 \cdot \left(\frac{2 \cdot 2}{3}\right)^3} = 24.1 \frac{\text{m}^3}{\text{s}}$$

Given the roughness and slope specified, we can use the Excel Goal Seek tool to determine a normal depth of 3.1 m. Clearly the initial assumption of critical flow is invalid since a flow with a depth of 3.1 m must have more energy than the 2 m of energy provided by the lake elevation. Therefore, the discharge must be something less than calculated above, and the reach must be mild.

- b. The process now becomes iterative. We must assume a depth of uniform flow in the downstream reach, determine the discharge from Manning's equation, and from that discharge determine the specific energy. Iteration continues until the assumed depth produces a specific energy consistent with the 2 m of energy provided by the lake level upstream. The results are best presented in a table.

Illustration of Iterative Approach to Discharge Calculation from Lake

Normal Depth $y_0$ (m)	Area A ( $\text{m}^2$ )	Wetted Perimeter P (m)	Hydraulic Radius R (m)	Velocity v ( $\text{m}/\text{s}$ )	Discharge Q ( $\text{m}^3/\text{s}$ )	Specific Energy $E_0$ (m)
1.0	5.0	7.0	0.71	1.00	4.99	1.05
1.8	9.0	8.6	1.05	1.29	11.6	1.88
1.9	9.5	8.8	1.08	1.32	12.5	1.99
1.95	9.75	8.9	1.10	1.33	12.6	2.04
1.91	9.55	8.82	1.08	1.32	12.6	2.00

Thus the discharge from the lake is about  $12.6 \text{ m}^3/\text{s}$ , slightly more than half the discharge when we assumed the downstream reach was steep. The flow is immediately at normal depth,  $y_0 = 1.91 \text{ m}$  at the head of downstream reach. Note that although this example presents several trial depths before the iterative procedure concludes, this is an application that readily lends itself to the use of the Excel Goal Seek tool. Problem 5.15 provides the reader with a different set of circumstances in which to further explore the lake discharge problem.

### Animation: discharge\_problem.avi

Flow conditions:

$$E_{Lake} = 102.2 \text{ ft}$$

Elevation of channel bottom at lake outlet is 100 feet

$$n = 0.03$$

$$b = 10 \text{ ft}$$

Apparent movement:

$S_0$  = varies from 0.024 (steep) to 0.00017 (mild) ft/ft

Rectangular cross-section

Still image of animation shown in Figure 5.17

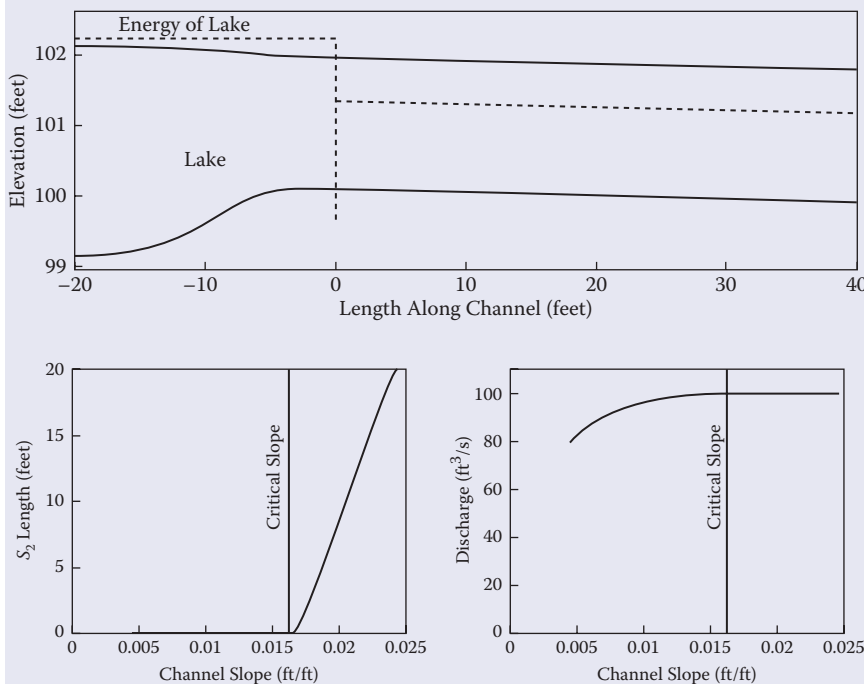


**FIGURE 5.17** Screen capture from *discharge\_problem.avi* animation. The effect of varying downstream reach slope on discharge from a lake. As the slope decreases in the animation, the initially steep reach eventually is equal to, and is then less than, the critical slope. Once the downstream reach is mild, the reach slope controls the discharge from the lake. The lower left subplot shows the diminishing length of the  $S_2$  curve on the downstream reach as the slope decreases, while the lower right subplot shows how the reach slope affects discharge for slopes less than the critical slope.

This animation shows the effect of diminishing slope on discharge from a reach that drains a lake. The animation begins with initially steep conditions prevailing in the draining reach. The slope of the reach is gradually reduced. Eventually, the reach slope corresponds to critical conditions ( $S_0 = 0.016 \text{ ft}/\text{ft}$ , approximately). When the slope is further reduced, the reach becomes mild, and the reduction in slope leads to a reduction in discharge from the lake. In essence, the resistance to flow offered by the reach is holding back discharge from the lake. The smaller the reach slope, the more this is true.

When the draining reach is steep, the flow goes through critical depth at the lake outlet and an  $S_2$  curve evolves downstream from the lake outlet into the reach until normal depth is encountered. The lower left subplot shows the length of this  $S_2$  profile as a function of the reach slope. The  $S_2$  profile has zero length as the slope reaches the critical slope. This smallest slope corresponds to the full discharge of  $100 \text{ ft}^3/\text{s}$  from the lake.

Once the slope in the reach is smaller than the slope corresponding to critical flow conditions, the reach holds back the flow from the lake and discharge becomes a function of the reach slope. This function is shown in the lower right subplot. The flow tends to zero as the reach slope approaches zero. If the slope is zero, the reach is now simply an extension of the lake and is no longer supporting any discharge from the lake.

## 5.8 CONJUGATE CURVE CONCEPT

Hydraulic jumps occur where a supercritical upstream flow depth,  $y_1$ , meets a subcritical downstream flow depth,  $y_2$ , such that  $y_1$  and  $y_2$  are conjugate to one another. To this point in the chapter the issue of precisely where such a conjugate pair meets has been avoided, generally by specifying either an upstream or downstream flow boundary condition that corresponds to normal depth. However, there is no reason for a hydraulic jump to begin or end at normal depth—this has just been a convenience taken to simplify the posing of examples.

Figure 5.18 presents a situation that clearly deviates from others presented in this chapter. We have a mild reach that ends at a free overfall. Thus, an  $M_2$  curve propagates backward from the overfall starting from critical depth at the downstream end and tending toward normal depth as the profile traces upstream. At the same time, a sluice gate imposes an upstream boundary condition of a known, supercritical depth with an  $M_3$  profile propagating downstream from there. The distance,  $\Delta x$ , separating the sluice gate upstream and

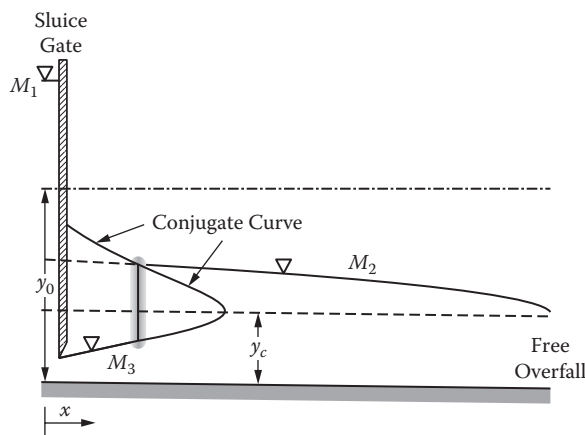


**FIGURE 5.18** The conjugate curve concept. Here, a sluice gate sets up an  $M_3$  profile slightly upstream of a free overfall. The conjugate curve to the  $M_3$  profile is shown. An (idealized vertical) hydraulic jump occurs at the location where the conjugate curve and the actual  $M_2$  profile intersect.

the free overfall downstream is understood to be short, such that the  $M_2$  profile requires a distance longer than  $\Delta x$  in order to return to normal depth for the reach. It follows that there is a hydraulic jump somewhere within the confines of this reach, but clearly the jump is not to normal depth but to a subcritical depth,  $y_2$ , somewhat smaller than normal depth. Considering the shape of the  $M$ - $y$  diagram, it thus also follows that the conjugate depth of  $y_2$ ,  $y_1$ , is somewhat larger than the conjugate to normal depth on this reach. Two interesting questions arise: (1) How do we identify the location where the hydraulic jump occurs? and (2) How does the position of the hydraulic jump within the reach vary as the overall length of the reach,  $\Delta x$ , lengthens or shortens?

The position of the hydraulic jump along the reach follows naturally from the development of a *conjugate curve*. Figure 5.18 shows the subcritical conjugate curve that corresponds to the  $M_3$  profile propagating downstream from the sluice gate. The conjugate curve is shown as an imaginary surface. It is not a profile that actually exists. As the conjugate curve is shown here, it is a visual representation of the depth that must be encountered by the actual flow that would correspond to the actual flow depth's conjugate at that location. Unless  $\Delta x$  is very short, the subcritical conjugate curve to the  $M_3$  profile will intersect the  $M_2$  profile somewhere along the reach. Treating the hydraulic jump as an instantaneous feature (i.e., the jump is vertical), the jump occurs where the conjugate curve and the  $M_2$  profile intersect.

The question of how the jump propagates upstream or downstream as  $\Delta x$  changes also depends on the reasoning embedded in this conjugate curve

approach. Before focusing on this problem, consider a couple of simple, limiting cases. If  $\Delta x$  is zero or a very short length, then the  $M_3$  curve propagating downstream from the upstream boundary is not even able to reach critical depth before reaching the downstream boundary and passing over the free overfall. In other words, no  $M_2$  profile ever forms because the depth at the downstream boundary is not able to reach critical depth. Mechanically, the subcritical conjugate curve and the  $M_2$  profile never meet. In the limit, the longest  $\Delta x$  can be without a jump is the length needed for the  $M_3$  profile to just reach critical depth before reaching the downstream boundary. In this limiting case, the subcritical conjugate curve just intersects the  $M_2$  profile at the downstream boundary. As  $\Delta x$  increases beyond this limiting condition, then an  $M_2$  profile truly does form and propagates backward to the point of intersection with the subcritical conjugate curve. Thus, as  $\Delta x$  increases beyond this limiting condition, we find that location of the hydraulic jump propagates upstream. The  $M_2$  profile grows longer and the  $M_3$  profile grows shorter as  $\Delta x$  increases. Further discussion of this conjugate curve concept, and an associated animation, will appear in Section 6.5 of the next chapter. The channel\_length.avi animation appearing there closely matches the discussion presented here.

## 5.9 SUMMARY

The focus of this chapter has been non-uniform flow. We have learned how non-uniform flow derives from a net difference between the friction slope,  $S_f$ , and the channel slope,  $S_0$ . With this difference in mind, a taxonomy of surface water profiles for mild, steep, critical, horizontal, and adverse reaches was presented, with an almost exclusive focus on mild and steep reaches.

We have returned to the in-stream obstructions of the sluice gate, step, and constriction and have seen how these features will set up surface water profiles both upstream and downstream of the obstructions. This discussion also put to rest the conundrum presented in Chapter 2 concerning which flow regime—supercritical or subcritical—is chosen by the flow downstream of such obstructions. The set of surface water profiles outlined in this chapter provides for a single possibility to end such problems, thus resolving the conundrum.

In the context of composite profiles, we have seen that mild and steep reaches function differently. At a simple level, the flow profile taxonomy is obviously different between mild and steep reaches. More importantly, the concept of information propagation in subcritical versus supercritical flows was found to lead to fundamentally different behavior for the different paired reach scenarios investigated in this chapter.

The concept of the conjugate curve was presented. This curve is an imaginary surface that is paired with an actual flow profile along the reach. A worked example and several animations showed how this concept can be used to determine the location of a hydraulic jump and how this location will propagate upstream or downstream under changing conditions within a reach.

Although boundary conditions and flow depths at the upstream and downstream ends of surface water profiles were often presented quantitatively, this chapter did not broach the calculation of the actual profile length or shape. This is what was meant by the term *qualitative* in the chapter title. These remaining pieces of the puzzle, profile length and shape, are discussed in Chapter 6.

## Problems

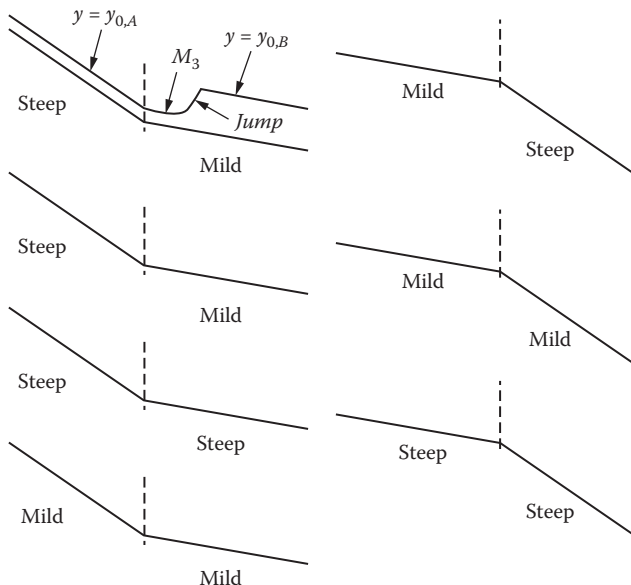
For Problems 5.1 through 5.3, perform the following:

- a. Calculate  $y_0$ .
  - b. Determine if the reach is mild, steep, or critical.
  - c. Sketch all profiles both upstream and downstream of the obstructions.
  - d. On your sketch, indicate the upstream and downstream depths of each profile you draw and provide supporting calculations.
  - e. Sketch the cycle of points on the  $E$ - $y$  diagram for each of the upstream and downstream depths identified in part (d) and label sections of the cycle that correspond to any surface water profiles, jumps, or in-stream obstructions.
- 5.1. A rectangular channel, 5 m wide, carries a flow of  $20 \text{ m}^3/\text{s}$ . The slope of the channel  $S_0 = 0.005 \text{ m/m}$ , and Manning's  $n$  is 0.030. The flow encounters a sluice gate open to 0.60 meters. The depths far upstream and downstream of the gate are equal to the normal depth,  $y_0$ .
  - 5.2. A rectangular channel, 5 m wide, carries a flow of  $20 \text{ m}^3/\text{s}$ . The slope of the channel  $S_0 = 0.005 \text{ m/m}$ , and Manning's  $n$  is 0.030. The flow encounters a step of height 0.50 meters. The depths far upstream and downstream of the step are equal to the normal depth,  $y_0$ .
  - 5.3. A rectangular channel, 5 m wide, carries a flow of  $20 \text{ m}^3/\text{s}$ . The slope of the channel  $S_0 = 0.02 \text{ m/m}$ , and Manning's  $n$  is 0.030. The flow enters a rectangular constriction to a width of 3 meters. The depths far upstream and downstream of the constriction are equal to the normal depth,  $y_0$ .
  - 5.4. For the sluice gate and flow conditions specified in Problem 5.1, design an equivalent:
    - a. Step
    - b. Constriction

- 5.5. For the step and flow conditions specified in Problem 5.2, design an equivalent:
- Sluice gate opening
  - Constriction
- 5.6. For the constriction and flow conditions specified in Problem 5.3, design an equivalent:
- Sluice gate opening
  - Step
- 5.7. Given  $q = 3 \text{ m}^2/\text{s}$  and  $y_0 = 1.40$  meters:
- Is the reach mild, steep, or critical?
  - For a gate opening of 0.80 meters:
    - Find the depth immediately upstream of the gate.
    - What is observed downstream of the gate?
    - Sketch the profiles and indicate all relevant depths on the sketch.
  - For a gate opening of 0.68 meters:
    - Find the depth immediately upstream of the gate.
    - What is observed downstream of the gate?
    - Sketch the profiles and indicate all relevant depths on the sketch.
  - For a gate opening of 0.60 meters:
    - Find the depth immediately upstream of the gate.
    - What is observed downstream of the gate?
    - Sketch the profiles and indicate all relevant depths on the sketch.
- 5.8. Given the junction of two rectangular reaches, A and B, carrying a discharge of  $30 \text{ m}^3/\text{s}$  as in the following table:

<i>Property</i>	<i>Upstream Reach A</i>	<i>Downstream Reach B</i>
Channel width (meters)	10 meters	10 meters
Channel roughness – Manning's $n$	0.030	0.030
Channel slope ( $\text{m/m}$ )	0.02	0.005
Critical depth (meters)		
Normal depth (meters)		
Reach type (mild, critical, steep)		
Conjugate to normal depth (meters)		

- Fill in the missing entries in the last four rows of the above table.
  - Does the hydraulic jump appear on the upstream (*A*) or downstream (*B*) reach? Justify your answer.
  - Using normal depths as the upstream (entrance) and downstream (exit) conditions, sketch the flow profile through the two reaches. Label all profiles and indicate all key depths.
  - Answer the appropriate one of the two questions below:
    - If your answer to Problem 5.8b placed the jump on Reach *A*, what is the least steep new slope for Reach *A* such that the jump moves downstream to Reach *B*?
    - If your answer to Problem 5.8b placed the jump on Reach *B*, what is the least steep new slope for Reach *A* such that the jump moves upstream to Reach *A*?
- 5.9. Repeat Problem 5.8 above except now the channel slope on Reach *B* is 0.0075 m/m.
- 5.10. For each of the reach transitions shown below, sketch the water surface profile and label all curves (e.g.,  $M_1$ ,  $S_3$ , etc.), jumps, and regions of normal flow as illustrated. Note that there are two *steep* to *mild* transitions. One possibility is shown as an example. You must sketch the other possibility. Assume all upstream and downstream boundary conditions are normal depth.



- 5.11. Use the flow conditions outlined in Example 5.9, except replace the channel slope with  $S_0 = 0.020 \text{ m/m}$ . For this new slope, repeat the questions addressed in Example 5.9.
- 5.12. A 10 m wide rectangular reach with slope,  $S_0 = 0.015 \text{ m/m}$ , carries a discharge,  $Q = 4 \text{ m}^3/\text{s}$ , and has a Manning's  $n = 0.025$ . A sluice gate imposes an upstream flow depth of 0.18 meters.
- Determine normal depth and whether the upstream flow is supercritical or subcritical.
  - What profile results downstream of the gate? Draw a sketch of the profile.
- 5.13. A channel carries a discharge of  $10 \text{ m}^3/\text{s}$  in a 5 m wide rectangular cross-section. Downstream of the gate, the normal depth is 1.7 m. The flow encounters a sluice gate with an upstream depth as specified below. The sluice gate is set to an opening of 0.30 m.
- If the upstream depth is 1.9 m, show that the jump is a drowned jump and determine the energy dissipated in the drowned jump.
  - Repeat from (a) with upstream depth 2.1 m.
  - Repeat from (a) with upstream depth 2.4 m.
  - Determine the minimum depth upstream of the sluice gate so that the jump is not drowned. How much energy is dissipated in this jump?
  - Plot upstream energy dissipation versus upstream depth for your calculations in parts (a) through (d).
- 5.14. A discharge of  $10 \text{ m}^3/\text{s}$  enters a reach at a depth of 0.30 m. The reach is rectangular with a width of 5 m, and Manning's  $n = 0.022$ . The reach tends toward normal depth downstream.
- If the reach has a channel slope,  $S_0 = 0.01$ , determine any profile(s) or jumps downstream. Indicate depths and the beginning and end of all features downstream.
  - If the reach has a channel slope,  $S_0 = 0.004$ , determine any profile(s) or jumps downstream. Indicate depths and the beginning and end of all features downstream.
- 5.15. A lake has an elevation 1.5 m greater than the invert at the head of a downstream reach. The downstream reach has a rectangular cross-section, 4.2 m in width, a Manning's  $n$  of 0.035, and a channel slope of 0.0045 m/m.
- Show that the downstream reach is mild.
  - Find the discharge in the downstream reach.



# **Quantitative Gradually Varied Flow**

## **CHAPTER OBJECTIVES**

1. Examine governing equation for determining surface water profiles.
2. Apply governing equation to calculate distance from depth in a spreadsheet application.
3. Apply governing equation to calculate depth from distance in a spreadsheet application.
4. Explore basics of the US Army Corps of Engineers Program: Hydrologic Engineering Center River Analysis System (HEC-RAS).
  - a. Solve for a single surface water profile using both the standard step method and HEC-RAS and compare results.
  - b. Using mixed flow option, show a drowned jump and hydraulic jump using both the standard step method and HEC-RAS and compare results.

### **6.1 INTRODUCTORY COMMENTS**

In the previous chapter we introduced a taxonomy for the surface water profiles that are associated with gradually varied flow. The focus then was on identifying the profile by name and quantifying only the beginning and/or ending depths of that profile. In this chapter we present several approaches to quantify the exact shape and length of the surface water profile. Specifically, three spreadsheet-based approaches using a finite difference approximation of

equation 4.10 will be presented. Additionally, the US industry-standard software application, HEC-RAS, which calculates surface water profiles, will be presented with its results compared to those previously calculated by spreadsheet methods.

Some surface water profiles are relatively short (on the order of several meters) while other profiles may evolve over tens or hundreds of meters. The finite length of a reach may lead to more complex flow profiles than were previously considered in Chapter 5. For instance, consider the three reaches shown in Figure 6.1. From the previous chapter, we know that in some cases (see Example 5.7a) a hydraulic jump will occur in Reach B. We also expect from Example 5.4 an  $M_2$  curve on the latter part of Reach B followed by an  $S_2$  curve on Reach C. The above will be true, provided that Reach B (length is  $\Delta x_B$  in this figure) is of sufficient length. But what if  $\Delta x_B$  is so short that a hydraulic jump never occurs? Material presented in Chapter 5 is unable to answer how long Reach B must be for the hydraulic jump to exist. In this chapter, we will develop the tools necessary to determine a minimum value for  $\Delta x_B$  such that a hydraulic jump does exist.

## 6.2 GOVERNING EQUATION

Returning to equation 4.10,

$$\frac{dE}{dx} = S_0 - S_f \quad (4.10)$$

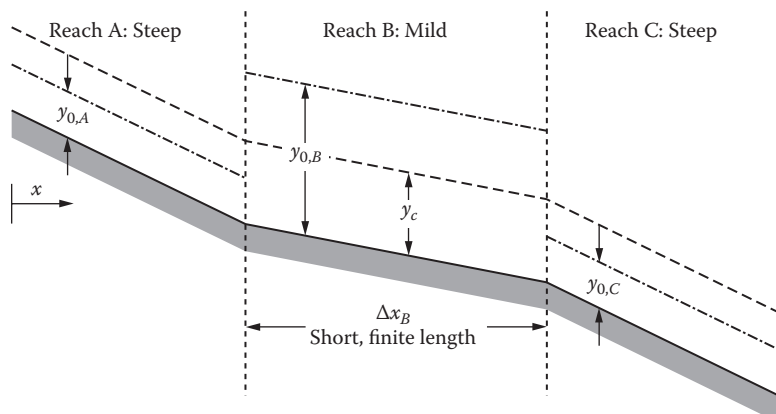


**FIGURE 6.1** Three sequential reaches supporting differing flow regimes. Differing lengths for Reach B may lead to different flow profiles on this reach.

we plan to solve a finite difference representation of equation 4.10. To do so, we will establish a mesh along the longitudinal direction of the reach. We will need to apply appropriate boundary conditions defining the flow at the upstream and downstream extremes of the reach.

Our mesh is composed of cross-sections taken perpendicular to the direction of flow. We focus on two typical cross-sections,  $i$  and  $i + 1$ , as shown in Figure 6.2. We can write

$$\frac{E_{i+1} - E_i}{x_{i+1} - x_i} = S_0 - \left( \frac{S_{f,i} + S_{f,i+1}}{2} \right) \quad (6.1)$$

We note that  $S_f$  can be determined by isolating this term from a rearrangement of Manning's equation:

$$S_{f,i} = \frac{v_i^2 \cdot n^2}{c^2 \cdot R_i^{4/3}} \quad (6.2)$$

where  $c$  is either 1 (metric units) or 1.49 (English units). Combining equations 6.1 and 6.2 and solving for  $x_{i+1}$ , we have

$$x_{i+1} = x_i + \frac{\frac{E_{i+1} - E_i}{n^2}}{S_0 - \frac{1}{2c^2} \cdot \left( \frac{v_i^2}{R_i^{4/3}} + \frac{v_{i+1}^2}{R_{i+1}^{4/3}} \right)} \quad (6.3)$$

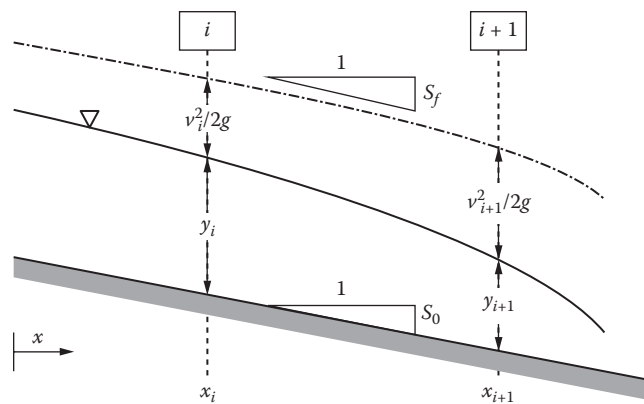


**FIGURE 6.2** Definition sketch for finite difference representation of equation 4.10.

Notice that quantities  $E$ ,  $v$ , and  $R$  are all simple functions of depth,  $y$ . Thus, in equation 6.3, if the upstream location,  $x_i$ , is known, and if depths  $y_i$  and  $y_{i+1}$  are known (or assumed), the right-hand side of this equation is calculable so that the next location downstream,  $x_{i+1}$ , can be determined. In this way, if one starts at a known location and depth at the upstream end of the profile, a new depth downstream, say  $y_i + \Delta y$  (synonymous with  $y_{i+1}$ ), can be assumed and the location,  $x_{i+1}$ , where this depth is realized can be determined using equation 6.3. In actuality, although this method is described as proceeding from upstream to downstream, the method may proceed in either direction depending on the flow profile modeled and the depths involved.

### 6.3 STANDARD STEP METHOD

We present here a recipe for developing a tabular solution to equation 6.3. This is commonly known as the *standard step method*. Envision a table with 13 columns as shown in Table 6.1. Each row (we will use index,  $i$ ) of the table corresponds to a location within the reach with depth specified by the reader and horizontal location determined by the table.

(Columns 1 through 8 correspond to a specific location in the reach where the depth indicated in column 1 is observed.)

*Column 1:* Depth [=]  $L$ : the reader specifies the depth in this column manually. The first row should correspond to the most upstream (or downstream) location along the profile. Subsequent rows indicate depths known to exist somewhere along the profile. Increments can be evenly spaced or irregularly spaced as desired. The last row should correspond to the depth at the opposite end of the profile being modeled.

*Column 2:* Area [=]  $L^2$ : this entry employs the depth indicated in column 1 and the known cross-sectional geometry to determine the cross-sectional area. For instance, if the depth is 1.5 meters and the channel is rectangular with width 10 m, the area is  $15 \text{ m}^2$ .

*Column 3:* Wetted Perimeter [=]  $L$ : this entry employs the depth indicated in column 1 and the known cross-sectional geometry to determine the wetted perimeter. For instance, if the depth is 1.5 meters and the channel is rectangular with width 10 m, the wetted perimeter is 13 m.

*Column 4:* Hydraulic Radius [=]  $L$ : this entry is area divided by wetted perimeter (i.e., column 2 divided by column 3).

*Column 5:* Velocity [=]  $L/T$ : this entry is calculated employing the continuity equation. The known discharge is divided by the area in column 2.

*Column 6:* Friction Slope [=] dimensionless: this entry is determined by solving the flow resistance equation for the friction slope. For instance, equation 6.2 presents such a rearrangement for Manning's equation.

*Column 7:* Velocity Head [=]  $L$ : this entry is the velocity head,  $v^2/2g$ , determined using the velocity indicated in column 5.

*Column 8:* Specific Energy [=]  $L$ : this entry is the sum of the elevation and velocity heads (i.e., column 1 and column 7).

(Columns 9 through 12 correspond to the segment of the reach existing between  $y_i$  and  $y_{i+1}$  [i.e., row  $i$  and row  $i + 1$ .])

*Column 9:* Average Friction Slope [=]  $L$ : this entry is the average between the entries in column 6 for rows  $i$  and  $i + 1$ .

*Column 10:* Slope Difference [=]  $L$ : this entry is the quantity  $(S_0 - S_f)$  calculated as the known channel slope minus the average friction slope tabulated in column 9.

*Column 11:* Energy Difference [=]  $L$ : this entry is the specific energy in column 8 (row  $i + 1$ ) minus the specific energy in column 8 (row  $i$ ). It is important to have the order of subtraction correct, otherwise a sign error will propagate through the solution.

*Column 12:* Horizontal distance [=]  $L$ : this entry is essentially equation 6.3 rearranged slightly by moving  $x_i$  to the left-hand side. This entry is the horizontal distance separating the depths at locations  $x_i$  and  $x_{i+1}$ . Note that if this quantity evaluates to a negative number, it means that the profile that is being modeled is propagating upstream from location  $i$  to location  $i + 1$ .

(Column 13, like columns 1 through 8, corresponds to a specific location in the reach where the depth indicated in column 1 is observed.)

*Column 13:* Horizontal location [=]  $L$ : this entry is calculated as column 13 (row  $i$ ) plus column 12 (corresponding to the segment between rows  $i$  and  $i + 1$ ). This entry contains the cumulative distance along the modeled profile from row  $i = 1$ , to row  $i + 1$ . The reader arbitrarily specifies the entry in column 13, row  $i + 1$ , typically assigning this entry the value 0.

We demonstrate the application of this recipe to solve equation 6.3 in Example 6.1.

***Example 6.1***

In Example 5.1 we analyzed a 10 m wide rectangular channel carrying a discharge of  $30 \text{ m}^3/\text{s}$ , with a channel slope of  $0.005 \text{ m/m}$ , and Manning's roughness is  $0.030$ . We determined that the normal and critical depths were  $y_0 = 1.26 \text{ m}$  and  $y_c = 0.97 \text{ m}$ , respectively. Therefore, the reach is mild.

- a. Determine the length of the  $M_2$  curve that varies over the entire depth distance between  $y_c$  and  $y_0$ .
- b. Make a plot of this curve showing also the channel bottom, and  $y_c$  and  $y_0$  over the full length of this profile.
- c. Examine the sensitivity of the length calculation in part (a) to
  - i. The depth increment used in the application of equation 6.3
  - ii. A small variation in the bounding depth near  $y_c$
  - iii. A small variation in the bounding depth near  $y_0$
- d. Use your results from sensitivity analysis in part (c) to provide guidance on calculation of surface water profiles with this method.

***Solution:***

- a. Table 6.1 provides a spreadsheet application of the standard step method to the calculation of the  $M_2$  profile using a vertical resolution of  $0.05 \text{ m}$ . The overall length of the profile is approximately  $136 \text{ m}$ . Notice that the negative sign for the  $\Delta x$  increments (and thus the overall profile length) indicates that as the depths increase within the table, the direction of the profile traces upstream. This is, of course, consistent with the shape of the  $M_2$  profile presented in Chapter 5.
- b. Figure 6.3 shows the requested plot.
- c. Sensitivity of length calculation:
  - i. Figure 6.4 shows the sensitivity of the overall profile length to vertical resolution ( $\Delta y$ ) used in the table such as that shown in Table 6.1. As the vertical resolution gets smaller, we see that the overall length of the calculated profile increases, though the profile length seems to be converging on a length of roughly  $160 \text{ m}$ .
  - ii. To four decimal places, the critical depth in this reach is  $0.9717 \text{ m}$ . Using the standard step method, the profile length was calculated for the distance between three different approximations of critical depth:  $0.9717 \text{ m}$ ,  $0.972 \text{ m}$ , and  $0.975 \text{ m}$  and a depth  $0.98 \text{ m}$ . Table 6.2 summarizes the findings:

**TABLE 6.1** Spreadsheet-Based Approach to Solution of Equation 6.3 for Example 6.1

<i>(1)</i> $y$ (m)	<i>(2)</i> $A$ ( $m^2$ )	<i>(3)</i> $P$ (m)	<i>(4)</i> $R$ (m)	<i>(5)</i> $v$ ( $m/s$ )	<i>(6)</i> $S_f$ ( $m/m$ )	<i>(7)</i> $v^2/2g$ (m)	<i>(8)</i> $E$ (m)	<i>(9)</i> $S_{f,avg}$ ( $m/m$ )	<i>(10)</i> $S_{\sigma}S_{f,avg}$ ( $m/m$ )	<i>(11)</i> $\Delta E$ (m)	<i>(12)</i> $\Delta x$ (m)	<i>(13)</i> $\Sigma x$ (m)
0.9717 <sup>a</sup>	9.7	11.94	0.8136	3.0874	0.0113	0.4858	1.4575					0.00
1.00	10.0	12.00	0.8333	3.0000	0.0103	0.4587	1.4587	0.0108	-0.0058	0.0012	-0.20	-0.20
1.05	10.5	12.10	0.8678	2.8571	0.0089	0.4161	1.4661	0.0096	-0.0046	0.0074	-1.60	-1.80
1.10	11.0	12.20	0.9016	2.7273	0.0077	0.3791	1.4791	0.0083	-0.0033	0.0130	-3.97	-5.78
1.15	11.5	12.30	0.9350	2.6087	0.0067	0.3469	1.4969	0.0063	-0.0022	0.0178	-8.10	
1.20	12.0	12.40	0.9677	2.5000	0.0059	0.3186	1.5186			0.0217	-16.85	-13.87
1.25	12.5	12.50	1.0000	2.4000	0.0052	0.2936	1.5436	0.0055	-0.0005	0.0250	-47.20	-30.72
1.2619 <sup>b</sup>	12.6	12.52	1.0076	2.3774	0.0050	0.2881	1.5500	0.0051	-0.0001	0.0064	-58.14	-77.92
												-136.06

<sup>a</sup> This is the critical depth,  $y_0$ , to four decimal places.

<sup>b</sup> This is the depth at 99% of the depth interval between critical and normal depth.

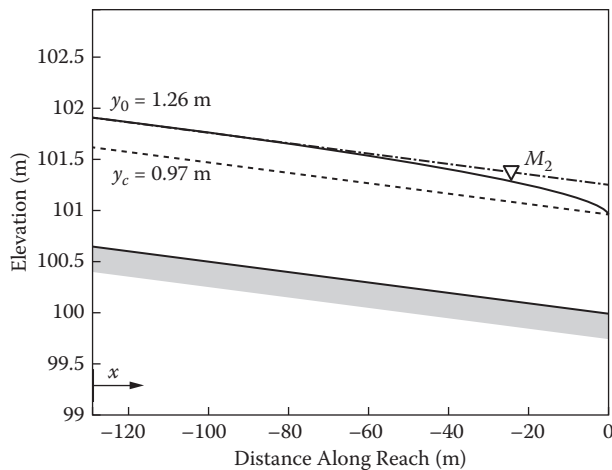


**FIGURE 6.3**  $M_2$  profile for Example 6.1. Vertical resolution of profile is  $\Delta y = 0.05 \text{ m}$ .

- iii. To four decimal places, the normal depth in this reach is 1.2648. Using the standard step method, the profile length was calculated for the distance between five different approximations of normal depth: 1.2648 m, 1.264 m, 1.263 m, 1.262 m, 1.2619 m, and a depth of 1.26 m. Table 6.3 summarizes the findings.

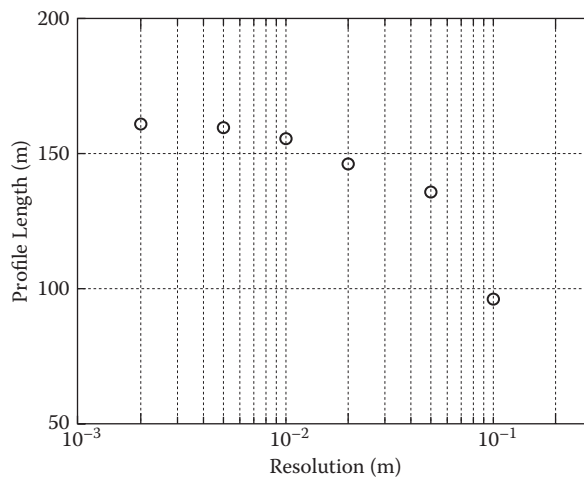


**FIGURE 6.4** Sensitivity of length of  $M_2$  profile in Example 6.1 to vertical resolution,  $\Delta y$ , in the standard step method.

**TABLE 6.2** Sensitivity of Incremental Profile Length to Precision of Critical Depth,  $y_c$ 

<i>Depth Interval</i>	<i>Incremental Profile Length (m)</i>
0.9717 m to 0.98 m	0.0172 m
0.972 m to 0.98 m	0.0172 m
0.975 to 0.98 m	0.0146 m

- d. The sensitivity results show the following:
- A smaller resolution (smaller depth increments,  $\Delta y$ ) results in generally longer calculated profile lengths.
  - There is not much sensitivity in incremental profile length to the precision of approximation of critical depth,  $y_c$ .
  - There is considerable sensitivity in incremental profile length to the precision of approximation of normal depth,  $y_0$ . Notice that the denominator in the second term of the right-hand side of equation 6.3 is an approximation of  $S_0 - S_f$ . At normal depth  $S_0 = S_f$ . Thus, the second term of equation 6.3 tends toward infinity in the neighborhood of normal depth. Because of this strong sensitivity, it is advisable not to have

**TABLE 6.3** Sensitivity of Incremental Profile Length to Precision of Normal Depth,  $y_0$ 

<i>Depth Interval</i>	<i>Incremental Profile Length (m)</i>
1.26 m to 1.2648 m	88.3 m
1.26 m to 1.264 m	63.1 m
1.26 m to 1.263 m	40.2 m
1.26 m to 1.262 m	23.3 m
1.26 m to 1.2619 m <sup>a</sup>	21.8 m

<sup>a</sup> Note that the depth 1.2619 m is 99% of the depth difference between normal depth 0.9717 m and 1.2648 m.

the standard step method end at normal depth, but to have the depth be within a close approximation of normal depth. For instance, the last row of Table 6.3 ends at 1.2619 m. This number is, to four decimal places, equal to 99% of the difference between  $y_c$  and  $y_0$ . Explicitly,

$$\begin{aligned}\tilde{y}_0 &= y_c + 0.99 \cdot (y_0 - y_c) = 0.9717 + 0.99 \cdot (1.2648 - 0.9717) \\ &= 1.2619 \text{ m}\end{aligned}$$

where  $\tilde{y}_0$  is a close approximation of the true value of  $y_0$  but is sufficiently far away from the actual value of  $y_0$  to limit the sensitivity of the divide-by-zero issue with equation 6.3. The 99% is somewhat arbitrary but accomplishes the intended purpose here. Note that if one were approximating an  $M_1$  profile, the desired approximation of  $y_0$  would necessarily be slightly bigger than  $y_0$ , and thus 101% of the depth difference between  $y_0$  and  $y_c$  would be a good approximation (approximately 1.2677 m). Finally, if one were calculating an  $M_3$  profile, this issue is not a concern since the  $M_3$  profile is supercritical and does not exist near normal depth.

## 6.4 VARIATIONS OF AND ALTERNATIVES TO THE STANDARD STEP METHOD

The standard step method presented in the previous section appears under different names in older books on this topic. Henderson (1966) calls it the “Standard Step Method—Distance Calculated from Depth,” while more recently Chaudhry (2008) calls it the “Direct Step Method.” Regardless of the name, the method presented in the previous section is attractive because it is easy to implement and requires no iteration. As long as the desired depth range is known and the sensitivity issues of step size and of calculations near normal depth are understood, the method works well.

However, there are limitations or shortcomings to this method. One shortcoming is that the method is based on depth, rather than position. A more natural way to approach the calculation of surface water profiles is from the standpoint of position along the reach and determination of the depth at that position. This involves an iterative approach but is rather easily achieved. From a mechanical standpoint the reader may use the same spreadsheet employed

in the previous example, coupling that approach with the aforementioned Excel® Goal Seek tool to automate the iteration needed. We demonstrate this approach in Example 6.2.

### **Example 6.2**

We return to Example 6.1 with a 10 m wide rectangular channel carrying a discharge of  $30 \text{ m}^3/\text{s}$ , with a channel slope of  $0.005 \text{ m/m}$ , and Manning's roughness is 0.030. Determine the depths along the  $M_2$  profile at the following locations:  $x = -0.1 \text{ m}, -0.2 \text{ m}, -0.3 \text{ m}, -0.4 \text{ m}, -0.5 \text{ m}, -1.0 \text{ m}, -2.0 \text{ m}, -5.0 \text{ m}, -10 \text{ m}, -20 \text{ m}, -30 \text{ m}, -40 \text{ m}, -50 \text{ m}, -100 \text{ m}$ , and  $-140 \text{ m}$ .

- Present the table generated for the requested depths and compare to information in Table 6.1.
- Describe the differences in approach and effort behind the standard step method when using  $y$  to determine  $x$  (as done in Example 6.1) and the standard step method when using  $x$  to determine  $y$  (as done in this example).

#### **Solution:**

- Table 6.4 provides a spreadsheet application of the standard step method having used the Goal Seek tool to determine depths at the specific locations (right-most column) requested in the problem statement.
- Although Tables 6.1 and 6.4 appear identical in presentation, the difference concerns the independent and dependent variables and the level of user intervention to populate the table. In Table 6.1, the depths,  $y$ , presented in column 1 are the independent variable, and the channel locations,  $x$  (or  $\Sigma x$ ), presented in column 13 are the dependent variable. In Table 6.1,  $x$  is calculated directly from the specification of  $y$ . In Table 6.4 the opposite is the case, the  $x$  values are the independent variable with  $y$  being calculated through an iterative approach, using the Goal Seek tool. More work is needed to generate a table like 6.4 because each row requires its own iterative solution before the next row can be calculated. Further, there is a need to proceed sequentially from the control (critical depth,  $y_c$ , in this case) upstream to normal depth,  $y_0$ . If one were to insert an additional row, say for  $x = -75 \text{ m}$ , its calculation would likely

**TABLE 6.4** Spreadsheet-Based Approach for Example 6.2

$y$ (m)	$A$ ( $m^2$ )	$P$ (m)	$R$ (m)	$v$ (m/s)	$S_f$ (m/m)	$v^2/2g$ (m)	$E$ (m)	$S_{f,avg}$ (m/m)	$S_{0-f,avg}$ (m/m)	$\Delta E$ (m)	$\Delta x$ (m)	$\Sigma \Delta x$ (m)
0.9717	9.7	11.94	0.8136	3.0874	0.0113	0.4858	1.4575	0.0109	-0.0059	0.0006	-0.10	0.00
0.992	9.9	11.98	0.8275	3.0254	0.0106	0.4665	1.4581	0.0105	-0.0055	0.0005	-0.10	-0.10
0.999	10.0	12.00	0.8329	3.0018	0.0103	0.4593	1.4587	0.0103	-0.0053	0.0005	-0.10	-0.20
1.005	10.1	12.01	0.8370	2.9842	0.0102	0.4539	1.4592	0.0101	-0.0051	0.0005	-0.10	-0.30
1.010	10.1	12.02	0.8404	2.9695	0.0100	0.4494	1.4597	0.0099	-0.0049	0.0005	-0.10	-0.40
1.014	10.1	12.03	0.8434	2.9571	0.0099	0.4457	1.4602	0.0096	-0.0046	0.0023	-0.50	-0.50
1.031	10.3	12.06	0.8546	2.9103	0.0094	0.4317	1.4625	0.0091	-0.0041	0.0041	-1.00	-1.00
1.053	10.5	12.11	0.8696	2.8501	0.0088	0.4140	1.4666	0.0083	-0.0033	0.0100	-2.00	-2.00

1.092	10.9	12.18	0.8961	2.7477	0.0079	0.3848	1.4766	0.0075	-0.0025	0.0124	-5.00	-5.00
1.129	11.3	12.26	0.9213	2.6564	0.0071	0.3597	1.4890	0.0067	-0.0017	0.0170	-10.00	-10.00
1.172	11.7	12.34	0.9495	2.5594	0.0063	0.3339	1.5060	0.0061	-0.0011	0.0112	-10.00	-20.00
1.197	12.0	12.39	0.9659	2.5061	0.0059	0.3201	1.5172	0.0058	-0.0008	0.0080	-10.00	-30.00
1.214	12.1	12.43	0.9767	2.4715	0.0057	0.3113	1.5252	0.0056	-0.0006	0.0059	-10.00	-40.00
1.226	12.3	12.45	0.9844	2.4475	0.0055	0.3053	1.5311	0.0053	-0.0003	0.0155	-50.00	-50.00
1.256	12.6	12.51	1.0036	2.3894	0.0051	0.2910	1.5465	0.0051	-0.0001	0.0019	-20.00	-100.00
1.261	12.6	12.52	1.0072	2.3784	0.0050	0.2883	1.5497				-140.00	

have a small effect on friction slope calculations upstream of this location and thus all rows below this inserted row would require recalculation for the specified cross-sectional locations to remain as requested in the problem statement. The time required to perform these individual iterations is modest but is still a greater level of user intervention in comparison to the “ $y$  from  $x$ ” approach presented in Example 6.1.

A second, more global limitation of the method as presented so far is that the channel cross-section, channel slope, and roughness are assumed to remain static. Certainly this would not be the general case in the natural world as we would expect all of these quantities to potentially vary along a channel reach. We present a generalized approach that allows these parameters to vary. Similar to the algorithm presented earlier, we will present the method from the perspective of a spreadsheet application with the contents of each column explicitly described.

(Columns 1 through 8 correspond to the specific location indicated in column 1.)

*Column 1:* Cross-Section location [=]  $L$ : the reader specifies the horizontal location in this column manually. Often this follows from the survey identifier for the cross-section (e.g., meters, kilometers, miles upstream from an understood zero location; in the United States, such an identifier is often referred to as a *river mile* marker). As before, the first row should correspond to the most upstream (or downstream) location along the profile. Subsequent rows indicate locations known to exist somewhere along the profile.

*Column 2:* Stage [=]  $L$ : this entry represents the water surface elevation relative to some datum. As such, this entry is the sum of the water depth and the elevation of the channel bottom above the datum.

*Column 3:* Area [=]  $L^2$ : this entry uses the stage indicated in column 2 and the known cross-sectional geometry at the location indicated in column 1 to determine the cross-sectional area.

*Column 4:* Wetted Perimeter [=]  $L$ : like cross-sectional area, this entry uses the stage indicated in column 2 and the known cross-sectional geometry at the location indicated in column 1 to determine the wetted perimeter.

*Column 5:* Hydraulic Radius [=]  $L$ : this entry is area divided by wetted perimeter (i.e., column 3 divided by column 4).

*Column 6:* Velocity [=]  $L/T$ : this entry is calculated employing the continuity equation. The known discharge is divided by the area in column 3.

*Column 7:* Friction Slope [=] dimensionless: this entry is determined by solving the flow resistance equation for the friction slope. For instance, equation 6.2 presents such a rearrangement for Manning's equation.

*Column 8:* Velocity Head [=]  $L$ : this entry is the velocity head,  $v^2/2g$ , determined using the velocity indicated in column 6.

*Column 9:* Total Energy 1 [=]  $L$ : this entry is the sum of the stage and velocity heads (i.e., columns 2 and 7).

(Columns 10 through 12 correspond to the segment of the reach existing between  $y_i$  and  $y_{i+1}$  [i.e., row  $i$  and row  $i + 1$ .])

*Column 10:* Average Friction Slope [=]  $L$ : this entry is the average between the entries in column 6 for rows  $i$  and  $i + 1$ .

*Column 11:* Reach Length [=]  $L$ : this entry is the difference between the entries in column 1 for rows  $i$  and  $i + 1$ .

*Column 12:* Friction Head Loss [=]  $L$ : this entry is the product of columns 10 and 11 and represents the energy loss due to friction over the reach.

(Columns 1 through 8 correspond to a specific location in the reach where the stage indicated in column 2 is observed.)

*Column 13:* Total Energy 2 [=]  $L$ : this entry is calculated based on the total energy indicated in column 13 (row  $i + 1$ ) minus the friction head loss indicated in column 12 for the segment between rows  $i$  and  $i + 1$ . The column 13 value in a given row is the same as the total energy reported in that same row for column 9.

This spreadsheet approach again involves iteration. In this case, stage (Column 2) is varied until  $H_{tot,1}$  (column 9) and  $H_{tot,2}$  (column 13) agree. As in previous applications, the Goal Seek tool is a convenient tool to automate this iterative approach.

### Example 6.3

An  $S_2$  water surface profile starts from critical depth at the upstream end of the reach (channel bottom is 100 m at this location) and transitions to normal depth some distance downstream. The channel carries a discharge of 30  $\text{m}^3/\text{s}$ , with a channel slope of 0.01 m/m, and Manning's roughness is 0.030. The channel cross-section is trapezoidal with 2H:IV side slopes and a width of 10 m at the upstream end of the reach. The channel bottom widens linearly for the first 20 m downstream to a width of 11 m, remaining fixed at this new width thereafter.

- Determine critical depth for the trapezoidal channel with width 10 m. This is the boundary condition at the upstream end of the reach.

- b. Determine normal depth for the trapezoidal channel with width 11 m. This is the downstream boundary condition.
- c. If  $x = 0$  m represents the upstream end of the reach and  $x = 50$  m represents the downstream end of the reach, use the generalized table approach just presented to quantitatively solve for this flow profile through this reach.
- d. Comment on the relative magnitude of the  $S_f$  versus  $S_0$  along this reach and indicate how  $S_0$  is communicated to the profile in this approach.
- e. Comment on the effort behind calculating Table 6.5 versus Tables 6.1 and 6.4 presented in the earlier examples.

***Solution:***

- a. Using Figure 2.23 or the Goal Seek tool (to determine the depth in a trapezoidal channel that produces a Froude number = 1), the reader should be able to verify that  $y_c = 0.9116$  m for the flow conditions indicated.
- b. Using the Goal Seek tool, the reader should be able to verify that  $y_0 = 0.6820$  m.
- c. Table 6.5 illustrates the application of the generalized step method approach to the problem posed in Example 6.3. The generalized approach is needed because the channel cross-section varies with location along the reach. The reader should keep in mind that although nature of the cross-sectional variation is simple to model, in general the cross-sectional shape, channel bottom, and roughness may vary in a much more complicated fashion. To help make the tabulation more clear, three columns (columns a, b, and c) have been added to the left of the general table so the reader is able to quickly track the channel width, depth, and channel bottom elevation, respectively.
- d. At the top of the reach  $S_f$  is not even half the magnitude of  $S_0$  (0.0044 versus 0.01). Because of this, as the  $S_2$  profile evolves, the flow gains energy supercritically with the friction slope increasing as the flow tends toward normal depth. The flow is very close to normal conditions at  $x = 20$  m just as the trapezoidal bottom finishes growing and becomes fixed at a new width of 11 m. Examining the friction slope column, we see that the flow actually slightly overshoots normal conditions (to two decimal places  $y = 0.67$  m at  $x = 20$  m and  $x = 25$  m), briefly shifting to an  $S_3$  curve before easing back to normal depth near the downstream end of the reach.

**TABLE 6.5** Spreadsheet-Based Approach for Example 6.3

<i>(a)</i>	<i>(b)</i>	<i>(c)</i>	<i>(1)</i> Loc. <i>y<sub>bot</sub></i> (m)	<i>(2)</i> <i>A</i> (m <sup>2</sup> )	<i>(3)</i> <i>P</i> (m)	<i>(4)</i> <i>R</i> (m)	<i>(5)</i> <i>v</i> (m/s)	<i>(6)</i> <i>v<sup>2</sup>/2g</i> (m)	<i>(7)</i> <i>S<sub>f</sub></i> (m/m)	<i>(8)</i> <i>H<sub>tot,1</sub></i> (m)	<i>(9)</i> <i>H<sub>tot,2</sub></i> (m)	<i>(10)</i> <i>S<sub>f,orig</sub></i> (m/m)	<i>(11)</i> <i>ΔL</i> (m)	<i>(12)</i> <i>Δh<sub>f</sub></i> (m)	<i>(13)</i> <i>H<sub>tot,2</sub></i> (m)
10.000	0.9116	100.0000	0.0	100.91	10.7775	14.0766	0.7656	2.7836	0.3949	0.0044	101.3065	0.0049	0.5000	0.0024	101.3065
10.025	0.86	100.00	0.5	100.86	10.1407	13.8843	0.7304	2.9584	0.4461	0.0053	101.3040	0.0055	0.5000	0.0028	101.3040
10.050	0.84	99.99	1.0	100.83	9.9117	13.8261	0.7169	3.0267	0.4669	0.0057	101.3013	0.0059	0.5000	0.0029	101.3013
10.075	0.83	99.99	1.5	100.82	9.7472	13.7892	0.7069	3.0778	0.4828	0.0060	101.2984	0.0061	0.5000	0.0031	101.2984
10.100	0.82	99.98	2.0	100.80	9.6159	13.7635	0.6987	3.1198	0.4961	0.0063	101.2953	0.0065	1.0000	0.0035	101.2953
10.150	0.80	99.97	3.0	100.77	9.4104	13.7312	0.6853	3.1879	0.5180	0.0067	101.2888	0.0069	1.0000	0.0039	101.2888
10.200	0.79	99.96	4.0	100.75	9.2513	13.7146	0.6746	3.2428	0.5360	0.0071	101.2819	0.0073	1.0000	0.0043	101.2819
10.250	0.77	99.95	5.0	100.72	9.1213	13.7080	0.6654	3.2890	0.5513	0.0074	101.2746	0.0073	1.0000	0.0046	101.2746

(continued)

**TABLE 6.5** Spreadsheet-Based Approach for Example 6.3

(a) $b \text{ (m)}$	(b) $y \text{ (m)}$	(c) $y_{bar} \text{ (m)}$	(1) Loc. (m)	(2) Stage (m)	(3) $A \text{ (m}^2\text{)}$	(4) $P \text{ (m)}$	(5) $R \text{ (m)}$	(6) $v \text{ (m/s)}$	(7) $v^2/2g$ (m)	(8) $S_f \text{ (m/m)}$	(9) $H_{tot,1} \text{ (m)}$	(10) $S_{f,org}$ (m/m)	(11) $\Delta L \text{ (m)}$	(12) $\Delta h_r \text{ (m)}$	(13) $H_{tot,2} \text{ (m)}$
10.375 0.75	99.93	7.5	100.67	8.8748	13.7186	0.6469	3.3804	0.5824	0.0082	101.2551	0.0078	2.5000	0.0195		101.2551
10.500 0.73	99.90	10.0	100.63	8.6979	13.7537	0.6324	3.4491	0.6063	0.0088	101.2339	0.0085	2.5000	0.0212		101.2339
10.625 0.71	99.88	12.5	100.59	8.5641	13.8043	0.6204	3.5030	0.6254	0.0093	101.2113	0.0090	2.5000	0.0226		101.2113
10.750 0.70	99.85	15.0	100.55	8.4601	13.8657	0.6101	3.5460	0.6409	0.0097	101.1876	0.0095	2.5000	0.0237		101.1876
11.000 0.67	99.80	20.0	100.47	8.3122	14.0108	0.5933	3.6092	0.6639	0.0105	101.1372	0.0101	5.0000	0.0504		101.1372
11.000 0.67	99.75	25.0	100.42	8.3358	14.0186	0.5946	3.5989	0.6602	0.0104	101.0851	0.0104	5.0000	0.0520		101.0851
11.000 0.68	99.70	30.0	100.38	8.3550	14.0248	0.5957	3.5907	0.6571	0.0103	101.0335	0.0103	5.0000	0.0516		101.0335
11.000 0.68	99.60	40.0	100.28	8.3831	14.0340	0.5973	3.5786	0.6527	0.0102	100.9311	0.0102	10.0000	0.1024		100.9311
11.000 0.68	99.50	50.0	100.18	8.4012	14.0399	0.5984	3.5709	0.6499	0.0101	100.8297	0.0101	10.0000	0.1015		100.8297

How is  $S_0$  actually communicated to the flow? This is done through the specification of the channel bottom elevation (column c) in the chart. In a more real-world example, cross-sectional survey data would replace the simple trapezoidal geometry at each of the  $x$  locations. The difference in minimum bottom elevation between adjacent cross-sections divided by the separation distance between these sections would communicate the channel slope to the flow being modeled in this approach.

- e. The effort spent in this example is comparable to the effort spent working through Table 6.4 in solving Example 6.2. This is because both tables require an iterative approach. In Table 6.4, that iteration was to find the depth that corresponds to a fixed horizontal location. Here, in Table 6.6, that iteration was to find the stage that is consistent with total energy calculated two different ways at a given location. Both methods require more effort than was expended in the direct approach presented in Example 6.1.
- 

## **6.5 CONJUGATE CURVE: QUANTITATIVE APPLICATION**

In Section 5.8, the conjugate curve concept was presented in qualitative detail. Recall that this concept was presented in the context of a mild reach with a sluice gate defining the upstream boundary condition and a free overfall serving as the downstream boundary condition. Thus, an  $M_3$  curve defines the upstream portion of the reach and an  $M_2$  curve prevails on the downstream portion of the reach. Somewhere in between a hydraulic jump marks the transition from one curve to the other. Idealizing the hydraulic jump to be vertical, the location of the jump is determined by generating the conjugate curve to, for instance, the  $M_3$  profile and identifying the location where the conjugate curve intersects the actual  $M_2$  profile. This was previously illustrated in Figure 5.18. We will return to this situation now in a quantitative form.

---

### ***Example 6.4***

We use the same flow conditions as in Examples 6.1 and 6.2. We have a 10 m wide rectangular channel carrying a discharge of  $30 \text{ m}^3/\text{s}$ , with a channel slope of  $0.005 \text{ m/m}$ , and Manning's roughness is 0.030. The upstream boundary condition is set by a sluice gate imposing a depth of

0.60 m. The downstream boundary condition is a free overfall. The total reach length is 50 meters.

- Using the conjugate curve to the  $M_3$  profile, provide a plot of the water surface over the entire length of the reach showing both profiles and the conjugate curve.
- Using the plot from (a), visually approximate the location of the hydraulic jump and indicate the depths on the  $M_3$  and  $M_2$  curves. Show that these depths are conjugate to one another.
- Repeat (a) and (b) but use the conjugate curve to the  $M_2$  profile.

**Solution:**

- Figure 6.5 shows a plot of the  $M_3$  and  $M_2$  curves along with the conjugate curve to the actual  $M_3$  profile. Note that an arbitrary elevation of 100 m has been assigned to the upstream end of the reach. The dashed vertical line indicates the approximate location where the  $M_2$  profile and the conjugate curve intersect. Idealizing the jump as being perfectly vertical, this is the location of the jump.
- Therefore, examining the figure, the jump is slightly more than 10 m downstream from gate, say at approximately 10.3 m. The depth on the  $M_3$  curve is approximately 0.76 m while the depth

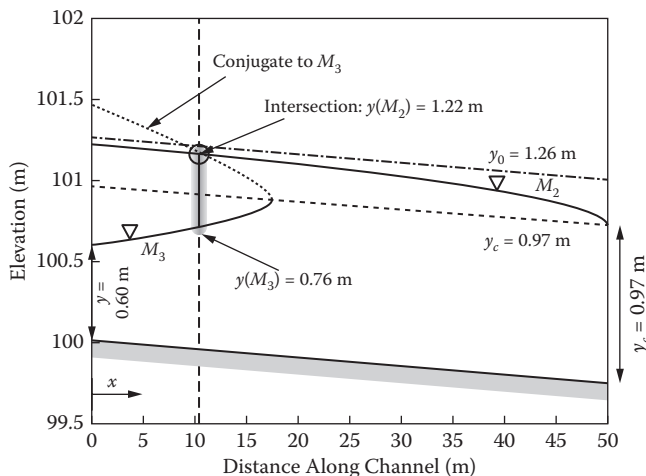


**FIGURE 6.5** Application of conjugate curve method to identify location of hydraulic jump in Example 6.4. Conjugate curve is shown for  $M_3$  profile.

at the intersection of the conjugate curve and the  $M_2$  profile is 1.22 m. Applying the momentum equation to these two depths, we find

$$M(y=0.76 \text{ m}) = \frac{y^2}{2} + \frac{q^2}{gy} = \frac{(0.76)^2}{2} + \frac{(3)^2}{(9.81) \cdot (0.76)} = 1.50 \text{ m}^2$$

$$M(y=1.22 \text{ m}) = \frac{y^2}{2} + \frac{q^2}{gy} = \frac{(1.22)^2}{2} + \frac{(3)^2}{(9.81) \cdot (1.22)} = 1.50 \text{ m}^2$$

To two decimal places, the momentum associated with both the upstream and downstream depths is the same confirming that these two depths are a conjugate pair.

- c. Figure 6.6 is a similar plot to Figure 6.5 except that the conjugate curve shown corresponds to the  $M_2$  profile. A close inspection by the reader should confirm that the location of the intersection of the conjugate curve and the  $M_3$  profile is the same as was determined above and therefore the jump is in the same location and the depths on opposite sides of the jump are the same. The reader can correctly conclude that the conjugate curve approach can be applied to either of the two profiles that are to meet at the jump with the same conclusion being reached in either case.

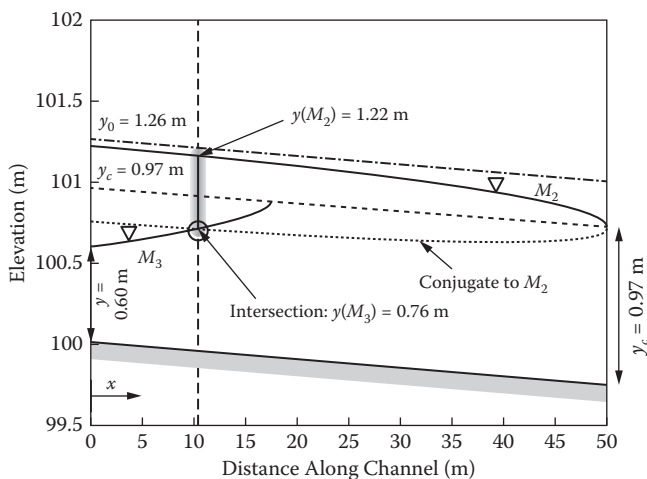


**FIGURE 6.6** Application of conjugate curve method to identify location of hydraulic jump in Example 6-4. Conjugate curve is shown for  $M_2$  profile.

The conjugate curve approach can also be used to identify the case of a drowned hydraulic jump as was originally discussed in Section 5.6. Let us return to Figure 6.5. In this figure, we note that the conjugate curve to the  $M_3$  profile right at the upstream boundary condition shows a water surface elevation of approximately 101.5 m corresponding to a depth of approximately 1.5 m. If conditions downstream were to impose a depth greater than this (for instance, an  $M_1$  profile propagating upstream from a second sluice gate at the downstream boundary), then the jump at the upstream sluice gate would be drowned. We know this because there is no depth on the conjugate curve that is greater than 1.5 m; thus, there is no suitable supercritical depth at or near the upstream boundary that would be conjugate to the hypothetical  $M_1$  curve propagating from the downstream gate. We examine this possibility in Example 6.5.

### Example 6.5

We use the same flow conditions and upstream boundary conditions as in Example 6.4. The downstream boundary condition is now a sluice gate set to an opening of 0.55 m. As before, the total reach length is 50 meters.

- Determine the alternate depth on the upstream side of the downstream sluice gate so that the step method can trace the  $M_1$  curve upstream from this depth.
- Using the conjugate curve to the  $M_3$  profile, provide a plot of the water surface over the entire length of the reach showing both profiles and conjugate curve. Verify that the jump caused by the upstream gate is drowned.
- Determine the depth of flow that exists just upstream of the upstream sluice gate.
- Recalculate the expected profiles if the downstream boundary condition is changed to a sluice gate set to an opening of 0.74 m.
- Determine the depth of flow that exists just upstream of the upstream sluice gate and compare to your answer to part (c) above.

#### **Solution:**

- The downstream sluice gate is set to a depth of 0.55 m. Assuming the gate is a choke, the depth on the upstream side of the gate is the alternate to the gate opening (1.94 m):

$$y_2 = \frac{2y_1}{-1 + \sqrt{1 + \frac{8gy_1^3}{q^2}}} = \frac{2 \cdot (0.55)}{-1 + \sqrt{1 + \frac{8 \cdot (9.81) \cdot (0.55)^3}{(30/10)^2}}} = 1.94 \text{ m}$$

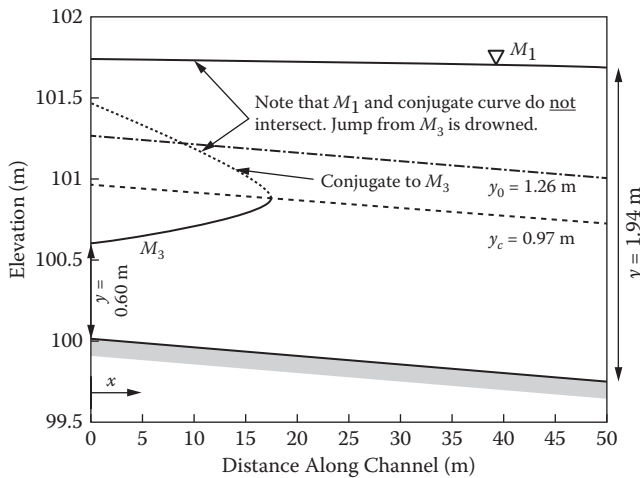


**FIGURE 6.7** Application of conjugate curve method for Example 6.5. Jump is drowned because  $M_1$  curve does not intersect conjugate curve within the modeled reach.

- b. The standard step method was used to generate an  $M_1$  curve propagating upstream from a depth of 1.94 m. Figure 6.7 shows how the  $M_1$  water surface profile remains deeper than the conjugate curve to the  $M_3$  profile even at the upstream end of the reach. Thus, the  $M_3$  profile (shown in dashed lines) does not actually exist and the upstream sluice gate does not set up supercritical flow; the hydraulic jump is drowned.
- c. Since there is no energy loss across the upstream sluice gate, the depth just upstream of the gate is the same as just below the gate, dictated by the  $M_1$  profile propagating upstream from the downstream sluice gate. As shown in the figure, this depth is approximately 1.75 m.
- d. The alternate depth to a sluice gate opening of 0.74 m is

$$y_2 = \frac{2y_1}{-1 + \sqrt{1 + \frac{8gy_1^3}{q^2}}} = \frac{2 \cdot (0.74)}{-1 + \sqrt{1 + \frac{8 \cdot (9.81) \cdot (0.74)^3}{(30/10)^2}}} = 1.31 \text{ m}$$

- e. Again using the standard step method, but for an  $M_1$  curve propagating upstream from a depth of 1.31 m, we arrive at conditions as reflected in Figure 6.8. We immediately see that this smaller depth  $M_1$  profile does intersect the conjugate curve to the  $M_3$

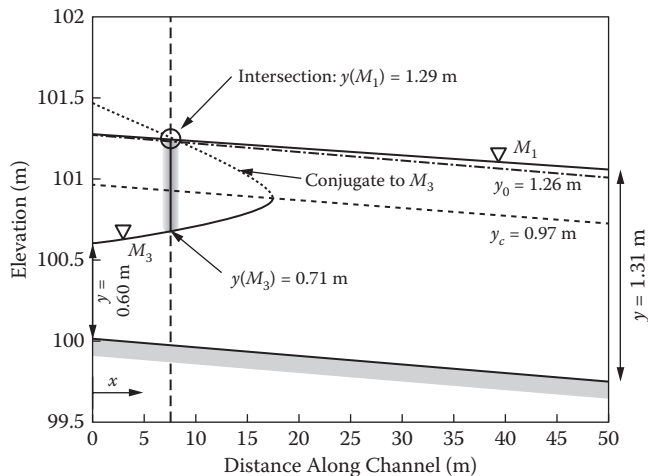


**FIGURE 6.8** Application of conjugate curve method for Example 6.5. Jump is located approximately 7.5 meters downstream of upstream sluice gate.

profile set up by the upstream sluice gate. Figure 6.8 shows an intersection of the  $M_1$  profile with the conjugate curve of  $M_3$  at approximately 7.5 m downstream of the upstream sluice gate.

Animations appear below to visually reinforce the conjugate curve concept.

### Animation: channel\_length.avi

Flow conditions:

$$Q = 4 \text{ m}^3/\text{s}$$

$$n = 0.03$$

$$b = 3 \text{ m}$$

$$S_0 = 0.001 \text{ m/m}$$

Apparent movement:

$L$  varies from 1000 m to 5 m in varying decrements

$$y_{gate} = 0.11 \text{ m}$$

Rectangular cross-section

Still image of animation shown in Figure 6.9

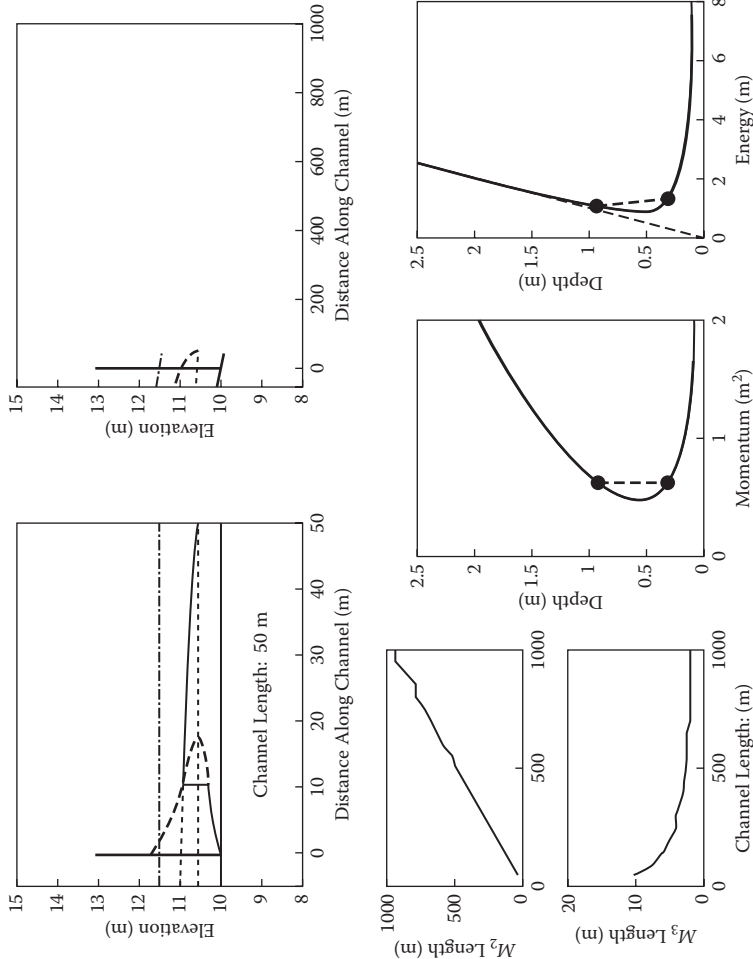


**FIGURE 6.9** Screen capture from channel\_length.avi animation. The capture shows the effect of diminishing length of channel downstream of a gate and upstream of a free overfall. As the downstream channel length decreases in the animation, the hydraulic jump propagates forward with the  $M_3$  curve lengthening more than the  $M_2$  curve shown in this figure.

This animation shows a sluice gate with a fixed opening on a mild reach. An  $M_2$  curve propagates upstream from a free overfall at the downstream end. The free overfall is initially 1000 m downstream of the gate; however, this length diminishes to as little as 5 m over the course of the animation.

The upper left subplot focuses on profiles in the first 50 meters downstream of the gate, while the upper right subplot shows the entire length of the reach downstream of the gate. Initially, the hydraulic jump is located just a few meters downstream of the gate. As the channel length diminishes, the  $M_2$  profile is not able to evolve upstream to as great a depth as was originally the case. The result is that the conjugate curve to the  $M_3$  profile intersects the  $M_2$  profile at locations that are increasingly further downstream as the channel length reduces. In short, the jump translates downstream as the channel length diminishes. When the channel length reaches approximately 18 m, the  $M_3$  profile ends at the free overfall and the hydraulic jump disappears. Any subsequent reduction in channel length simply means a shorter  $M_3$  profile.

The lower left subplots show the lengths of the  $M_2$  and  $M_3$  profiles as a function of overall channel length while the lower middle and lower right subplots show the  $M$ - $y$  and  $E$ - $y$  relationships, respectively, and the prevailing hydraulic jump as conditions evolve with diminishing channel length. The jagged appearance of the  $M_2$  and  $M_3$  profiles is a meaningless numerical artifact. In reality, the curves are smooth.

### Animation: m3m2\_animation.avi

Flow conditions:

$$Q = 100 \text{ ft}^3/\text{s}$$

$$n = 0.03$$

$$b = 10 \text{ ft}$$

$$S_0 = 0.001 \text{ ft/ft}$$

$$L = 100 \text{ ft (downstream of gate)}$$

$$L = 2000 \text{ ft (upstream of gate)}$$

Apparent movement:

$y_{gate}$  varies from 1.4 ft to 0.15 ft

Rectangular cross-section

Still image of animation shown in Figure 6.10

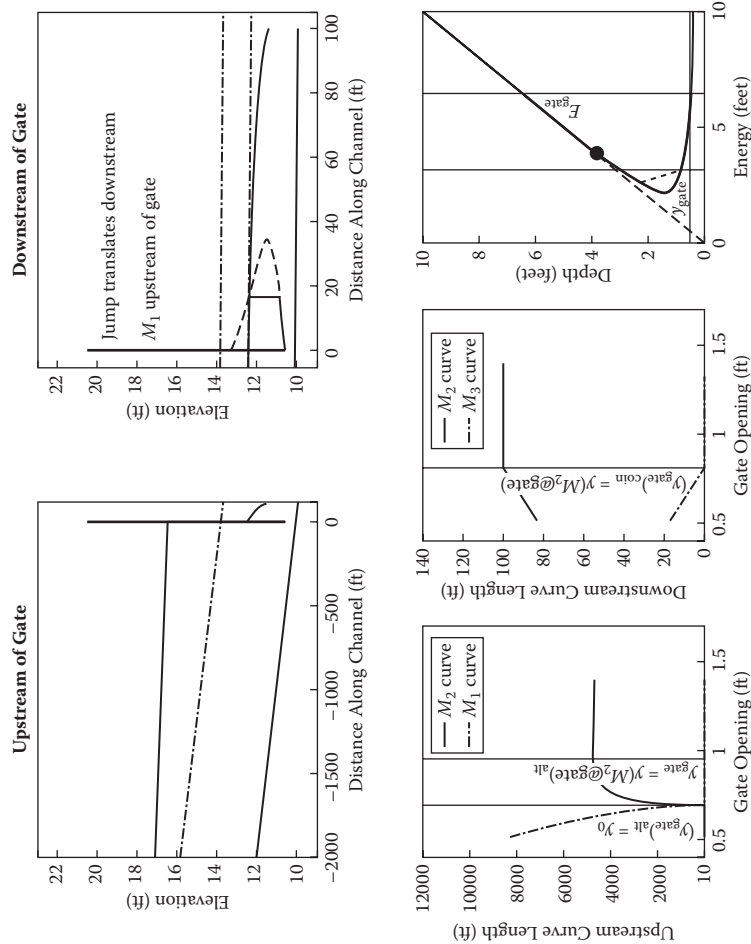


**FIGURE 6.10** Screen capture from m3m2\_animation.avi animation. The capture shows the effect of a sluice gate lowering into a reach with an existing  $M_2$  profile. Depending on the gate opening different surface water profiles are set up both upstream and downstream of the gate. See the text for further explanation of the subplots shown in this figure.

This animation shows a sluice gate lowering on a mild reach. An  $M_2$  curve propagates upstream from a free overfall at the downstream end. The gate produces the potential for an  $M_3$  curve immediately downstream. If the  $M_3$  curve exists, it is followed by a hydraulic jump to the  $M_2$  profile. Depending on the size of the gate opening, either an  $M_1$  or  $M_2$  profile exists upstream of the gate.

The upper left subplot focuses on profiles upstream of the gate, while the upper right subplot focuses on profiles downstream of the gate. Initially, the gate has no influence and is simply being lowered into an existing  $M_2$  profile. As the gate lowers past critical depth it begins to set up a potential  $M_3$  curve immediately downstream (with the conjugate curve to this potential  $M_3$  also shown). These potential curves become reality when the conjugate curve intersects the existing  $M_2$  profile. As the gate lowers further, the conjugate curve intersects the  $M_2$  profile increasingly further downstream, meaning that as the gate lowers, the location of the hydraulic jump translates downstream. Meanwhile, as the gate lowers deeper into the flow it becomes a choke, first raising the depth along the truncated  $M_2$  profile upstream of the gate. Eventually, the choke is great enough to cause conditions upstream of the gate to become an  $M_1$  profile. This latter choke condition occurs when the energy associated with the gate opening equals the energy associated with flow at normal depth.

The lower subplots provide graphical information about profile lengths and energy-depth relationships. The lower left and lower middle subplots show the length of each of the  $M_x$  profile lengths as a function of the gate opening. Several vertical lines are indicated at gate openings which mark key transition points in the existence or disappearance of one or more  $M_x$  profiles. The lower right subplot presents the  $E-y$  relationship for this animation with a vertical line slowly migrating to the right to indicate the energy associated with the current gate opening.

## 6.6 HEC-RAS: AN INDUSTRY STANDARD SOFTWARE PACKAGE FOR SURFACE WATER PROFILES

We turn now to the HEC-RAS program (HEC 2014) as a tool for calculating surface water profiles. HEC-RAS is a computer program produced by the US Army Corps of Engineers, Hydrologic Engineering Center (HEC). The second

part of the program name, RAS, stands for “River Analysis System.” HEC-RAS is capable of modeling both steady and unsteady flow in open channels. That flow may be subcritical, supercritical, or mixed (meaning a combination of subcritical and supercritical). Single reaches can be studied, or profiles within an entire dendritic drainage network can be modeled. The HEC-RAS program has many applications, though one of the most common is its application to flood mapping and its use in flood insurance studies. HEC-RAS was first introduced in 1995, but it has its origins in an earlier program, HEC-2 (HEC 1991), which has been used for similar purposes since the mid-1970s. HEC-RAS represents a substantial improvement over HEC-2 both algorithmically and visually.

Computer advances and program changes render documentation of any software package too ephemeral for a textbook. While this section will show selected screen captures from the HEC-RAS program that are current at the time of the writing of this text, the specific menu choices and software functions necessary to model surface water profiles within a reach will not be enumerated here. Instead, the emphasis here is on physical interpretation of the HEC-RAS model input and output, and on comparison of this program’s results to those from the spreadsheet-based techniques presented earlier in this chapter. The reader is encouraged to obtain both the software and user’s manual for the HEC-RAS program to complement the presentation provided in this text. The citations for these materials are provided in the references, and these materials are available at no cost from HEC. The opportunity to use HEC-RAS is reinforced through some of the exercises at the end of this chapter that specifically direct the reader to employ this program in developing problem solutions.

HEC-RAS requires data input in three basic categories: geometric data, flow data, and plan data:

*Geometric data:* These data include both cross-sectional and longitudinal information. In general, the greatest single effort in creating a HEC-RAS input file will be spent specifying this information.

*Flow data:* These data generally amount to indicating the channel discharge and the boundary conditions that apply at both the upstream and downstream ends of the modeled channel(s).

*Plan data:* In indicating plan data, the user is generally simply specifying the anticipated flow regime(s), typically subcritical only, supercritical only, or possibly the appearance of both flow regimes within the system being modeled.

We will introduce the reader to the use of HEC-RAS through a return to Example 6.2, but solved now through the use of HEC-RAS.

### Example 6.6

Repeat the modeling of an  $M_2$  curve as posed in Example 6.2, but using HEC-RAS as the analysis tool. Compare the calculated profile from the two examples and comment on the nature and source of any differences between them.

#### **Solution:**

We first repeat the flow conditions and requested locations. The system is a 10 m wide rectangular channel carrying a discharge of  $30 \text{ m}^3/\text{s}$ , with a channel slope of  $0.005 \text{ m/m}$ , and Manning's roughness is 0.030. Depths are to be determined along the  $M_2$  profile at the following locations:  $x = -0.1 \text{ m}, -0.2 \text{ m}, -0.3 \text{ m}, -0.4 \text{ m}, -0.5 \text{ m}, -1.0 \text{ m}, -2.0 \text{ m}, -5.0 \text{ m}, -10 \text{ m}, -20 \text{ m}, -30 \text{ m}, -40 \text{ m}, -50 \text{ m}, -100 \text{ m}, \text{ and } -140 \text{ m}$ .

**Project Setup/Initial Activities:** A new project was started in HEC-RAS. The HEC-RAS program defaults to English units so one of the initial steps of the project definition is to switch to metric (SI) units. As stated, the problem involves a single reach of a single river so these, too, must be nominally specified.

**Geometric Data:** Figure 6.11 shows the “Cross Section Data” dialog with the initial downstream cross-section specified. This dialog requests station ( $x$ ) and elevation ( $y$ ) data pairs which are sequential horizontal and vertical measurements, respectively, along the stream cross-section

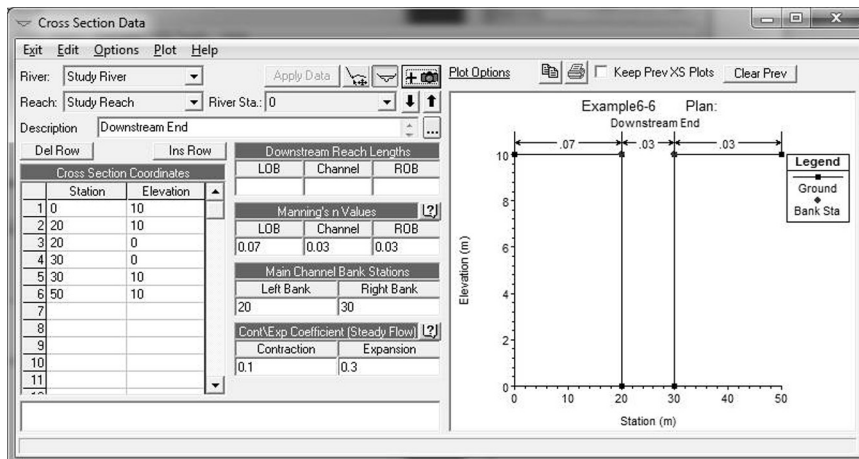


**FIGURE 6.11** “Cross Section Data” dialog in HEC-RAS program. Data entered corresponds to downstream end of reach modeled in Example 6.6.

from the left edge of the stream cross-section to the right. The user must identify the station coordinate that represents the left and right bank of the channel. Because the project is understood to be working in SI units, all length measurements are understood to be in meters. In addition, a Manning's roughness needs to be specified for the left overbank (LOB) region, the channel, and the right overbank (ROB) region. The user indicates the distance from the indicated cross-section to the next cross-section downstream. These distances are again separated into LOB, channel, and ROB components. Channel meandering is indicated when these distances are not equal. The software automatically creates a plot of the entered cross-section as shown in the right half of the dialog. This plot is useful to minimize the possibility of errors in data entry.

Cross-sections are ordered sequentially through their identified "River Station." The lowest value river station is understood to be the downstream end of the reach being modeled. In practice in the United States, river stations are generally expressed in units of river miles such that a given river station's value indicates the distance that cross-section is located from some starting location downstream, often the confluence of that stream or reach with a larger river downstream. The river station value is used by HEC-RAS simply to create an order in which cross-sections are sequenced. The actual separation distance between cross-sections is conveyed through the three downstream reach lengths entered elsewhere.

In Figure 6.11, the cross-section that marks the downstream end of the stream reach is shown. The problem definition did not address absolute elevations or the overall depth of the channel, so these measurements (0 m for the channel bottom at the downstream end and 10 m deep channels) were arbitrarily assumed. Note that the downstream reach length entries are left blank because the illustrated channel cross-section is at the bottom of the reach being modeled. Any other cross-section would need these three distances to be specified.

Because the channel shape is constant in this problem, the user can take advantage of features in the HEC-RAS software to rapidly generate additional cross-sections. Special features that the user might employ include a tool that replicates entered cross-sections, a tool that adds or subtracts a fixed value to all cross-sectional elevations, and a tool that allows for interpolation between cross-sections. Using these tools, the only significant input the user needs to provide is the downstream reach lengths. The overall channel slope is effectively communicated to the program through the combination of the elevation difference between successive cross-sections and the downstream reach length separating them.

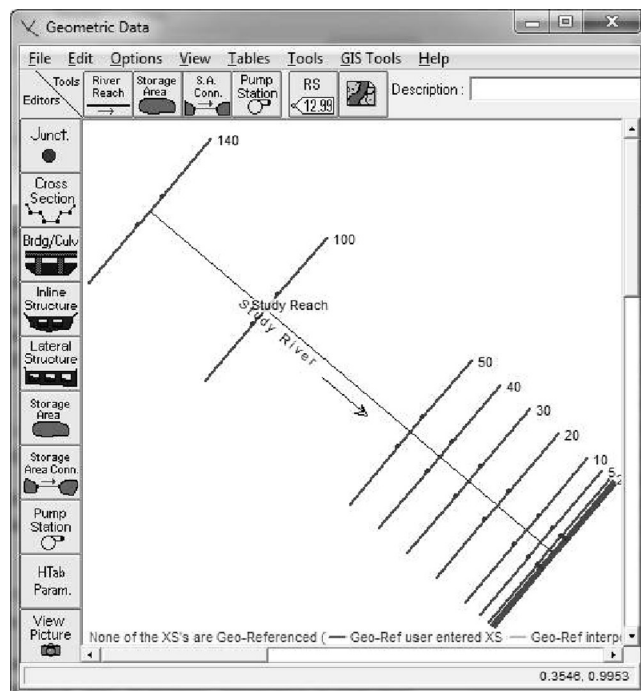


**FIGURE 6.12** Plan view of modeled reach for Example 6.6 within HEC-RAS program. Cross-sections are spaced irregularly to capture expected curvature of  $M_2$  profile.

Figures 6.12 and 6.13 show a plan and profile view, respectively, of the reach entered into HEC-RAS to model this example problem. Figure 6.12 shows the channel as if viewed from above with the cross-sectional locations indicated by the lines perpendicular to the study river/study reach. Notice that the spacing of cross-sectional locations varies with much greater density at the downstream (lower right) end of the reach. This greater density helps capture the greater curvature in the  $M_2$  profile as the flow nears critical depth at the downstream boundary. Figure 6.13 shows the channel viewed in profile, with each square dot indicating a cross-sectional location. It is especially useful to create this profile plot to confirm that the intended overall channel slope has been correctly entered into the program. The constant slope of the channel at 0.005 m/m is confirmation of successful data entry in this case.

**Flow Data:** Figures 6.14 and 6.15 show the “Steady Flow Data” and the “Steady Flow Boundary Conditions” dialogs, respectively. The flow data dialog is quickly completed as shown in Figure 6.14 with “30” (indicating

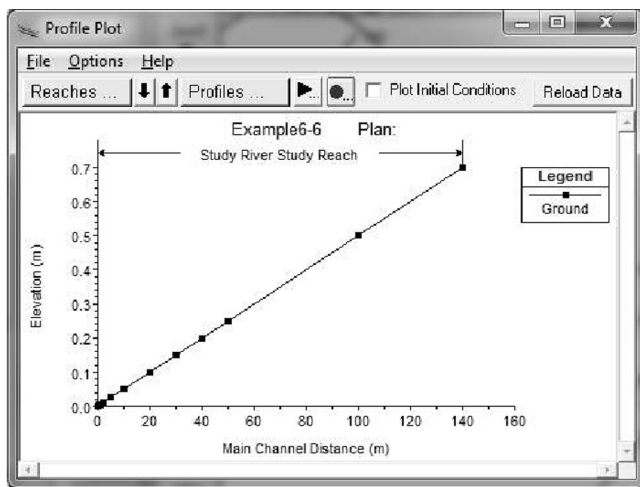


**FIGURE 6.13** Profile view of modeled reach for Example 6.6 within HEC-RAS program. Channel slope is 0.005 m/m. The straight slope of the channel bottom in the figure confirms accurate depiction of reach within the program.

30 m<sup>3</sup>/s) entered for PF 1 (Profile Flow rate for profile 1). The user will also click on the “Reach Boundary Conditions” button in this dialog to obtain the dialog shown in Figure 6.15. This figure has the user indicate both the upstream and downstream boundary conditions. As shown here, the

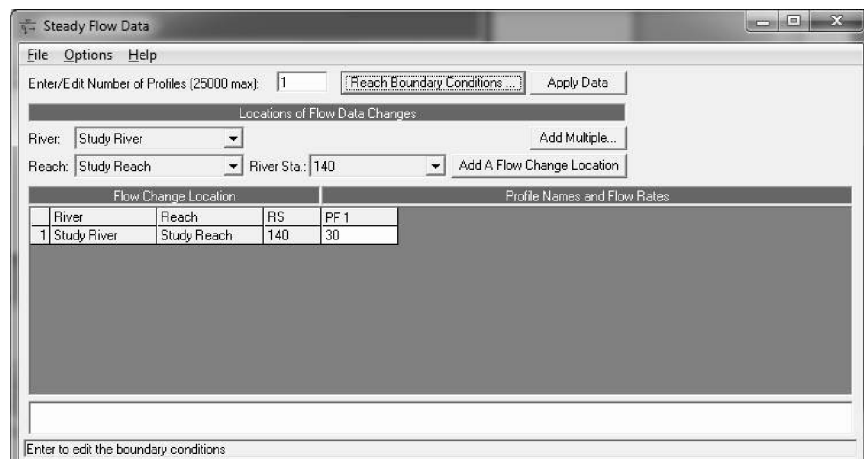


**FIGURE 6.14** “Steady Flow Data” dialog in the HEC-RAS program. Data entry corresponds to 30 m<sup>3</sup>/s discharge at upstream end, “RS = 140” in Example 6.6.

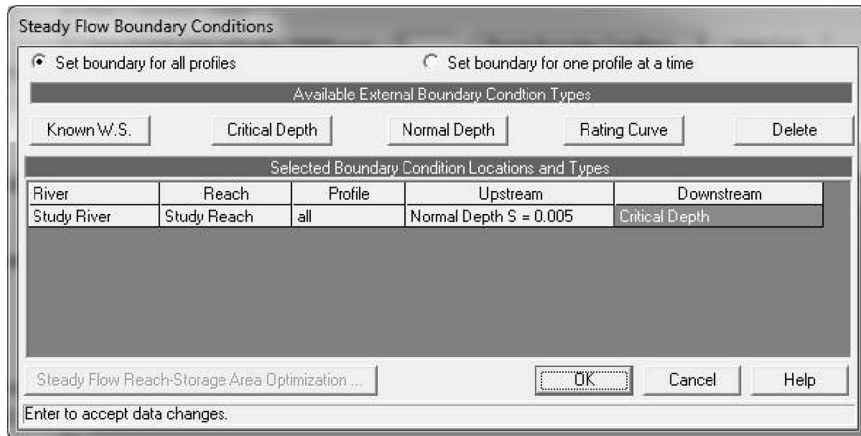


**FIGURE 6.15** “Steady Flow Boundary Conditions” dialog in the HEC-RAS program. Data entry shows normal depth (upstream) and critical depth (downstream) boundary conditions in Example 6.6.

downstream boundary condition is “Critical Depth” while the upstream boundary condition is “Normal Depth  $S = 0.005$ .” The user can also specify boundary conditions using the “Known W.S.” (Water Surface elevation) and “Rating Curve” tools. The “Known W.S.” entry can be useful for specifying a depth that might be imposed by a sluice gate, for instance.

Figure 6.16 presents a tabular accounting of the surface water profile determined by the HEC-RAS program. The software provides a

Profile Output Table - Standard Table 1													
HEC-RAS Plan: Plan 01 River: Study River Reach: Study Reach Profile: FF 1 (Released 03/03)													
Reach	River Sta	Profile	Hyd Depth	D Total	Min Ch El	W.S. Elev	Crit W.S.	E.G. Elev	E.G. Slope	Vel Chnl	Flow Area	Top Width	Froude # Chnl
Study Reach	140	FF 1	1.26	30.00	0.70	1.96		2.25	0.005018	2.37	12.63	10.00	0.67
Study Reach	100	FF 1	1.26	30.00	0.50	1.75		2.05	0.005120	2.39	12.55	10.00	0.68
Study Reach	50	FF 1	1.22	30.00	0.25	1.47		1.78	0.005654	2.47	12.15	10.00	0.71
Study Reach	40	FF 1	1.20	30.00	0.20	1.40		1.72	0.006851	2.50	12.02	10.00	0.73
Study Reach	30	FF 1	1.18	30.00	0.15	1.33		1.66	0.008136	2.54	11.83	10.00	0.74
Study Reach	20	FF 1	1.16	30.00	0.10	1.26		1.60	0.008590	2.59	11.56	10.00	0.77
Study Reach	10	FF 1	1.11	30.00	0.05	1.16		1.53	0.007534	2.71	11.07	10.00	0.82
Study Reach	5	FF 1	1.07	30.00	0.02	1.09	1.00	1.49	0.008423	2.81	10.68	10.00	0.87
Study Reach	2	FF 1	0.98	30.00	0.01	1.00	0.98	1.47	0.010521	3.02	9.94	10.00	0.97
Study Reach	1	FF 1	0.98	30.00	0.00	0.99	0.98	1.46	0.010919	3.05	9.82	10.00	0.98
Study Reach	0.6	FF 1	0.98	30.00	0.00	0.98	0.97	1.46	0.011110	3.07	9.77	10.00	0.99
Study Reach	0.4	FF 1	0.97	30.00	0.00	0.98	0.97	1.46	0.011209	3.09	9.74	10.00	1.00
Study Reach	0.2	FF 1	0.97	30.00	0.00	0.97	0.97	1.46	0.011287	3.09	9.72	10.00	1.00
Study Reach	0	FF 1	0.97	30.00	0.00	0.97	0.97	1.46	0.011336	3.09	9.71	10.00	1.00

**FIGURE 6.16** “Profile Output Table” window showing a tabular accounting of the calculated profile in Example 6.6.

standardized table; however, HEC-RAS allows the user to modify this table by inserting or deleting columns. The table shown in Figure 6.16 has been modified by adding the “Hydr Depth” column to explicitly report the depths simulated by the HEC-RAS program.

Figure 6.17 presents a comparison of the  $M_2$  water surface profiles calculated here using the HEC-RAS program and calculated previously using the standard step method in Example 6.2. Overall, the two profiles compare favorably, although a close examination (see inset within the figure) shows the tendency of the HEC-RAS profile to report slightly smaller depths in the immediate vicinity of the downstream end of the reach. Some of this difference can be simply attributed to the number of decimal places reported by the HEC-RAS program. The reason for the remainder of the difference is unclear but may be a function of the solution algorithm, the precise value used for gravitational acceleration,  $g$ , or possibly by internal metric-English units conversion. Additionally,

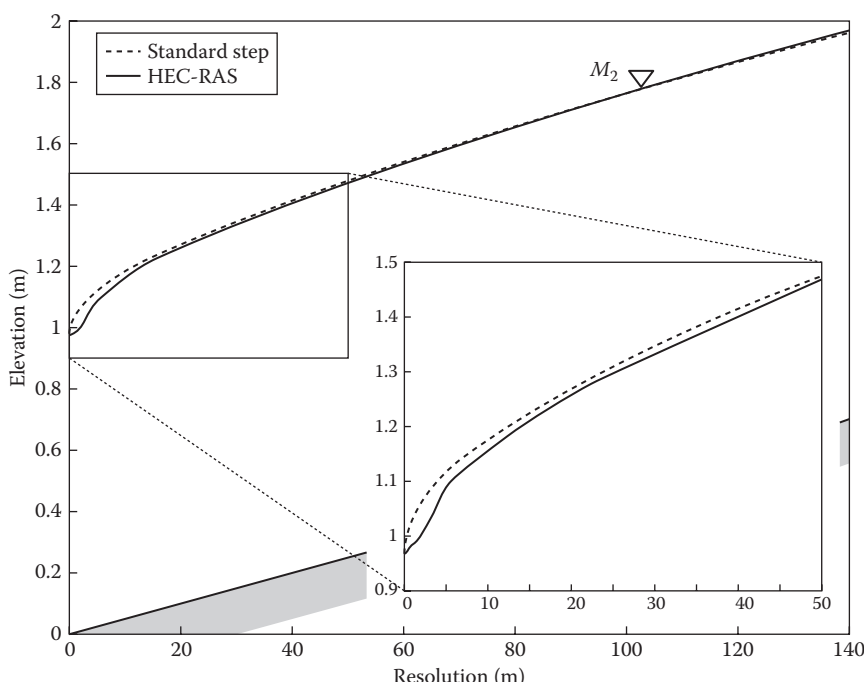


**FIGURE 6.17** Graphical comparison of  $M_2$  profiles determined using the HEC-RAS program (solid line) in Example 6.6 versus the standard step method (dashed line) in earlier Examples 6.1 and 6.2. The inset shows an enlarged view of the downstream end of the two computed profiles.

because of the small channel slope being modeled and the three decimal place vertical elevation precision supported by the HEC-RAS program, the smallest spacing,  $\Delta x$ , that could be modeled in HEC-RAS is 0.2 m, rather than the 0.1 m used in the standard step method in Example 6.2. That is,

$$\Delta z = \Delta x \cdot S_0 = (0.2) \cdot (0.005) = 0.001 \text{ m}$$

---

Let's examine one more application of the HEC-RAS program with regard to what HEC-RAS refers to as "mixed flow," that is a reach where the conditions favor a hydraulic jump so the flow is expected to transition from supercritical to subcritical flow. We perform this examination by returning to the conditions in Example 6.5 in which an upstream sluice gate was setting up supercritical flow at the top of the modeled reach and a downstream sluice gate was imposing subcritical flow at the bottom of the reach. The reader may recall that depending on the opening at the downstream gate, the hydraulic jump within the reach was drowned in one case and realized in the other.

---

### ***Example 6.7***

Using HEC-RAS, re-examine the two flow profiles initially presented in Example 6.5:

- a. Explicitly describe your approach for setting up stream cross-sections.
- b. Indicate your approach for specifying upstream and downstream boundary conditions.
- c. Indicate the HEC-RAS flow plan for this analysis.
- d. Present the flow profile plots for both downstream gate settings and interpret your findings.
- e. Comment on the solution consistency with the findings from Example 6.5.

#### ***Solution:***

- a. The general cross-sectional shape is identical to that defined in Example 6.6. The easiest approach for setting up the stream cross-sections is to first specify the downstream reach the same as in the previous example. Second, use tools within HEC-RAS to copy the cross-section, specifying a location of 50 m (the upstream end of the reach). Third, for the copied

cross-section, use tools within HEC-RAS to add an elevation of 0.25 m. Fourth, specify the downstream reach length of 50 m to the LOB, channel, and ROB. Finally, use tools within HEC-RAS to interpolate cross-sections between these two defined cross-sections at a spacing of 2 m.

- b. Recall that the sluice gates can impose both an upstream depth and a downstream depth. The upstream gate imposes a depth of 0.60 m. The downstream gate is set at two different openings imposing a depth of first 1.94 m and later a depth of 1.31 m. As the problem is posed, the best way to manage the boundary conditions is to use a "Known WS" (known water surface elevation). The reader should be careful not to confuse depth with water surface elevation. The water surface elevation is the sum of the depth and the elevation of the channel bottom at the location in question. For the downstream boundary condition, the channel elevation, as modeled, is 0 m so the water surface elevation and the depth are the same (i.e., 1.94 m and later 1.31 m). At the upstream boundary, the reader should note that the channel bottom has an elevation of 0.25 m (channel slope of 0.005 m/m multiplied by the reach length of 50 m). Therefore, the boundary condition of a known water surface elevation is  $0.25\text{ m} + 0.60\text{ m} = 0.85\text{ m}$ .
- c. The upstream gate imposes supercritical flow while the downstream gate dictates subcritical flow. From Example 6.5, there is an expectation of a drowned jump for the deeper downstream depth. This information would not typically be known without separate analysis, so the proper flow regime to specify in the HEC-RAS program is "mixed flow," which will allow for the potential of calculating a hydraulic jump within the study reach.
- d. Figures 6.18 and 6.19 show profile plots of the 1.94 m and 1.31 m downstream water surface elevation settings, respectively. It should be clear from a quick examination of Figure 6.18 that the hydraulic jump is drowned as the water surface elevation is close to 2 m at the upstream boundary. In Figure 6.19, a hydraulic jump is indicated at a main channel distance between 44 and 46 m. The location of this jump cannot be determined from the output with any greater resolution than this as HEC-RAS only reports depths at cross-sectional locations.
- e. Recall that in Example 6.5 a drowned jump was determined for the downstream boundary condition depth of 1.94 m while a jump was calculated to occur at approximately 7.5 m

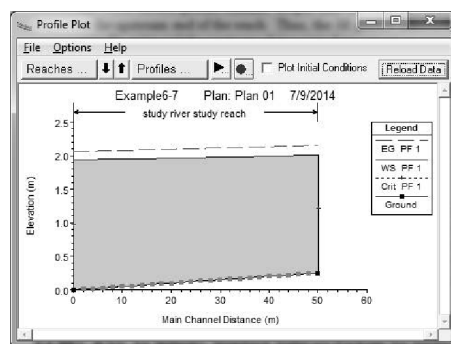


**FIGURE 6.18** “Profile Plot” window showing the drowned jump calculated when the downstream boundary condition is a water surface elevation of 1.94 m in Example 6.7.

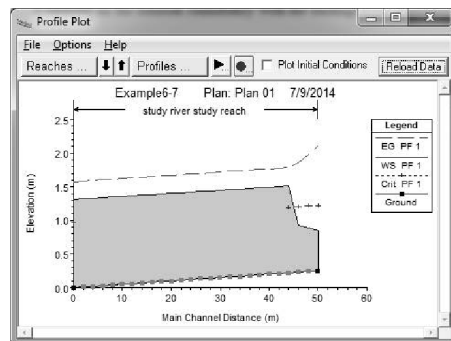


**FIGURE 6.19** “Profile Plot” window showing the hydraulic jump calculated when the downstream boundary condition is a water surface elevation of 1.31 m in Example 6.7.

downstream of the upstream boundary. The results determined by HEC-RAS are comparable, but not identical, to these findings. The drowned jump result is consistent across the two examples for the larger downstream water surface elevation. For the smaller downstream water surface elevation, Example 6.5 indicates a jump near 7.5 m downstream while HEC-RAS places this jump between 4 and 6 m downstream.

## 6.7 SUMMARY

This chapter presented the fundamental equations governing the calculation of gradually varied surface water profiles. Several different spreadsheet-based approaches were first presented as a tool for quantitatively calculating these profiles. The first method, known as the *standard step method*, involved the calculation of location,  $x$ , given depth,  $y$ , in a regular, constant-shaped channel. Subsequent spreadsheet-based approaches that allowed for the calculation of  $y$  given  $x$  and for the calculation of surface water profiles in a channel of varying size/shape/roughness were presented. These subsequent approaches required iteration to apply, while the first approach ( $x$  given  $y$ ) is direct and does not require iteration.

In the previous chapter, the *conjugate curve* concept was presented. In this chapter this concept was used to determine the location of a hydraulic jump within a stream reach of finite length. This concept was also used to illustrate the occurrence of a drowned jump, which occurs when a downstream depth propagates upstream and is too deep to match the upstream momentum of a supercritical flow created, for instance, by a sluice gate.

Finally, this chapter presented the commonly used program, HEC-RAS, for the calculation of quantitative surface water profiles. Although a thorough user's manual-type approach to using HEC-RAS was not presented in this chapter, the basics of required input in terms of channel geometry, slope, roughness, discharge, and boundary conditions were presented in the form of several illustrative examples. Typical graphical and tabular outputs were also presented and contrasted with the results obtained earlier using spreadsheet-based approaches.

## References

- Chaudhry, M.H. (2008). *Open-Channel Flow*, Springer, New York.  
 Henderson, F.M. (1966). *Open Channel Flow*, Macmillan, New York.  
 Hydrologic Engineering Center (HEC). (1991). *HEC-2 Water Surface Profiles User's Manual*, US Army Corps of Engineers, Davis, CA.  
 Hydrologic Engineering Center (HEC), HEC-RAS, US Army Corps of Engineers, <http://www.hec.usace.army.mil/software/hec-ras/> (accessed on July 14, 2014).

## Problems

- 6.1. A 2 m wide rectangular reach with slope,  $S_0 = 0.005 \text{ m/m}$ , carries a discharge,  $Q = 5 \text{ m}^3/\text{s}$ , and has a Manning's  $n = 0.055$ . A sluice gate imposes an upstream flow depth of 0.10 m. At the downstream end of the channel critical flow conditions prevail. Assume a large overall reach length of 1000 or 2000 m.

- a. Determine normal depth and whether flow at normal conditions is supercritical or subcritical.
  - b. What profile(s) do you expect in this reach? Draw a sketch of the profiles anticipated within the reach.
  - c. Use the standard step method ( $x$  calculated from  $y$ ) to quantitatively calculate all flow profiles and to determine the location of all jumps.
  - d. Use an alternative spreadsheet approach to calculate depth ( $y$ ) given location ( $x$ ) for this same reach.
  - e. Use HEC-RAS to solve for water surface profile(s) in this reach and provide an output table that indicates location, depth, and water surface elevation within the reach.
  - f. Prepare a plot that shows the three profiles calculated in parts (c), (d), and (e) on a single graph. Briefly discuss similarities and differences between these three profiles.
- 6.2. Repeat Problem 6.1 except the reach is 100 m long.
- 6.3. Repeat Problem 6.1 except the reach is 100 m long and the downstream boundary is a sluice gate open to a depth of 0.35 m. Hint: you will first want to convert this downstream gate into a downstream boundary condition corresponding to the depth that exists just upstream of the gate.
- 6.4. A 5 m wide rectangular reach with slope,  $S_0 = 0.015 \text{ m/m}$ , carries a discharge,  $Q = 5 \text{ m}^3/\text{s}$ , and has a Manning's  $n = 0.019$ . Flow enters at critical depth. At the downstream end of the channel a sluice gate is open to 0.21 m. Assume a large overall reach length of 1000 m.
- a. Determine normal depth and whether flow at normal conditions is supercritical or subcritical.
  - b. What profile(s) do you expect in this reach? Draw a sketch of the profiles anticipated within the reach.
  - c. Use the standard step method ( $x$  calculated from  $y$ ) to quantitatively calculate all flow profiles and to determine the location of all jumps.
  - d. Use HEC-RAS to solve for water surface profile(s) in this reach and provide an output table that indicates location, depth, and water surface elevation within the reach.
  - e. Prepare a plot that shows the two profiles calculated in parts (c) and (d) on a single graph. Briefly discuss similarities and differences between these two profiles.
- 6.5. Repeat Problem 6.4 focusing on the region from the upstream end to the sluice gate and limiting the length to 50 m.

- 6.6. For the  $S_2$  profile in Problem 6.4, revisit the sensitivity analysis of Example 6.1c, examining the profile length for small increments of depth,  $\Delta y$ , near both  $y_c$  and  $y_0$ . In spirit, are the results the same or different from those found in Example 6.1c?
- 6.7. Return to Problem 5.8 in the Chapter 5.
  - a. Redo (or re-copy your past response to) part (a) from Problem 5.8.
  - b. Re-do (or re-copy your past response to) part (b) from Problem 5.8.
  - c. Use the standard step method to quantitatively calculate the water surface profiles in these two reaches. Provide a single composite plot of the profiles in this system based on your calculations.
  - d. Use HEC-RAS to calculate the water surface profiles in these two reaches. Provide two plots (one for each reach) that show the profiles you determined for this system.
  - e. Based on your findings in parts (c) and (d) of this problem, what is the minimum length of each reach such that the flow enters and leaves the system at normal depth as specified?
- 6.8. Repeat Problem 6.7 based on the conditions specified in Problem 5.9 in Chapter 5.



# **Fundamentals of Sediment Transport**

## **CHAPTER OBJECTIVES**

1. Define some basic properties of sediment: size, size distribution, and density.
  - a. Density and specific gravity
  - b. Particle shape
  - c. Sediment size—different classification schemes
  - d. Size distribution ( $d_{50}$ ,  $d_{84}$ , etc.)
    - i. USGS relationship to Manning's  $n$
2. Quantify the onset of sediment transport.
  - a. Present Shields diagram for initiation of sediment motion.
3. Define transport: bed load, suspended load, and washload.
  - a. Present dimensional analysis for sediment transport.
  - b. Illustrate calculation of bed load transport rate.
  - c. Illustrate calculation of suspended load transport rate.
4. Show use of rating curve approach for estimating total sediment load.
5. Examine sediment transport estimation accuracy and precision.

### **7.1 INTRODUCTORY COMMENTS**

The focus in the previous chapters has been placed exclusively on flowing water. This final chapter is a departure from that theme. In this chapter we explore the most basic elements of sediment transport. Sediment transport is a natural process that occurs primarily during times of flood or elevated flow

conditions. Water flowing in open channels has the capacity to set sediment in motion and to carry this sediment to points downstream. This chapter presents the most fundamental concepts relevant to sediment transport.

From an engineering perspective, sediment transport is of interest because problems arise when sediment is eroded from or deposited to a given location. For instance, bridge piers placed within the channel may collapse or fail if scour surrounding the pier is sufficient to undermine the foundation of the pier. At the other extreme, sediment transported downstream commonly deposits in ponds or reservoirs and may accumulate to the point that the water body is filled, reducing or eliminating water storage capacity. In addition to concerns of erosion and deposition is the basic desire to design a stable channel. Many decades past, this took the form of designing canals while in more recent times stream restoration generally has the same objective of seeking a channel design that will be stable.

In short, then, this chapter is concerned with addressing four basic questions: (1) How are water and sediment characterized with respect to sediment transport? (2) At what point does sediment start to move? (3) How do we quantify the amount of sediment that moves? and (4) In general terms, what can be said of the estimation of sediment transport in terms of accuracy and precision? This chapter proceeds in four parts. The first part (Section 7.2) introduces terminology and quantities relevant to matters of sediment characterization and transport—Question 1 above. The second part (Section 7.3) focuses on the question of sediment motion—Question 2 above. The third part (Section 7.4) focuses on quantifying sediment transport rates and loads—Question 3 above. In the fourth part (Section 7.5), the chapter concludes with a brief summary addressing Question 4 above.

## 7.2 CHARACTERIZATION OF WATER AND SEDIMENT

The first step in understanding sediment transport is to quantify the relevant characteristics of both the flowing fluid—water—and the transported material—sediment. One might assume that the relevant characteristics of water—density, unit weight, dynamic and kinematic viscosity—do not vary considerably with temperature. Over the temperature range from 0 to 30°C, this assumption would be a good one in the context of density or unit weight. However, it is a poor one in terms of viscosity, which decreases by more than a factor of two over this temperature range as shown in Table 7.1.

The remainder of this section focuses on several important characteristics of sediment: weight, size, shape, and distribution. Sediment weight is maybe the most simple characteristic to understand and to quantify. The composition of

**TABLE 7.1** Some Physical Properties of Water as a Function of Temperature

Temperature (°C)	Density $\rho$ (kg/m <sup>3</sup> )	Unit Weight $\gamma$ (N/m <sup>3</sup> )	Dynamic Viscosity $\mu$ (N·s/m <sup>2</sup> )	Kinematic Viscosity $v$ (m <sup>2</sup> /s)
0	999.8	9805	$1.781 \times 10^{-3}$	$1.785 \times 10^{-6}$
5	1000	9807	$1.518 \times 10^{-3}$	$1.519 \times 10^{-6}$
10	999.7	9804	$1.307 \times 10^{-3}$	$1.306 \times 10^{-6}$
15	999.1	9798	$1.139 \times 10^{-3}$	$1.139 \times 10^{-6}$
20	998.2	9789	$1.002 \times 10^{-3}$	$1.003 \times 10^{-6}$
25	997.0	9777	$8.90 \times 10^{-4}$	$8.93 \times 10^{-7}$
30	995.7	9764	$7.98 \times 10^{-4}$	$8.00 \times 10^{-7}$

a piece of sediment will vary depending on the geology of the region, and the density of this sediment will vary accordingly. As a practical matter, however, although sediment density does vary, a specific gravity,  $S_s = 2.65$ , is almost universally used. This value applies well to quartz and is used exclusively in this text.

The weathering process and the composition of sediment source material lead to a wide range of sediment sizes from the very small (< 0.002m) to the very large (> 256 mm). Here we present two common approaches that allow for the measurement of sediment size. The first scale is the  $\phi$ -scale, based on powers of 2. It is defined as:

$$D = 2^{-\phi} \quad (7.1)$$

where  $D$  is in millimeters. For instance, the  $\phi$ -scale of an 8 mm sediment particle is

$$8 = 2^{-\phi}$$

thus,

$$\phi = -\frac{\log(8)}{\log(2)} = -3$$

Another common approach for measuring sediment size is to use the US standard sieve series. These sieve sizes are based on mesh screens with a fixed number of openings per inch. These meshes only cover a subset of the total range of sediment sizes, as indicated in Table 7.2. Table 7.2 provides a commonly accepted set of grain size class ranges on both the  $\phi$ -scale and on the US standard sieve series.

**TABLE 7.2** Sediment Class Names and Size Ranges

Sediment Class Name	Size Range (mm)	$\phi$ -Scale	Sieve Openings/inch
Very coarse cobble up to boulders	> 256	< -8	
Coarse cobble	128 to 256	-7 to -8	
Fine cobble	64 to 128	-6 to -7	
Very coarse gravel	32 to 64	-5 to -6	
Coarse gravel	16 to 32	-4 to -5	
Medium gravel	8 to 16	-3 to -4	5
Fine gravel	4 to 8	-2 to -3	10
Very fine gravel	2 to 4	-1 to -2	18
Very coarse sand	1 to 2	0 to -1	35
Coarse sand	0.5 to 1	1 to 0	60
Medium sand	0.25 to 0.5	2 to 1	120
Fine sand	0.125 to 0.25	3 to 2	230
Very fine sand	0.063 to 0.125	4 to 3	
Very coarse silt	0.031 to 0.063	5 to 4	
Coarse silt	0.016 to 0.031	6 to 5	
Medium silt	0.008 to 0.016	7 to 6	
Fine silt	0.004 to 0.008	8 to 7	
Very fine silt	0.002 to 0.004	9 to 8	
Clay	< 0.002	> 9	

Sediment shape also varies depending on the weathering process and sediment source material. Because measuring the surface area of a natural sediment particle is difficult, a secondary approach used by McNown and Malaika (1950) to describe particle shape imposes an orthogonal set of axes on the particle and measures its length dimensions along each of these three axes. With  $a$  being the longest length measurement along one axis,  $c$  being the shortest length measurement along another axis, and  $b$  the length measurement along

the remaining axis, these three measurements are used to calculate a shape factor:

$$SF = \frac{c}{\sqrt{a \cdot b}} \quad (7.2)$$

A shape factor of 1 is indicative of a particle with equal lengths in all three dimensions such as a sphere or cube. A value of about 0.7 is typical for natural sands. Sediment shape is important because more irregular or angular sediment is generally more difficult to mobilize than a smoother, more rounded material.

The sediment size distribution is perhaps the most crucial characteristic with regard to sediment transport. This is because a more diverse set of sediment sizes tends to pack more efficiently, limiting the ability of a flow to mobilize the sediment. A more uniform sediment distribution packs with greater void space between particles, allowing the flow to have greater access to dislodge the sediment material.

The sediment distribution is determined using a set of different-sized mesh screens. Mechanically, these mesh screens are attached to the bottom of individual frames that stack and interlock. A stacked set of frames with mesh sizes growing finer from top to bottom is assembled. The sediment sample is introduced at the top of the stack and the entire stack is then mechanically shaken. Fractions of the overall sample will naturally separate in individual frames according to their size. A sediment gradation distribution such as shown in Figure 7.1 is subsequently generated by weighing the sediment caught in each frame and developing a cumulative distribution of sediment sizes. Several key size fractions of the sediment sample are  $d_{16}$ ,  $d_{50}$ , and  $d_{84}$ , which are the sediment diameters for which 16%, 50%, and 84% of the overall sample are finer by weight, respectively. The overall distribution of the sizes within the sample often approximates a log-normal distribution, meaning that the cumulative distribution of the sediment, as shown in Figure 7.1, approximates a straight line when plotted on log-probability paper. Additionally, the slope of this line gives the standard deviation of the sediment size distribution:

$$\sigma = \frac{1}{2} \log_{10} \left( \frac{d_{84}}{d_{16}} \right) \quad (7.3)$$

A sediment sample that contains uniformly sized material will have a small standard deviation,  $\sigma$ , and is referred to as well sorted or poorly graded. If  $\sigma$  is large the material spans a wide range of sizes and is referred to as poorly sorted or well graded.

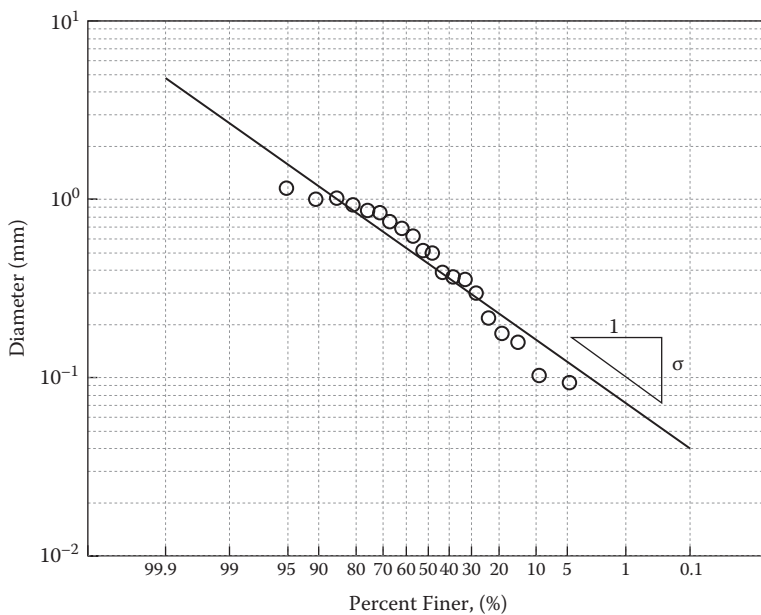


FIGURE 7.1 Sample sediment size distribution.

### 7.2.1 Manning's $n$ as a Function of Channel and Sediment Characteristics

There are many predictive equations of Manning's roughness,  $n$ , that make use of channel and sediment characteristics. The purpose here is to establish a linkage between Manning's  $n$ , used so extensively in previous chapters with the discussion of sediment characteristics presented here. We list here just a few predictive equations to illustrate some of the equations that have been proposed. The first is from Strickler (1923):

$$n = 0.039d_{50}^{1/6} \quad (7.4)$$

where  $d_{50}$  is the median sediment size in meters. A still more complex formulation for Manning's  $n$  was proposed by Limerinos (1970):

$$n = \frac{0.0926R^{1/6}}{1.16 + 2.0\log_{10}\left(\frac{R}{d_{84}}\right)} \quad (7.5)$$

where  $d_{84}$  is as defined earlier and additionally corresponds to the intermediate axis of the sediment particle ( $b$  in equation 7.2) and both  $R$  and  $d_{84}$  are in units of feet. Finally, the most complex equation we present was offered by Brownlie (1983):

$$n = 0.034 \left[ 1.6940 \left( \frac{R}{d_{50}} \right)^{0.1374} S^{0.1112} \sigma^{0.1605} \right] \cdot d_{50}^{0.167} \quad (7.6)$$

where  $R$  and  $d_{50}$  are in units of meters,  $S$  is the slope, and  $\sigma$  is

$$\sigma = 0.5 \left( \frac{d_{84}}{d_{50}} + \frac{d_{50}}{d_{16}} \right) \quad (7.7)$$

Note that the definition of  $\sigma$  in equation 7.7 differs from earlier in equation 7.3. Equation 7.3 assumes the sediment is log-normally distributed while equation 7.7 makes no such assumption and simply defines  $\sigma$  for purposes of use in equation 7.6.

## 7.3 SEDIMENT MOTION

In this section we examine sediment motion, first in terms of its fall velocity in a still column of water, and then in terms of its motion along a channel bed subjected to flowing water.

### 7.3.1 Particle Fall Velocity: Stokes' Law

Before we begin to examine sediment mobilization and transport, it is useful to first examine the movement of sediment in a quiescent or still column of water. In such a setting, a sediment particle rapidly reaches a force balance between gravitational forces acting downward and the drag force acting upward. This is a terminal velocity, analogous to the conditions considered in Chapter 4 that gave rise to uniform flow. In a still column of water, the gravity force is

$$F_g = (\rho_s - \rho)g \cdot V_s \quad (7.8)$$

where  $F_g$  is the force due to gravity,  $\rho_s$  is the density of the sediment particle,  $\rho$  is the density of water, and  $V_s$  is the volume of the sediment particle. Note that the term in parentheses is the effective density of the sediment particle which allows for the buoyancy of the sediment particle in water. Idealizing the particle to be a sphere with diameter,  $d$ , we get

$$F_g = \gamma(S_s - 1) \cdot \frac{1}{6} \pi \cdot d^3 \quad (7.9)$$

where  $S_s$  is the ratio  $\rho_s/\rho$ , the specific gravity of the sediment drag force opposes gravity, thus acting upward:

$$F_D = \frac{C_D \cdot A}{2} \rho \cdot v_f^2 \quad (7.10)$$

where  $C_D$  is the drag coefficient,  $A$  is the area of the particle perpendicular to the direction of flow, and  $v_f$  is the velocity at which the particle is falling through the water column. At values of the Reynold's number,  $R_e$ , less than approximately 1, Stokes' law applies and the drag coefficient can be approximated by

$$C_D = \frac{24}{R_e} = \frac{24\infty}{\rho \cdot v \cdot d} \quad (7.11)$$

where  $\mu$  is the dynamic viscosity. Noting that area,  $A$ , is simply the area of a circle with diameter,  $d$ , we can substitute equation 7.11 into equation 7.10, yielding

$$F_D = \frac{24\infty \cdot \left( \pi \frac{d^2}{4} \right)}{2 \cdot \rho \cdot v_f \cdot d} \rho \cdot v_f^2 = 3\infty \cdot \pi \cdot d \cdot v_f \quad (7.12)$$

At terminal velocity, the gravitational force is balanced by the drag force. We can thus equate equations 7.9 and 7.12 and solve for the terminal or fall velocity,  $v_f$ :

$$v_f = \frac{\gamma(S_s - 1) \cdot \frac{1}{6} \pi \cdot d^3}{3\infty \cdot \pi \cdot d} = \frac{\gamma(S_s - 1)d^2}{18\infty} \quad (7.13)$$

The reader should be able to verify that equation 7.13 obeys the Stokes' law criterion of  $R_e \leq 1$  for particle diameters of approximately 0.1 mm or less (see Problem 7.2) which corresponds to a very fine sand. As shown in Figure 7.2, for values of the Reynolds number exceeding 1, the drag coefficient is larger than would be predicted by Stokes' law. Morrison (2013) presents a numerical approximation of the relationship between drag coefficient and the Reynolds number:

$$C_D = \frac{24}{R_e} + \frac{2.6 \cdot \left( \frac{R_e}{5} \right)^{1.52}}{1 + \left( \frac{R_e}{5} \right)^{1.52}} + \frac{0.411 \cdot \left( \frac{R_e}{263,000} \right)^{-7.94}}{1 + \left( \frac{R_e}{263,000} \right)^{-8.00}} + \left( \frac{R_e^{0.80}}{461,000} \right) \quad (7.14)$$

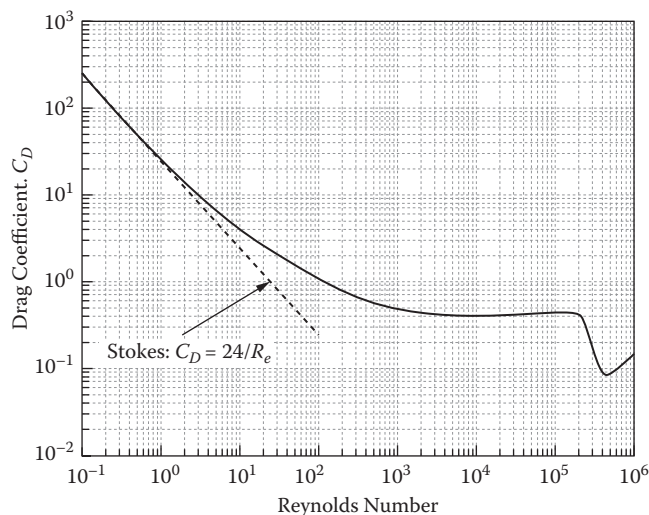


**FIGURE 7.2** Drag coefficient on a sphere as a function of the Reynolds number.

Using equation 7.14 rather than Figure 7.2 can be preferable in cases where automated iteration is necessary, as demonstrated in Example 7.1.

### Example 7.1

Determine the fall velocities for particles of the following sizes: 0.1 mm, 0.2 mm, 0.5 mm, 1 mm, 2 mm, and 10 mm. For each particle size, report the corresponding Reynolds number, true drag coefficient, Stokes' law-based drag coefficient, and the percent difference between these two drag coefficient estimates. Use a specific gravity for the sediment of 2.65, and assume conditions at 10°C. Briefly explore sensitivity to temperature by calculating the fall velocity of a 1 mm particle at 20°C.

#### **Solution:**

Letting  $F_g$  in equation 7.9 equal  $F_D$  in equation 7.10 and assuming each sediment particle is well-approximated as a sphere, we get the following relationship:

$$v_f = \sqrt{\frac{3g \cdot d(S_s - 1)}{4C_D}} \quad (7.15)$$

The solution process is iterative.  $C_D$  depends on the Reynolds number, as shown in equation 7.14, and the Reynolds number depends on the fall velocity determined from equation 7.15.

Consider the 2 mm particle size. As a starting point, we assume that Stokes' law applies and that the Reynolds number is 1. Thus,

$$C_D = \frac{24}{R_e} = \frac{24}{1} = 24$$

and using equation 7.15,

$$v_f = \sqrt{\frac{3g \cdot d(S_s - 1)}{4C_D}} = \sqrt{\frac{3 \cdot (9.81) \cdot \left(\frac{2}{1000}\right) \cdot (2.65 - 1)}{4 \cdot (24)}} = 0.032 \frac{\text{m}}{\text{s}}$$

The Reynolds number based on this fall velocity is

$$R_e = \frac{\rho \cdot v_f \cdot d}{\infty} = \frac{999.7 \cdot (0.032) \cdot \left(\frac{2}{1000}\right)}{0.001307} = 49.0$$

Clearly the assumed Reynolds number of 1 and the Reynolds number calculated here are not consistent. Examining Figure 7.2 or equation 7.15, the larger Reynolds number calculated here is suggestive of a smaller drag coefficient somewhere in  $1 < C_D < 2$ . We can assume a value of  $C_D = 1.5$ , for instance, and return to equation 7.15 to calculate a new fall velocity. Better yet, equation 7.11 can be programmed into an Excel® spreadsheet and the Goal Seek function can be used to iterate between the calculation of the drag coefficient, the fall velocity, and Reynolds number, until the assumed Reynolds number at the front end of the calculations is consistent with the calculated value of the Reynolds number at the back end (see Problem 7.2). Using this approach, Table 7.3 was constructed for the particle sizes requested.

This table shows that as particle sizes get smaller, the Reynolds number decreases and the drag coefficient increases. It is only at the smallest sediment particle size that the difference between the Stokes' law estimate of the drag coefficient and the actual drag coefficient becomes small (less than 1%).

**TABLE 7.3** Reynolds Number, Drag Coefficients, and Fall Velocities of Various Sediment Sizes in Water at 10°C

Particle Diameter $d$ (mm)	Reynolds Number $R_e$	Drag Coefficient $C_D$	Stokes' Law ( $C_D = 24/R_e$ )	Percent Difference in Calculated $C_D$	Fall Velocity (m/s)
10	4180	0.407	0.00574	98.6	0.546
2	291	0.669	0.0824	87.7	0.191
1	77.7	1.18	0.309	73.7	0.102
0.5	18.0	2.73	1.33	51.3	0.0472
0.2	2.16	12.2	11.1	8.86	0.0141
0.1	0.295	81.7	81.4	0.406	0.00386

Relative to 10°C, at 20°C, the water density decreases very slightly but dynamic viscosity decreases by almost 25% (from  $1.307 \times 10^{-3}$  to  $1.002 \times 10^{-3}$  N·s/m<sup>2</sup>; see Table 7.1). For a sediment particle of 1 mm diameter, the result is a calculated fall velocity of 0.111 m/s, about 9% greater than the 0.102 m/s determined at 10°C. The change in fall velocity with temperature will be more dramatic for particles of even smaller size.

An alternative equation for the fall velocity of a particle is provided by Rubey (1933):

$$v_f = F \cdot \sqrt{g(S_s - 1)d} \quad (7.16)$$

where

$$F = \sqrt{\frac{2}{3} + \frac{36v^2}{g(S_s - 1)d^3}} - \sqrt{\frac{36v^2}{g(S_s - 1)d^3}} \quad (7.17)$$

Remember that the kinematic viscosity term,  $v$ , should not be mistaken for the velocity,  $v$ , in equation 7.17.

**Example 7.2**

Repeat Example 7.1 using the Rubey (1933) formula and compare against the results reported in the previous example.

**Solution:**

Using the Rubey (1933) formula, the fall velocity of a sediment particle is a simple, direct calculation using equations 7.16 and 7.17 which, for a fixed temperature, is only a function of the particle size. Figure 7.3 shows fall velocity as a function of particle size over the range of sizes examined in Example 7.1. The curve shown is from the Rubey formula while the individual points shown are from Example 7.1. The figure shows there is reasonable agreement between the two approaches; however, the Reynolds number and drag coefficient approach in Example 7.1 tends to produce smaller estimates of the fall velocity for smaller particles and larger estimates of the fall velocity for larger sediment particles. The break-even point between the two approaches occurs at roughly 1 mm.

Examining the sensitivity of the Rubey formula to temperature, the viscosity terms in the formula will shift from  $v = 1.306 \times 10^{-6}$  to  $v = 1.003 \times 10^{-6} \text{ m}^2/\text{s}$ . Moving from 10°C to 20°C, the fall velocity for a 1 mm particle shifts from 0.0963 m/s to 0.0980 m/s, an increase of a little under

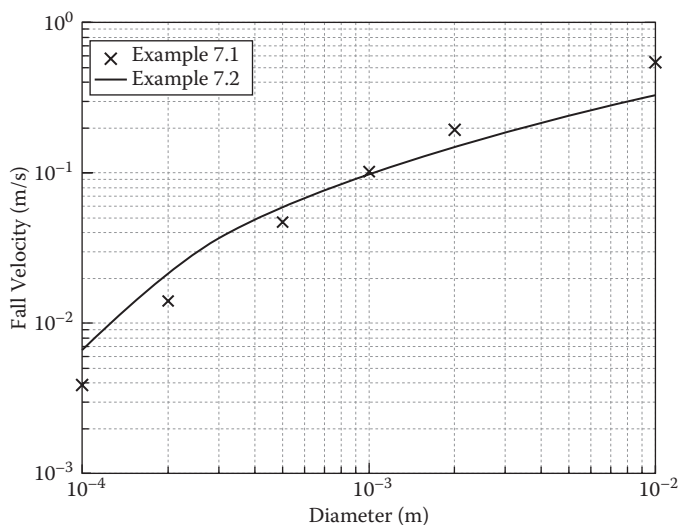


**FIGURE 7.3** Comparison of fall velocities estimated from Reynolds number and drag coefficient (Example 7.1) versus Rubey equation (Example 7.2).

2%. Recall that the same sensitivity analysis for the Reynolds number and drag coefficient approach in Example 7.1 gave a 9% increase. Clearly the Rubey formula, at least in the vicinity of a 1 mm sediment particle, shows a smaller sensitivity to temperature change than did the Reynolds number and drag coefficient approach explored in Example 7.1.

The particle fall velocity will appear as an element for estimating sediment transport in later sections of this chapter.

### **7.3.2 Incipient Motion and Shields' Diagram**

Many of us have spent some part of our childhood playing in the neighborhood creek. At times of low flow, we observed that the water appeared clear with the bed of the channel visible through the flowing water. That same creek, during and after storms, not only produced greatly elevated flows, but that flowing water was no longer clear but was instead an opaque brown owing to the sediment being carried in the flood waters. To oversimplify, our creek during low flow carries no sediment while at high flow it carries sediment.

This section deals with the concept of incipient motion, the point at which sediment motion begins. We propose there is some threshold condition for sediment transport to begin. Below this threshold, sediment remains fixed in place and the water flows clear. Above this threshold, the flow is able to mobilize the sediment, transporting it downstream.

Identifying sediment and flow parameters that would likely characterize sediment transport conditions within an open channel, a reasonable list of such quantities might include the shear stress,  $\tau_0$ ; gravity,  $g$ ; the dynamic viscosity of the fluid,  $\mu$ ; the diameter of a sediment particle,  $d$ ; the density of the flowing water,  $\rho$ ; and the density of the sediment particle,  $\rho_s$ . These six quantities collectively span the three dimensions of mass, length, and time. Using dimensional analysis such as the Buckingham Pi theorem (see Problem 7.3), allows for assembly of  $6 - 3 = 3$  dimensionless terms that should be relevant to the problem of characterizing sediment motion. The precise result of this analysis will vary, but one possible outcome is

$$\Pi_1 = \frac{\rho_s}{\rho} \quad (7.18a)$$

$$\Pi_2 = \frac{\tau_0}{\rho \cdot g \cdot d} \quad (7.18b)$$

$$\Pi_3 = \frac{d}{\sqrt{\rho \cdot \tau_0}} \quad (7.18c)$$

Before going further, notice the conspicuous absence of a velocity term in the dimensional analysis exercise. This was intentional as a pseudo-velocity term constructed from the shear stress and water density is now introduced:

$$\nu_s^* = \sqrt{\frac{\tau_0}{\rho}} \quad (7.19)$$

where  $\nu_s^*$  will be referred to as the shear velocity.

Inspired by the dimensional analysis, we note that the first  $\Pi$  term, in equation 7.18a, is the sediment specific gravity,  $S_s$ . Drawing from the fall velocity analysis earlier, we introduce the specific gravity term from  $\Pi_1$  and the concept of effective weight of the sediment from equation 7.9 into the  $\Pi_2$  term to generate the Shields (1936) entrainment function,  $1/\psi$ :

$$\frac{1}{\psi} = \frac{\tau_0}{\gamma(S_s - 1)d} \quad (7.20)$$

which can be thought of as a form of dimensionless shear stress. Notice that the identity  $\rho \cdot g = \gamma$  is invoked in translating equation 7.18b into equation 7.20. Again, taking motivation from the fall velocity analysis, we wish to examine how shear stress varies with some appropriate form of Reynolds number. Using the shear velocity defined in equation 7.19 to substitute for  $\tau_0$  in the  $\Pi_3$  term in equation 7.18c, we get

$$\Pi_3 = \frac{d}{\infty} \sqrt{\rho \tau_0} = \frac{d}{\infty} \sqrt{\rho \cdot \nu_s^* \sqrt{\rho}} = \frac{d \nu_s^*}{v} = R_e \quad (7.21)$$

where we have converted from the dynamic to the kinematic viscosity using the relationship  $v = \mu/\rho$ . Making measurements of flow and sediment conditions just on the brink of motion, we can graph these conditions in terms of equation 7.20 on the ordinate and the extreme right-hand-side term of equation 7.21 on the abscissa. The result is known as the Shields diagram as shown in Figure 7.4.

The curve for the entrainment function shown in the Shields diagram (1936) is indicative of three distinct flow regime regions. Analogous to the Moody diagram for energy loss in pipes, the Shields diagram spans from laminar flow at the left edge ( $R_e < 1$ ) of the diagram, turbulent flow at the far right ( $R_e > 1000$ ), and a transition zone in between.

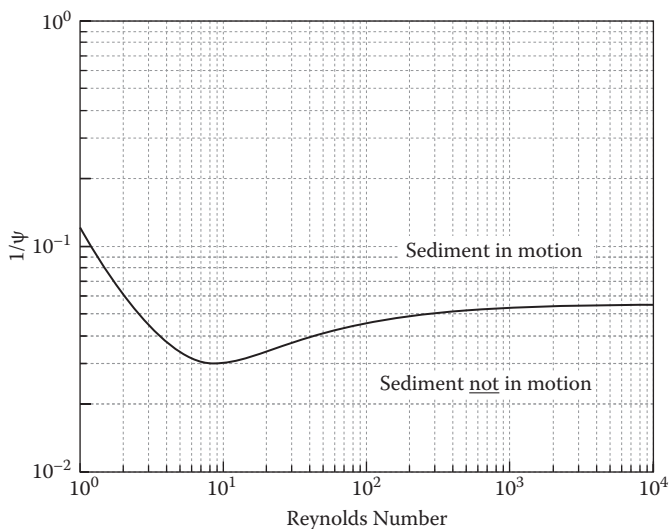


**FIGURE 7.4** The Shields diagram for incipient motion.

### Example 7.3

For a trapezoidal channel flowing at normal depth with  $Q = 2 \text{ m}^3/\text{s}$ , bottom width,  $b = 6 \text{ m}$ , and 2H:1V side slopes, channel slope,  $S_0 = 0.005 \text{ m/m}$ , and Manning's roughness,  $n = 0.03$ , determine the average sediment particle size that will be on the verge of motion within the channel. Assume conditions at  $10^\circ\text{C}$ , but briefly explore sensitivity of the solution to water temperature.

#### **Solution:**

The first step is to determine the normal depth in the reach. For the stated discharge, channel geometry, roughness, and channel slope, the normal depth is 0.292 m and the hydraulic radius,  $R$ , is 0.233 m. Average shear stress across the channel cross-section is then calculated using equation 4.9:

$$\tau_0 = \gamma \cdot R \cdot S_0 = 9804 \cdot (0.233) \cdot (0.005) = 11.4 \frac{\text{N}}{\text{m}^2}$$

Both the Reynolds number and the Shields entrainment function depend on the particle diameter,  $d$ . Assume a value for  $d = 1 \text{ mm}$ . We can now calculate the Reynolds number using equation 7.21:

$$R_e = \frac{d}{\infty} \sqrt{\rho \tau_0} = \frac{\left( \frac{1}{1000} \right) \cdot \sqrt{(999.7) \cdot (11.4)}}{1.307 \cdot 10^{-3}} = 81.7$$

To determine the value of the Shields entrainment function we could refer to Figure 7.4, or for more precision, the function can be approximated by

$$\frac{1}{\psi} = 0.118 \cdot R_e^{-0.979} + 0.056 \cdot e^{-5.31 \cdot R_e^{-0.679}} \quad (7.22)$$

For a Reynolds number of 81.7, the entrainment function is approximately

$$\frac{1}{\psi} = 0.118 \cdot (81.7)^{-0.979} + 0.056 \cdot e^{-5.31 \cdot (81.7)^{-0.679}} = 0.0445$$

The entrainment function, is also defined by equation 7.20:

$$\frac{1}{\psi} = \frac{\tau_0}{\gamma(S_s - 1)d} = \frac{11.4}{9804 \cdot (2.65 - 1) \left( \frac{1}{1000} \right)} = 0.705$$

Clearly, there is a mismatch between these two estimates of the entrainment function,  $1/\psi$ . This simply means that the assumed particle diameter of 1 mm is incorrect. An iterative process can now begin making new estimates of the particle diameter until there is agreement in the value of the entrainment function. This could be a tedious process, but similar to the sediment fall velocity calculation, the iterative process can be automated with the Excel Goal Seek function, allowing estimates of particle diameter to vary until the two entrainment function values are equal. For the values posed in this problem, the solution is,  $d = 13.2 \text{ mm}$ ,  $R_e = 1080$ , and the entrainment function is 0.053. Note that the entrainment function approaches a constant of  $1/\psi = 0.056$  for large Reynolds numbers, and the actual value calculated in this problem,  $1/\psi = 0.053$ , is obviously only slightly less than this. The flow conditions in this problem are in the turbulent region of the Shields diagram.

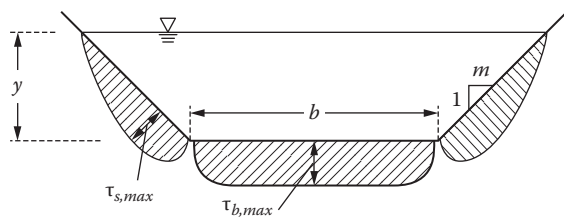


**FIGURE 7.5** Shear stress distribution in a trapezoidal section.

Investigating the sensitivity of this result to temperature, we find that the Reynolds number increases a bit to 1400 and the entrainment function increases slightly to 0.054. However, the particle diameter that is just on the brink of motion is unchanged at  $d = 13.2$  mm. Because the flow is well into the turbulent region, there simply is not much sensitivity of entrainment function to the Reynolds number, and thus the stable particle size is unchanged.

It is important to note that the shear stress value,  $\tau_0$ , used in Example 7.3 and derived from equation 4.9 is simply a representative average value of shear stress across the channel wetted perimeter. In truth, shear stress varies over the wetted perimeter as is indicated schematically in Figure 7.5. Figures 7.6 and 7.7 show how the maximum shear stress in a

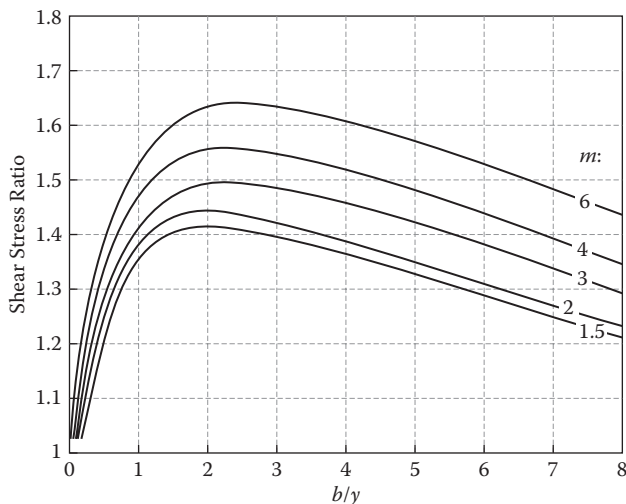


**FIGURE 7.6** Maximum value of shear stress on channel bed in a trapezoidal channel as a function of channel side slope and width/depth ratio. (After Olsen and Florey 1952.)

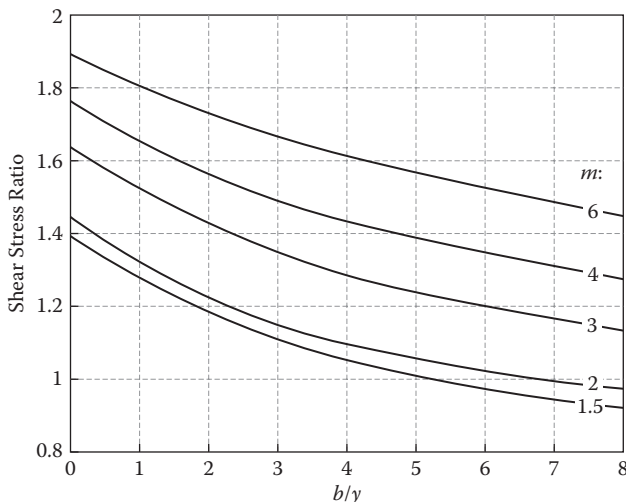


**FIGURE 7.7** Maximum value of shear stress on channel sides in a trapezoidal channel as a function of channel side slope and width/depth ratio. (After Olsen and Florey 1952.)

trapezoidal cross-section varies as a function of the side slope parameter,  $m$ , and the width-to-depth ratio,  $b/d$ , varies (Olsen and Florey 1952) on the channel bed and banks, respectively. These figures depict the ratio of the maximum shear observed on the channel bottom and sides relative to the average shear stress given by equation 4.9.

Let's explore the implications in shear stress variation by re-examining Example 7.3.

### Example 7.4

For the trapezoidal channel and discharge specified in Example 7.3, determine the maximum shear stress ratios that apply on both the bed and banks of the channel. For these ratios, determine the sediment particle sizes that would be on the verge of motion. Compare to the solution found in Example 7.3. Again, assume conditions at 10°C.

#### **Solution:**

In Example 7.3, a normal depth,  $y_0 = 0.292$  m was determined. Thus,  $b/D = 6/0.292 = 6.8$ . Examining Figure 7.6 for  $m = 2$ , the channel bottom shear stress ratio is approximately 1.28, while the channel side shear stress ratio determined from Figure 7.7 is essentially 1.

**Channel bed:**

The maximum shear stress on the bed of the channel is equal to the product of the maximum channel bottom shear stress ratio and the average channel shear stress:

$$\tau_{b,\max} = S_R \cdot (\gamma \cdot R \cdot S_0) = S_R \cdot \tau_0 = 1.28 \cdot (11.4) = 14.6 \frac{\text{N}}{\text{m}^2}$$

where  $S_R$  is the shear stress ratio indicated by either Figure 7.6 (for the channel bed) or Figure 7.7 (for the channel sides). The same iterative procedure as used in Example 7.2 now applies. For the values posed in this problem, the solution is  $d = 16.6$  mm,  $R_e = 2000$ , and the entrainment function is 0.054. This particle diameter is about 25% bigger than the particle diameter of 13.2 mm determined in Example 7.2. The Reynolds number is almost double (2000 versus 1080), and the entrainment function,  $1/\psi$ , has changed only slightly (now 0.054 versus 0.053) in Example 7.3.

**Channel sides:**

Since the shear stress ratio in Figure 7.7 is essentially 1 for the conditions found in this problem, the same sediment diameter and flow conditions calculated in Example 7.3 apply here to the channel sides.

The take-away message from this example is that average shear stress varies considerably over the wetted perimeter of the channel. Thus, using average shear stress to determine a stable particle size is not sufficient. A quick examination of Figures 7.6 and 7.7 indicates that the shear stress ratio,  $S_R$ , is greater than 1 under all conditions along the channel bottom and greater than 1 for all but the  $m = 1.5$  and  $m = 2$  sections and wide channels (high width-to-depth ratios). If one's goal is to specify the minimum channel bed and sides particle size for stability, it would generally be the case that average shear stress needs to be magnified to guarantee stability. In the case of channel bottoms, this magnification factor varies but can be as great as approximately 1.65 for  $m = 6$ . In the case of channel sides, the magnification is, again, greatest for the  $m = 6$  geometry, approaching  $S_R = 1.9$ .

## **7.4 SEDIMENT TRANSPORT**

Sediment being transported within an open channel is typically subdivided into one of three separate categories: washload, suspended load, and bed load. Washload is the material that is brought to the channel from points within the watershed. Generally this material is composed of very fine particles. As

such, this material often remains suspended in the flow and simply washes through the channel, rather than settling within it, to become part of the channel bed or banks. No attempt will be made in this text to examine or further quantify this material. Suspended load has its source in the bed and banks of the channel and is composed of the finer-sized fractions of this material. When mobilized by flowing water, this material is incorporated across the entire depth of flow, though its concentration will naturally be highest nearest the channel edges and bottom. This material gives flood waters their characteristic brown color. Bed load also has its source in the bed and banks of the channel. This term refers to the coarser-sized fractions of the channel material. This material generally is not carried within the flowing water, but rather it tends to hop and roll along the channel bottom in a process referred to as *saltation*. The term *bed material load* is generally used to refer to the sum of both the suspended load and bed load, both having the channel as the source of this material. Equations to estimate these loads often are developed for just suspended load or just bed load, because these two parts of the bed material are transported somewhat differently.

### 7.4.1 Bed Load Transport Rate

There are numerous approaches for estimating bed load transport rate, and an exhaustive enumeration of these approaches is beyond the scope of this text. Instead, we examine a single, widely cited approach known as the Einstein-Brown (1950) equation that built on the earlier work of Einstein (1942). We refer the reader to other texts on sediment transport for comparison of alternative techniques.

The Einstein-Brown approach is based on Figure 7.8 which presents the function,  $\Phi$ , a dimensionless representation of bed load transport rate, as function of the Shields entrainment function ( $1/\psi$ ), a dimensionless representation of shear stress. The dimensionless bed load transport rate,  $\Phi$ , is defined as

$$\Phi = \frac{q_s}{\gamma \cdot S_s \cdot d \cdot v_f} \quad (7.23)$$

where  $q_s$  is the unit bed load transport in N/(m-s); and the fall velocity,  $v_f$ , is specifically determined using the Rubey (1933) formula presented earlier. For convenience, the Einstein-Brown curve shown in Figure 7.8 can be approximated as follows:

$$\Phi = 0.425 \sqrt{\frac{1}{\psi} - 0.1} \quad \text{for } 0.056 \leq \frac{1}{\psi} \leq 0.08 \quad (7.24)$$

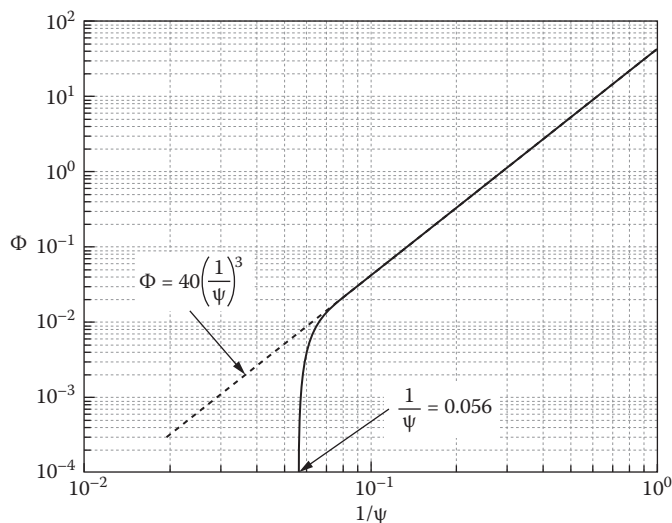


**FIGURE 7.8** Dimensionless bed load transport rate,  $\Phi$ , as a function of the dimensionless Shields entrainment function,  $1/\psi$ .

and

$$\Phi = 40 \left( \frac{1}{\psi} \right)^3 \quad \text{for } \frac{1}{\psi} > 0.08 \quad (7.25)$$

If  $1/\psi$  is less than 0.056, then  $\Phi = 0$ . Bed load estimates are made on individual size fractions by rearranging equation 7.23:

$$q_{s,i} = \Phi_i \cdot \gamma \cdot S_s \cdot d_i \cdot v_{f,i} \quad (7.26)$$

with  $d_i$  (in units of L) representing the geometric mean of the  $i^{\text{th}}$  fraction of the overall bed material sample,  $\Phi_i$  being the dimensionless bed load associated with the  $i^{\text{th}}$  size fraction, and  $q_{s,i}$  being the bed load [in units of F/(L·T)] associated with that fraction. The overall unit bed load [also in units of F/(L·T)] is then determined as the weighted sum of bed loads across all size fractions:

$$q_s = \sum p_i \cdot q_{s,i} \quad (7.27)$$

where  $p_i$  is the decimal fraction of the overall bed material sample within size classification,  $i$ . Finally, the overall sediment transport,  $Q_s$  (in units of F/T), is simply the product of the unit bed load and the channel width:

$$Q_s = q_s \cdot w \quad (7.28)$$

The following example illustrates a procedure for calculating the bed load using the Einstein-Brown relationship.

### **Example 7.5**

Calculate the total bed load transport rate associated with the channel and flow conditions specified in Example 7.3. The bed material of the channel is composed as indicated in Table 7.4.

Show sample calculations for the 4.0 to 4.75 mm size fraction and present a table giving the entrainment function, dimensionless bed load transport, fall velocity, unit bed load transport, and incremental unit bed load transport for each size fraction. Use the average shear stress from Example 7.3 and assume a 10 m wide channel at 10°C.

#### **Solution:**

We first calculate the geometric mean of this size fraction:

$$d_{4.0 \text{ to } 4.75} = \sqrt{\left(\frac{4.0}{1000}\right) \cdot \left(\frac{4.75}{1000}\right)} = 0.00436 \text{ m}$$

**TABLE 7.4** Sieve Analysis of Bed Material for Examples 7.5 and 7.6

<i>Sieve Opening (mm)</i>	<i>% Passing</i>
16.0	100
13.2	83
11.2	71
8.0	55
6.3	42
4.75	34
4.0	26
2.0	18
1.0	9
1.0	0

The average shear stress determined in Example 7.3 was  $11.4 \text{ N/m}^2$ . Using this value, the entrainment function can be determined next:

$$\frac{1}{\Psi} = \frac{\tau_0}{\gamma(S_s - 1)d} = \frac{11.4}{9804 \cdot (2.65 - 1) \cdot (0.00436)} = 0.162$$

The Einstein-Brown dimensionless bed load transport function is

$$\Phi = 40 \left( \frac{1}{\Psi} \right)^3 = 40(0.162)^3 = 0.169$$

To convert the dimensionless bed load to actual bed load, we need to calculate the Rubey (1933) fall velocity. We first calculate  $F$  from equation 7.17:

$$\begin{aligned} F &= \sqrt{\frac{2}{3} + \frac{36v^2}{g(S_s - 1)d^3}} - \sqrt{\frac{36v^2}{g(S_s - 1)d^3}} \\ &= \sqrt{\frac{2}{3} + \frac{36(1.306 \cdot 10^{-6})^2}{9.81(2.65 - 1)(0.00436)^3}} - \sqrt{\frac{36(1.306 \cdot 10^{-6})^2}{9.81(2.65 - 1)(0.00436)^3}} = 0.810 \end{aligned}$$

The fall velocity from equation 7.16 is

$$v_f = F \cdot \sqrt{g(S_s - 1)d} = 0.810 \sqrt{9.81 \cdot (2.65 - 1) \cdot 0.00436} = 0.215 \frac{\text{m}}{\text{s}}$$

The unit bed load for this size fraction is then

$$\begin{aligned} q_{s,i} &= \Phi \cdot \gamma \cdot S_s \cdot d_i \cdot v_{f,i} = (0.169) \cdot (9804) \cdot (2.65) \cdot (0.00436) \cdot (0.215) \\ &= 4.12 \frac{\text{N}}{\text{m} \cdot \text{s}} \end{aligned}$$

For the 4.75 mm sieve opening, 34% passes, while for 4.0 mm, 26% passes. Thus, there is 8% of the overall material that resides in this size fraction, so the incremental unit bed load is

$$p_i \cdot q_{s,i} = (0.08) \cdot (4.12) = 0.329 \frac{\text{N}}{\text{m} \cdot \text{s}}$$

**TABLE 7.5** Bed Load Transport Rates across all Sediment Sizes for Example 7.5

Size Range (mm)	Fraction (%)	$d_i$ (mm)	$1/\psi$	$\Phi$	$v_f$ (m/s)	$q_{s,i}$ [N/(m-s)]	$p_i \cdot q_{s,i}$ [N/(m-s)]
13.2 to 16.0	17	0.0145	0.0485	0	0.395	0	0
11.2 to 13.2	12	0.0122	0.0580	0.00232	0.362	0.265	0.0318
8.0 to 11.2	16	0.00947	0.0745	0.0160	0.319	1.25	0.200
5.3 to 8.0	13	0.00710	0.0993	0.0391	0.276	1.99	0.259
4.75 to 6.3	8	0.00547	0.129	0.0855	0.242	2.94	0.235
4.0 to 4.75	8	0.00436	0.162	0.169	0.215	4.12	0.329
2.0 to 4.0	8	0.00283	0.249	0.619	0.172	7.82	0.625
1.0 to 2.0	9	0.00141	0.498	4.95	0.118	21.5	1.93
<1.0	9	0.00050	1.41	112	0.0594	86.5	7.78
					Sum	11.4	

Finally, for a 10 meter wide channel, the bed load transport rate in this size fraction is

$$p_i \cdot q_{s,i} \cdot w = (0.329) \cdot (10) = 3.29 \frac{N}{s}$$

The bed load transport calculations for the remainder of the size fractions of the material are presented in Table 7.5.

From the table, the total bed load for this channel is

$$w \sum p_i \cdot q_{s,i} = (10) \cdot (11.4) = 114 \text{ N/s.}$$

#### 7.4.2 Suspended Load Transport Rate

While bed load transport rates are generally given in units of F/T (e.g., N/s), the units of suspended load modeling reflect the nature of material being suspended in a fluid and are typically given in units of concentration (e.g., parts

per million, ppm). Thus, conversion of suspended load to a transport rate involves multiplication by the flow rate of the fluid:

$$q_{ss} = \frac{\gamma \cdot S_s \cdot q}{1 \cdot 10^6} \cdot \sum p_i \cdot C_{s,i} \quad (7.29)$$

where the subscript,  $i$ , again refers to a single size fraction in the overall distribution of the bed material sample,  $q_{ss}$  is the unit transport rate [in units of  $F/(L \cdot T)$ ] of suspended material,  $q$  is the unit or specific discharge (in units of  $L^2/T$ ),  $p_i$  is again the decimal fraction of the overall bed material sample, and  $C_{s,i}$  is the concentration (in units of ppm) of suspended sediment in the flow. As with the bed load transport rate, the suspended load transport rate is determined using

$$Q_{ss} = q_{ss} \cdot w \quad (7.30)$$

The key, then, is to identify an effective means to estimate  $C_{s,i}$  in equation 7.29. Similar to bed load transport, an exhaustive enumeration of suspended load transport formulas is not the goal of this text. Instead we will focus on, again, a single approach using the formula presented by Pizzuto (1984):

$$C_{s,i} = 3404 \cdot \left( \frac{v_s^*}{v_{f,i}} \right)^2 \cdot \left( \frac{d_{50}}{y_0} \right)^{0.60} \quad (7.31)$$

where  $C_{s,i}$  is the concentration of suspended sediment (in ppm) of sediment in size fraction  $i$ ,  $v_s^*$  is the shear velocity (in units of  $L/T$ ) as defined earlier in equation 7.19,  $v_{f,i}$  is the fall velocity (in units of  $L/T$ ) for sediment in size fraction  $i$ ,  $d_{50}$  is the median sediment size (in units of L) of the overall distribution of bed material, and  $y_0$  is the depth of flow (in units of L), assumed to be the normal depth. Note that both terms in parentheses are dimensionless so the overall equation can be applied in any internally consistent set of units.

### **Example 7.6**

Using the Pizzuto (1984) formula, calculate the overall suspended load transport rate associated with a channel whose bed material is composed as was previously indicated in Table 7.4 and again use the average shear stress from Example 7.3. Assume a 10 m wide channel flowing at a normal depth of 0.30 m and carrying a discharge of  $2.80 \text{ m}^3/\text{s}$  and

temperature at 10°C. As in the previous example, show sample calculations for the 4.0 to 4.75 mm size fraction and present a table giving the fall velocity, the sediment concentration, and the unit sediment transport rate for each size fraction.

**Solution:**

As was calculated in the previous example, the geometric mean sediment diameter for the 4.0 to 4.75 mm size fraction is 0.00436 m. Using the Reynolds number and drag coefficient approach from Example 7.1, we find by iteration that  $v_{f,i} = 0.334 \text{ m/s}$  at a Reynolds value of approximately 1110. The shear velocity is

$$v_s^* = \sqrt{\frac{\tau_0}{\rho}} = \sqrt{\frac{11.4}{999.7}} = 0.107 \frac{\text{m}}{\text{s}}$$

We need to estimate  $d_{50}$ . The sediment size distribution shows 55% of the material passing a sieve opening of 8.0 mm and 42% passing an opening of 6.3 mm. Linearly interpolating based on the logarithms of the two sizes, we find

$$\log(d_{50}) = \left( \frac{50 - 42}{55 - 42} \right) \cdot [\log(8.0) - \log(6.3)] + \log(6.3)$$

$$\therefore d_{50} = 7.30 \text{ mm or } 0.0073 \text{ m}$$

Applying equation 7.31,

$$C_{s,i} = 3404 \cdot \left( \frac{v_s^*}{v_{f,i}} \right)^2 \cdot \left( \frac{d_{50}}{y_0} \right)^{0.60} = 3404 \cdot \left( \frac{0.107}{0.334} \right)^2 \cdot \left( \frac{0.0073}{0.30} \right)^{0.60} = 37.6 \text{ ppm}$$

The increment of the unit suspended sediment transport rate in this size fraction is,

$$q_{ss, 4.0 \text{ to } 4.75} = \frac{\gamma \cdot S_s \cdot q}{1 \cdot 10^6} \cdot p_i \cdot C_{s,i} = \frac{(9804) \cdot (2.65) \cdot (0.28)}{1 \cdot 10^6} \cdot (0.08) \cdot (37.6)$$

$$= 0.0219 \frac{\text{N}}{\text{m-s}}$$

This value, multiplied by the 10 m width of the channel, produces a total suspended sediment transport rate of 0.219 N/s, which is an order of magnitude smaller than the bed load transport rate of this same size

**TABLE 7.6** Suspended Load Transport Rates across all Sediment Sizes for Example 7.6

Size Range (mm)	Fraction (%)	$d_i$ (mm)	$v_f$ (m/s)	$C_{s,i}$ (ppm)	$q_{ss,i}$ [ $N/(m\cdot s)$ ]	$p_i \cdot q_{ss,i}$ [ $N/(m\cdot s)$ ]
13.2 to 16.0	17	0.0145	0.667	9.4	0.0685	0.0116
11.2 to 13.2	12	0.0122	0.607	11.4	0.0827	0.0099
8.0 to 11.2	16	0.00947	0.530	14.9	0.109	0.0174
5.3 to 8.0	13	0.00710	0.450	20.7	0.151	0.0196
4.75 to 6.3	8	0.00547	0.385	28.2	0.206	0.0164
4.0 to 4.75	8	0.00436	0.334	37.6	0.274	0.0219
2.0 to 4.0	8	0.00283	0.248	68.0	0.494	0.0396
1.0 to 2.0	9	0.00141	0.142	209.0	1.52	0.137
<1.0	9	0.00050	0.0472	1885.9	13.7	1.23
				Sum	1.51	

fraction of the bed material. The suspended sediment transport calculations for the remainder of the size fractions of the material are presented in Table 7.6.

From the above table, the total suspended load for this channel is

$$w \sum p_i \cdot q_{ss,i} = (10) \cdot (1.51) = 15.1 \frac{N}{s}$$

### 7.4.3 Sediment Load Estimation

The formulas for estimating bed load and suspended load transport rates described in the previous subsections are useful to develop instantaneous estimates of transport rate based on an instantaneous flow condition. Of course, an open channel is subject to a wide range of discharges. The total sediment transport load between times  $t_1$  and  $t_2$  is therefore the integral of the instantaneous loads:

$$L = \int_{t_1}^{t_2} [Q_s(t) + Q_{ss}(t)] \cdot dt \quad (7.32)$$

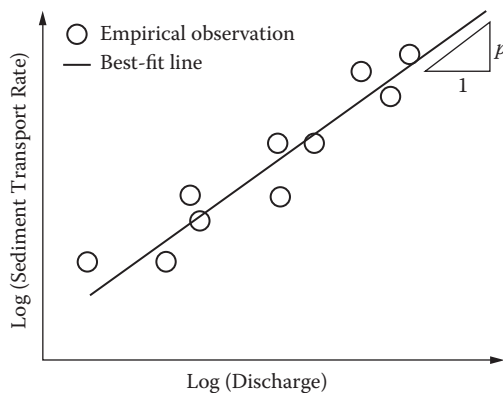


**FIGURE 7.9** An empirically derived sediment rating curve. Best-fit line suggests  $Q_s \sim Q^p$ .

where  $L$  is the total sediment load (in units of  $F$ ) and it is understood that both  $Q_s(t)$  and  $Q_{ss}(t)$  are functions of the time-varying discharge.

While equation 7.32 is tautologically valid, it trivializes the complications in developing a continuous time series of both  $Q_s(t)$  and  $Q_{ss}(t)$ . While methods have been presented in Sections 7.4.1 and 7.4.2 for calculating an instantaneous value for these quantities, generating a continuous time series of each by the methods presented is intractable. Further, even if that were accomplished, there exist other confounding behaviors such as differences in sediment transport rates on the rising versus falling limb of a hydrograph, seasonality effects, temperature dependencies, and so on, that the instantaneous sediment transport rate methods neglect or assume constant.

The solution to estimating total sediment load must be to simplify the approach. This is most readily accomplished through development of a sediment rating curve such as shown in Figure 7.9. Ideally, a rating curve is generated from empirically collected data over a wide range of flows. An empirical rating curve has the advantage of capturing the range of idiosyncrasies of transport behavior in the stream in question. However, it has the disadvantage of applicability only to the stream in question. Applying that rating curve elsewhere is an extrapolation, only as good as the observed stream and applied location are similar. Further, empirically deriving a sediment rating curve is expensive, requiring many observations and possibly considerable time to develop a representative relationship across the spectrum of large flows that are responsible for the majority of sediment transport.

An alternative to empirical observation is to apply bed load and suspended load formulas, like the ones presented in the previous subsections, to the range

of relevant discharges for the stream being studied. This approach can be done more quickly and at little cost but is limited by the representativeness of the chosen formulas and calibration to the stream in question.

An even more simplified approach is to view sediment transport behavior in the stream at a macro level. Such an approach reduces the need for the characterization of the bed material distribution into a single threshold at which sediment movement begins. This approach is conceptually consistent with the incipient motion threshold of the Shields diagram presented earlier. The threshold can be phrased in terms of a critical shear stress,  $\tau^*$ , a critical velocity,  $v^*$ , or a critical discharge,  $Q^*$ . For example,

$$Q_s = f_{\tau}(\tau_0 - \tau^*) \quad (7.33a)$$

$$Q_s = f_v(v - v^*) \quad (7.33b)$$

$$Q_s = f_Q(Q - Q^*) \quad (7.33c)$$

where  $f_x(.)$  is understood to be some possibly complicated function depending on the difference between the actual quantity,  $x$ , and the threshold value of that quantity,  $x^*$ , for sediment movement to begin. If  $x < x^*$ , then no movement occurs and sediment transport is understood to be zero. The reader should recognize that shear stress is arguably the physical quantity that best approximates the cause of movement of a sediment particle, regardless of the specific dimensions of the channel in question. Thus, equations of the form 7.33a are generally more robust to variations in scales of flow and sediment than are equations in the form of 7.33b or 7.33c. Regardless, assuming any of equations 7.33a through 7.33c can be reasonably calibrated to a location, a rating curve that ultimately relates discharge to sediment transport rate can be developed. Once in possession of such a rating curve, one need only have an accompanying time series of stream discharges to estimate the total load of sediment transported in the stream. This approach is illustrated in Example 7.7.

---

### **Example 7.7**

The cross-section of a natural stream is reasonably approximated by a trapezoidal section with bottom width,  $b = 8.2$  m, and 3H:1V side slopes. The bankfull depth is 2.1 m. Manning's roughness is  $n = 0.041$ , and the channel slope is  $S_0 = 0.0037$  m/m. It is found that total sediment transport can be estimated by  $Q_s = 0.0017Q^{1.1}(\tau_0 - 16)$  with  $Q_s$  in N/s,  $Q$  in  $m^3/s$ , and

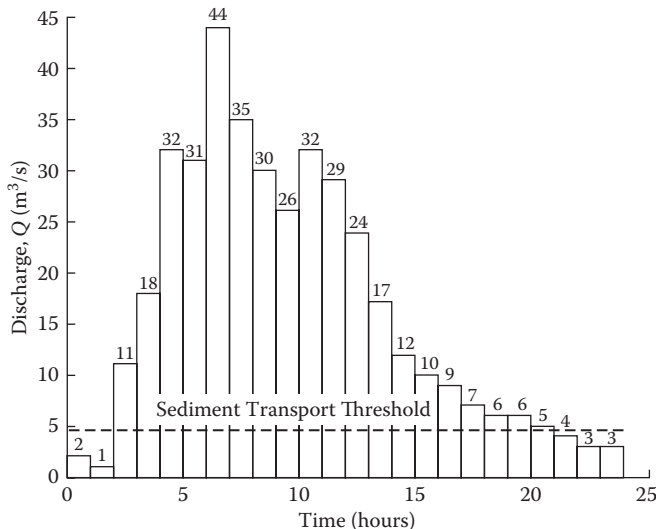


**FIGURE 7.10** Discharge hydrograph for Example 7.7. Discharges greater than the dashed line of  $Q = 4.33 \text{ m}^3/\text{s}$  result in sediment transport.

$\tau_0$  in  $\text{N}/\text{m}^2$ . An hourly time series of discharge is presented in Figure 7.10 corresponding to a single flood event. Assume a temperature of  $10^\circ\text{C}$ .

- Determine the discharge at which sediment transport begins.
  - Present a graph of the sediment transport rating curve over a relevant range of discharges.
  - At high discharges, determine the approximate exponent,  $p$ , in the equation
- $$Q_s \propto Q^p$$
- Use the rating curve to estimate the total sediment load transported by the flood event.

### Solution:

- Sediment transport begins when  $\tau_0 > \tau_c$  where  $\tau_c$  is  $16 \text{ N}/\text{m}^2$ . Thus, we seek the conditions that produce  $\tau_0$  equal to 16:

$$\tau_0 = 16 = \gamma \cdot R \cdot S_0$$

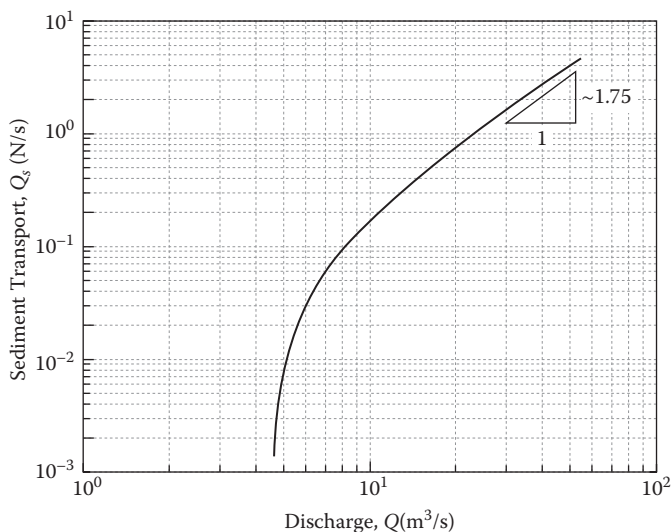


**FIGURE 7.11** Sediment rating curve for Example 7.7. Note that at high discharge, the rating curve approaches becomes linear, with  $Q_s \propto Q^p$  with  $p$  approximately equal to 1.75 for the combined effects of the transport formula and channel geometry provided.

So,

$$R = \frac{16}{\gamma \cdot S_0} = \frac{16}{(9804) \cdot (0.0037)} = 0.441 \text{ m}$$

By iteration, the hydraulic radius,  $R$ , is attained when  $y_0 = 0.514 \text{ m}$ , and the resulting discharge,  $Q = 4.53 \text{ m}^3/\text{s}$ . In other words, sediment discharge,  $Q_s = 0$  if the discharge is below  $4.53 \text{ m}^3/\text{s}$ .

- b. Figure 7.11 shows the relationship between discharge and sediment transport rate for the coupling of channel conditions and the transport equation provided. The strong nonlinearity in transport rate as the discharge just exceeds  $4.53 \text{ m}^3/\text{s}$  is an obvious consequence of the threshold structure of the sediment transport rate equation. The relationship approaches a linear behavior when viewed on a log-log set of axes as shown in Figure 7.11 when discharge is large.
- c. Examining the sediment transport rating curve shown in Figure 7.11 for the largest discharges, the slope of this line, corresponding to the exponent,  $p$ , is approximately 1.7 to 1.8.\*

---

\* It has been generally observed that sediment transport increases with roughly the square of the discharge (Henderson 1966).

- d. Table 7.7 presents the calculations to determine the total sediment volume transported by the flood shown in Figure 7.10. The third time interval (from hours 2 to 3) is used to illustrate the tabulations. For a discharge of  $11 \text{ m}^3/\text{s}$ , the normal depth is determined to be 0.85 m, corresponding to a hydraulic radius of 0.68 m. The average shear stress is

$$\tau_0 = \gamma \cdot R \cdot S_0 = (9804) \cdot (0.68) \cdot (0.0037) = 24.7 \frac{\text{N}}{\text{m}^2}$$

Because this shear stress exceeds the critical shear stress, there is sediment transport during hour 3. That transport rate is

$$Q_s = 0.0017 \cdot Q^{1.1} \cdot (\tau_0 - 16) = (0.0017) \cdot (11)^{1.1} \cdot (24.7 - 16) = 0.206 \frac{\text{m}^3}{\text{s}}$$

The sediment load for the entire 1 hour period is

$$L = Q_s \cdot \Delta t = \left( 0.206 \frac{\text{m}^3}{\text{s}} \right) \cdot (3600 \text{ s}) \cdot \left( \frac{1 \text{ kN}}{1000 \text{ N}} \right) = 0.743 \text{ kN}$$

Table 7.7 shows the cumulative sediment load is 66.3 kN for the flood shown in Figure 7.10 and the provided sediment rating curve.

## 7.5 ESTIMATION OF SEDIMENT TRANSPORT: ACCURACY AND PRECISION

The examples provided in this chapter have generally exhibited two or three significant figures. This has been done to add clarity to the formulas and computations that have been presented and illustrated. However, this may have mistakenly conveyed the impression that phenomena pertaining to sediment transport estimates are understood to a high degree of precision. They are not.

There are many confounding issues and sources of uncertainty in estimating sediment transport. A couple of these have been demonstrated in examples within this chapter: sensitivity to temperature and sensitivity to the equation used to estimate particle fall velocity. Sensitivity to time resolution is examined in Problem 7.9. But there are myriad other sources of uncertainty including accurate knowledge of the bed material distribution, sediment shape, armoring of the bed, presence of cohesive sediments, hysteresis

**TABLE 7.7** Determination of Total Sediment Load on an Hourly Time Interval for Example 7.7

Hour	$Q$ ( $m^3/s$ )	$y_0$ (m)	$R$ (m)	$\tau$ ( $N/m^2$ )	$Q_s$ ( $N/s$ )	Load (kN)
0–1	2	0.32	0.29	10.5	0	0
1–2	1	0.21	0.20	7.2	0	0
2–3	11	0.85	0.68	24.7	0.21	0.74
3–4	18	1.12	0.85	31.0	0.61	2.21
45	32	1.52	1.10	40.0	1.85	6.64
5–6	31	1.50	1.09	39.4	1.74	6.27
6–7	44	1.80	1.26	45.8	3.26	11.73
7–8	35	1.60	1.15	41.6	2.17	7.82
8–9	30	1.47	1.07	38.9	1.64	5.90
9–10	26	1.36	1.01	36.5	1.26	4.52
10–11	32	1.52	1.10	40.0	1.85	6.64
11–12	29	1.45	1.06	38.3	1.54	5.55
12–13	24	1.31	0.97	35.3	1.08	3.89
13–14	17	1.08	0.83	30.2	0.54	1.96
14–15	12	0.89	0.71	25.7	0.25	0.91
15–16	10	0.81	0.65	23.6	0.16	0.58
16–17	9	0.76	0.62	22.4	0.12	0.44
17–18	7	0.66	0.55	19.9	0.06	0.20
18–19	6	0.60	0.51	18.4	0.03	0.11
19–20	6	0.60	0.51	18.4	0.03	0.11
20–21	5	0.54	0.46	16.8	0.01	0.03
21–22	4	0.48	0.41	15.0	0	0
22–23	3	0.41	0.36	12.9	0	0
23–24	3	0.41	0.36	12.9	0	0
					Sum	66.3

effects, characterization of channel geometry in both the vertical and horizontal planes, and accurate estimates of the water discharge.

This chapter has sought to illustrate the most basic concepts of sediment transport and motivate the enthusiastic reader to explore deeper. Sediment transport estimation suffers from being at the tail end of many other sources of natural variability and uncertainty, compromising the accuracy of any estimate. It cannot be overstated that estimating sediment loads carried by a channel on either a storm-by-storm or annual basis is difficult. One is generally doing well simply to estimate the load within the correct order of magnitude. The reader would do well to keep this fact well in mind when performing any computation. An honest assessment of uncertainty and variability in the numerous inputs to a given computation, coupled with ample application of sensitivity analysis, should help lead to the appropriate precision of presentation of sediment transport rate or load estimates.

## References

- Brown, C.B. (1950). Sediment transportation, Chapter XII in *Engineering Hydraulics*, H. Rouse, ed., Wiley, New York.
- Brownlie, W.R. (1983). Flow depth in sand-bed channels, *Journal of Hydraulic Engineering*, ASCE, 109(7): 959–990.
- Einstein, H.A. (1942). Formulas for the transportation of bed load, *Transactions*, ASCE, 107: 561–573.
- Henderson, F.M. (1966). *Open Channel Flow*, Macmillan, New York.
- Limerinos, J.T. (1970). Determination of the Manning coefficient from measured bed roughness in natural channels. US Geological Survey, Water Supply Paper 1898-B, 47 p.
- McNown, J.S., and J. Malaika. (1950). Effects of particle shape on settling velocity at low Reynolds numbers. *Transactions, American Geophysical Union*, 31(1): 74–82.
- Morrison, F.A. (2013). *An Introduction to Fluid Mechanics*, Cambridge University Press, New York.
- Olsen, R.B., and Q.L. Florey (1952). Sedimentation studies in open channels: Boundary shear and velocity distribution by membrane analogy, analytical, and finite-difference methods. Laboratory Report Sp-34, U.S. Bureau of Reclamation.
- Pizzuto, J.E. (1984). An evaluation of methods for calculating the concentration of suspended bed material in rivers. *Water Resources Research*, 20(10): 1381–1389.
- Rubey, W.W. (1933). Equilibrium-conditions in debris-laden streams. *Transactions, American Geophysical Union*, 14: doi: 10.1029/TR014i001p00497.
- Shields, A. (1936). Anwendung der Ähnlichkeitsmechanik und der Turbulenzforschung auf die Geschiebebewegung (Application of similitude and turbulence experiments in bed-load movement), Mitteilungen der Prüssischen Versuchanstalt für Wasserbau und Schiffbau, Berlin, Germany. Translated to English by W.P. Ott and J.C. van Uchelen, California Institute of Technology, Pasadena, CA, 1936.
- Strickler, A. (1923). Beiträge zur Frage der Geschwindigkeits-formel und der Raugegekeitszahlen fur Strom, Kanale und geschlossene Leitungen (Some contributions to the problem of the velocity formula and roughness factors for rivers, canals, and closed conduits), Bern, Switzerland, Mitt. Eidgeno assicshen Amtes Wasserwirtschaft, no. 16.

## Problems

In all problems below, assume sediment specific gravity is  $S_s = 2.65$ .

- 7.1. Assume a hydraulic radius,  $R = 0.83$  m, a friction slope of  $S_f = 0.0065$  m/m, and  $d_{16}$ ,  $d_{50}$ , and  $d_{84}$  are 1.6 mm, 11 mm, and 26 mm, respectively. Assume  $d_{84}$  is particle size of intermediate axis. Use the equations provided by Strickler, Limerinos, and Brownlie to estimate Manning's  $n$ .
- 7.2. Using iteration, determine the largest particle diameter for which Stokes' law still holds. Note that this will be the diameter of a particle that corresponds to a Reynolds number of approximately 1.
- 7.3. Use the Buckingham-Pi theorem to develop a dimensionless term for sediment transport based on the following parameters: shear stress,  $\tau_0$ ; gravity,  $g$ ; dynamic viscosity,  $\mu$ ; particle diameter,  $d$ ; density of the water,  $\rho$ ; and density of the sediment,  $\rho_s$ . Verify that your result is either identical to or equivalent to the findings shown in equations 7.18a through 7.18c.
- 7.4. For a trapezoidal channel flowing at normal depth with  $Q = 1.6$  m<sup>3</sup>/s, bottom width,  $b = 3.0$  m, and 3H:1V side slopes, channel slope,  $S_0 = 0.0021$  m/m, and Manning's roughness,  $n = 0.032$ , determine the average sediment particle size that will be on the verge of motion within the channel. Assume conditions at 10°C, but briefly explore the effect on solution if water is 20°C.
- 7.5. Continue with Problem 7.4 but now determine the following:
  - a. Maximum shear stress on channel bed
  - b. Maximum shear stress on channel sides
  - c. Size of sediment particle on both channel bed and channel sides that will be just on the verge of motion
- 7.6. Use the channel geometry and flow conditions specified in Problem 7.4 and the bed material composition from Example 7.5 to perform the same bed load transport rate analysis as in Example 7.5. Since the channel is trapezoidal, simply assume its width is equal to the average of the bottom width,  $b = 3$  m, and the top width at normal depth. As in the example, show sample calculations for the 4 to 4.75 mm size fraction.
- 7.7. Repeat Example 7.6 for the overall suspended load transport rate associated with a channel whose bed material is composed as in Example 7.5. Use the channel geometry and flow conditions from Problem 7.4. Since the channel is trapezoidal, simply assume its width is equal to

the average of the bottom width,  $b = 3$  m, and the top width at normal depth. As in the previous problem, show sample calculations for the 4 to 4.75 mm size fraction.

- 7.8. The cross-section of a natural stream is reasonably approximated by a trapezoidal section with bottom width,  $b = 9.1$  m, and 2H:1V side slopes. The bankfull depth is 3.1 m. Manning's roughness is  $n = 0.033$  and the channel slope is  $S_0 = 0.0043$  m/m. It is found that total sediment transport can be estimated by  $Q_s = 0.027Q^{1.3}(\nu-1.4)$  with  $Q_s$  in N/s,  $Q$  in  $\text{m}^3/\text{s}$ , and  $\nu$  in  $\text{m}/\text{s}$ . The following is an hourly time series of a single storm event:  $Q = \{2, 1, 12, 20, 37, 35, 50, 28, 21, 17, 13, 8\}$  in  $\text{m}^3/\text{s}$ .
- Determine the discharge at which sediment transport begins.
  - Present a graph of the sediment transport rating curve over a relevant range of discharges.
  - At high discharges, determine the approximate exponent,  $p$ , in the equation

$$Q_s \propto Q^p$$

- Use the rating curve to estimate the total sediment load transported by the storm event.
- 7.9. Examine the sensitivity of the 1 hour time resolution used in Example 7.7. Consider that the actual discharges, in 6 minute intervals from the start to the end of hour 6 are  $\{36, 42, 45, 52, 51, 50, 44, 42, 40, 38\}$   $\text{m}^3/\text{s}$ . Note that these discharges average to the  $44 \text{ m}^3/\text{s}$  reported for this same hour in the original calculations.

# Appendix

**Key:**  $y$ : flow depth;  $D$ : channel diameter;  $A$ : cross-sectional area;  $P$ : wetted perimeter;  $R$ : hydraulic radius ( $A/P$ );  $B$ : top width;  $A/B$ : hydraulic depth;  $\bar{y}$ : centroid depth from water surface.

Table of Circular Channel Properties								
$\frac{y}{D}$	$\frac{A}{D^2}$	$\frac{P}{D}$	$\frac{R}{D}$	$\frac{B}{D}$	$\frac{A/B}{D}$	$\frac{\bar{y}}{D}$	$\frac{AR^{2/3}}{D^{8/3}}$	
0.01	0.0013	0.2003	0.0066	0.1990	0.0067	0.0040	0.0000	
0.02	0.0037	0.2838	0.0132	0.2800	0.0134	0.0080	0.0002	
0.03	0.0069	0.3482	0.0197	0.3412	0.0201	0.0120	0.0005	
0.04	0.0105	0.4027	0.0262	0.3919	0.0269	0.0161	0.0009	
0.05	0.0147	0.4510	0.0326	0.4359	0.0337	0.0201	0.0015	
0.06	0.0192	0.4949	0.0389	0.4750	0.0405	0.0241	0.0022	
0.07	0.0242	0.5355	0.0451	0.5103	0.0474	0.0282	0.0031	
0.08	0.0294	0.5735	0.0513	0.5426	0.0542	0.0322	0.0041	
0.09	0.0350	0.6094	0.0575	0.5724	0.0612	0.0363	0.0052	
0.10	0.0409	0.6435	0.0635	0.6000	0.0681	0.0404	0.0065	
0.11	0.0470	0.6761	0.0695	0.6258	0.0751	0.0444	0.0079	
0.12	0.0534	0.7075	0.0755	0.6499	0.0821	0.0485	0.0095	

(continued)

Table of Circular Channel Properties

$\frac{y}{D}$	$\frac{A}{D^2}$	$\frac{P}{D}$	$\frac{R}{D}$	$\frac{B}{D}$	$\frac{A/B}{D}$	$\frac{\bar{y}}{D}$	$\frac{AR^{2/3}}{D^{8/3}}$
0.13	0.0600	0.7377	0.0813	0.6726	0.0892	0.0526	0.0113
0.14	0.0668	0.7670	0.0871	0.6940	0.0963	0.0567	0.0131
0.15	0.0739	0.7954	0.0929	0.7141	0.1034	0.0608	0.0152
0.16	0.0811	0.8230	0.0986	0.7332	0.1106	0.0650	0.0173
0.17	0.0885	0.8500	0.1042	0.7513	0.1178	0.0691	0.0196
0.18	0.0961	0.8763	0.1097	0.7684	0.1251	0.0732	0.0220
0.19	0.1039	0.9021	0.1152	0.7846	0.1324	0.0774	0.0246
0.20	0.1118	0.9273	0.1206	0.8000	0.1398	0.0816	0.0273
0.21	0.1199	0.9521	0.1259	0.8146	0.1472	0.0857	0.0301
0.22	0.1281	0.9764	0.1312	0.8285	0.1546	0.0899	0.0331
0.23	0.1365	1.0004	0.1364	0.8417	0.1621	0.0941	0.0362
0.24	0.1449	1.0239	0.1416	0.8542	0.1697	0.0983	0.0394
0.25	0.1535	1.0472	0.1466	0.8660	0.1773	0.1025	0.0427
0.26	0.1623	1.0701	0.1516	0.8773	0.1850	0.1067	0.0461
0.27	0.1711	1.0928	0.1566	0.8879	0.1927	0.1110	0.0497
0.28	0.1800	1.1152	0.1614	0.8980	0.2005	0.1152	0.0534
0.29	0.1890	1.1374	0.1662	0.9075	0.2083	0.1195	0.0572
0.30	0.1982	1.1593	0.1709	0.9165	0.2162	0.1237	0.0610
0.31	0.2074	1.1810	0.1756	0.9250	0.2242	0.1280	0.0650
0.32	0.2167	1.2025	0.1802	0.9330	0.2322	0.1323	0.0691
0.33	0.2260	1.2239	0.1847	0.9404	0.2404	0.1366	0.0733

Table of Circular Channel Properties

$\frac{y}{D}$	$\frac{A}{D^2}$	$\frac{P}{D}$	$\frac{R}{D}$	$\frac{B}{D}$	$\frac{A/B}{D}$	$\frac{\bar{y}}{D}$	$\frac{AR^{2/3}}{D^{8/3}}$
0.34	0.2355	1.2451	0.1891	0.9474	0.2485	0.1410	0.0776
0.35	0.2450	1.2661	0.1935	0.9539	0.2568	0.1453	0.0820
0.36	0.2546	1.2870	0.1978	0.9600	0.2652	0.1496	0.0864
0.37	0.2642	1.3078	0.2020	0.9656	0.2736	0.1540	0.0910
0.38	0.2739	1.3284	0.2062	0.9708	0.2821	0.1584	0.0956
0.39	0.2836	1.3490	0.2102	0.9755	0.2907	0.1628	0.1003
0.40	0.2934	1.3694	0.2142	0.9798	0.2994	0.1672	0.1050
0.41	0.3032	1.3898	0.2182	0.9837	0.3082	0.1716	0.1099
0.42	0.3130	1.4101	0.2220	0.9871	0.3171	0.1760	0.1148
0.43	0.3229	1.4303	0.2258	0.9902	0.3261	0.1805	0.1197
0.44	0.3328	1.4505	0.2295	0.9928	0.3353	0.1850	0.1248
0.45	0.3428	1.4706	0.2331	0.9950	0.3445	0.1895	0.1298
0.46	0.3527	1.4907	0.2366	0.9968	0.3539	0.1940	0.1349
0.47	0.3627	1.5108	0.2401	0.9982	0.3634	0.1985	0.1401
0.48	0.3727	1.5308	0.2435	0.9992	0.3730	0.2031	0.1453
0.49	0.3827	1.5508	0.2468	0.9998	0.3828	0.2076	0.1506
0.50	0.3927	1.5708	0.2500	1.0000	0.3927	0.2122	0.1558
0.51	0.4027	1.5908	0.2531	0.9998	0.4028	0.2168	0.1611
0.52	0.4127	1.6108	0.2562	0.9992	0.4130	0.2214	0.1665
0.53	0.4227	1.6308	0.2592	0.9982	0.4234	0.2261	0.1718

(continued)

Table of Circular Channel Properties								
$\frac{y}{D}$	$\frac{A}{D^2}$	$\frac{P}{D}$	$\frac{R}{D}$	$\frac{B}{D}$	$\frac{A/B}{D}$	$\frac{\bar{y}}{D}$	$\frac{AR^{2/3}}{D^{8/3}}$	
0.54	0.4327	1.6509	0.2621	0.9968	0.4340	0.2308	0.1772	
0.55	0.4426	1.6710	0.2649	0.9950	0.4448	0.2355	0.1826	
0.56	0.4526	1.6911	0.2676	0.9928	0.4558	0.2402	0.1879	
0.57	0.4625	1.7113	0.2703	0.9902	0.4671	0.2449	0.1933	
0.58	0.4724	1.7315	0.2728	0.9871	0.4785	0.2497	0.1987	
0.59	0.4822	1.7518	0.2753	0.9837	0.4902	0.2545	0.2041	
0.60	0.4920	1.7722	0.2776	0.9798	0.5022	0.2593	0.2094	
0.61	0.5018	1.7926	0.2799	0.9755	0.5144	0.2642	0.2147	
0.62	0.5115	1.8132	0.2821	0.9708	0.5269	0.2690	0.2200	
0.63	0.5212	1.8338	0.2842	0.9656	0.5398	0.2739	0.2253	
0.64	0.5308	1.8546	0.2862	0.9600	0.5530	0.2789	0.2306	
0.65	0.5404	1.8755	0.2881	0.9539	0.5665	0.2839	0.2358	
0.66	0.5499	1.8965	0.2900	0.9474	0.5804	0.2889	0.2409	
0.67	0.5594	1.9177	0.2917	0.9404	0.5948	0.2939	0.2460	
0.68	0.5687	1.9391	0.2933	0.9330	0.6096	0.2990	0.2511	
0.69	0.5780	1.9606	0.2948	0.9250	0.6249	0.3041	0.2560	
0.70	0.5872	1.9823	0.2962	0.9165	0.6407	0.3093	0.2610	
0.71	0.5964	2.0042	0.2975	0.9075	0.6571	0.3144	0.2658	
0.72	0.6054	2.0264	0.2987	0.8980	0.6741	0.3197	0.2705	
0.73	0.6143	2.0488	0.2998	0.8879	0.6919	0.3250	0.2752	

Table of Circular Channel Properties

$\frac{y}{D}$	$\frac{A}{D^2}$	$\frac{P}{D}$	$\frac{R}{D}$	$\frac{B}{D}$	$\frac{A/B}{D}$	$\frac{\bar{y}}{D}$	$\frac{AR^{2/3}}{D^{8/3}}$
0.74	0.6231	2.0715	0.3008	0.8773	0.7103	0.3303	0.2798
0.75	0.6319	2.0944	0.3017	0.8660	0.7296	0.3357	0.2842
0.76	0.6405	2.1176	0.3024	0.8542	0.7498	0.3411	0.2886
0.77	0.6489	2.1412	0.3031	0.8417	0.7710	0.3466	0.2928
0.78	0.6573	2.1652	0.3036	0.8285	0.7933	0.3521	0.2969
0.79	0.6655	2.1895	0.3039	0.8146	0.8169	0.3577	0.3008
0.80	0.6736	2.2143	0.3042	0.8000	0.8420	0.3633	0.3047
0.81	0.6815	2.2395	0.3043	0.7846	0.8686	0.3691	0.3083
0.82	0.6893	2.2653	0.3043	0.7684	0.8970	0.3748	0.3118
0.83	0.6969	2.2916	0.3041	0.7513	0.9276	0.3807	0.3151
0.84	0.7043	2.3186	0.3038	0.7332	0.9605	0.3866	0.3183
0.85	0.7115	2.3462	0.3033	0.7141	0.9963	0.3927	0.3212
0.86	0.7186	2.3746	0.3026	0.6940	1.0354	0.3988	0.3239
0.87	0.7254	2.4039	0.3018	0.6726	1.0785	0.4050	0.3264
0.88	0.7320	2.4341	0.3007	0.6499	1.1263	0.4113	0.3286
0.89	0.7384	2.4655	0.2995	0.6258	1.1800	0.4177	0.3305
0.90	0.7445	2.4981	0.2980	0.6000	1.2409	0.4242	0.3322
0.91	0.7504	2.5322	0.2963	0.5724	1.3110	0.4308	0.3335
0.92	0.7560	2.5681	0.2944	0.5426	1.3933	0.4376	0.3345

(continued)

Table of Circular Channel Properties

$\frac{y}{D}$	$\frac{A}{D^2}$	$\frac{P}{D}$	$\frac{R}{D}$	$\frac{B}{D}$	$\frac{A/B}{D}$	$\frac{\bar{y}}{D}$	$\frac{AR^{2/3}}{D^{8/3}}$
0.93	0.7612	2.6061	0.2921	0.5103	1.4917	0.4445	0.3351
0.94	0.7662	2.6467	0.2895	0.4750	1.6131	0.4517	0.3353
0.95	0.7707	2.6906	0.2865	0.4359	1.7681	0.4590	0.3349
0.96	0.7749	2.7389	0.2829	0.3919	1.9771	0.4665	0.3339
0.97	0.7785	2.7934	0.2787	0.3412	2.2819	0.4743	0.3322
0.98	0.7816	2.8578	0.2735	0.2800	2.7916	0.4823	0.3294
0.99	0.7841	2.9413	0.2666	0.1990	3.9401	0.4908	0.3248
1.00	0.7854	3.1416	0.2500	0.0000	$+\infty$	0.5000	0.3117

# Index

## A

Accessibility, *see* Flow accessibility  
Adverse reach  
    definition, 115  
    profiles on, 122, 132  
Alternate depth  
    contrasted with conjugate depth, 70, 73–74  
    definition, 24  
    determination by goal seek function, 52–54  
    duality with conjugate depth, 83–86  
    equation in rectangular channel, 24, 64, 83–86  
    in constriction.avi animation, 38  
    in gatejump.avi animation, 81–83  
    in momentum example, 77–78, 80  
    in non-rectangular channel, 49, 51–55  
    in qualitative profiles example, 134, 136, 138, 152  
    in quantitative profiles example, 188–189  
    in solved energy examples, 26, 28, 30, 32, 36  
Animations  
    channel\_length.avi, 190–192

constriction.avi, 38–39  
discharge\_proble.avi, 158–159  
gatejump.avi, 81–83  
mild\_vary.avi, 143–144  
m3m2\_animation.avi, 192–194  
normal depth summary, 115–116  
steep\_vary.avi, 150–151  
step.avi, 34–35  
step\_transient.avi, 43–44  
ynorm\_discharge.avi, 117  
ynorm\_n.avi, 118  
ynorm\_slope.avi, 121  
ynorm\_width\_mild.avi, 119  
ynorm\_width\_stEEP.avi, 120

## B

Bank  
    bed load, 228  
    HEC-RAS specification, 196–197  
    shear stress, 226  
Bed load  
    related to suspended load transport rate, 232–234  
    related to sediment load estimation, 235–236  
    transport rate, 227–232

Bernoulli equation, 4, 6, 13–14, 16  
 Boundary conditions

in HEC-RAS, *see* HEC-RAS  
 qualitative, 153–156, 159, 162  
 quantitative, 169, 181–182, 186,  
 188, 205

Buckingham Π theorem, 221

## C

Circular cross-section

alternate depth in, 49–50  
 computation of energy in, 49  
 computation of momentum in,  
 86–89, 97–98  
 critical depth in, 55–56, 61–63,  
 64  
 critical energy in, 57, 64  
 graphical calculation of conjugate  
 depth, 90–91, 91–92,  
 94–95, 97  
 hydraulic jump in, 90–91, 91–92,  
 94–95, 97  
 normal depth, 112, 114  
 properties (*see* Appendix),  
 245–250

Chézy equation, 103, 108–110

Choke

caused by constriction, 38–39  
 caused by sluice gate, 82–83  
 caused by step, 34–35  
 definition, 41  
 general discussion, 39–41, 132,  
 139, 154  
 in qualitative profiles example, 134,  
 136, 152, 154  
 in quantitative profiles example,  
 188, 194  
 transient conditions, 41–44

Composite profiles

general discussion of, 140,  
 148–149  
 mild to less mild, 141–142  
 mild to steep, 140–141  
 steep to more steep, 144–145  
 steep to mild, 145–148

Conjugate curve, 159–161, 162,  
 185–194, 205

Conjugate depth, 70, 97–98, 139,  
 149  
 definition, 74  
 determination by goal seek  
 function, 96  
 duality with alternate depth,  
 83–86  
 equation in rectangular channel,  
 74–75  
 in circular channel, 90–91  
 in gatejump.avi animation, 81–83  
 in qualitative profiles example,  
 134, 136, 146–147  
 in trapezoidal channel, 89–90  
 in solved momentum examples,  
 75–78, 80–81, 91–95  
 summary, non-rectangular  
 calculation of, 97  
 with changing normal depth,  
 117–121

Constriction

choke conditions at, 38–39,  
 40–43  
 general discussion of, 35–38,  
 63–64  
 gradually varied flow profiles  
 caused by, 126, 134, 138,  
 139, 145  
 transient flow at, 40–44

Continuity equation, 4, 5, 16, 17, 24,  
 69, 112, 171, 180

Control, 48–49, 177

Critical depth

equation in rectangular channel,  
 19–20, 43, 48, 64  
 graphical solution for circular or  
 trapezoidal channel, 55–56,  
 59–63  
 maximum discharge  
 interpretation, 20–21, 59

Critical energy

equation in rectangular channel,  
 19–20, 42, 64  
 graphical solution for circular or  
 trapezoidal channel, 55–58,  
 63

minimum energy interpretation,  
 18, 20, 40–42, 61

- Critical flow**  
 as function of discharge, 117  
 chokes and, 39–41, 78  
 general discussion of, 18–21,  
 21–24, 63–69  
 occurrence of, 46–49  
 relationship to energy dissipation,  
 152  
 relationship to lake discharge  
 problem, 157, 159
- Critical reach**  
 definition, 114  
 profiles on, 122, 131
- D**
- Depth**  
 alternate, *see* Alternate depth  
 conjugate, *see* Conjugate depth  
 critical, *see* Critical depth  
 normal, *see* Normal depth
- Discharge**  
 definition, 3  
 specific or unit, 16
- Drag coefficient**, 216–221, 234
- E**
- Efficient channel**, 124
- Einstein-Brown equation**, 228–231
- Energy equation**, 15, 17, 49
- Energy**  
 kinetic, 14  
 loss in jump, 70–71, 77, 78–79,  
 82–83, 97  
 loss from friction, 108–109, 122,  
 141, 181, 222  
 loss in drowned jump, 152  
 potential, 14  
 in non-rectangular channel, 49  
 in rectangular channel, 15, 17  
 specific, 14  
 units of, 14
- F**
- Fall velocity**, *see* Terminal velocity
- Flow accessibility**, 45–46, 145, 151
- Friction slope**, 107–110, 112, 122  
 in estimation equation of  
 Manning's  $n$ , 215  
 importance to gradually varied  
 flow, 127–128, 161  
 numerical calculation of, 171, 173,  
 175, 178–184
- Froude number**  
 definition, 4–7  
 relationship to critical conditions,  
 21–22  
 relationship to information flow,  
 22–24  
 relationship to mild and steep  
 reaches, 115
- G**
- Gate**, *see* Sluice gate
- Goal seek function**  
 applied to alternate depths, 51,  
 52–54, 64  
 applied to conjugate depths, 93,  
 95, 96, 97, 98  
 applied to fall velocity, 218  
 applied to normal depth, 114, 122  
 applied to qualitative gradually  
 varied flow, 133, 136, 146,  
 147, 157  
 applied to quantitative gradually  
 varied flow, 177  
 applied to Shields entrainment  
 function, 224  
 general demonstration, 52–54
- H**
- HEC-RAS**  
 about, 194–195  
 boundary conditions, 195, 198–  
 200, 202–204  
 hydraulic jump example, 202–204  
 $M_2$  example, 196–202  
 modifying tabular output,  
 200–201
- Horizontal reach**  
 definition, 115  
 profiles on, 122, 131

- Hydraulic depth, 55, 87, 201, 245–250
- Hydraulic grade line, 107–108
- Hydraulic jump
- equation in rectangular channels, 74–75
  - graphical solution in circular channels, 90–91
  - graphical solution in trapezoidal channels, 89–90
- Hydraulic radius
- and shear stress, 106–107
  - and normal depth, 107–110, 112–114
  - calculation in standard step method, 171, 180
  - definition, 107
  - in lake discharge problem, 157
  - in normal depth animations, 116–121
  - in sediment motion and transport, 223, 239–240
- Hydrograph, 236, 238
- I**
- Incipient motion, 221, 223, 237
- J**
- Jump, *see* Hydraulic jump
- K**
- L**
- Lake discharge problem, 156–159
- M**
- Manning equation
- and normal depth, 112–114, 116, 118
  - general discussion of, 108–110, 122
  - roughness from sediment characteristics, 214–215
- specification in HEC-RAS, 196–197
- table of roughness coefficients, 110–111
- Mild reach; *see also* Animations; Composite profiles
- definition, 114–115
  - normal depth in channel of varying width, 116, 119
  - profiles on, 122, 126–127, 129–130, 133–135
- Momentum
- contrasted with energy, 69–71
  - in non-rectangular channel, 86–88
  - in rectangular channel, 71–72
  - loss at gate, 78–83
  - units of, 72
- N**
- Non-rectangular cross-section; *see also* Circular cross-section; Trapezoidal cross-section
- energy in, 49–52, 55–57
  - momentum in, 86–89
- Normal depth, 7, 103, 112–122
- definition, 112
- Non-uniform flow, *see* Surface water profiles
- O**
- Outfall, 48, 58, 60–62, 140
- P**
- Q**
- Quiescent column of water, 215
- R**
- Reach terminology, 114–115
- Rectangular cross-section
- critical depth in, *see* Critical depth
  - critical energy in, *see* Critical energy

- energy in, *see* Energy  
 momentum in, *see* Momentum  
 Resistance equation, *see* Chézy  
     equation; Manning equation
- S**
- Sediment  
     shape, 212–213  
     size, 211–212  
     size distribution, 213–214  
     example distribution, 230  
     specific gravity, 210–211  
     rating curve, 236–240
- Shear stress  
     and sediment transport, 233–234,  
         237–238, 240  
     and Shields function, *see* Shields  
         entrainment function  
     as source of friction, 106–108,  
         122  
     distribution in trapezoidal cross-  
         section, 225–227
- Shields entrainment function,  
     221–224, 228–231
- Sluice gate  
     alternate depths at, 25–26  
     causing choke conditions, 81–83  
     drowned hydraulic jump at,  
         151–152  
     energy conservation at, 24, 79–80,  
         138  
     momentum loss at, 78–80, 82, 98
- Specific energy, *see* Energy
- Stage, 180–181, 183–185
- Standard step method  
     comparison to HEC-RAS, 196,  
         201–202, 202–204  
     distance from depth, 170–176  
     depth from distance, 176–180  
     with varying channel cross-section,  
         180–185
- Steady flow, 7, 195, 198–200
- Steep reach; *see also* Animations;  
     Composite profiles  
     critical flow at head of, 48, 58,  
         60–62, 140–141  
     definition, 114–115
- normal depth in channel of varying  
     width, 116, 120  
     profiles on, 122, 126–127, 129–130,  
         135–138
- Step  
     choke conditions at, 34–35  
     Froude number changed by,  
         46–48  
     general discussion of, 26–35  
     gradually varied flow profiles  
         caused by, 126, 138–139, 145  
         transient flow at, 43–44
- Stokes' law, 216–219
- Surface water profiles  
     on adverse reaches, 132  
     on critical reaches, 131  
     on horizontal reaches, 131  
     on mild reaches, 130  
     on steep reaches, 130
- Suspended load, 227–228, 232–235,  
     235–236
- T**
- Terminal velocity  
     normal depth analog, 103–106,  
         121  
     sediment fall velocity, 215–221,  
         222, 224, 228, 230–231,  
         233–234, 240
- Transient flow,  
     at constriction, 41–43  
     general discussion of, 7, 39, 41  
     in step animation, 43–44
- Trapezoidal cross-section  
     alternate depth in, 51–54  
     computation of energy in, 49–50  
     computation of momentum in,  
         86–88, 96–98  
     critical depth in, 55–56, 60–61, 64  
     critical energy in, 55–57, 58–59,  
         64  
     graphical calculation of conjugate  
         depth, 89–90, 91–94, 97  
     hydraulic jump in, 89–90, 91–94,  
         97  
     normal depth in, 112–114  
     momentum function in, 86–87, 96

**U**

Uniform flow, *see also* Normal depth  
definition, 7, 121  
general discussion of, 103–106,  
108, 121–122

Unsteady flow, 7

**V**

Velocity  
from continuity equation, 5, 17  
definition, 2, 13, 16

general discussion of, 2–6, 13–18  
of shallow wave, 4–6, 22–23

**W**

Water  
physical properties of, 210–211  
Washload, 227–228  
Wetted perimeter  
in circular cross-section, 87, 245–250  
numerical calculation of, 170–171,  
180  
role in flow resistance, 107, 114  
role in sediment transport, 225, 227